Impact of global change on coastal plankton: a multiple environmental driver approach - from cellular processes to food webs

Dissertation zur Erlangung des Grades eines

Doktors der Naturwissenschaften

- Dr. rer. nat. –

Fachbereich 2 Biologie/Chemie

Vorgelegt von

Hugo Duarte Moreno

Universität Bremen

Januar 2023

GEFÖRDERT VOM

Bundesministerium
für Bildung
und Forschung

ALFRED-WEGENER-INSTITUT
HELMHOLTZ-ZENTRUM FÜR POLAR-
UND MEERESFORSCHUNG

Betreuer: Prof. Dr. Maarten Boersma

Prüfungsausschuss:

1. Gutachter: PD Dr. Cédric Meunier (PlanktoSERV, Shelf Sea System Ecology, Alfred-Wegener-Institut, Helmholtz-Zentrum für Polar-und Meeresforschung, Biologische Anstalt Helgoland)
2. Gutachterin: Dr. Cordula Scherer (Trinity Centre for Environmental Humanities, the University of Dublin, Trinity College)

1. Prüfer: Prof. Dr. Tilmann Harder (Meereschemie, Universität Bremen)
2. Prüfer: Prof. Dr. Marko Rohlfs (Populations- und Evolutionsökologie, Universität Bremen)

Tag des Promotionskolloquiums: 10. März 2023

Acknowledgments

I would like to thank my supervisor PD Dr. Cédric Meunier for his support throughout this process, for making this project possible and for giving me the chance to be part of his team. Many thanks also to Prof. Dr. Maarten Boersma for his valuable suggestions and advices during my PhD. I sincerely thank the members of my examination committee, Prof. Dr. Tilmann Harder, Prof. Dr. Marko Rohlfs and Dr. Cordula Scherer for their effort and time on evaluating my dissertation.

I am truly grateful to the researchers who directly supported me during experiments, inspiring discussions, sample analysis and reviewing processes: Dr. Nelly Tremblay, Dr. Elisabeth Groß, Dr. Sebastian Rokitta, Prof. Dr. Karen H. Wiltshire, Dr. Julien di Pane, Martin Köring, PD Dr. Bernhard Fuchs and Helena Klip. Many thanks to the great technical support from the AWI team as well, especially Julia Haafke, Ursula Ecker, Silvia Peters, Kristine Carstens and Petra Kadel.

I sincerely thank Prof. Dr. Herwig Stibor for his support as member of my thesis advisory committee. I would like to thank the AWI graduate school POLMAR for their great support. Many thanks also to the Federal ministry of Education and Research (BMBF) for financing this project.

Special thanks to my fellow Helgoland PhD students who went or are going on the same roller coaster and have shared many moments with me on that small island. Thank you, Laura, Eli, Aldi and Nelly for your company and trust, and for making my life on Helgoland so much better. Thank you, Thomas, for your support and for being on my side during these last crazy years.

Table of Contents

List of Figures

Supplementary Figures

List of Tables

Supplementary Tables

Supplementary Information

Frequently used abbreviations

ANOVA	Analysis of variance
AOX	Alternative oxidase
C	Carbon
Chl-a	Chlorophyll *a*
DIC	Dissolved inorganic carbon
DIN	Dissolved inorganic nitrogen
DIP	Dissolved inorganic phosphorus
DOC	Dissolved organic carbon
DSi	Dissolved silica
ERCP	Extended representative concentration pathway
ETC	Electron transport chain
GLM	Generalized linear model
IPCC	Intergovernmental Panel on Climate Change
N	Nitrogen
LMM	Linear mixed-effects model
LRT	Likelihood ratio test
MDA	Malondialdehyde
P	Phosphorus
PCA	Principal component analysis
pCO_2	Partial pressure of carbon dioxide
POC	Particulate organic carbon
PRC	Principeal response curve
RCP	Representative concentration pathway
ROS	Reactive oxygen species

Thesis summary

Phytoplankton are responsible for approximately 50% of global primary production and are the basis of pelagic food webs. Seasonal phytoplankton blooms in temperate coastal habitats boost productivity in these systems, while the dynamics of blooms are directly dependent on abiotic factors. Human activities have led to global changes in environmental conditions, including higher temperature, partial pressure of carbon dioxide (pCO_2) and nitrogen:phosphorus ratio of dissolved inorganic nutrients, which have been putting plankton communities under pressure. Such environmental changes have raised questions about how these communities will react to future conditions. In my thesis I applied a multiple-driver approach to investigate the effect of global change drivers on phytoplankton cells as well as on plankton communities during seasonal bloom events. Using future scenarios from the Intergovernmental Panel on Climate Change (IPCC) together with predicted shifts in N:P ratios in coastal system, my thesis aims to realistically simulate environmental conditions expected for the year 2100.

Given the importance of phytoplankton to the biological carbon pump, I investigated the impact of global change drivers on the carbon metabolism and antioxidant capacity of the diatom *Phaeodactylum tricornutum*. This phytoplankton was exposed to the environmental conditions of the RCP 8.5 scenario (+3°C and pCO_2 1000 µatm) from the IPCC as well as higher N:P ratio of dissolved nutrients in a full-factorial design. The results of this experiment indicate that temperature is the main driver behind cellular processes. Warming led to lower antioxidant capacity, while positively affected DOC exudation and growth rate. The cells were mostly unaffected by pCO_2 and N:P ratio at current temperature, and only under increased temperatures, cells became prone to these environmental drivers. Higher pCO_2 stimulated primary production under warmer conditions, while dampened dark respiration. Higher N:P ratio also positively affected DOC exudation. As a result, cells had lower carbon content when exposed to the RCP 8.5 scenario conditions. Antioxidant enzymes were less active under warming and photoprotective pigments concentration was lower. Alternative Oxidase (AOX) activity increased under warming, as well as the accumulation of Malondialdehyde in the cells, indicating cellular oxidative stress.

To assess if changes in phytoplankton cellular dynamics are also parallel to changes in plankton community structure and composition, two mesocosm experiment were conducted during a spring and fall bloom with natural plankton food webs. The plankton community was

exposed to an integrated multiple driver approach. Two different scenarios with higher temperature and pCO_2, RCP 6.0 (+1.5°C and pCO_2 800 µatm) and RCP 8.5 (+3.0°C and pCO_2 1000 µatm) were tested against ambient conditions. The scenarios were extended (ERCP) also to include higher N:P ratios. These experiments revealed the resilience of the phytoplankton spring bloom against global change drivers, where phytoplankton, microzooplankton and bacterioplankton biomass and community composition remained similar across scenarios. Mesozooplankton, namely copepods, however, showed an increase in abundance in spring in the ERCP 8.5, demonstrating that more energy went up from primary producers to higher trophic levels in this scenario. The higher abundance of copepods took place despite the higher N:P and C:P ratio of the seston under the ERCP scenarios, which proved not to be a limiting factor for mesozooplankton growth under such conditions. In fall, results revealed that phytoplankton community underwent restructuring under the ERCP 8.5 scenario, being mostly dominated by smaller species at the expense of large diatoms. The rise of the coccolithophore *Emiliania huxleyi* under this scenario also indicates potential functional changes in the biological carbon pump, due to the calcification capacity of this species. Conversely, mesozooplankton were negatively impacted by the ERCP 8.5 scenario conditions, and were partially replaced by microzooplankton. The microbial loop was strengthened in the ERCP 8.5 scenario, indicating lower flux of energy to higher trophic levels. Nonetheless, in both experiments, the ERCP 6.0 scenario proved to be more similar to the Ambient conditions, compared to the ERCP 8.5.

Finally, the results of the fall mesocosm experiment were reassessed though an inverse modelling and network analysis to quantify carbon fluxes and interactions between the food web compartments. This analysis identifies that functioning of the plankton food web was similar in the Ambient and ERCP 6.0 scenario, while substantial alterations were seen in the ERCP 8.5. These results reveal the higher fluxes of carbon through the microbial loop in the ERCP 8.5 scenario, and, therefore, a higher capacity to recycle carbon within the system. Microzooplankton also showed higher herbivory degree in this scenario, exerting higher grazing pressure on the phytoplankton than mesozooplankton.

Overall, this thesis presents a comprehensive picture of the impact of global change drivers on phytoplankton physiology and its implications to the plankton food web, as well as evidences of structural and functional shifts in plankton communities under future scenarios. Due to the fact that plankton food webs remained similar in the ERCP 6.0 scenarios and

Ambient, compared to the ERCP 8.5 scenario, this thesis also identifies that the worst case ERCP scenario may lead to substantial alterations in the plankton community.

Zusammenfassung

Phytoplankton ist für ca. 50% der globalen Primärproduktion verantwortlich und bildet die Grundlage pelagischer Nahrungsnetze. Saisonale Phytoplanktonblüten in gemäßigten Küstenlebensräumen steigern die Produktivität in diesen Systemen, während die Dynamik der Blüten direkt von abiotischen Faktoren abhängt. Menschliche Aktivitäten haben zu globalen Veränderungen der Umweltbedingungen geführt, einschließlich höherer Temperatur, Partialdruck von Kohlendioxid (pCO_2) und Konzentration gelöster Nährstoffe, die die Planktongemeinschaften unter Druck setzen. Solche Umweltveränderungen haben Fragen darüber aufgeworfen, wie diese Gemeinschaften auf zukünftige Bedingungen reagieren werden. In meiner Doktorarbeit habe ich einen Multi-Driver-Ansatz angewendet, um die Auswirkungen globaler Veränderungstreiber auf Phytoplanktonzellen sowie auf Planktongemeinschaften während saisonaler Blütenereignisse zu untersuchen. Unter Verwendung von Zukunftsszenarien des „Intergovernmental Panel on Climate Change“ (IPCC) zusammen mit vorhergesagten Verschiebungen der N:P-Verhältnisse im Küstensystem zielt meine Doktorarbeit darauf ab, die für das Jahr 2100 erwarteten Umweltbedingungen realistisch zu simulieren.

Angesichts der Bedeutung von Phytoplankton für die biologische Kohlenstoffpumpe untersuchte ich den Einfluss von Treibern des globalen Wandels auf den Kohlenstoffstoffwechsel und die antioxidative Kapazität der Diatomee *Phaeodactylum tricornutum*. Diese Phytoplankton Art wurde den Umweltbedingungen des RCP 8.5-Szenarios (+3°C und pCO_2 1000 µatm) des IPCC sowie einem höheren N:P-Verhältnis gelöster Nährstoffe in einem vollfaktoriellen Design ausgesetzt. Die Ergebnisse dieses Experiments zeigen, dass die Temperatur der Haupttreiber hinter zellulären Prozessen ist. Die Erwärmung führte zu einer geringeren antioxidativen Kapazität, während sie die DOC-Exsudation und die Wachstumsrate positiv beeinflusste. Die Zellen waren bei der aktuellen Temperatur größtenteils unbeeinflusst von pCO_2 und dem N:P-Verhältnis, und nur bei erhöhten Temperaturen wurden die Zellen anfällig für diese Umwelttreiber. Ein höherer pCO_2 stimulierte die Primärproduktion unter wärmeren Bedingungen, während die Zellatmung gedämpft wurde. Ein höheres N:P-Verhältnis wirkte sich auch positiv auf die DOC-Exsudation aus. Als Ergebnis hatten die Zellen einen niedrigeren Kohlenstoffgehalt, wenn sie den Bedingungen des RCP 8.5-Szenarios ausgesetzt wurden. Antioxidative Enzyme waren unter Erwärmung weniger aktiv und die

Konzentration der lichtschützenden Pigmente war geringer. Alternative Oxidase-Aktivität (AOX), sowie die Akkumulation von Malondialdehyd in den Zellen erhöhte sich unter Erwärmung, was auf zellulären oxidativen Stress hinweist.

Um zu beurteilen, ob Veränderungen in der Zelldynamik des Phytoplanktons auch parallel zu Veränderungen in der Struktur und Zusammensetzung der Planktongemeinschaft verlaufen, wurden zwei Mesokosmenexperimente während einer Frühlings- und Herbstblüte mit natürlichen Plankton-Nahrungsnetzen durchgeführt. Die Planktongemeinschaft wurde einem integrierten Ansatz mit mehreren Treibern ausgesetzt. Es wurden zwei verschiedene Szenarien mit höherer Temperatur und pCO_2, RCP 6.0 (+1,5 °C und pCO_2 800 µatm) und RCP 8.5 (+3°C und pCO_2 1000 µatm) gegen Umgebungsbedingungen getestet. Die Szenarien wurden erweitert (ERCP), um auch höhere N:P-Verhältnisse einzubeziehen. Diese Experimente zeigten die Widerstandsfähigkeit der Phytoplankton-Frühlingsblüte gegenüber Treibern des globalen Wandels, bei denen die Biomasse und die Zusammensetzung der Gemeinschaft von Phytoplankton, Mikrozooplankton und Bakterioplankton in allen Szenarien ähnlich blieben. Mesozooplankton, nämlich Ruderfußkrebse, zeigten jedoch im Frühling im ERCP 8.5 eine Zunahme der Abundanz, was zeigt, dass in diesem Szenario mehr Energie von Primärproduzenten zu höheren trophischen Ebenen aufstieg. Die höhere Abundanz von Ruderfußkrebsen fand trotz des höheren N:P- und C:P-Verhältnisses des Sestons unter den ERCP-Szenarien statt, was sich unter solchen Bedingungen als kein limitierender Faktor für das Wachstum von Mesozooplankton erwies. Im Herbst zeigten die Ergebnisse, dass die Phytoplanktongemeinschaft im Rahmen des ERCP 8.5-Szenarios umstrukturiert wurde und hauptsächlich von kleineren Arten auf Kosten großer Diatomeen dominiert wurde. Der Anstieg des Coccolithophoren *Emiliania huxleyi* in diesem Szenario deutet auch auf mögliche funktionelle Veränderungen in der biologischen Kohlenstoffpumpe aufgrund der Verkalkungskapazität dieser Art hin. Umgekehrt wurde Mesozooplankton durch die Bedingungen des ERCP 8.5-Szenarios negativ beeinflusst und teilweise durch Mikrozooplankton ersetzt. Die mikrobielle Schleife wurde im ERCP 8.5-Szenario verstärkt, was auf einen geringeren Energiefluss zu höheren trophischen Ebenen hindeutet. Nichtsdestotrotz erwies sich in beiden Experimenten das ERCP 6.0-Szenario im Vergleich zu ERCP 8.5 als ähnlicher zu den Umgebungsbedingungen.

Schließlich wurden die Ergebnisse des Herbst-Mesokosmen-Experiments durch eine inverse Modellierung und Netzwerkanalyse neu bewertet, um Kohlenstoffflüsse und Wechselwirkungen zwischen den Nahrungsnetzbestandteilen zu quantifizieren. Diese Analyse

zeigt, dass die Funktionsweise des Plankton-Nahrungsnetzes im Ambient- und ERCP 6.0-Szenario ähnlich war, während im ERCP 8.5 wesentliche Änderungen festgestellt wurden. Diese Ergebnisse zeigen die höheren Kohlenstoffflüsse durch die mikrobielle Schleife im ERCP 8.5-Szenario und damit eine höhere Kapazität zum Recycling von Kohlenstoff innerhalb des Systems. Mikrozooplankton zeigte in diesem Szenario auch einen höheren Herbivory-degree und übte einen höheren Fraßdruck auf das Phytoplankton aus als Mesozooplankton.

Insgesamt präsentiert diese Arbeit ein umfassendes Bild der Auswirkungen globaler Veränderungstreiber auf die Phytoplanktonphysiologie und ihre Auswirkungen auf das Plankton-Nahrungsnetz sowie Hinweise auf strukturelle und funktionelle Veränderungen in Planktongemeinschaften unter Zukunftsszenarien. Aufgrund der Tatsache, dass Plankton-Nahrungsnetze im ERCP 6.0-Szenario und Ambient im Vergleich zum ERCP 8.5-Szenario ähnlich blieben, identifiziert diese Arbeit auch, dass das Worst-Case-ERCP-Szenario zu erheblichen Veränderungen in der Planktongemeischaft führen kann.

Chapter 1

General Introduction

1.1. Plankton communities

Plankton communities are the basis of pelagic food webs. This group comprises all autotrophic and heterotrophic pelagic organisms that cannot actively move against currents. Autotrophic plankton, or phytoplankton, are unicellular microalgae able to photosynthesize, while heterotrophic plankton contain nano- and microzooplankton (< 200 µm in size), mesozooplankton (200 - 20,000 µm) and larger animals, such as jellyfish and krill. Marine phytoplankton are responsible for approximately 50% of global primary production (Field et al., 1998; Behrenfeld et al., 2001) and for more than 90% of all primary production in the seas (Duarte and Cebrian, 1996). Due to the their incredibly high biomass and capacity to convert inorganic nutrients into organic compounds, phytoplankton are major players in biogeochemical cycles of different elements, especially carbon, nitrogen, phosphorus and silica (Buesseler, 1998; Bowler et al., 2010). Phytoplankton can assimilate dissolved inorganic carbon (DIC) from the water column and, once taken up, DIC is converted into carbohydrates through photosynthesis, which then can be used by the phytoplankton cell for growth, energy production through dark respiration, or exuded as dissolved organic carbon (DOC) (Marra and Barber, 2004; Tortell et al., 2008; Thornton, 2014). Carbon present in phytoplankton biomass can be transferred to higher trophic levels through zooplankton grazing, remineralized as CO_2 when phytoplankton cells decay and are decomposed by detritivores, or exported to deeper oceanic layers, where it can buried and sequestrated (Honjo and Manganini, 1993). These carbon fluxes are some of the most important components of the marine carbon pump and globally influence the carbon concentration in the atmosphere (Falkowski, 1994; Falkowski et al., 1998).

Carbon fluxes associated with the marine carbon pump are largely influenced by processes taking place within the microbial loop, a trophic pathway where heterotrophic bacterioplankton (planktonic prokaryotes) incorporate DOC into biomass (Azam et al., 1983). Once incorporated as biomass, organic carbon can be transferred to the classic planktonic food

web, as bacterioplankton are consumed by zooplankton. The microbial loop benefits from phytoplankton production, since bacterioplankton rely on exuded DOC (Larsson and Hagström, 1979), and, in turn, it supplies important elements to phytoplankton production, such as inorganic nitrogen and phosphorus via decomposition. When inorganic nutrients are incorporated into phytoplankton biomass, they are passed on to microzooplankton that graze on the microalgae. Microzooplankton can also directly consume pelagic bacteria, making a straight link between the bacterioplankton, phytoplankton and microzooplankton (Azam et al., 1983). Alternatively, mesozooplankton can graze on microzooplankton and phytoplankton, directing carbon from phytoplankton and the microbial loop to higher trophic levels, as mesozooplankton are an important food source for planktivorous fish, for example.

Phytoplankton is also responsible for seasonal events typically occurring in temperate regions, the spring and fall blooms. Phytoplankton blooms are a rapid and massive increase of phytoplankton abundance that takes place when environmental conditions are favourable. These blooms are largely controlled by environmental conditions, especially the degree of turbulence, which maintains the water column well mixed and a good supply of dissolved nutrients. Well mixed seawater also keeps microalgae cells close to the surface, where sunlight irradiance is high, therefore, providing energy supply for photsyntehtic activity (Margalef, 1978; Jones and Gowen, 1990; Winder and Sommer, 2012; Wiltshire et al., 2015). Phytoplankton benefits from high dissolved nutrient concentration as well as increasing temperature and sunlight irradiance at the beginning of spring, which support their growth. When phytoplankton growth exceeds losses by, for instance, grazing and virus lysis, a phytoplankton bloom can take place. This exponential increase in phytoplankton biomass boosts zooplankton production, which in turn, increases grazing pressure on phytoplankton and, along with dissolved nutrient depletion, leads to reduction in microalgae abundance (Huppert et al., 2002; Sun et al., 2013). By the beginning of fall, zooplankton abundances decrease, and, reduced top-down pressure coupled with nutrient remineralisation by bacteria enable a second bloom event (Figure 1.1). The fall bloom is, however, not always guaranteed to occur and yields lower phytoplankton biomass than the spring bloom.

Spring and fall phytoplankton blooms do not differ only in biomass, but are also characterized by a different community composition. The fall bloom is commonly dominated by dinoflagellates and smaller microalgae. Conversely, spring blooms are often dominated by large diatoms (Cullen et al., 2002). These two groups, diatoms and dinoflagellates, are long recognized as r- and K-strategist phytoplankton, respectively. R-strategists, will typically thrive

under beginning of spring conditions, highly turbulent and high nutrient concentration environments. Due to their low affinity for nutrients, diatoms have a longer way to reach saturation of nutrient uptake, making this group very competitive under high nutrient availability. On the other hand, dinoflagellates can sustain low, but constant, growth when nutrient concentration is low, which are common conditions in low turbulent, warm waters at the beginning of fall (Margalef, 1978; Smayda and Reynolds, 2001). Common taxa present in spring blooms in the North Sea include: *Guinardia delicatula*, *Odontella* sp., *Thalassiosira* sp., *Chaetoceros* sp., *Skeletonema costatum*, *Rhizosolenia setigera* and *Ditylum brightwellii*. Typical taxa present during late summer and fall are *Protoperidinium* sp., *Ceratium* sp., *Noctiluca scintillans*, *Prorocentrum* sp., *Katodinium* sp., *Guinardia flaccida*, *Leptocylindrus danicus* and *Detonula pumila* (Kraberg et al., 2010; Wiltshire et al., 2010; Löder et al., 2010; Löder, et al., 2011; Scharfe and Wiltshire, 2019). Phytoplankton bloom events are associated with biotic and abiotic conditions that affect the triggering and development of the bloom with escalating impacts to the whole marine food web. Phytoplankton physiology and community dynamics are connected to, among other factors, temperature conditions and nutrient concentrations (Strom et al., 2001; Häder and Gao, 2015). However, these environmental drivers have been undergoing intense changes over the last decades due to human activities, raising questions about their impact on plankton communities.

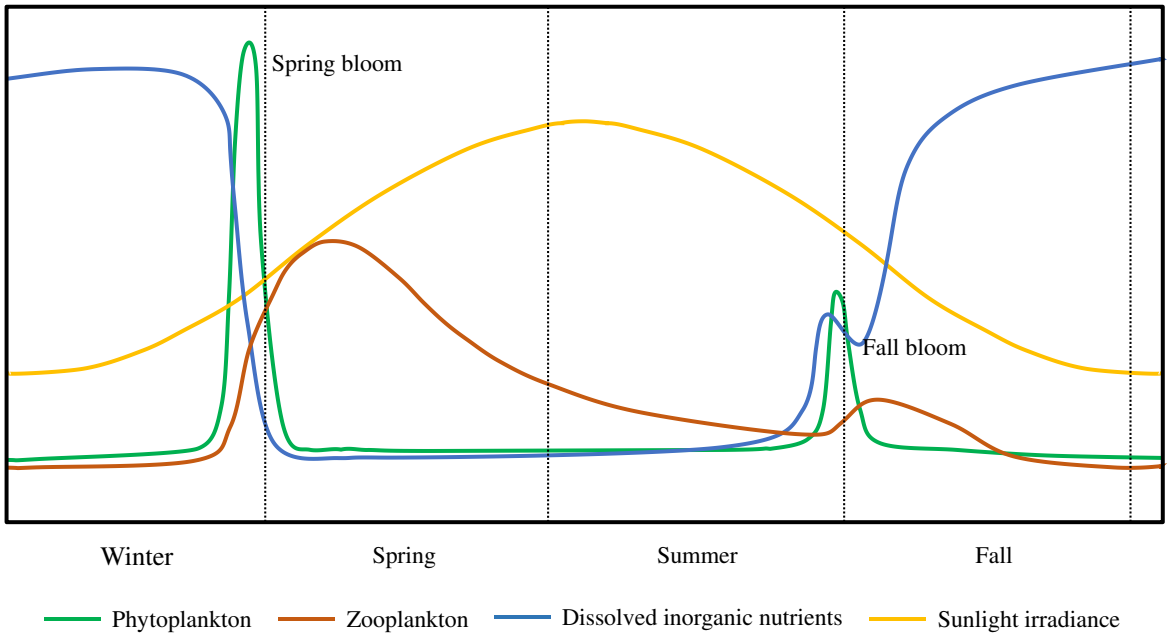

Figure 1.1: The seasonal pattern of phytoplankton blooms in temperate marine habitats (based on 2004 Pearson Prentice Hall, Inc.)**.**

1.2. Global change: pCO_2, warming and dissolved nutrients ratio

Since the industrial revolution, fossil fuels have been applied as energy source at large scales, leading to a rise of atmospheric partial pressure of carbon dioxide (pCO_2) from 277 ppm in 1750 to 412 ppm in 2020 (Friedlingstein et al., 2022). Although CO_2 is the primary source of C for photosynthetic organisms and a key component of the carbon cycle, it is also a greenhouse gas, able to indirectly trap part of the sunlight energy in the atmosphere, which would be otherwise reflected from the Earth's surface as infrared light, warming the planet's surface and lower atmosphere (Easterbook, 2016). Atmospheric CO_2 is partially absorbed by the oceans, most of it by direct dissolution through the sea surface. CO_2 reacts with H_2O, forming carbonic acid (H_2CO_3), once hydrated CO_2 engages a series of reactions to reach equilibrium, releasing protons (H^+) and resulting in the formation of bicarbonate (HCO_3^-) and carbonate (CO_3^{2-}). The concentration of these compounds is pH-dependent, with CO_3^{2-} being more abundant at higher pH and HCO_3^- and free dissolved CO_2 at lower pH (Andersen, 2002). Dissolved inorganic carbon can be incorporated by primary producers, mainly phytoplankton, while free protons will lead to a reduction of seawater pH, a process known as ocean acidification (Doney et al., 2009). Due to their capacity to store carbon as carbonate and bicarbonate, the oceans contain 50 times more carbon than the atmosphere, representing the largest pool of carbon on the planet (Raven and Falkowski, 1999). Although seawater tends to reach equilibrium with the atmosphere, this process is slow (hundreds of years), and the capacity of the ocean to absorb CO_2 decreases with pH reduction. The Intergovernmental Panel on Climate Change (IPCC) predicts an increase of global average temperature of 1-5°C and decrease of 0.1-0.4 pH in the sea surface layer by the year 2100 depending on efforts to reduce greenhouse gas emissions (IPCC, 2021). The IPCC has developed future climate scenarios based on Representative Concentration Pathways (RCP), which predict the concentration of CO_2-eq in the atmosphere depending on the amount of greenhouse gas (GHG) emissions by human society until the year 2100 (Figure 1.2). There are four main scenarios: RCP 2.6, a very stringent scenario that predicts CO_2-eq emissions to decline from the year 2020 and reach 0 by 2100, resulting in atmospheric pCO_2 of 430-480 ppm and mean temperature increase of 0.3-1.7°C; RCP 4.5 predicts CO_2-eq emissions to peak around 2040 to reach half of the emissions of 2050 by 2100 resulting in atmospheric pCO_2 to be 530-720 ppm and mean temperature increase of 1.1-2.6°C; RCP 6.0 expects GHG emissions to decline from 2080, what would make the atmospheric pCO_2 to rise to 720-1000 ppm by 2100 and temperature increase of 1.4-3.1°C; RCP 8.5, the worst-case scenario, that predicts GHG emissions to continue to rise throughout

the 21st century, resulting in atmospheric pCO_2 around 1000 ppm and temperature increase of 2.6-4.8°C. Hence, increasing pCO_2 causes three major changes in environmental conditions which are likely to influence marine plankton: temperature increase, fertilization by DIC and lower pH.

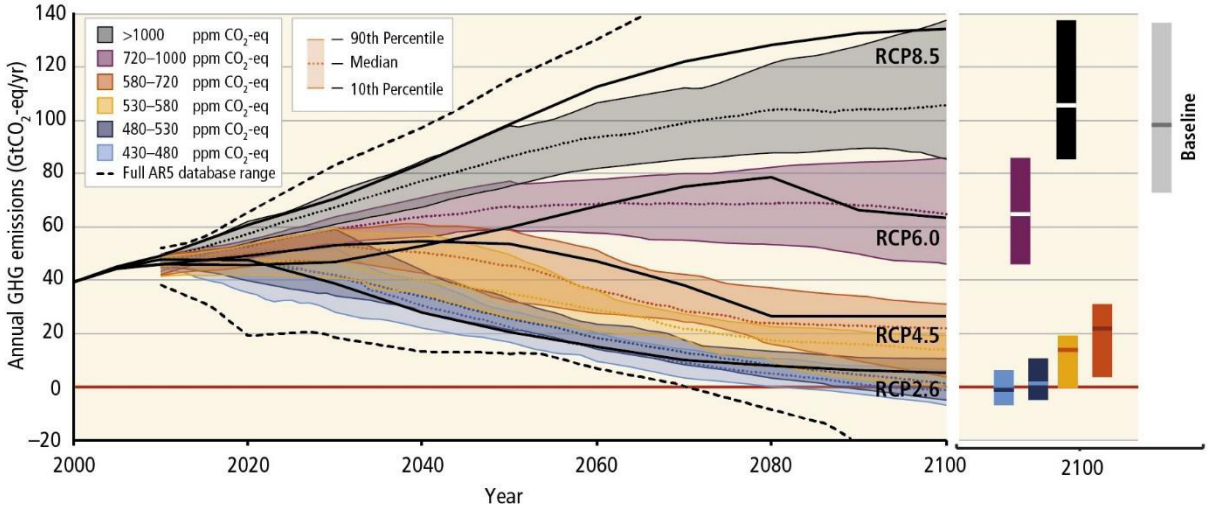

Figure 1.2: Representative Concentration Pathway scenarios developed by the IPCC. The graph displays the predicted GHG emissions in each scenario to reach the CO_2-eq concentration showed in the box on the top-left by 2100 (modified from IPCC, 2014).

Global sea surface temperature increased by 0.9°C on average since 1901 (EPA, 2020). However, the warming is not uniform across the globe. For instance, the North Sea has faced an increasing mean temperature of 0.2-0.4°C per decade (Tinker and Howes, 2020). In parallel to ocean acidification and warming, Europeans coastal waters have experienced a reduction of dissolved nutrient concentrations, especially nitrogen and phosphorus, important macronutrients for phytoplankton growth (Grizzetti et al., 2012). Human activity strongly influences nitrogen and phosphorus cycling at global scale through, for example, the use of fertilizer in agriculture. A large portion of fertilizers are washed down to rivers, loading coastal waters with dissolved inorganic nutrients, which can induce phytoplankton growth (Beman et al., 2005). In order to control nutrients loads into the sea, European governments have applied different strategies to reduce eutrophication of coastal waters by nitrogen and phosphorus. These strategies have worked, yet more effectively on nitrogen than phosphorus, causing not only a general reduction of dissolved inorganic nutrients concentrations, but also an increase on the N:P ratio, for instance in the North Sea (Grizzetti et al., 2012; Burson et al., 2016), representing an increasing potential of P-limitation for phytoplankton productivity (Peñuelas et al., 2013). Consequently, marine planktonic organisms are faced with simultaneous changes in

seawater temperature, pCO_2 and dissolved N:P ratios, which altogether may impact the whole planktonic food web and the biogeochemical cycles of nutrients.

1.3. Phytoplankton physiology response to global change

The physiological processes involved in carbon fluxes within a phytoplankton cell have direct influence on the oceanic carbon pump as a whole (Falkowski, 1994; Del Giorgio and Duarte, 2002). Annually, phytoplankton incorporate 50 Pg of carbon into their cells worldwide (Field et al., 1998), which is five times higher than the roughly 10 Pg global energy-related carbon emissions in 2021 (IEA, 2022). Three physiological processes are essential to determine the phytoplankton cell carbon fluxes: photosynthesis, dark respiration and DOC exudation. Photosynthesis and dark respiration are known to be positively correlated to temperature (Xu et al., 2011; Sett et al., 2014; Edwards et al., 2016; Gao et al., 2017), although respiration is reported to be more thermally sensitive than photosynthesis (Padfield et al., 2016). Photosynthetic rate is insensitive to temperature when light is a limiting factor, but it increases with temperature under light saturated conditions (Tilzer et al., 1986). The balance between photosynthesis and respiration can determine the carbon content of phytoplankton cells (Mantikci et al., 2017). Parallel to the effect of warming, the higher pCO_2 can stimulate phytoplankton photosynthesis (Hein and Sand-Jensen, 1997), it also represents lower seawater pH. This influences the membrane potential, intracellular pH, activity of enzymes and energy partitioning (Riebesell, 2004; Giordano et al., 2005; Rokitta et al., 2012), counterbalancing the positive effect of DIC fertilization. Lower availability of phosphorus can also limit phytoplankton metabolic rates as it is an elemental component for the biosynthesis of different compounds in the cells, such as nucleic acids and phospholipids (Berdalet et al., 1994; Litchman et al., 2006; van Mooy et al., 2009). To some extent, phytoplankton can cope with low availability of phosphorus by inducing the expression of alkaline phosphatases and other enzymes, such as phosphodiesterases and nucleotidases, to scavenge phosphates from organic phosphorus sources, and by increasing expression of high-affinity transporters to increase P uptake (Dyhrman et al., 2012; Yamaguchi et al, 2014; Rokitta et al., 2016; Alipanah et al., 2018). Another strategy applied by phytoplankton to cope with higher dissolved N:P ratios is DOC exudation (Li and Sun, 2016). As an attempt to balance biomass stoichiometry, the phytoplankton cell exudates excessive organic carbon products from photosynthesis (Thornton, 2014). DOC exudation has also been found to be stimulated by warming and higher pCO_2

(Zlotnik and Dubinsky, 1989; Baines and Pace, 1991; Riebesell et al., 2007; Wetz and Wheeler, 2007; Engel et al., 2011; Torstensson et al., 2015). As a result, higher DOC exudation by phytoplankton fuels carbon into the microbial loop, instead of to higher trophic levels (Thornton, 2014), whilst lower carbon content cells could also limit the available energy for higher trophic levels.

Elevated rates of respiration and photosynthesis in phytoplankton (Hancke et al., 2008; Padfield et al., 2016), are coupled with increases in the electron transport rates in mitochondria and choloroplasts. This may lead to overreduction of the associated electron transport chains (ETC) in these organelles (Mittler et al., 2004; Janknegt et al., 2008). Electrons may 'leak' from an overreduced ETC and react with free O_2, which is extensively produced during photosynthesis, creating superoxide radicals ($O_2^{-\bullet}$) (Gechev et al., 2006). Superoxide is a primary reactive oxygen species (ROS) that will undergo a chain of reactions to form the highly reactive hydroxyl radical ($HO^{\bullet}$), able to oxidize lipids, proteins, and DNA, damaging several cellular apparatus (Halliwell, 1987). Oxidative damage can cause membrane lipid peroxidation and lead to lower photosynthetic capacity (Rajagopal et al., 2000; Juan et al., 2004; Carrara, et al., 2021), as well as lower growth rates, chlorophyll *a* content (Mallick et al., 2002) and, ultimately, cell death (Bidle, 2016). Phytoplankton can apply different strategies to avoid the formation of ROS in the chloroplast, such as photoprotective pigments (Kuczynska et al., 2015), as well as an alternative pathway for electrons in the mitochondrion (Prihoda et al., 2012). Additionally, microalgal cells are equipped with a set of antioxidant enzymes to combat free radicals, including Catalase (CAT) and Superoxide Dismustases (SOD) (Barros et al., 2003; Janknegt et al., 2008). Nevertheless, oxidative stress indirectly caused by global change drivers can impose additional pressure on phytoplankton. Once there is a change on the common threshold of environmental conditions, the most resistant species will be favoured at the cost of the least adapted, altering the food web structure and community diversity (Fogg, 2001). Although there are diverse studies of the individual effect of CO_2, temperature and dissolved inorganic nutrients on phytoplankton physiology, multiple driver approaches are still scarce, despite the fact that these environmental drivers are undergoing changes simultaneously. Hence, it remains broadly unknown if multiple environmental drivers have additive, synergistic or antagonistic effects on plankton dynamics, therefore, we cannot accurately predict how these communities will be influenced by global change multiple drivers. Physiological processes in phytoplankton can have consequences not only for carbon fluxes but also for species assemblages, and overall food web structure, which are especially critical aspects during blooms.

1.4. Plankton community response to global change

Some studies have revealed that timing and magnitude of phytoplankton blooms and zooplankton development shift in response to temperature changes in temperate regions, which can create a mismatch between food availability and demand by higher trophic levels (Edwards and Richardson, 2004; Sommer and Lewandowska, 2011; Hjerne et al., 2019). At the same time, phytoplankton stockings stands worldwide have shown a decline of 1% per year over the past century related to increase in sea surface temperature (Boyce et al., 2010). The analyses of the 'Helgoland roads' time series, one of the longest marine data sets available for the North Sea, clearly indicates a correlation between changing environmental drivers, such as increasing temperature, and changes in phytoplankton communities over the last decades (Wiltshire et al., 2010). The success of phytoplankton under warming will depend on the characteristics of each species, ultimately shaping phytoplankton community composition (Huertas et al., 2011). For instance, higher temperature leads to higher metabolic rates in phytoplankton and higher need for nutrient uptake, and as surface:volume ratio of smaller cells allows more efficient nutrient uptake and exchange rate with the environment, smaller cells are usually benefited under warming and lower nutrient availability (Agawin et al., 2000; Morán et al., 2010; Peter and Sommer, 2012). Smaller cells also have lower sinking rates, which could have negative implications for the biological carbon pump (Bopp et al., 2005). Other studies suggest that increased temperature causes higher DOC exudation by phytoplankton, channelling more carbon into the microbial loop (Engel et al., 2011; Guo et al., 2022). Zooplankton are also temperature sensitive, as warming is known to drive up cellular respiration rates, thus increasing energy demand and grazing pressure on phytoplankton communities (Castellani et al., 2005; Garrido et al., 2013), which leads to faster development and reproduction rates of grazers (Sommer et al., 2007). The increased grazing pressure caused by warming is expected to delay the phytoplankton bloom development in spring, revealing that not only individual responses, but also interactions between the food web compartments can be altered (Gaedke et al., 2010).

Higher aqueous CO_2 availability could benefit photosynthetic organisms and stimulate their growth (Riebesell et al., 2007; Bach et al., 2019). However, the increase in [H+] concentration lowers seawater pH and can affect phytoplankton membrane potential, intracellular pH, energy partitioning and enzymatic activity (Riebesell, 2004; Giordano et al., 2005; Rokitta et al., 2012), making the effects of ocean acidification more complex than simply DIC fertilization. The phytoplankton sensitivity to pCO_2 levels is taxon-specific and, therefore, can influence the competition between species (Gao and Campbell, 2014). Concentrations of

DIC can also modulate phytoplankton response to light irradiance, with high pCO_2 stimulating growth under low light, but inhibiting growth under high light in the diatoms *Phaeodactylum tricornutum* and *Thalassiosira pseudonana*, while other studied species seem to be unaffected (Gao et al., 2012). Even though calcification is known to be negatively impacted by ocean acidification, some strains of the coccolithophore *Emiliania huxleyi* proved to be able to calcify under higher pCO_2 than present days' (Langer et al., 2016). Indeed, an increase of coccolithophores abundance has been seen in the North Atlantic phytoplankton blooms over the last decades, despite the higher pCO_2, which can lead to changes in the oceanic carbon cycling due to the capacity of this group to utilize dissolved Ca^{2+} and CO_3^{2-} (Rivero-calle et al., 2015). Stoichiometric quality of phytoplankton can also be affected by high pCO_2, where microalgal C:P and C:N can increase when DIC availability is high, but N and P remain constant (Meunier et al., 2016). Riebesell et al. (2018) also reported changes in plankton communities, where ocean acidification triggered a bloom of the toxic microalga *Vicicitus globosus*, preventing the development of zooplankton and disrupting the energy transfer to higher trophic levels. On the other hand, micro- and mesozooplankton are largely insensitive to variations in pCO_2 (Aberle et al., 2013; McConville et al., 2013; Horn et al., 2016; Bailey et al., 2017). However, copepods can be indirectly effected by the higher phytoplankton C-to-nutrient, showing lower growth (Meunier et al., 2016), and influencing fluxes of nutrients and productivity across the food web compartments.

Although still scarce, a few studies have revealed some of the combined effects of higher pCO_2 and warming on natural planktonic communities. For instance, higher pCO_2 and temperature resulted in structural changes of species composition during a phytoplankton bloom, where coccolithophores gained in prominence at the expense of diatoms (Feng et al., 2009). Conversely, Sommer et al. (2015) found no significant effect of higher temperature and pCO_2 on taxonomic composition of a phytoplankton community without the presence of coccolithophores in spring, but rather a reduction of phytoplankton biomass under these conditions. Another study with plankton communities from the Mediterranean Sea found that warming and, to a lower degree, higher pCO_2 favoured the growth of smaller phytoplankton species (Maugendre et al., 2015). Similarly, Hyun et al. (2020) reported the same environmental drivers being more selective towards nanophytoplankton and heterotrophic dinoflagellates, suggesting that the combined effect of warming and ocean acidification can strengthen the energy transfer through the microbial loop. Trophic interactions can, indeed, become more prominent under the effects of warming and ocean acidification, where top-down effects are

stronger in shaping the plankton community than current conditions with bottom-up controls playing a larger role (Murphy et al., 2019).

Phytoplankton productivity is largely limited by the concentration of dissolved inorganic nutrients. Human activities influence and alter biogeochemical cycles through nutrient runoffs, leading to a general increase of N:P ratios in European coastal waters (Grizzetti et al., 2012). Dissolved nutrient ratios have been found to be correlated to phytoplankton community composition off the Florida west coast, where diatoms were more abundant under higher N:P while dinoflagellates were more present at lower N:P ratio (Heil et al., 2007). Environmental ratios of inorganic N:P are known to influence cellular quotas of POC, photosynthetic and growth rate in phytoplankton (Rasdi and Qin, 2014; Li and Sun, 2016), as well as DOC exudation rate (Obernosterer and Herndl, 1995). Phytoplankton acquire nutrients and energy from different sources: light, DIC, dissolved nutrients; and because these elements are mostly not coupled in ideal ratios for microalgae, their stoichiometry is widely flexible. In contrast, heterotrophs tend to have a homeostatic nutrient stoichiometry (van de Waal et al., 2010). The changes in phytoplankton cellular stoichiometry caused by imbalanced N:P ratios can negatively affect grazers, which have specific nutritional demands. For instance, the copepod *Acartia tonsa* showed lower gross growth efficiency and egg production, when feeding on high C-to-nutrient ratio phytoplankton (Bi and Sommer, 2020). On the other hand, the microzooplankton *Oxyrrhis marina* applies different physiological strategies and shows more flexibility in cell stoichiometry, when feeding on poor quality prey (Meunier et al., 2012). Additionally, the effect of warming and acidification coupled with increasing N:P ratios can all together lead to perturbations in planktonic biological processes and disturb the biogeochemical cycle of nutrients in the ocean (Le Quéré et al., 2010; Winder and Sommer, 2012). For instance, De Senerpont Domis et al., (2014) demonstrated how warming can aggravate an increase in C-to-nutrient ratio of a phytoplankton community when coupled with higher N:P ratio of dissolved inorganic nutrient. Van de Waal et al. (2010) predicted an increase in phytoplankton C-to-nutrient ratio, and especially in C:P, in response to climate change. This increase is expected due to the higher availability of DIC in the ocean, which can benefit photosynthesis, and due to lower availabilities of other dissolved inorganic nutrients. Indeed, several studies (Boersma et al., 2016; Malzahn et al., 2016; Laspoumaderes et al., 2022) show that temperature plays a major role in the metabolic demands of ectotherms, indicating that higher C-to-nutrient ratio in plankton can be favourable at higher temperature. Grazers might need more carbon under warming conditions due to the increasing energetic demand. This, in turn, can result in a

stronger grazing pressure on phytoplankton, which contain higher C-to-nutrient ratios than heterotrophic prey (Boersma et al., 2016).

Although the importance of single driver studies is undeniable for the understanding of primary plankton dynamics, this sort of approach suffers from limited realism and ecological relevance. As previously discussed, the combined effect of different environmental drivers can lead to different responses in phytoplankton physiology with potential consequences for the whole community. Despite the urgent need to understand the effect of current global change drivers, warming, higher pCO_2 and N:P ratios, there is still a wide paucity of scientific research on the simultaneous impacts of these drivers on phytoplankton processes. Therefore, literature regarding the combined effect of global change drivers on phytoplankton populations and communities remains limited. Multi-trophic experiment are especially complex and are even less represented in the current scientific literature. This represents a huge knowledge gap in realistically understanding the impacts of global change on trophic interactions, community response and carbon budgets regarding plankton food webs. Hence, in this thesis, my main purpose is to contribute to filling knowledge gaps in comprehending the processes regarding phytoplankton carbon metabolism and antioxidant response to global change drivers. Due to the high importance of phytoplankton blooms to pelagic food webs, I also investigate if changes in cell processes are coupled with changes in phytoplankton bloom structure, including biomass and community composition. Moreover, as changes in food web structure are most likely associated with difference in interactions within the plankton community, I further investigate the effect of these changes on carbon fluxes between the food web compartments. By applying a simultaneous multiple driver approach, I aim to go beyond the available literature on single stressors and assist improving our understanding of complex environmental changes of ecological processes of phytoplankton.

Aims of this thesis

The main aim of this thesis is to investigate the effect of multiple global change drivers on phytoplankton carbon metabolism and antioxidant response, as key aspects also influencing seasonal bloom dynamics, biomass, community composition and interactions within planktonic food webs. The main hypothesis of this thesis is that future scenarios will lead to alterations in phytoplankton carbon metabolism and food web structure, channelling a higher amount of primary production into the microbial loop. I applied a multiple drivers approach to simulate future environmental conditions in coastal seawaters based on scenarios developed by the Intergovernmental Panel on Climate Change (IPCC, 2021). These conditions included warmer temperature and higher pCO_2, as well as higher N:P ratio of dissolved inorganic nutrients predicted for European coastal habitats. To investigate the impact of these three drivers on phytoplankton carbon metabolism and antioxidant response, I conducted a full-factorial experiment on a single phytoplankton population. To investigate if changes in cell physiology are also parallel to changes in plankton food webs, two integrated multiple driver mesocosm experiment were conducted during a spring and fall bloom with natural plankton communities. These experiments assessed the influence of global change on the plankton community biomass and composition. Furthermore, an inverse modelling and network analysis were applied on the data collected from the fall mesocosm experiment to further investigate the changes caused by the tested environmental drivers on the carbon fluxes across the compartments within the plankton food web. The specific aims and research questions of this thesis include:

Chapter II is guided by the research question: What is the effect of global change on carbon metabolism and antioxidant response of the diatom *Phaeodactylum tricornutum*? I hypothesize that the multiple global change drivers will lead to increase of primary production, respiration and DOC exudation rate, resulting in cells with lower POC. The second hypothesis predicts that cells will invest more energy in antioxidant capacity under the future ERCP 8.5 scenario. To investigate this aspect, this phytoplankton species was exposed over generations to elevated temperature and pCO_2 based on the RCP 8.5 scenario derived from the IPCC, as well as higher N:P ratio. The full-factorial approach of this experiment revealed the isolated and combined effect of the environmental drivers on the phytoplankton physiology. To quantify carbon fluxes entering and leaving the phytoplankton cell, I measured rates of primary production, dark respiration and dissolved organic carbon production, as well as growth rate

after the acclimation period. Additionally, different biomarkers were also investigated in order to understand the effect of the global change on the phytoplankton antioxidant capacity, including carotenoids content, antioxidant enzymes activity, alternative oxidase activity and malondialdehyde content.

Chapter III is guided by the research question: What is the effect of global change on plankton food web biomass and community composition during a spring bloom? I hypothesize that under the conditions of future scenarios plankton communities will be dominated by smaller species included in the microbial loop, as well as diminished populations of mezoooplankton. This chapter shows and discusses the results obtained from a mesocosm experiment conducted during a phytoplankton spring bloom event containing a natural plankton community with species up to 1000 µm in size. The community was exposed to an integrated multiple driver approach, where two different scenarios with higher temperature and pCO_2, RCP 6.0 and 8.5, also including higher N:P ratios, were tested against Ambient conditions. I quantified biomass and species composition of phytoplankton, microzooplankton, bacterioplankton and mesozooplankton to assess the effect of these three scenarios on the different compartments of the food web. Seston stoichiometry was also measured to investigate changes in the elemental quality of the phytoplankton community.

Chapter IV is guided by the research question: What is the effect of global change on plankton food web biomass and community composition during a fall bloom? Similarly to the previous chapter, I hypothesize that the microbial loop will play a larger role in the plankton community under the conditions of future scenarios, with negative impact to mesozooplankton. Applying the same strategy as in Chapter III, the community was exposed to an integrated multiple driver approach, where two different future scenarios were tested against Ambient conditions. Biomass and species composition of phytoplankton, microzooplankton, bacterioplankton and mesozooplankton were also quantified to investigate the impact of global change on the planktonic food web. Additionally, seston stoichiometry was also measured to investigate changes in the elemental quality of the phytoplankton community.

Chapter V is guided by the research question: What is the effect of global change on interactions within a plankton food web during a fall bloom? Here, I hypothesize that under future scenario conditions carbon flows in the plankton food web will be redirected to the microbial loop, demising energy fluxes to higher trophic levels. This chapter reassesses the results of the fall mesocosm experiment by applying an inverse analysis to determine interactions across the different compartments of the plankton food web that were not quantified

in Chapter IV. The model aims to reveal changes in the functioning of the plankton assemblages under different future scenarios, due to the effect of warming, ocean acidification and higher N:P ratios. From the ecological network, various indices were derived to assist understanding carbon fluxes within the food web, such as sum of energy flows, relative internal ascendancy, flow diversity, finn cycling index, degree of herbivory, detrivory:herbivory ratio, mean trophic level and efficiency of energy transfer. The composition of zooplankton diet was also estimated.

Publications and manuscripts

This thesis is based on the following papers:

Paper I (Chapter 2)	**Moreno, H. D.**, Rokitta, S., Tremblay, N., Boersma, M., Groß, E., Klip, H., Wiltshire, K. H., Meunier, C. L. Global change induces oxidative stress and alters the carbon metabolism of the phytoplankton *Phaeodactylum tricornutum*. *Under review in Global Change Biology.*
Paper II (Chapter 3)	**Moreno, H. D.**, Köring, M., Wiltshire, K. H., Boersma, M., Meunier, C. L. Resilience of planktonic communities to warming, ocean acidification and higher dissolved N:P ratios during a spring bloom event. Manuscript.
Paper III (Chapter 4)	**Moreno, H. D.**, Köring, M., Di Pane, J., Tremblay, N., Wiltshire, K. H., Boersma, M., Meunier, C. L. An integrated multiple driver mesocosm experiment reveals the effect of global change on planktonic food web structure. Communications Biology, 5 (1), 1-9.
Paper IV (Chapter 5)	Di Pane, J., Bourdaud, P., Horn, S., **Moreno, H. D.**, Meunier, C. L. Global change alters plankton food webs by promoting the microbial loop: An inverse modelling and network analysis approach on a mesocosm experiment. *Under review in Limnology and Oceanography.*

My contribution to the papers:

Paper I: I developed the experimental design and scientific concept together with CLM, SR, NT, MB and EG. NT, HK, EG and I conducted the experiment. I analysed the samples, evaluated the data and wrote the manuscript. All co-authors commented and improved the manuscript.

Paper II: I developed the experimental design and scientific concept together with CLM, MB, and MK. CLM, MK and I conducted the experiment. I analysed the samples, evaluated the data and wrote the manuscript. All co-authors commented and improved the manuscript.

Paper III: I developed the experimental design and scientific concept together with CLM, MB, and MK. CLM, MK, NT and I conducted the experiment. MK and I analysed the samples. JDP and I evaluated the data. I wrote the manuscript and all co-authors commented and improved the manuscript.

Paper IV: The experimental design and scientific concept were developed by JDP, CLM, SH, PB and me. JDP and SH analysed and evaluated the data. JDP wrote the manuscript. Together with the other co-authors, I commented and improved the manuscript.

Chapter 2

Global change induces oxidative stress and alters the carbon metabolism of the phytoplankton *Phaeodactylum tricornutum*

Hugo Duarte Moreno[1a], Sebastian Rokitta[2a], Nelly Tremblay[1,3], Maarten Boersma[1,4], Elisabeth Groß[1], Helena Klip[1], Karen H. Wiltshire[5], Cédric L. Meunier[1]

[a]These authors contributed equally to this study

[1]Alfred-Wegener-Institut, Helmholtz-Zentrum für Polar- und Meeresforschung, Biologische Anstalt Helgoland, Germany

[2]Alfred-Wegener-Institut, Helmholtz-Zentrum für Polar- und Meeresforschung, Bremerhaven, Germany

[3]Pêches et Océans Canada, Mont-Joli, QC, Canada

[4]University of Bremen, Bremen, Germany

[5]Alfred-Wegener-Institut, Helmholtz-Zentrum für Polar- und Meeresforschung, Wattenmeerstation, List auf Sylt, Germany

Under review in Global Change Biology

2.1. Abstract

Phytoplankton are responsible for about 90% of the oceanic primary production, largely supporting marine food webs, and actively contributing to the biogeochemical cycling of carbon. Yet, increasing temperature and pCO_2, along with higher dissolved nitrogen:phosphorus ratios in coastal waters have consequences for phytoplankton physiology. Here, we conducted a full-factorial experiment to identify the individual and combined effects of temperature, pCO_2, and N:P ratio on the antioxidant capacity and carbon metabolism of the diatom *Phaeodactylum tricornutum*. Our results demonstrate that, among these three drivers, temperature is the most influential factor on the physiology of this species, with warming causing oxidative stress and lower activity of antioxidant enzymes. Furthermore, photosynthetic rate was higher under warmer conditions and higher pCO_2, and, together with lower dark respiration rate and higher dissolved organic carbon exudation, generated cells with lower carbon content. If we expect similar responses from other phytoplankton species, an enhanced oceanic CO_2 uptake and an overall stimulated microbial loop benefiting from higher dissolved organic carbon exudation might be the longer-term consequences of rising temperatures, elevated pCO_2 as well as shifted dissolved N:P ratios.

2.2. Introduction

Phytoplankton species are responsible for about 90% of the total oceanic primary production (Duarte & Cebrián, 1996), making them major contributors to the biogeochemical cycling of carbon (Buesseler, 1998; Bowler et al., 2010). Two distinct marine carbon pools derive directly from the biological activity of photosynthetic organisms: particulate organic carbon (POC), bound in cell biomass, and dissolved organic carbon (DOC), released by living phytoplankton or decaying cells, through sloppy feeding of grazers, consumption and excretion by higher trophic levels or viral lysis (Jiao et al., 2010). Some phytoplankton species are also able to take up DOC from seawater (Villanova et al., 2017). Once fixed as phytoplankton biomass, carbon can be transferred via trophic processes through the food web or sink to the deep sea (Honjo and Manganini, 1993). These fluxes are essential components of biogeochemical cycling and the 'marine organic carbon pump', and are influenced by phytoplankton cellular physiological processes.

After inorganic carbon is assimilated into carbohydrates through photosynthesis, it can take different pathways in a phytoplankton cell: the carbon can be used for storage and growth; it can be remineralized for mitochondrial energy generation and fuel cellular processes; or it can be exuded in the form of organic molecules (Marra and Barber, 2004; Tortell et al., 2008; Thornton, 2014). The relative proportions of these intracellular carbon fluxes are directly influenced by environmental conditions, such as temperature, partial pressure of carbon dioxide (pCO_2), and concentration of dissolved nutrients (Neori and Holm-Hansen, 1982; Alipanah et al., 2015; Padfield et al., 2016) all of which have experienced large perturbations due to human activities. Indeed, anthropogenic CO_2 emissions and the resulting increase in atmospheric pCO_2 contribute to the greenhouse effect, i.e. global warming. In addition, part of this CO_2 dissolves into the ocean, and lowers seawater pH, leading to ocean acidification (Doney et al., 2009; Anderson et al., 2016). Human activities have also altered dissolved nutrient concentrations through nutrient runoffs, leading to a general increase of dissolved nitrogen:phosphorus (N:P) ratios, especially in European coastal waters (Grizzetti et al., 2012), thus increasing the potential of P limitation for phytoplankton.

Aqueous CO_2 concentrations increase could have positive effects on primary producers that profit from the higher availability of CO_2 (Bach et al., 2019). However, other studies have shown that responses of phytoplankton to increasing oceanic pCO_2 may be complex (Beardall and Raven, 2004; Taucher et al., 2015; Alvarez-Fernandez, et al. 2018), and the consequences

for photosynthesis and wider phytoplankton ecophysiology are still to be clarified. Studies have found different effects of warming and ocean acidification on various physiological processes related to carbon metabolism in phytoplankton including increase in photosynthesis and respiration rates (Wu et al., 2010; Goldman et al., 2017), higher DOC production (Engel et al., 2010), and down-regulation of carbon-concentrating mechanisms (Rokitta et al. 2022; Thangaraj and Sun, 2021). Environmental ratios of dissolved inorganic N:P influence cellular quotas of particulate organic carbon (POC), photosynthetic and growth rate in phytoplankton (Rasdi and Qin, 2014; Li and Sun, 2016), as well as DOC exudation (Obernosterer and Herndl, 1995). The uncertainties about the interactions of environmental drivers and the co-dependency of cellular carbon pathways on different environmental drivers make the responses of phytoplankton cells to future environmental change even more difficult to predict (Gao and Campbell, 2014; Wolf et al., 2019).

Environmental conditions modulate the rates of respiration and photosynthesis in phytoplankton (Hancke et al., 2008; Padfield et al., 2016), and the associated electron transport rates which determine the degree of reduction of the electron transport chains (ETCs) in chloroplasts and mitochondria (Mittler et al., 2004; Janknegt et al., 2008). When ETCs are overreduced, electrons can 'leak' and react with free O_2, extensively generated as a photosynthesis by-product, creating superoxide radicals ($O_2^{-\bullet}$) (Gechev et al., 2006). This primary reactive oxygen species (ROS) is further converted into other oxidative compounds, such as hydrogen peroxide (H_2O_2) and the highly reactive hydroxyl radical ($HO^{\bullet}$), which are able to cause oxidative damage to lipids, proteins, and DNA (Halliwell, 1987). Oxidative damage can lead to loss of photosynthetic capacity, due to membrane lipid peroxidation (Rajagopal et al., 2000; Juan et al., 2004), to lower growth rates as well as decreased chlorophyll *a* content (Mallick et al., 2002). Phytoplankton can apply different strategies to prevent the formation of ROS and combat such compounds when their formation cannot be avoided. In the chloroplast, excess light absorbed by the antenna complex can be quenched as thermal energy by activating the xanthophyll cycle (Janknegt et al., 2008), while the proportions of photoprotective versus light-harvesting pigments can be rearranged to better tune energy flow to the photosystems (Dubinsky and Stambler, 2009). Activation of the Alternative Oxidase (AOX) pathway within the mitochondria can relieve electron flow through the ETC in order to prevent leakages, yet at the cost of lower energy yield by dark respiration (Day and Wiskich, 1995; Allen et al., 2008). Antioxidant enzymes also play an important role in scavenging ROS. Superoxide dismutases (SODs) are potent antioxidants widely utilized to catalyse the dismutation of $O_2^{-\bullet}$ into O_2 and H_2O_2 (Janknegt et al., 2008). Once formed, H_2O_2 can be further

decomposed into harmless O_2 and H_2O by other enzymes, such as Catalase and Glutathione Peroxidase (Barros et al., 2003; Vega-López et al., 2013). While several studies have reported modulation of antioxidant response and oxidative stress by temperature, pCO_2, and dissolved nutrient concentrations in different classes of photosynthetic organisms (Lesser, 1997; Choo et al., 2004; Yakovleva et al., 2009; Gillespie et al., 2011; Brutemark et al., 2015; Kvernvik et al., 2020), the potential interactions between these environmental factors affecting the antioxidant capacity of marine phytoplankton remain poorly understood.

In this study, we tested the influence of temperature, pCO_2, and dissolved N:P ratios on the cellular carbon fluxes and antioxidant response of the diatom *Phaeodactylum tricornutum*. Overall, our work assesses how multiple global change drivers may act separately and in concert to influence physiological processes related to carbon metabolism, mainly primary production, respiration and DOC production. These processes involve electron transfer chains in chloroplasts and mitochondria and are directly related to the formation of ROS in phytoplankton cell. Therefore, we also assessed the antioxidant response and oxidative stress in parallel to potential changes in carbon metabolism.

2.3. Materials and Methods

A full factorial design was applied to test the influence of two CO_2 partial pressures (400 and 1000 µatm), temperatures (18 and 21°C), and N:P ratios of dissolved inorganic nutrients (16 and 25 molar), forming eight independent treatments in quadruplicates. The pCO_2 levels were chosen to represent the contemporary and the RCP 8.5 scenario atmospheric pCO_2 based on predictions of CO_2 emissions by the Intergovernmental Panel on Climate Change for the end of the 21st century (IPCC, 2021). Eighteen °C is the mean temperature value for summer (July-August) at the Helgoland roads time-series station (North Sea) and 21°C represents the +3.0°C increase expected according to the RCP 8.5 scenario. We included different nutrient regimes to this experiment as well, where an N:P of 16 represents the balanced Redfield ratio, while an N:P of 25, achieved by lowering the concentrations of dissolved P, resembles the increasing P-limitation predicted for the future (Grizzetti et al., 2012). This diatom has a worldwide distribution and is common in coastal waters (Hendey, 1964). Despite the uncommon capacity of this diatom to grow in the absence of silica (Hendey, 1954), the sequencing of its genome, as well as ecophysiological studies identified this species as a model organism representative of the Bacillariophyceae group (Oudot-Le Secq et al., 2007; Bowler et al., 2008; Martin-

Jézéquel and Tesson, 2013). Carbon fluxes were measured through the rates of primary production, dark respiration, DOC production and POC contents, representing organic carbon production, organic carbon consumption, organic carbon exudation and organic carbon in the cells biomass, respectively. The antioxidant response was assessed based on different biomarkers, including the contents of protective carotenoids (β-carotene, diadinoxanthin and violaxanthin), the prevalence of the alternative oxidase pathway (AOX), antioxidant enzyme activities (Catalase, Manganese Superoxide Dismutase, Glutathione Peroxidase, Glutathione S-transferase), and by determination of Malondialdehyde (MDA) formation as proxy for oxidative damage to membrane lipids.

Culture conditions

Cultures of *Phaeodactylum tricornutum* (Strain CCAP 1052/1A) were grown at 18 or 21°C in a temperature-controlled room in 2 L glass bottles (Duran, Mainz, Germany) closed with airtight lids. The cultures were grown in F/20 medium (Guillard, 1975) prepared with artificial seawater according to the protocol of Harrison et al. (1980) modified by Berges et al. (2001), and sterile filtered (0.2 µm) to avoid contamination. Total alkalinity (TA) was adjusted by the addition of NaOH until it reached natural seawater levels (~2350 µmol kg SW^{-1}). To yield N:P ratios of 16 and 25, nitrate was added to reach a concentration of 88 µmol NO_3 L^{-1}, and phosphate concentrations in the growth medium were set to 5.5 µmol PO_4 L^{-1} and 3.5 µmol PO_4 L^{-1}, respectively (Supplementary Figure 2.1). The pCO_2 of the medium was adjusted by bubbling it for 24 hours with air mixtures containing either 400 or 1000 µatm CO_2, which were obtained from a CO_2-mixing system (GDZ 401, Denkendorf, Germany) (Schoo et al., 2013). Cultures were irradiated with 100 µmol photons m^{-2} s^{-1} by LED light bars (Mitras 2 Daylight, GHL, Germany) under a 14:10 hours light:dark cycle. The culture bottles were continuously rotated on a roller table to prevent cell sedimentation. The diatom cultures were pre-acclimated to every treatment for at least 20 generations. The experiment was subdivided into two periods. In the first period of four days, we measured dissolved organic carbon production and particulate organic carbon, whereas the second period was focused on the measurements of antioxidant response, pigment and rates of photosynthesis and respiration. Samples for production rates of dissolved organic carbon (DOC) were collected daily over a four-day period during the first incubation phase, following the acclimation period. Samples for particulate organic carbon (POC) were collected on the last day of the first incubation phase. Initial cell concentration was always ~400 cells mL^{-1}. After the first incubation phase of four days, cells were diluted back to ~400 cells mL^{-1} with described media and grown for a second incubation

phase of four days in order to acquire more biomass for further measurements. On the last day of the second incubation phase, cells were harvested for assessments of dark respiration, primary production, AOX activity, antioxidant enzyme assays and MDA concentration, as well as for the analyses of pigments as indicators of antioxidant capacity and photoprotective capacities. Cultures were kept dilute to avoid self-shading, fluctuations in pH during the experiment, and drifts in carbonate chemistry. Cells were harvested during exponential growth phase before ~10% of the dissolved inorganic carbon (DIC) in the culture was consumed. This limit was ascertained through modelling the carbonate system with the help of the CO_2SYS Excel Macro (Pierrot et al., 2006).

Seawater carbonate system and dissolved macronutrients

The seawater carbonate system was calculated based on determined DIC, pH, temperature, and salinity using the CO_2SYS Excel Macro (Pierrot et al., 2006) with acidity constants defined by Mehrbach et al. (1973) refitted by Dickson and Millero (1987). Salinity was measured with a salinometer (WTW Cond 3110 SET 1, Weilheim, Germany) directly from total alkalinity samples. An aliquot of each culture was taken daily to measure pH with a WTW Tetracon® 925 probe. Samples for dissolved inorganic nutrients, salinity, TA and DIC were taken from the medium prior to cell inoculation, and on the last day of each incubation phase. Total alkalinity samples were by filling an airtight 100 mL transparent glass bottle, avoiding air bubbles, with filtered culture medium (GF/F filter 0.45 µm, Whatman, Buckinghamshire, UK). The samples were stored at 4°C before analysis through linear Gran-titration (Dickson, 1981) using a TitroLine alpha plus (Schott, Mainz, Germany). Samples for DIC samples were filtered through 0.45 µm polytetrafluoroethylene (PTFE) filters and kept in 5 mL brown glass bottles, free of air bubbles, at 4°C prior to analysis with the colorimetric method of Stoll et al. (2001). Dissolved inorganic nutrients (DIP = PO_4^{3-} and DIN = NO_x) samples were kept frozen at -20°C until being measured with a continuous-flow analyzer (QuAAtro39, Seal Analytical, Norderstedt, Germany) according to Strickland and Parsons (1972). Results of dissolved inorganic nutrient analyses and seawater carbonate chemistry are available as Supplementary Figure 2.1 and Supplementary Table 2.1, respectively. There was not enough biomass growth during the experiment to exhaust the dissolved nutrient supply. Thus, the cells did not face nutrient limitation during the experiment.

Photosynthesis and dark respiration rate

Photosynthesis and dark respiration rates were measured as net O_2 evolution rates. We used a high-resolution O_2k-FluoRespirometer (Oroboros Instruments, Innsbruck, Austria)

calibrated with each treatment medium. The 2 mL incubation chambers of the respirometer are airtight, temperature controlled and equipped with magnet stirrers to keep the cells in suspension. In order to acquire enough cells to reach rates within the equipment resolution, cells were concentrated by gently filtering 100-200 mL of each culture on a polycarbonate filter (0.45 µm pore size) with suction pressure lower than 200 mbar relative to the atmosphere. The volume used depended on cell concentration in the culture. Phytoplankton cells were resuspended in 5 mL of 30 µmol L^{-1} 4-(2-hydroxyethyl)-1-piperazineethanesulfonic acid (HEPES) buffered culture medium to maintain constant pH during the measurements. This aliquot was dark acclimated in the instrument for 10 minutes at the respective experimental temperatures before applying a rapid light curve (RLC), where the aliquot was exposed for 10 minutes to irradiance of 50, 100, 150 and 300 µmol photons m^{-2} s^{-1} provided by LEDs. A last light intensity step of 600 µmol photons m^{-2} s^{-1}, was provided by a Zeiss / Schott CL 1500 ECO lamp (Colombes, France). Each light step was followed by 10 minutes of darkness to account for variation in dark respiration due to higher photosynthetic rate. Dark respiration was calculated as the mean of all respiration measurements taken during every dark period. To quantify carbon fluxes, O_2 fluxes were converted into CO_2 fluxes using a photosynthetic quotient of 1.56 and a respiratory quotient of 0.6 determined for *P. tricornutum* (Wagner et al., 2005). We used least-squares fitting on the obtained data to derive physiological photosynthesis parameters, such as compensation point, as well as photochemical efficiency (α), light acclimation index (I_k) and maximum net photosynthesis rate (V_{max}), following equations from Rokitta and Rost (2012). The compensation point obtained in the procedure represents the irradiance where respiration rate is equal to photosynthesis rate, α is the initial slope of the RLC and indicates efficiency of light energy conversion into chemical energy via photosynthesis, I_k represents the irradiance where photosynthesis transitions into saturation and V_{max} shows the highest electron transport rate attained during the RLC.

Determination of growth rates, elemental quotas and DOC production

Cell concentrations were measured by flow cytometry (BD Accuri C6 Plus, BD Biosciences) with 100 µL samples processed at a flow rate of 35 µL min^{-1}. Specific growth rate (μ) was calculated as:

$$\mu = (ln_{C1} - ln_{C0}) * \Delta t^{-1}$$

where c_0 and c_1 are the initial and final cell concentrations and Δt is the time interval in days. The growth rate was calculated based on cell concentrations on the initial and final day

of each incubation phase and computed as mean of both incubation phases, generating one growth rate value per replicate.

Samples for particulate organic carbon were taken by filtering 200 mL of each phytoplankton culture on precombusted (12h, 500°C) GF/F filters (0.45 µm, Whatman, Buckinghamshire, UK), with suction pressure of 200 mbar relative to the atmosphere. The filters were then soaked with 200 µL of 0.2 mol L^{-1} HCl to remove any calcite contaminants, and dried in an oven at 60°C. Carbon content on the filters was determined with an elemental analyzer (Vario Micro Cube, Elementar, Hanau, Germany).

To quantify dissolved organic carbon, samples of 20 mL were collected from the artificial seawater batch produced to prepare the medium prior to cells' incubation (initial), and from every culture bottle on the last, fourth, day of the first incubation phase. Samples were collected with a sterile plastic syringe and filtered through a 0.45 µm PTFE filter. The first 2 mL of the sample was used to rinse the filter and were discarded. The samples were collected in technical duplicates and stored in HCl washed and precombusted glass vials. Samples were acidified with HCl and kept at -20°C until analysis. Dissolved organic carbon was determined by high temperature catalytic oxidation and subsequent nondispersive infrared spectroscopy and chemiluminescence detection, automatically conducted in a TOC-$L_{CPH/CPN}$ analyzer (Shimadzu, Kyoto, Japan). Net dissolved organic carbon production per cell (D) was calculated based on the following formula derived from the integral of total DOC production in the culture and cell growth:

$$D = \frac{DOC_p}{C_0} \cdot \frac{\mu}{\left(\frac{C_1}{C_0} - 1\right)}$$

where DOC_p is the total DOC production in the culture over the whole incubation period (pmol mL^{-1}), C_0 and C_1 are the initial and final phytoplankton cell concentrations (cells mL^{-1}), and μ is the specific growth rate (d^{-1}; see Supplementary Information 2.1 for the integral resolution).

We chose not to work with axenic cultures to avoid potential effects of the absence of microbiome in the culture, which interacts with phytoplankton in natural conditions (Stock et al., 2019), as well as negative impacts of antibiotics on phytoplankton physiology (Siedlewicz et al., 2020). Therefore, to account for bacterial DOC consumption, 200 mL of each culture was filtered through a polycarbonate filter (3 µm pore size, Millipore, USA) to remove phytoplankton cells, and subsequently filtered through a polycarbonate filter (0.45 µm pore

size). The bacterial cells captured on the 0.45 µm filter were resuspended and incubated in an O_2k-FluoRespirometer to measure their respiration rate as for the phytoplankton cells (see above). This procedure ensured enough bacterial cell biomass for accurate measurements. The aliquots of each incubation for respirometry were also subsequently preserved to determine bacterial cell concentrations. Bacterial respiration rate (pmol O_2 cell^{-1} d^{-1}) was as well converted to C consumption using an average respiratory quotient of 1.55 (Allesson et al., 2016), and the bacterial carbon consumption was added to the phytoplankton DOC production, since DOC is the carbon source for bacteria in the culture. Bacterial DOC consumption (DOC_c) was calculated using the formula:

$$DOC_c = \frac{B_{0\,.\,\left(B_1/B_0 - 1\right)\,.\,c}}{\mu}$$

where c is the bacterial respiration rate (pmol C cell^{-1} d^{-1}), B_0 and B_1 are the bacterial cell initial and final concentrations in the cultures (cells mL^{-1}), and µ is the specific bacterial growth rate (d^{-1}) based on the initial and final bacterial cell concentration in the culture and calculated as for phytoplankton.

Bacterial cell concentration was also determined from each phytoplankton aliquot in incubated in the respirometer for photosynthesis and dark respiration rates to ensure that bacterial biomass accounted for less than 10% of the total carbon biomass. These samples were fixed with glutaraldehyde (0.1% final concentration) and frozen at -80°C until analysis. The samples were thawed in a water bath (20°C) and stained with SYBR Green (Invitrogen) as described in Marie et al. (2005). Bacterial cells were quantified by processing the samples through flow cytometry (BD AccuriTM C6 Plus, BD Biosciences) at a flow rate of 12 µL min^{-1} for 1-2 minutes. Samples were diluted with sterile filtered seawater (0.2 µm) when flow cytometry events were higher than 400 events s^{-1}. Bacteria cell counts were converted into carbon using the 20 fg C cell^{-1} factor defined by Lee & Fuhrman (1987). Nevertheless, bacteria concentration was low, representing on average 11.6% of total carbon biomass in the culture on the harvesting day and less than 5% during measurements with the respirometer.

Enzyme assays and pigment detection

A concentrated phytoplankton aliquot (obtained as described in 'Photosynthesis and dark respiration rate') was incubated in the two chambers of the O_2k-FluoRespirometer (Oroboros Instruments, Innsbruck, Austria). Alternative Oxidase activity (AOX) was determined using Substrate-uncoupler-inhibitor titration (SUIT, 022

www.bioblast.at/index.php/SUIT-022_O2_ce_D051 and 023 www.bioblast.at/index.php/SUIT-023_O2_ce_D053) protocols specifically developed to distinguish between oxygen consumption derived from mitochondrial AOX and from respiratory complex IV (CIV) As a first step, routine dark respiration was measured for both chambers. Then, one of the chambers was used to quantify AOX dependent respiration after inhibition of CIV with 1 mM potassium cyanide (KCN), while the other was used for CIV dependent respiration after inhibition of AOX with 1 mM salicylhydroxamic acid (SHAM). We expressed AOX as the ratio between SHAM inhibited respiration rate and routine respiration (AOX:Resp). The AOX:Resp ratio indicates the proportion of electrons that ends up in the alternative oxidase pathway compared to all electrons used during the dark respiration process.

Samples for the assessments of antioxidant enzyme activities and MDA as an oxidative stress marker were collected by filtering 200-250 mL of the culture through a polycarbonate membrane filter (3 µm pore size, Millipore, USA) to concentrate cells. The cells caught on the filter were resuspended in culture medium, transferred into a 1.5 mL assay reaction tube (Eppendorf, Hamburg, Germany) and centrifuged at 27,000 RCF for 3 minutes at treatment temperature to form a cell pellet. Then, the supernatant was removed and the phytoplankton cells were immediately frozen in liquid N_2 and kept at -80°C until analysis. For determination of malondialdehyde (MDA), the samples were thawed and homogenized in 250 µL of 1.1% H_3PO_4 (Mixer Mill MM301, Retsch, Haan, Germany) for 1 minute with frequency of 30 rotations s^{-1}. Measurements of MDA content were done in triplicate according to Uchiyama & Mihara (1978).

To quantify the antioxidant enzyme activities and soluble proteins, samples were homogenized with 125 µL of phosphate buffer solution [50 mmol L^{-1} potassium phosphate dibasic and monobasic mixture (K_2HPO_4/KH_2PO_4), 50 mmol L^{-1} Ethylenediaminetetraacetic acid (EDTA), 1 mmol L^{-1} Phenylmethylsulfonyl fluoride (PMSF; $C_7H_7FO_2S$), pH 7.5] and centrifuged at 27,000 RCF for 5 minutes at 4°C. The same supernatant extract was measured in technical triplicates for Catalase (CAT) following Aebi (1984), Manganese Superoxide Dismutase (SOD-Mn) following Suzuki (2000), Glutathione Peroxidase (GPx) following Ahmad and Pardini (1988), and Glutathione S-transferase (GST) following the protocol from Habig and Jakoby (1981). Soluble protein contents were determined following Bradford (1976) to report enzymatic activity in activity unit (U) mg $protein^{-1}$. All assays were conducted at room temperature (20°C) and measured with a spectrophotometer (Thermo Scientific Multiskan® Spectrum, Bremen, Germany). Activities of antioxidant enzymes and MDA contents are shown

in a star plot and were analyzed using the Integrated Biomarker Response (IBR) method suggested by Beliaeff and Burgeot (2002), which merge the results into one index. The IBR method allows clear visualization (using radar plots and one index) of biological effects of treatments and simplifies the interpretation as all data is normalized to the same scale with arbitrary units. The IBR only simplifies the data analysis and indicates changes in antioxidant response. A high IBR value can uncover negative or positive changes, i.e great antioxidant defense or oxidative stress, which become clear by looking at the corresponding radar plots. Individual results of antioxidant enzymatic activity and MDA concentration are shown in Supplementary Figure 2.2 and 2.3. Details about the calculation of the IBR are available in Beliaeff and Burgeot (2002).

Samples for chlorophyll *a* (Chl-a), and photosynthetic pigments were taken by filtering 250 mL of the culture on a polycarbonate filter (0.45 µm pore size, Millipore, USA) protected from direct irradiance. The filter was conserved in 2 mL of 100% acetone at -80°C until analysis. Pigments were extracted and subsequently analysed by high performance liquid chromatography (HPLC, Waters Alliance 2695, Agilent, California, USA), following methods described in Wiltshire et al. (2000). Pigments quantified in the analysis were chlorophyll *a*, fucoxanthin, diadinoxanthin, β-carotene and violaxanthin. Pigments were divided into 'photosynthetic pigments' (PSP, including chlorophyll *a* and fucoxanthin), and 'photoprotective carotenoids' (PPC, including diadinoxanthin, violaxanthin and β-carotene). Individual results of carotenoid contents are shown in Supplementary Figure 2.4.

Statistical analyses

Statistical analyses were performed using R 3.4.3 software (R Core Team, 2022). For all analyses, the threshold of significance was set to 0.05. Effects of different temperatures, pCO_2 and N:P were assessed through a three-way Analysis of Variance (3-way ANOVA) followed by a pairwise Tukey PostHoc test. Data was log-transformed when normality and homoscedasticity of residuals were not met. All results of the 3-way ANOVAs are presented in Table 2.1. Principal Component Analysis (PCA) was applied to assess multivariate response to the experimental treatments on the dependent variables using Temperature, pCO_2 and N:P ratio as supplementary variables.

Table 2.1: Statistical results of 3-way ANOVA models indicating treatment effects. * highlights significant p-values (< 0.05). The factors represent the enrivonmental drivers tested in the experiments alone or in combination. MS is the value for mean square and F represents the F ratio extracted from the model results.

Variable	Factor 1	Factor 2	Factor 3	MS	F	p-value	Effect indicated by Tukey's posthoc test
Primary production	Temperature	-	-	0.819	9.918	**0.004***	Higher at 21°C
	-	pCO_2	-	0.401	4.854	**0.037***	Higher at 1000 pCO_2
	-	-	N:P	0.194	2.348	0.138	-
	Temperature	pCO_2	-	0.152	1.843	0.187	-
	Temperature	-	N:P	0.301	3.644	0.068	-
	-	pCO_2	N:P	0.052	0.632	0.434	-
	Temperature	pCO_2	N:P	0.036	0.435	0.516	-
Dark Respiration rate	Temperature	-	-	0.061	30.34	**<0.001***	Lower at 21°C
	-	pCO_2	-	0.005	2.406	0.134	-
	-	-	N:P	0.005	2.297	0.143	-
	Temperature	pCO_2	-	0.065	30.86	**<0.001***	Lower dark respiration rate at 21°C when pCO_2 is 1000
	Temperature	-	N:P	0.005	2.688	0.114	-
	-	pCO_2	N:P	0.006	3.158	0.088	-
	Temperature	pCO_2	N:P	0.001	0.659	0.425	-
DOC Production	Temperature	-	-	7.276	400.2	**<0.001***	DOC exudation at 21°C and DOC uptake at 18°C
	-	pCO_2	-	0.010	0.523	0.476	-
	-	-	N:P	0.128	7.023	**0.014***	Higher DOC production when N:P is 25
	Temperature	pCO_2	-	0.173	9.542	**0.005***	Higher DOC production at 21°C when pCO_2 is 1000
	Temperature	-	N:P	0.001	0.054	0.817	-
	-	pCO_2	N:P	0.029	1.602	0.218	-
	Temperature	pCO_2	N:P	0.020	1.127	0.299	-
Particulate organic carbon	Temperature	-	-	1.096	272.8	**<0.001***	Lower at 21°C
	-	pCO_2	-	0.023	5.728	**0.025***	Lower at 1000 pCO_2
	-	-	N:P	0.001	0.378	0.545	-
	Temperature	pCO_2	-	0.015	3.685	0.067	-

Variable	Factor 1	Factor 2	Factor 3	MS	F	p-value	Effect indicated by Tukey's posthoc test
Growth rate	Temperature	-	N:P	0.027	6.730	**0.016***	Lower carbon content at 21°C when N:P is 25
	-	pCO_2	N:P	0.013	3.282	0.083	-
	Temperature	pCO_2	N:P	0.001	0.135	0.717	-
	Temperature	-	-	0.035	38.71	**<0.001***	Higher at 21°C
	-	pCO_2	-	0.001	0.266	0.610	-
	-	-	N:P	0.002	1.946	0.176	-
	Temperature	pCO_2	-	0.014	15.39	**<0.001***	No significant increase at 21°C when pCO_2 is 1000
	Temperature	-	N:P	0.001	0.857	0.364	-
	-	pCO_2	N:P	0.008	8.427	**0.008***	Higher growth rate at 1000 pCO_2 when N:P is 25
	Temperature	pCO_2	N:P	0.001	0.204	0.656	-
Photochemical efficiency	Temperature	-	-	0.002	0.124	0.728	-
	-	pCO_2	-	0.048	3.370	0.079	-
	-	-	N:P	0.001	0.083	0.775	-
	Temperature	pCO_2	-	0.001	0.090	0.767	-
	Temperature	-	N:P	0.033	2.309	0.142	-
	-	pCO_2	N:P	0.004	0.298	0.590	-
	Temperature	pCO_2	N:P	0.012	0.832	0.371	-
Maximum electron transport rate	Temperature	-	-	0.050	4.885	**0.037***	Higher at 21°C
	-	pCO_2	-	0.018	1.785	0.194	-
	-	-	N:P	0.001	0.153	0.699	-
	Temperature	pCO_2	-	0.014	1.321	0.262	-
	Temperature	-	N:P	0.235	2.273	0.145	-
	-	pCO_2	N:P	0.001	0.801	0.379	-
	Temperature	pCO_2	N:P	0.134	1.294	0.266	-
Light saturation point	Temperature	-	-	2463	14.03	**<0.001***	Higher at 21°C
	-	pCO_2	-	311.1	1.772	0.196	-
	-	-	N:P	1.200	0.007	0.937	-
	Temperature	pCO_2	-	565.7	3.222	0.852	-
	Temperature	-	N:P	34.40	0.196	0.662	-
	-	pCO_2	N:P	7.500	0.430	0.838	-
	Temperature	pCO_2	N:P	5.600	0.032	0.859	-

Variable	Factor 1	Factor 2	Factor 3	MS	F	p-value	Effect indicated by Tukey's posthoc test
Chlorophyll *a*	Temperature	-	-	0.001	2.115	0.159	-
	-	pCO_2	-	0.001	0.380	0.543	-
	-	-	N:P	0.001	0.386	0.540	-
	Temperature	pCO_2	-	0.001	0.887	0.356	-
	Temperature	-	N:P	0.001	1.207	0.283	-
	-	pCO_2	N:P	0.001	1.814	0.191	-
	Temperature	pCO_2	N:P	0.001	1.006	0.326	-
Integrated Biomarker Response	Temperature	-	-	3.295	19.41	**<0.001***	Higher at 21°C
	-	pCO_2	-	0.051	0.301	0.591	-
	-	-	N:P	0.181	1.068	0.317	-
	Temperature	pCO_2	-	0.004	0.026	0.875	-
	Temperature	-	N:P	0.046	0.272	0.609	-
	-	pCO_2	N:P	0.191	1.126	0.304	-
	Temperature	pCO_2	N:P	0.139	0.820	0.378	-
AOX:Resp	Temperature	-	-	0.234	15.97	**<0.001***	Higher at 21°C
	-	pCO_2	-	0.001	0.024	0.879	-
	-	-	N:P	0.028	1.883	0.183	-
	Temperature	pCO_2	-	0.053	3.621	0.069	-
	Temperature	-	N:P	0.009	0.600	0.446	-
	-	pCO_2	N:P	0.001	0.089	0.768	-
	Temperature	pCO_2	N:P	0.106	7.357	**0.012***	No significant increase at 21°C when N:P is 16 and pCO_2 is 400
PPC:PSP	Temperature	-	-	0.012	208.3	**<0.001***	Lower at 21°C
	-	pCO_2	-	0.001	0.865	0.362	-
	-	-	N:P	0.001	0.630	0.435	-
	Temperature	pCO_2	-	0.001	0.845	0.367	-
	Temperature	-	N:P	0.001	0.067	0.798	-
	-	pCO_2	N:P	0.001	0.309	0.583	-
	Temperature	pCO_2	N:P	0.001	0.749	0.395	-

2.4. Results

Carbon fluxes and cellular carbon content

Primary production, which represents the major share of organic carbon flow into the cell, was significantly affected by temperature as well as by pCO_2, but not by N:P ratios, or by any of the driver combinations. The primary production of *P. tricornutum* was 2.06 pmol C cell^{-1} d^{-1} at 18°C, and was higher at 21°C (2.38 pmol C cell^{-1} d^{-1}, $F_{1,24}$ 9.918, p = 0.004, Figure 2.1). Primary production was also higher at 1000 µatm pCO_2 than at 400 µatm pCO_2 (2.33 pmol C cell^{-1} d^{-1} vs. 2.11 pmol C cell^{-1} d^{-1}, $F_{1,24}$ 4.854, p = 0.037). Dark respiration rate did not differ between temperatures at pCO_2 of 400 µatm, but it was negatively affected by higher temperature when pCO_2 was 1000 µatm ($F_{1,24}$ 30.86, p < 0.001, Figure 2.1). Dark respiration rates were unaffected by dissolved N:P ratios. Concerning DOC production, we observed a significant stimulation by higher pCO_2 under 21°C conditions compared to 18°C (0.36 vs. 0.25 pmol cell^{-1} d^{-1}, $F_{1,24}$ 9.542, p = 0.005, Figure 2.1). In addition, DOC production was also significantly stimulated by higher N:P ratios, higher by about 0.13 pmol cell^{-1} d^{-1} ($F_{1,24}$ 7.023, p = 0.014). In all 21°C treatments, DOC production rates were positive, indicating exudation rates of 0.31 pmol C cell^{-1} d^{-1} on average, while under 18°C, values of DOC production were negative, indicating uptake rates of 0.65 pmol C cell^{-1} d^{-1} ($F_{1,24}$ 400.2, p < 0.001). Cellular carbon contents were significantly influenced by temperature, being higher at 18°C than at 21°C (1.26 pmol C cell^{-1} vs. 0.89 pmol C cell^{-1}, $F_{1,24}$ 272.8, p < 0.001, Figure 2.2a).

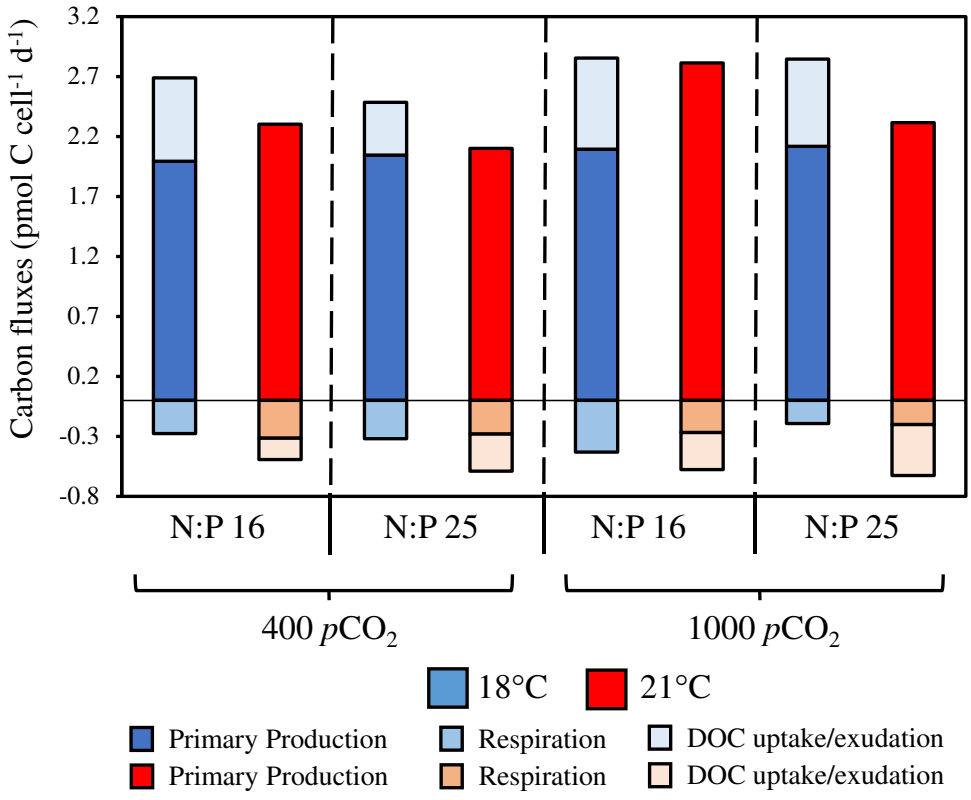

Figure 2.1: Carbon fluxes in the *Phaeodactylum tricornutum* cell under different treatments. Carbon production (primary production) and carbon consumption (net DOC production and dark respiration). Positive

DOC production represents DOC uptake by the cell, while negative DOC production represents DOC exudation by the cell. X-axis represents N:P ratios and pCO_2. Colours represent temperature (blue = 18°C, red = 21°C). Different shades represent Primary Production, Respiration and Net DOC production. Data as mean.

Growth rate

Growth rates of *P. tricornutum* were positively affected by higher temperature at 400 µatm pCO_2 but the increase was lower at 1000 µatm pCO_2 ($F_{1,24}$ 15.39, $p < 0.001$, Figure 2.2b). Furthermore, pCO_2 and N:P ratios in isolation did not significantly influence growth rates, but in combination, a significantly higher growth rate was achieved under 1000 µatm pCO_2 and an N:P of 25, thereby indicating an interactive effect of these drivers. The combination of temperature and N:P ratios, as well as all three drivers did not significantly influence growth rates.

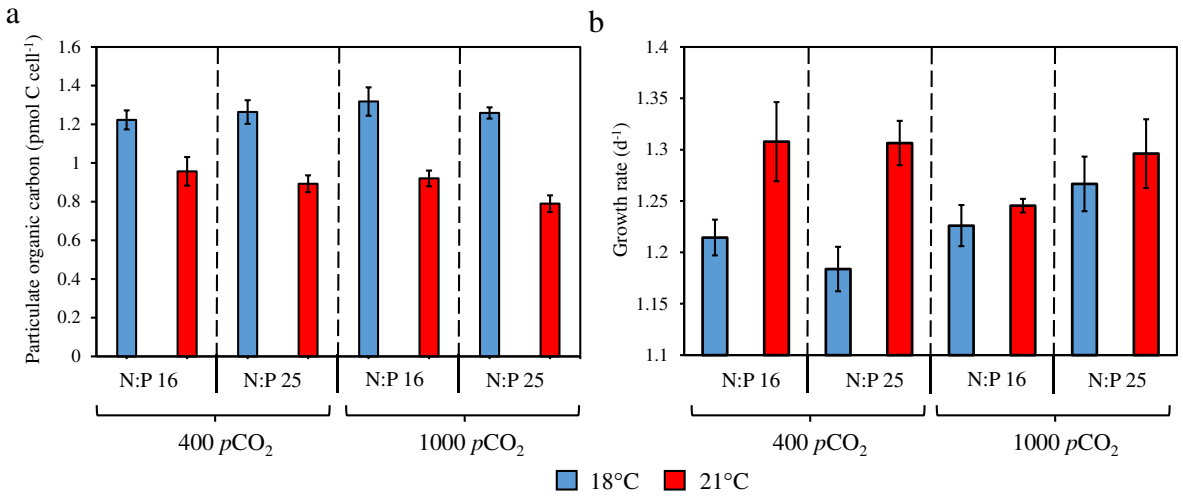

Figure 2.2: Cellular carbon content and *Phaeodactylum tricornutum* specific growth rate. (a) Particulate organic matter. (b) *P. tricornutum* specific growth rate. X-axis represents N:P ratios and pCO_2. Colours represent temperature (blue = 18°C, red = 21°C).

Photochemical performance and Chl-a content

Photochemical efficiency (α) was 0.016 on average in all treatments, and was neither affected by temperature, nor by pCO_2 or N:P ratio ($p > 0.05$, Table 2.2). The compensation point (cp) was significantly lower under 21°C and high pCO_2 (10.49 vs. 6.51 µmol photons m^{-2} s^{-1}) but no temperature effect could be detected under low pCO_2, showing the interactivity of these drivers ($F_{1,24}$ 48.31, $p < 0.001$; Table 2.2). Maximum rates of net photosynthesis (V_{max}) were positively affected by higher temperature ($F_{1,24}$ 4.885, $p = 0.037$), increasing from 1.25 to 1.46 µmol O_2 µg Chl-a^{-1} h^{-1}. No effects of pCO_2 and N:P were detected. The light saturation

point (I_k) was higher under high temperature (~85 vs. ~100 µmol photons m^{-2} s^{-1}, $F_{1,24}$ 14.03, $p < 0.001$, Table 2.2), irrespective of the applied pCO_2 levels and N:P ratios. None of the above-mentioned photochemical parameters was affected by N:P ratio ($p > 0.05$, Table 2.2). Chlorophyll *a* content was on average 0.15 pg $cell^{-1}$ and was not affected by temperature, pCO_2 or N:P ratio ($p > 0.05$, Table 2.2).

Antioxidant response

The integrated biomarker response index (IBR) was on average 4.48 under 18°C, but it was lower at 21°C (0.61, $F_{1,16}$ 19.41, $p < 0.001$, Figure 2.3a,b), showing that temperature is the main driver for antioxidant responses. We observed no statistically significant effect of pCO_2, dissolved N:P ratios, nor of any driver combination on the IBR. The temperature-driven decrease in IBR was mainly caused by the lower activity of antioxidant enzymes, especially GPx, GST and SOD-Mn (Figure 2.3a,b and Supplementary Figure 2.2). Cellular MDA concentrations were stimulated by temperature in all treatments ($F_{1,16}$ 18.06, $p < 0.001$). In all low-temperature treatments, MDA concentrations were highest under high pCO_2 and high N:P (Figure 2.3a). The ratio of AOX to dark respiration was significantly stimulated by high temperatures in all driver constellations, going from 0.20 to 0.40, except under low pCO_2 and low N:P (Figure 2.4a). The ratio of photoprotective carotenoids (violaxanthin, diadinoxanthin, β-carotene) to photosynthetic pigments (chl-a, fucoxanthin; PPC:PSP) decreased under high temperatures in all treatments ($F_{1,24}$ 208.3, $p < 0.001$, Figure 2.4b). Since photosynthetic pigments were not different across treatments, the reduction of this ratio was primarily driven by the decrease in photoprotective carotenoids (Supplementary Figure 2.4, Table 2.2).

Table 2.2: The rapid light curve fitted parameters under different treatments. Photochemical efficiency (α), light compensation point (cp), maximum electron transport rate (V_{max}), light saturation point (I_k) based on the rates of μmol O_2 μg Chl-a^{-1} h^{-1}. Chl-a content as pg $cell^{-1}$. Data as mean ± standard deviation.

Variable	18°C				21°C			
	400 pCO_2		1000 pCO_2		400 pCO_2		1000 pCO_2	
	N:P 16	N:P 25	N:P 16	N:P 25	N:P 16	N:P 25	N:P 16	N:P 25
α	0.015 (±0.003)	0.015 (±0.005)	0.016 (±0.003)	0.020 (±0.004)	0.015 (±0.003)	0.014 (±0.004)	0.019 (±0.004)	0.015 (±0.003)
cp (μmol photons m^{-2} s^{-1})	8.20 (±1.07)	8.21 (±0.28)	10.86 (±0.93)	9.99 (±0.73)	8.41 (±0.28)	8.17 (±0.93)	6.55 (±0.69)	6.17 (±0.49)
V_{max} (μmol O_2 μg Chl-a^{-1} h^{-1})	1.14 (±0.18)	1.09 (±0.35)	1.18 (±0.19)	1.57 (±0.43)	1.55 (±0.21)	1.38 (±0.37)	1.59 (±0.09)	1.33 (±0.12)
I_k (μmol photons m^{-2} s^{-1})	86.3 (±6.2)	82.1 (±1.7)	86.7 (±3.1)	86.1 (±8.1)	109.4 (±9.8)	110.9 (±20.4)	94.6 (±17.1)	96.4 (±11.5)
Chl-a content (pg $cell^{-1}$)	0.15 (±0.01)	0.15 (±0.03)	0.15 (±0.02)	0.12 (±0.02)	0.15 (±0.01)	0.16 (±0.03)	0.15 (±0.01)	0.16 (±0.01)

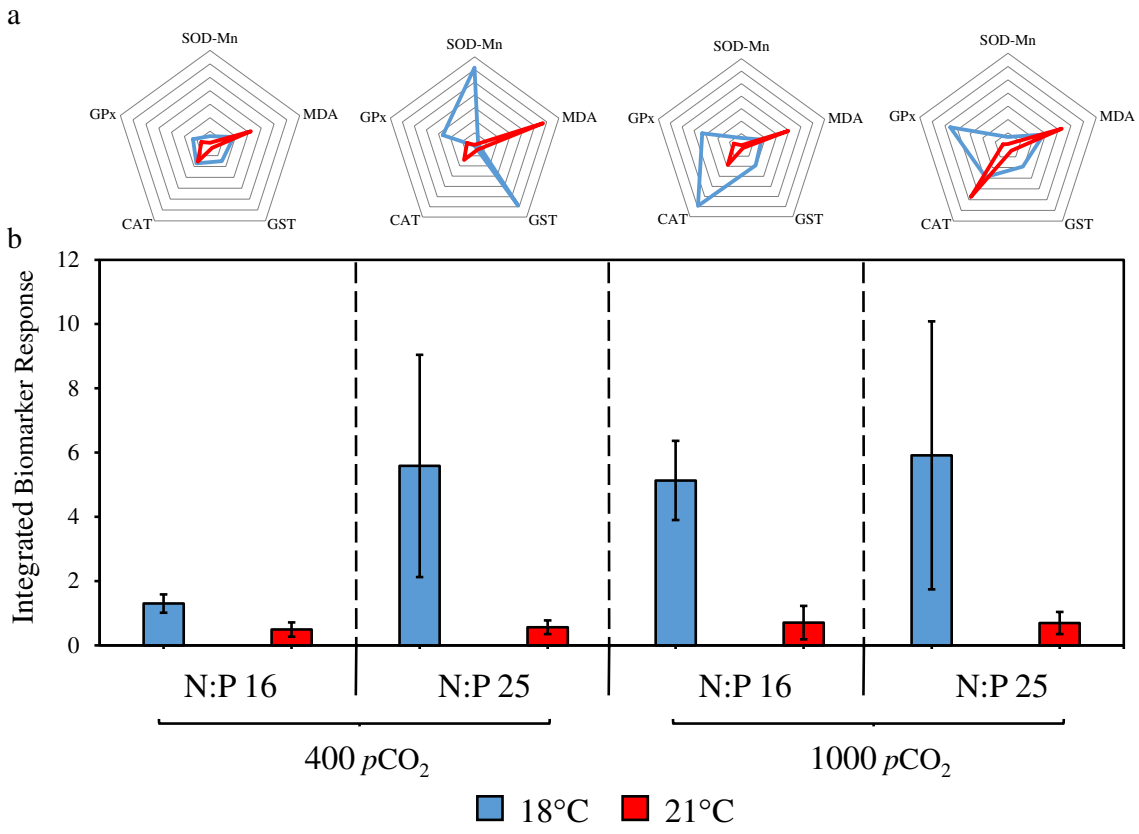

Figure 2.3: Antioxidant enzymatic response and oxidative stress. (a) Normalized radar plots of antioxidant enzyme activities and MDA as a biomarker for oxidative stress. MDA = Malondialdehyde, SOD-Mn = Managanese Superoxide Dismutase, GST = Glutathione S-transferase, CAT = Catalase, GPx = Glutathione Peroxidase. All radar plots are to the same scale. (b) Integrated Biomarker Response. X-axis represents N:P ratios and pCO_2. Colours represent temperature (blue = 18°C, red = 21°C). Data as mean ± standard deviation.

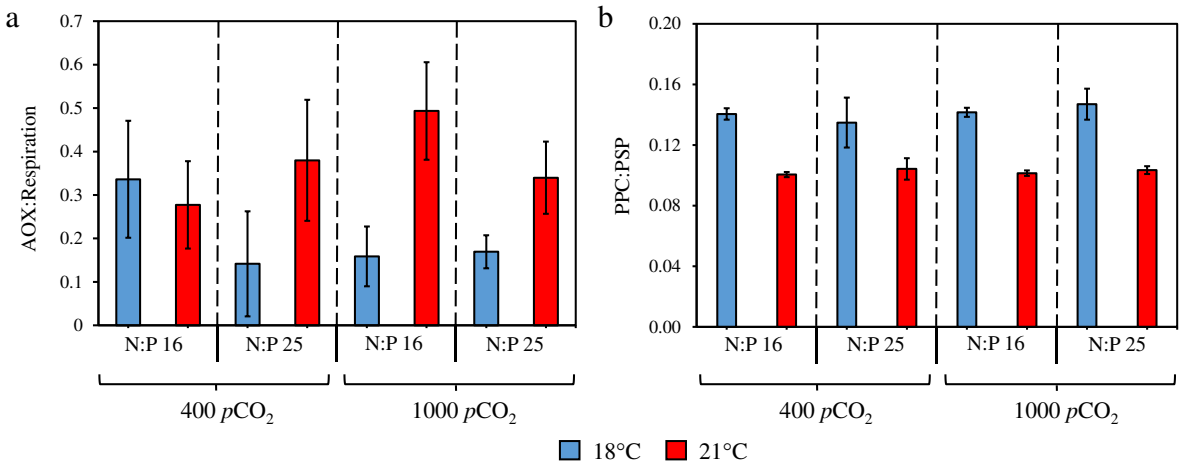

Figure 2.4: Alternative oxidase activity and carotenoids. (a) Ratio of Alternative oxidase (AOX) activity relative to dark respiration rate. (b) Ratio of Photoprotective Carotenoids (PPC, Diadinoxanthin, Violaxanthin and β-Carotene) relative to Photosynthetic Pigments (PSP, Chlorophyll a and Fucoxanthin). X-axis represents N:P ratios and pCO_2. Colours represent temperature (blue = 18°C, red = 21°C). Data as mean ± standard deviation.

Synthesis of cellular responses

Results from the PCA identified temperature as the most influential driver of changes in the measured variables, followed by pCO_2 and, to a lower degree, N:P ratio (Figure 2.5). The first two principal component axes of the PCA explained 60.2% of variance within all observations (Figure 2.5). Higher DOC production, growth rate, and MDA concentration were related to higher temperature (21°C), whilst higher POC, dark respiration rate, and antioxidant response were positively correlated to the lower temperature we tested (18°C). On the other hand, primary production and maximum net photosynthesis rates (V_{max}) were rather influenced by pCO_2 than by temperature, whereas contents of photosynthetic pigments, Chl-a and Fucoxanthin, were the least influenced by the environmental drivers.

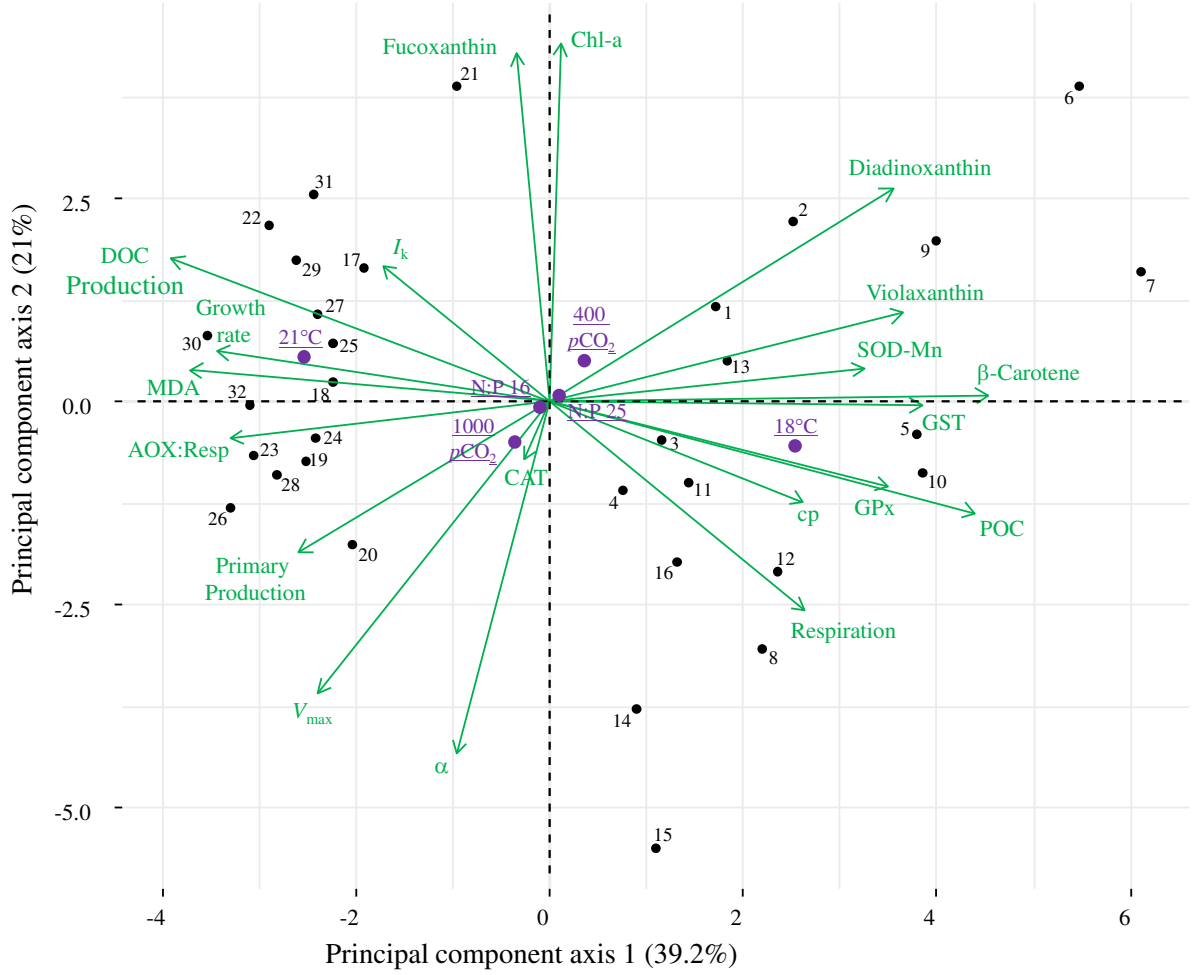

Figure 2.5: Principal Component Analysis (PCA) of the *Phaeodactylum tricornutum* response to global change factors. Dependent variables are displayed in green, supplementary variables are displayed in purple and black dots represent the individual observations (replicates). The two first principal component axes explain 60.2% of all variation within observations. Location of dependent variables near to supplementary variables indicates positive correlation of that experimental factor on the dependent variable. The position of the supplementary variables (drivers) relative to the point 0 show the intensity of the drivers on the dependent variables. The further

the drivers are from point 0, the stronger their effect is. Black dots represent individual replicates: 1-4 (T: 18°C, pCO_2 400 µatm, N:P 16), 5-8 (T: 18°C, pCO_2 400 µatm, N:P 25), 9-12 (T: 18°C, pCO_2 1000 µatm, N:P 16), 12-16 (T: 18°C, pCO_2 1000 µatm, N:P 25), 17-20 (T: 21°C, pCO_2 400 µatm, N:P 16), 21-24 (T: 21°C, pCO_2 400 µatm, N:P 25), 25-28 (T: 21°C, pCO_2 1000 µatm, N:P 16) and 29-32 (T: 21°C, pCO_2 1000 µatm, N:P 25).

2.5. Discussion

The full-factorial design of our experiment enabled us to identify that in the global change context tested in this study temperature has a greater influence than higher pCO_2 and dissolved N:P ratios on the antioxidant capacity and carbon metabolism of *Phaeodactylum tricornutum*. Higher temperatures led to higher photosynthesis, DOC exudation, growth rate and respiration, overall yielding a decrease in net C fluxes into the cell, and cells with lower carbon content. We also observed a synergy between temperature and pCO_2, and to a lesser extent between temperature and N:P. The cells were mostly unaffected by pCO_2 and N:P ratio at 18°C, and only under increased temperatures, cells became prone to these environmental drivers. At 21°C, the phytoplankton cells had higher oxidative stress and lower antioxidant enzymatic activity, indicating a reduced capacity to combat ROS generated under warmer conditions. These results indicate that the RCP 8.5 scenario predicted for 2100 will likely influence the carbon metabolism and oxidative stress management of this species. If we expect similar response from other phytoplankton species, a decrease in cellular carbon content and an increase of DOC production might represent a higher energetic input into the surface microbial loop and lower export of organic matter to deeper waters, as carbon fixed as biomass can be assimilated to higher trophic levels, while DOC is usually a source of energy for planktonic bacteria (Azam et al., 1983).

We observed higher cellular contents of MDA, and a higher electron flow through the AOX pathway under 21°C conditions than at 18°C. Both are indicators of oxidative stress, because the cells reroute electrons through the AOX pathway to alleviate flow through the inner mitochondrial membrane, and because MDA arises from harmful oxidation reactions in lipid membranes (Uchiyama and Mihara, 1978). The chloroplast and mitochondrion constantly exchange compounds such as ADP/ATP and electron carriers, whereby the mitochondrion can serve as an extra electron sink under photosynthetic overproduction by activating the AOX pathway. This generates less energy, but allows a more rapid supply of ADP and electron carriers to the chloroplast, avoiding photoinhibition due to the lack of these compounds in the chloroplast (Bailleul et al., 2015; Launay et al., 2020). The increase of AOX:Respiration we observed under elevated temperature, despite lower dark respiration and higher photosynthetic

rates, suggests that the mitochondrion was acting as an electron sink as a stress response mechanism (Allen et al., 2008; Prihoda et al., 2012). Regarding the detoxification of oxidative stress, we observed an overall lower activity of most antioxidant enzymes under high temperatures (GPx, GST, SOD-Mn; CAT under low N:P) which is counterintuitive, since higher contents of these enzymes could reduce oxidative stress. However, these results are supported by another study which also observed decreased activities of antioxidant enzymes in phytoplankton after high temperature acclimation (Perelman et al., 2006). We hypothesized that these lower enzyme activities reflect the inability of the mitochondria to maintain the respective gene expression, suggesting that 21°C past the optimum temperature of *P. tricornutum*, similar to other studies (Bitaubé Pérez et al., 2008 ; He et al., 2014; Tong et al. 2021).

We observed a higher photosynthetic rate at 21°C than at 18°C, which may be related to the enhanced activity of the CO_2 fixing enzyme RuBisCO under higher temperatures, causing a higher I_k (Table 2.2, Ras et al., 2013). In addition to warming, elevated pCO_2 further increased photosynthetic activity, likely as a result of higher C availability, which may enable a reallocation of energy possible due to a lower demand for the carbon concentration mechanism activity (Young et al., 2015; Rokitta et al., 2022). Light harvesting pigments (Chl-a, fucoxanthin) were not affected by any of the drivers, indicating that the light-harvesting portion of the antenna complex was not affected by temperature, pCO_2, or dissolved nutrient ratios. However, the concentration of protective carotenoids (especially diadinoxanthin and violaxanthin; Arbones et al., 2000 ; Wagner et al., 2006; Janknegt et al., 2008) and of their precursor, β-carotene (Kuczynska et al., 2015), decreased under high temperature. This likely enhanced the overall photosynthetic activity, because relatively more captured photons were directed to the light dependent reactions of photosynthesis. Protective carotenoids compete for light energy trapped in the photosystem and dissipate it as thermal energy before it reaches the reaction center, a useful photoprotection mechanism when light irradiance is higher than needed (Arbones et al., 2000; Wagner et al., 2006; Janknegt et al., 2008). On the one hand, the lower concentration of carotenoids can increase photosynthetic rates, on the other hand, this reduction decreases photoprotection, the main short-term response against the formation of ROS in the chloroplast (Kuczynska et al., 2015).

High pCO_2 increased the photosynthetic compensation points (Table 2.2), meaning that cells needed more light to reach positive net primary production, at 18°C, whereas at 21°C, high pCO_2 lowered the photosynthetic compensation point. Although elevated pCO_2 represents higher availability of DIC for phytoplankton and could stimulate their growth (Riebesell et al.,

2007), it also represents higher H^+ concentration. This lowers seawater pH, which influences the membrane potential, intracellular pH, activity of enzymes and energy partitioning (Riebesell, 2004; Giordano et al., 2005; Rokitta et al., 2012), and can even lead to lower growth rates (Berge et al., 2010), counterbalancing the positive effect of DIC fertilization. We hypothesize that the overall mitochondrial function was negatively affected by increasing temperature, which was exacerbated under high pCO_2. In other words, respiration had the opposite reaction to temperature and pCO_2 as photosynthesis. This is unexpected since, typically, the dark respiration is positively correlated with photosynthesis, acting as a sink for organic carbon (Yoshida et al., 2007), and also for the reduction equivalents (Bailleul et al., 2015). This disparity of chloroplast and mitochondrial activity reveals an imbalance under high temperature, which has been observed previously in this species, for instance, by Tong et al. (2021), who found that respiration peaked at 18°C while photosynthesis had an optimum around 20°C. The negative effect of high pCO_2 on dark respiration has also been observed in diatoms before (Shi et al., 2019). This imbalance causes high photosynthetic organic carbon production, as well as a reduced respiration, which should lead to higher organic carbon retention, i.e. both processes should support the net POC production of the cells. However, *P. tricornutum* cells did not accumulate POC, but rather, we observed an increased DOC exudation (especially under high N:P ratio), which may represent a mechanism to regulate cellular POC production rates. DOC exudation has previously been shown to range from 1 to 55% of the total carbon fixation in different phytoplankton taxa. In line with our data, DOC production was found to be stimulated by high temperatures, as well as by higher pCO_2 (Zlotnik and Dubinsky, 1989; Baines and Pace, 1991; Riebesell et al., 2007; Wetz and Wheeler, 2007; Engel et al., 2010; Torstensson et al., 2015). The stimulating effect of high N:P ratios on DOC production has been found before in phytoplankton (Li and Sun, 2016), and seems to be an additional supporting mechanism to balance cellular elemental stoichiometry (Thornton, 2014), since RuBisCO activity is more sensitive to low supplies of nitrogen than of phosphorus (Geider et al., 1993). Although, *P. tricornutum* and other phytoplankton species can take up DOC (Villanova et al., 2017), the net cellular flows of DOC were sensitive to the environmental drivers tested here. We measured DOC uptake at 18°C and exudation at 21°C, with a synergistic influence of warming, elevated pCO_2, and elevated N:P ratios on the degree of DOC exudation. These results are supported by another study which found higher DOC exudation by phytoplankton under oxidative stress (Mohamed, 2008). While the stimulated photosynthetic POC production and the lower consumption by mitochondrial respiration under high temperature were compensated by DOC exudation, other temperature effects could not be compensated, for

instance, the stimulation of growth rates that typically derives from enhanced nutrient uptake, more rapid DNA duplication, etc. Consequently, given the steady net POC production, the increased division rates resulted in cells with overall lower carbon content.

If the results obtained for this single strain of one species are indicative of what would happen with other species as well, an expected scenario for 2100 corresponding to RCP 8.5 with higher temperature and pCO_2 combined with increasing N:P ratio can significantly alter metabolic fluxes of microalgae and have the potential to alter the biogeochemical cycling of carbon in the oceans: increased photosynthesis, as well as decreased respiration might lower the overall CO_2 concentrations in surface waters and could thus both enhance the air-sea gas exchange, i.e. the uptake of atmospheric CO_2. The fact that organic carbon is not channeled into biomass and fed to higher trophic levels, but rather exuded, suggests an enhanced carbon input into the microbial loop (Azam et al., 1983). In line with this, cells with lower C content might be smaller and likely to have lower sinking velocities and also to become a better prey, especially for microzooplankton, which again will feed more carbon into the microbial loop (Legendre and Le Fèvre, 1995; Morán et al., 2010; Hillebrand et al., 2022). Similar results were obtained in a mesocosm experiment during which plankton communities were subjected to simultaneous changes in temperature, pCO_2, and N:P ratios (Moreno et al., 2022), and which identified an intensification of the microbial loop. These results highlight the sensitivity of microalgal physiology to the combined effects of multiple drivers. Remarkably, the manifestation of further effects of pCO_2 and N:P were enabled by elevated temperatures, underlining that temperature functions as a 'master variable' for phototrophic phytoplankton. An enhanced oceanic CO_2 uptake and an overall stimulated microbial loop may to be the longer-term consequences of rising temperatures, elevated pCO_2 as well as shifted dissolved N:P ratios.

2.6. Acknowledgements

We thank the colleagues from Alfred-Wegener-Institut for the technical and scientific support during the experiment, especially Julia Haafke, Marcel Machnik and Kristine Carstens. Sincere thanks to the colleagues who supported us in analyzing some of the samples, including Bernhard Fuchs (bacteria), Claudia Burau and Prof. Dr. Boris Koch (DOC), Nadine Rijsdijk (flow cytometry), and Johanna Strauß (total alkalinity). Special thanks for Dr. Mathias Wegner for lending us the flow cytometer, Ivan de Palma for supporting us with calculations for DOC production and Julien di Pane for the help with the PCA.

2.7. Supplementary Material

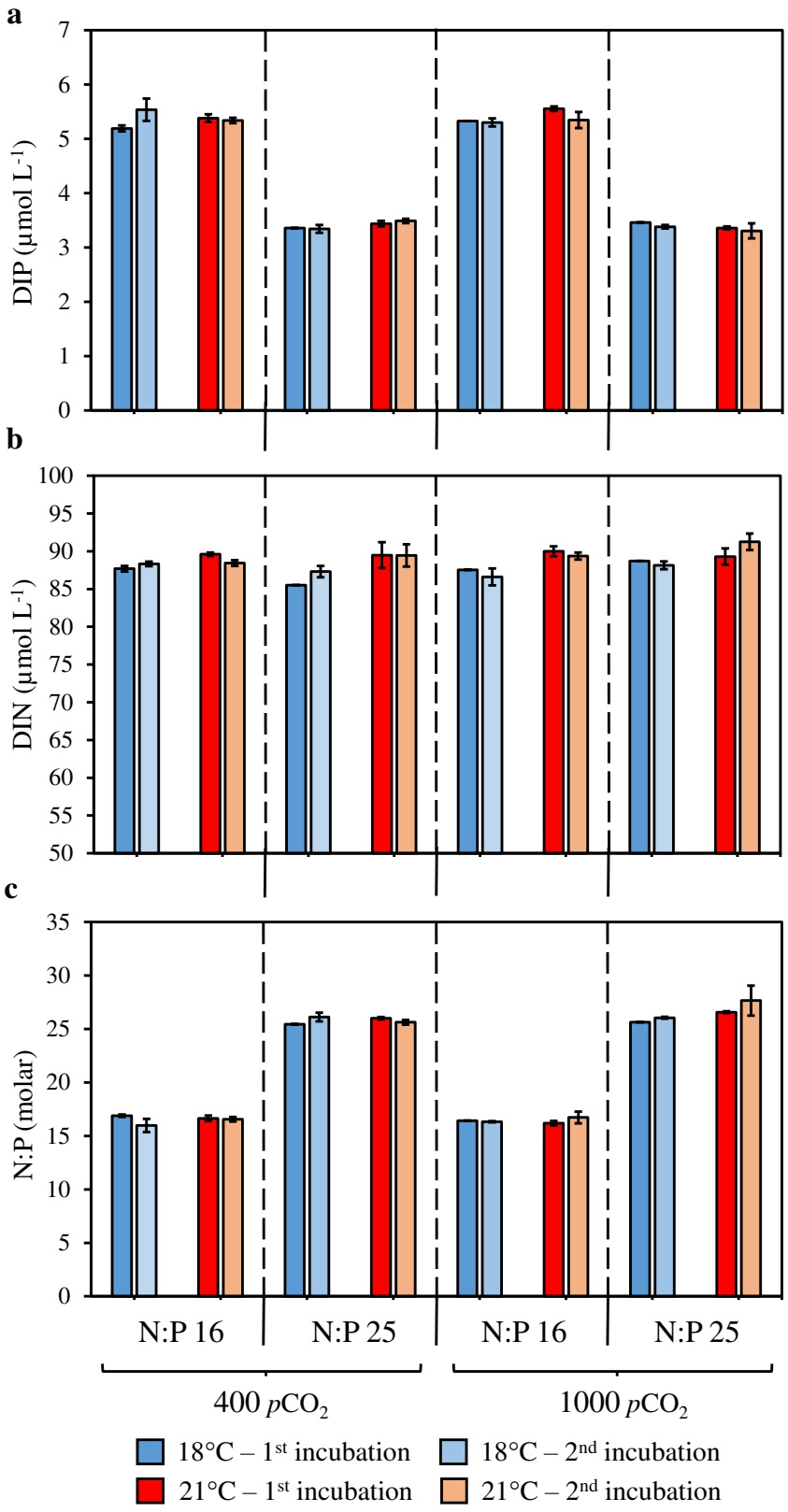

Supplementary Figure 2.1: Dissolved inorganic nutrients. Initial nutrient concentrations and N:P ratios across treatments. Incubation refers to first or second incubation. (a) Dissolved inorganic phosphorus (DIP = PO_4^{3-}). (b) Dissolved inorganic nitrogen (DIN = NO_x). (c) N:P ratio (molar). Data as mean ± standard deviation.

Supplementary Table 2.1: Seawater carbonate chemistry. Final and initial seawater carbonate chemistry across treatments. Incubation and day refers to first or second incubation, d_0 = initial, d_4 = final. Total alkalinity (TA), dissolved inorganic carbon (DIC), partial pressure of CO_2 (pCO_2), Bicarbonate (HCO_3^-), Carbonate (CO_3^{2-}) and Carbon dioxide (CO_2) were calculated based on pH and total alkalinity using CO2Sys (Pierrot et al., 2006). Data as mean ± standard deviation.

Incubation and day	Temperature (°C)	Target pCO_2 (µatm)	N:P	pH	TA (µmol KgSW^{-1})	DIC (µmol KgSW^{-1})	Attained pCO_2 (µatm)	HCO_3^- (µmol KgSW^{-1})	CO_3^{2-} (µmol KgSW^{-1})	CO_2 (µmol KgSW^{-1})
1 d_0	18	400	16	8.13 (±0.01)	2424.16 (±3.74)	2118.68 (±10.95)	456.80 (±18.44)	1946.68 (±13.85)	156.14 (±4.49)	15.85 (±0.64)
1 d_0	18	400	25	8.11 (±0.01)	2404.52 (±2.16)	2111.08 (±2.24)	484.79 (±5.10)	1946.19 (±2.21)	148.09 (±1.41)	16.78 (±0.18)
1 d_0	18	1000	16	7.79 (±0.01)	2411.68 (±2.98)	2229.64 (±4.31)	1084.99 (±27.18)	2114.48 (±3.62)	77.52 (±2.05)	37.65 (±0.94)
1 d_0	18	1000	25	7.79 (±0.01)	2391.67 (±0.94)	2233.07 (±8.80)	1083.20 (±25.50)	2117.11 (±9.06)	78.46 (±1.28)	37.50 (±0.88)
1 d_4	18	400	16	8.15 (±0.01)	2428.01 (±2.63)	2128.58 (±8.74)	436.62 (±6.81)	1949.73 (±9.23)	163.69 (±1.33)	15.15 (±0.24)
1 d_4	18	400	25	8.18 (±0.05)	2421.96 (±4.24)	2111.16 (±7.47)	413.28 (±9.83)	1926.57 (±9.28)	170.28 (±2.50)	14.31 (±0.34)
1 d_4	18	1000	16	7.86 (±0.03)	2433.69 (±5.13)	2226.87 (±5.40)	920.82 (±63.83)	2104.11 (±4.01)	90.81 (±6.07)	31.95 (±2.21)
1 d_4	18	1000	25	7.86 (±0.01)	2424.46 (±1.77)	2222.93 (±3.69)	930.79 (±22.71)	2100.78 (±2.82)	89.92 (±2.32)	32.23 (±0.79)
2 d_0	18	400	16	8.16 (±0.01)	2424.53 (±3.74)	2141.28 (±3.80)	434.0 (±13.77)	1959.73 (±6.71)	166.49 (±4.13)	15.06 (±0.48)
2 d_0	18	400	25	8.14 (±0.02)	2438.33 (±16.73)	2108.68 (±29.13)	443.71 (±21.70)	1934.32 (±23.26)	158.96 (±9.14)	15.40 (±0.75)
2 d_0	18	1000	16	7.78 (±0.01)	2411.56 (±2.94)	2259.87 (±1.87)	1119.04 (±20.84)	2143.81 (±1.22)	77.24 (±1.51)	38.83 (±0.72)

Incubation and day	Temperature (°C)	Target pCO_2 (µatm)	N:P	pH	TA (µmol KgSW^{-1})	DIC (µmol KgSW^{-1})	Attained pCO_2 (µatm)	HCO_3^- (µmol KgSW^{-1})	CO_3^{2-} (µmol KgSW^{-1})	CO_2 (µmol KgSW^{-1})
2 d_0	18	1000	25	7.78 (±0.01)	2442.33 (±0.01)	2233.74 (±3.62)	1113.38 (±13.89)	2119.39 (±3.63)	75.70 (±0.81)	38.65 (±0.48)
2 d_4	18	400	16	8.12 (±0.01)	2427.64 (±9.00)	2157.40 (±15.10)	476.57 (±15.67)	1985.29 (±16.43)	155.58 (±3.07)	16.53 (±0.54)
2 d_4	18	400	25	8.18 (±0.05)	2418.60 (±2.71)	2139.85 (±20.06)	423.80 (±53.44)	1953.54 (±35.87)	171.60 (±17.93)	14.70 (±1.85)
2 d_4	18	1000	16	7.81 (±0.01)	2421.16 (±1.55)	2235.12 (±3.46)	1037.85 (±28.49)	2117.81 (±4.16)	81.30 (±1.96)	36.01 (±0.99)
2 d_4	18	1000	25	7.80 (±0.01)	2418.97 (±1.91)	2235.36 (±4.12)	1069.99 (±38.38)	2119.36 (±4.65)	78.85 (±2.56)	37.15 (±1.33)
1 d_0	21	400	16	8.17 (±0.01)	2407.67 (±4.99)	2080.62 (±6.50)	423.32 (±7.69)	1885.48 (±4.05)	181.66 (±3.66)	13.47 (±0.24)
1 d_0	21	400	25	8.18 (±0.00)	2432.33 (±0.47)	2041.79 (±9.12)	402.28 (±6.11)	1845.11 (±9.70)	183.85 (±0.95)	12.82 (±0.19)
1 d_0	21	1000	16	7.80 (±0.02)	2451.28 (±7.48)	2195.87 (±8.55)	1081.54 (±40.73)	2074.37 (±8.41)	87.18 (±3.09)	34.32 (±1.29)
1 d_0	21	1000	25	7.79 (±0.02)	2453.33 (±11.90)	2169.63 (±9.92)	1087.59 (±38.88)	2050.3 (±9.53)	84.70 (±2.82)	34.51 (±1.23)
1 d_4	21	400	16	8.18 (±0.02)	2422.63 (±2.03)	2083.10 (±11.89)	406.12 (±21.96)	1881.33 (±14.13)	188.84 (±7.91)	12.93 (±0.69)
1 d_4	21	400	25	8.20 (±0.02)	2448.89 (±8.04)	2085.88 (±19.49)	390.34 (±23.55)	1876.16 (±23.89)	197.2 (±7.65)	12.40 (±0.75)
1 d_4	21	1000	16	7.87 (±0.02)	2435.82 (±7.96)	2185.69 (±8.31)	923.02 (±35.59)	2056.05 (±10.02)	100.35 (±3.05)	29.29 (±1.13)
1 d_4	21	1000	25	7.83	2434.82	2206.42	1032.24	2080.65	93.03	32.75

Incubation and day	Temperature (°C)	Target pCO_2 (µatm)	N:P	pH	TA (µmol KgSW^{-1})	DIC (µmol KgSW^{-1})	Attained pCO_2 (µatm)	HCO_3^- (µmol KgSW^{-1})	CO_3^{2-} (µmol KgSW^{-1})	CO_2 (µmol KgSW^{-1})
				(±0.06)	(±4.09)	(±28.23)	(±138.88)	(±32.49)	(±9.19)	(±4.41)
2 d_0	21	400	16	8.12 (±0.01)	2447.67 (±2.62)	2071.18 (±3.42)	469.40 (±9.79)	1890.29 (±4.37)	165.97 (±2.89)	14.91 (±0.31)
2 d_0	21	400	25	8.17 (±0.01)	2450.33 (±13.22)	2057.60 (±9.85)	419.68 (±9.03)	1863.79 (±9.23)	180.48 (±3.51)	13.33 (±0.29)
2 d_0	21	1000	16	7.82 (±0.01)	2424.41 (±6.53)	2183.45 (±15.50)	1032.82 (±13.68)	2060.99 (±14.71)	89.65 (±1.01)	32.81 (±0.43)
2 d_0	21	1000	25	7.83 (±0.01)	2427.80 (±4.90)	2191.87 (±9.26)	1005.99 (±20.99)	2067.14 (±9.65)	92.79 (±1.08)	31.94 (±0.66)
2 d_4	21	400	16	8.17 (±0.01)	2442.09 (±12.07)	2142.30 (±16.16)	437.20 (±12.64)	1940.9 (±15.37)	187.92 (±4.59)	13.88 (±0.40)
2 d_4	21	400	25	8.17 (±0.02)	2424.01 (±8.43)	2119.16 (±9.20)	421.83 (±17.42)	1915.88 (±12.69)	189.88 (±5.43)	13.40 (±0.55)
2 d_4	21	1000	16	7.85 (±0.02)	2433.41 (±9.02)	2227.99 (±4.31)	965.02 (±39.09)	2097.80 (±5.52)	99.54 (±3.58)	30.65 (±1.24)
2 d_4	21	1000	25	7.89 (±0.03)	2423.34 (±8.98)	2236.95 (±13.99)	902.24 (±53.18)	2101.17 (±16.66)	107.14 (±4.48)	28.64 (±1.69)

Supplementary Information 2.1: Net DOC Production Integral resolution. Step-by-step resolution of integral explaining the formula for Net DOC Production.

DOC_p = Total DOC production (ΔDOC pmol mL^{-1})

$DOC_p' = \frac{dQ}{dt}$

D = DOC production cell^{-1} d^{-1}

C_1 = final cells concentration

$D = \frac{Q'}{C_1}$

G = cells growth

t = time

$C_1(t)$ = Cell concentration in the function of time

C_0 = Initial cells concentration

Cells growth: $C_1(t) = C_0.e^{Gt}$

DOC production d^{-1}: $\frac{dDOCp}{dt} = D.C1(t)$

DOC production:

$$DOCp = \int_{to}^{t} \frac{dDOCp}{dt} dt = \int_{to}^{t} D.C1(t).dt$$

$$\int_{to}^{t} D.C1(t).dt = \int_{to}^{t} D.C0.e^{Gt}.dt$$

$$\int_{to}^{t} D.C0.e^{Gt}.dt = D.C0.\left[\frac{e^{Gt}}{G}\right]_{to}^{t}$$

$$D.C0.\left[\frac{e^{Gt}}{G}\right]_{to}^{t} = D.C0.\left(\frac{e^{Gt}}{G} - \frac{e^{Gto}}{G}\right)$$

$$DOCp = D.C0.\left(\frac{e^{Gt}}{G} - \frac{e^{Gto}}{G}\right)$$

$$DOCp = D.C0.\left(\frac{e^{G.4}}{G} - \frac{e^{G.0}}{G}\right)$$

$$(I)\ DOCp = D.C0.\left(\frac{e^{G.4}}{G} - \frac{1}{G}\right)$$

Determining G = $C1(t) = C0.e^{\mu t}$

$$C1(t) = C0.e^{Gt}$$

$$\frac{C1(t)}{C0} = e^{Gt}$$

$$ln\left(\frac{C1(t)}{C0}\right) = \ln\left(e^{Gt}\right)$$

$$ln\left(\frac{C1(t)}{C0}\right) = Gt$$

$$\frac{\ln C1(t) - lnC0}{t} = G$$

Applying $C1$, $C0$ and t measured during the experiment to determine G.

$$G = \frac{ln81290 - ln320}{4}$$

$$G = \frac{ln\,81290/320}{4}$$

$$G = \frac{ln256}{4} = \frac{ln4^4}{4} = \frac{4}{4} ln4$$

$$G = ln4\ (II)$$

Replacing II in I

$$DOCp = D.C0.\left(\frac{e^{ln4.4}}{ln4} - \frac{1}{ln4}\right)$$

$$\frac{DOCp}{C0.\left(\frac{e^{ln4.4}}{ln4} - \frac{1}{ln4}\right)} = D$$

$$\frac{DOCp}{C0.\left(\frac{e^{G.4}}{G} - \frac{1}{G}\right)} = D$$

Replacing *G* by the specific growth rate (μ)

$$D = \frac{DOCp}{C0} . \frac{\mu}{\left(\frac{C1}{C0} - 1\right)}$$

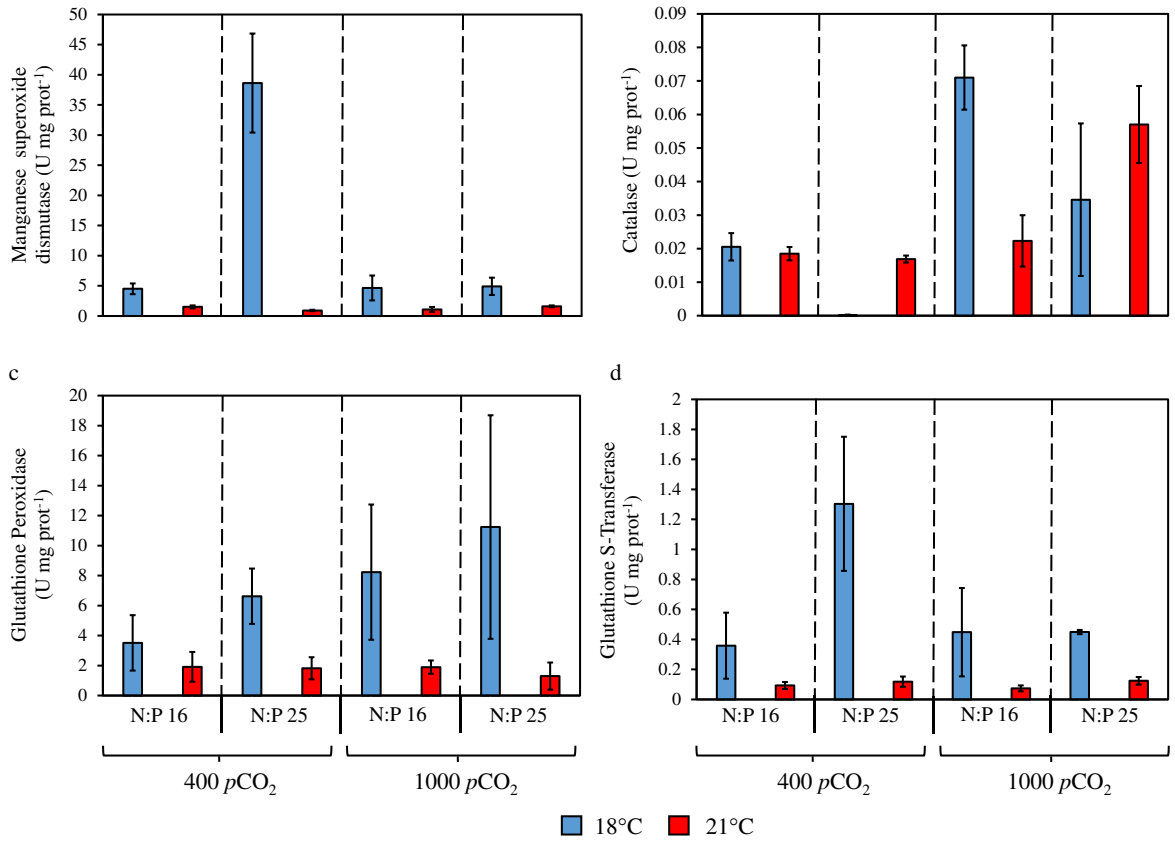

Supplementary Figure 2.2: Biomarkers of enzymatic antioxidant response. (a) Manganese Superoxide Dismutase (SOD-Mn) activity. (b) Catalase (CAT) activity. (c) Glutathione Peroxidase (GPx) activity. (d) Glutathione S-transferase (GST) activity. X-axis represents N:P ratios and pCO_2. Colours represent temperature (blue = 18°C, red = 21°C). Data as mean ± standard deviation.

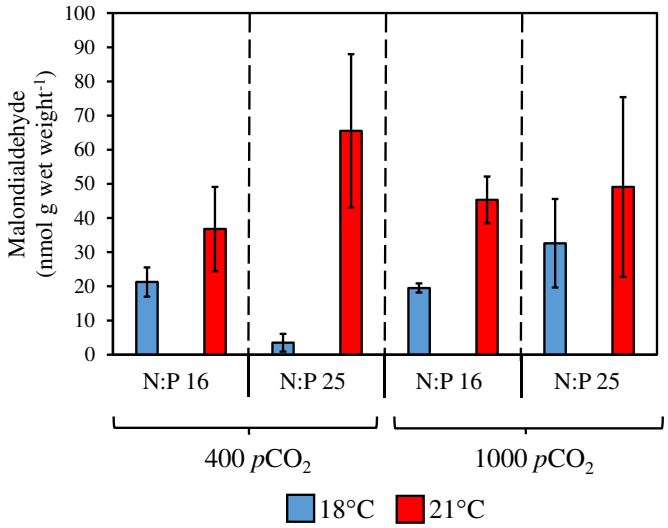

Supplementary Figure 2.3: Biomarker of oxidative stress. Malondialdehyde (MDA) cellular concentration. X-axis represents N:P ratios and pCO_2. Colours represent temperature (blue = 18°C, red = 21°C). Data as mean ± standard deviation.

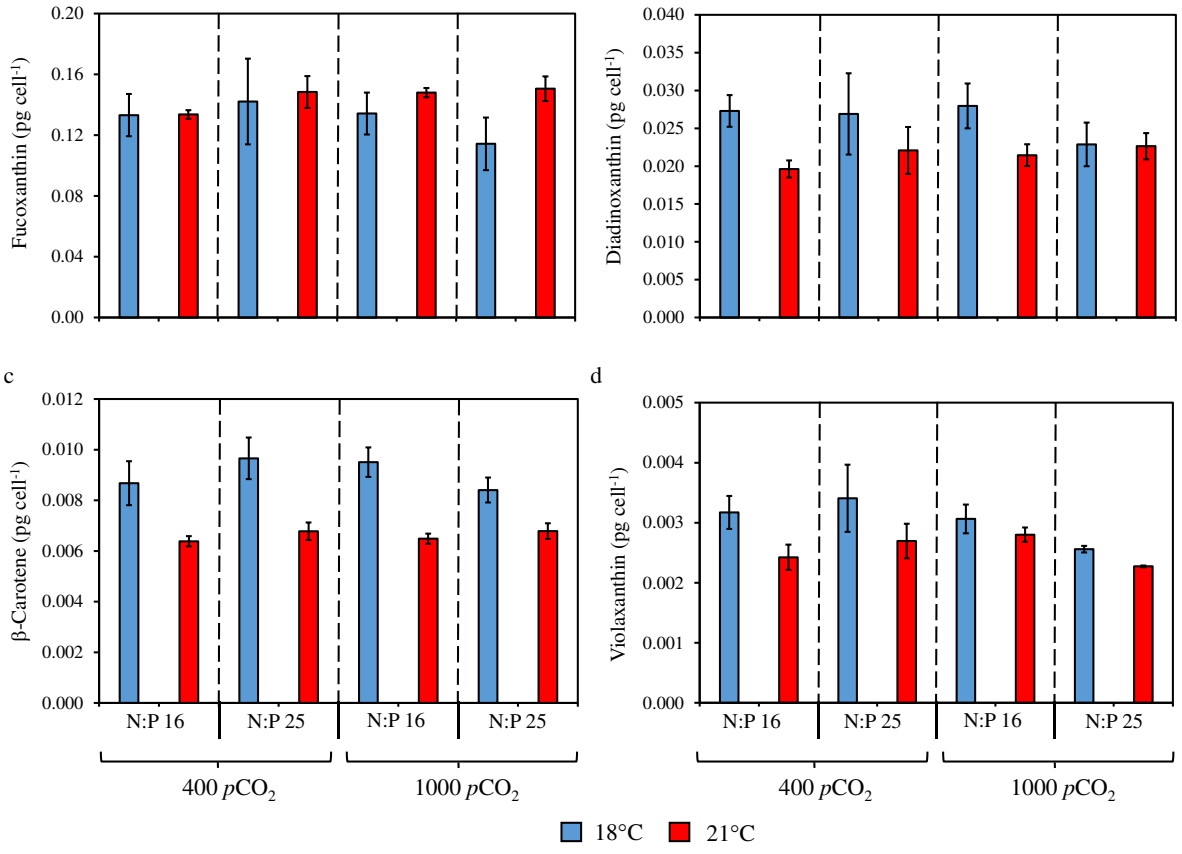

Supplementary Figure 2.4: Cellular carotenoids concentration. (a) Fucoxanthin, (b) Diadinoxanthin, (c) β-Carotene, (d) Violaxanthin. X-axis represents N:P ratios and pCO_2. Colours represent temperature (blue = 18°C, red = 21°C). Data as mean ± standard deviation.

Chapter 3

Resilience of coastal planktonic communities to warming, ocean acidification and higher dissolved nutrients N:P ratios during a spring bloom event

Hugo Duarte Moreno[1], Martin Köring[1], Karen H. Wiltshire[1,2], Maarten Boersma[1,3], Cédric L. Meunier[1]

[1]Alfred-Wegener-Institut, Helmholtz-Zentrum für Polar- und Meeresforschung, Biologische Anstalt Helgoland, Germany

[2]Alfred-Wegener-Institut, Helmholtz-Zentrum für Polar- und Meeresforschung, Wattenmeerstation, Germany

[3]University of Bremen, FB 2, Bremen, Germany

Manuscript

3.1. Abstract

Global change puts coastal marine systems under pressure, as higher temperature, pCO_2 and dissolved nutrients N:P ratios affect the structure and functioning of planktonic food webs. Here, we conducted a mesocosm experiment with a multiple-driver design to assess the impact of future global change scenarios on a typical temperature shelf sea plankton spring bloom. The experimental treatments were based on the RCP 6.0 and 8.5 scenarios developed by the IPCC, which were extended (ERCP) to integrate the future predicted changing nutrient inputs into coastal waters. Our results reveal a high degree of resilience of planktonic food webs against the environmental changing conditions, as we did not observe significant shifts in community composition and biomass of phytoplankton, microzooplankton, and bacterioplankton. However, the combined effect of warming, ocean acidification and higher N:P ratios in the ERCP 8.5 scenario favoured the development of copepods. These findings suggest that marine planktonic communities may be little affected by global change during spring blooms in temperate systems.

3.2. Introduction

Phytoplankton accounts for 50% of the global primary production (Behrenfeld et al., 2001), and for over 90% of all primary production in the oceans (Duarte and Cebrian, 1996). These photosynthetic organisms are the basis of pelagic food webs and play a major role in biogeochemical cycles of different elements, including carbon, nitrogen, phosphorus, and silica (Buesseler, 1998; Bowler et al., 2010). The phytoplankton spring bloom is the most productive annual event in temperate systems, and provides energy and nutrients to higher trophic levels after winter (Townsend et al., 1994). Spring blooms are mainly triggered by environmental conditions, such as increasing sunlight irradiance and temperature at the beginning of spring (Huppert et al., 2002; Wei et al., 2004; Wiltshire et al., 2008), and their intensity depends on nutrient availability and top-down control mechanisms. Therefore, human-induced changes in environmental conditions can alter the dynamics of a phytoplankton spring bloom event. For instance, warming was shown to cause shifts in the timing of spring phytoplankton blooms (Lewandowska and Sommer, 2010; Sommer and Lewandowska, 2011), which could disrupt energy flow to higher trophic levels, causing a mismatch of food supply and demand in aquatic systems (Cushing, 1990). A spring bloom mesocosm experiment has also revealed the negative effect of warming on phytoplankton biomass, mean cell size, and large diatoms (Sommer and Lengfellner, 2008). Furthermore, higher pCO_2 has been found to stimulate production and exudation of carbon-rich components by phytoplankton during a spring bloom, channelling more photosynthates into the microbial loop (Engel et al., 2014). Additionally, the dissolved nitrogen:phosphorus (N:P) ratio of European coastal seas has substantially increased over the past decades (Grizzetti et al., 2012), which may promote P-limitation of marine primary producers (Sarker, 2018). On the other hand, a time series analysis with data from the North Sea revealed that phytoplankton spring blooms dynamics hardly changed since 1975, despite the clear shifts in environmental conditions (Wiltshire et al., 2008). Since these changes in environmental conditions are expected to continue (IPCC, 2021), we urgently need to understand how multiple global change drivers (i.e., temperature, pCO_2, N:P ratios) concomitantly influence the dynamics and community structure of spring blooms.

The few existing studies on the combined effects of multiple global change drivers on phytoplankton blooms indicate that higher pCO_2 combined with warming alter phytoplankton assemblages by benefiting small-sized species (Hare et al., 2007; Maugendre et al., 2015; Hyun et al., 2020) and coccolithophores over diatoms (Feng et al., 2009). Conversely, Sett et al. (2018) found that warming and pCO_2 favour larger diatoms in a community experiment.

Another experiment, however, proved no significant effect of warming and ocean acidification on species composition in a community without coccolithophores, but rather a decrease in phytoplankton biomass under such conditions (Sommer et al., 2015). Limited nutrient supply can also intensify the impact of increasing temperatures, leading to cell size shrinking greater than only under warming (Peter and Sommer, 2012). At the same time, warming has been shown to intensify the increase of C-to-nutrient ratio of a phytoplankton community when combined with higher N:P ratios of dissolved inorganic nutrients during a spring bloom (De Senerpont Domis et al., 2014). This is especially critical for primary consumers because the elemental stoichiometry of autotrophs directly determines their quality as food (Sterner and Elser, 2002). Additionally, pCO_2 is also known to be positively correlated to C-to-nutrient ratios in phytoplankton biomass (Schoo et al., 2013), raising questions about how the interaction of different drivers can affect the planktonic food web as a whole. Overall, these studies indicate complex response mechanisms of phytoplankton communities to multiple drivers, with cascading effects to higher trophic levels.

Micro- and mesozooplankton represent major links between primary producers and higher trophic levels, a role which is particularly important during a spring bloom (Aberle et al., 2007). As any ectotherm, zooplankton are sensitive to temperature, since warming can increase respiration rates and, therefore, cause higher demands for energy intake, which can in turn influence the top-down control mechanisms on phytoplankton communities (Castellani et al., 2005; Garrido et al., 2013). Conversely, micro- and mesozooplankton are rather insensitive to direct effects of ocean acidification alone (Aberle et al., 2013; McConville et al., 2013; Horn et al., 2016; Bailey et al., 2017). Multiple driver experiments suggest that higher temperature and pCO_2 benefit microzooplankton abundance and grazing (Rose et al., 2009; Horn et al., 2016). The impacts of higher temperature and pCO_2 on zooplankton are complex, as grazers can also be indirectly impacted by the quality of their phytoplankton prey. Boersma et al., (2016) found that temperature influences dietary preference in omnivorous copepods, which preferentially consume phytoplankton over microzooplankton when temperature rises, suggesting a higher top-down control on phytoplankton under warmer conditions. The copepod demand for phosphorus is also expected to shift under warmer temperatures (Mathews et al., 2018), leaving open questions on how grazers will react to the effects of global change drivers, as well as to the changes in their prey quality induced by the same drivers.

Mesocosm approaches are among the most suitable experimental techniques to study dynamics of plankton communities. This method can incorporate large assemblages of natural

planktonic communities and addresses mechanistic relationships across many trophic levels that occur in complex natural systems, unlike small unrealistic controlled experiments. Hence, mesocosm experiments provide a high level of ecological relevance, whereas still convenient for experimental manipulation (Boyd et al., 2018). Even though studies on individual global change drivers are important to understand their effect on planktonic communities, there is still a paucity of scientific studies on multiple driver studies despite the simultaneous alterations of these drivers in natural environments. Here we applied an integrated multiple driver design to assess the effect of global change scenarios developed by the Intergovernmental Panel on Climate Change (IPCC), combined with altered N:P ratios, on natural coastal plankton communities during a spring bloom event.

3.3. Materials and Methods

Experimental design

In our mesocosm experiments, temperature and pCO_2 levels were chosen based on predictions by the IPCC for the end of the 21st century (IPCC, 2021). They represented (1) Ambient conditions, (2) a moderate global change scenario based on RCP 6.0 (+1.5°C and -0.2 pH), and (3) a more severe global change scenario based on RCP 8.5 (+3°C and -0.3 pH). As nutrient inputs are also predicted to change towards considerably higher nitrogen to phosphorus ratio (N:P) in coastal European seas (Grizzetti et al., 2012), we extended the RCP scenarios (ERCP) to include the predicted changing nutrient regime, with the Ambient and the ERCP scenarios having a dissolved inorganic nutrients N:P ratio (molar) of 16 (Redfield ratio), and 25, respectively, at the onset of the experiment.

Mesocosm system

The experiment was conducted in the mesocosm facility located at the Alfred-Wegener-Institut, Helmholtz-Zentrum für Polar- und Meeresforschung (AWI) Wadden Sea Station on the Island of Sylt (Pansch et al., 2016). The outdoor facility consists of 12 double-hulled, insulated, cylindrical tanks, made of UV stabilised high-density polyethylene (HDPE; Spranger Kunststoffe, Plauen, Germany). Each tank has a height of 85 cm, an inner diameter of 170 cm, and a net volume of 1800 L. To avoid introduction of unwanted material, each mesocosm tank is covered with a translucent lid made of HDPE, which allows penetration of 90% of the photosynthetically active radiation. An adjustable flow-through system from the AWI Wadden

Sea Station constantly supplies the tanks with fresh, unfiltered seawater. The temperature is regulated every 30 minutes by a Labview-based computer software (4H-Jena engineering, Jena, Germany), which periodically receives temperature data from Hydrolab DS5X Probes (OTT Messtechnik GmbH, Kempten, Germany) and controls external cooling units (Titan 2000 or Titan 4000 Aqua Medic, Bissendorf, Germany) and heaters (Titanium heater 500 W, Aqua Medic, Bissendorf, Germany).

We installed 450 L low-density polyethylene (LDPE) bags in each mesocosm tank. The LDPE bags were filled with seawater collected from the open North Sea with natural plankton communities (see details about filling procedures below). The bags were fixed in the centre of the tanks. By regulating the temperature and aerating the surrounding flow-through water as described above, we indirectly regulated temperature and pCO_2 in the LDPE bags. We replicated each treatment four times, for a total of 12 mesocosms. The temperature in the Ambient mesocosms was adjusted daily to the seawater temperature measured at Helgoland Roads station (54°11.3'N, 7°54.0'E) and was increased by 1.5 and 3.0°C for the ERCP 6.0 and ERCP 8.5 scenarios, respectively. We mounted small mortar mixer engines (TC-MX 1400-2 E, Einhell Germany AG, Landau/Isar, Germany) on top of each mesocosm tank, which were connected to a custom-made HDPE propeller (AWI, Helgoland, Germany). To avoid sedimentation of the planktonic organisms and mimic the relatively well mixed water column condition found in the southern part of the North Sea (van Leeuwen et al., 2015), the submerged propellers gently homogenised the water column of the LDPE bags at 50 rpm in a 1-minute-mixing/30-minutes-pause interval. To reach the desired pCO_2 in the different ERCP scenarios, streaming pipes aerated each tank with the desired gas mixture in the water outside the LDPE bags. The aeration outside the mesocosm bag was intended to prevent damage to fragile planktonic organisms that are sensitive to bubbling. The Ambient conditions mesocosms were bubbled with pressured air, ERCP 6.0 scenario with 800 µatm pCO_2 and the ERCP 8.5 with 1000 µatm pCO_2, which were determined by a central CO_2-mixing facility (GMZ 750, HTK, Hamburg, Germany). The mesocosm cover trapped the pCO_2-controlled atmosphere above the mesocosm water column, hence realistically mimicking future environmental conditions.

Seawater collection and filling of the mesocosm bags

On the 21st of March 2019, we collected water off the coast of Sylt (55°03'41.1" N 8°26'00.3" E), with the AWI research vessel Mya II during rising tide. During the water collection and filling procedure of the mesocosm bags, we did not use any pumps, but transferred seawater via gravity flow to prevent any damage to fragile organisms within the

planktonic community. To sample seawater onboard, we submerged a 500 L tub attached to a crane to fill it with seawater from the upper 5 meters sea surface. The tub was subsequently lifted up to let the water flow through a hose into 1000 L polyethylene Intermediate Bulk Containers (IBC, AUER Packaging GmbH, Amerang, Germany). We attached a 1000 µm mesh to the end of the hose, to exclude larger organisms, such as jellyfish and fish larvae. This procedure prevented any disproportionally large impact which larger consumers can have on the rest of the plankton community in a 450 L enclosed water volume. Furthermore, this approach enabled us to focus on bottom-up processes since there was no top-down control on mesozooplankton. The procedure was repeated until eight IBC tanks were filled (8000 L), which took about three hours.

Before filling the mesocosm bags, we first gently homogenised the water in the IBC tanks. Then, we attached a four-way-distributor to one IBC tank, and the tank was lifted by a wheel -loader to allow gravity flow of the seawater into the mesocosm bags. At the end of each connected hose, a flowmeter measured the exact volume of water which was released into each mesocosm bag. We filled 80 L of seawater simultaneously to four bags, and then filled the next quadruplet of mesocosms. This enabled an equal distribution of the water contained in each IBC tank among the twelve mesocosms. This procedure was repeated until all mesocosm bags were filled with 450 L of North Sea water. This procedure enabled us to achieve homogenous replicates at the onset of the experiment, which is a major challenge when conducting mesocosm experiments (Boyd et al., 2018). Once the filling procedure was completed, we directly measured the dissolved N and P concentrations in each mesocosm bag according to the method described in Grasshoff et al. (1999), and subsequently adjusted the dissolved N:P ratios to 16 (Ambient conditions) and 25 (ERCP scenarios). We added DIP to reach 2.4 µmol L^{-1} in the Ambient scenario and 1.5 µmol DIP L^{-1} in the ERCP 6.0 and 8.5 scenarios, following results of natural DIN concentrations (38.2 µmol L^{-1}) measured in the seawater we sampled. At the onset of the experiment, we bubbled a small volume of seawater with pure CO_2, which lowered its pH to 4.8 at saturation. Using a 50 mL plastic syringe connected to a 1 m hose, we injected 500 mL (ERCP 6.0) and 1100 mL (ERCP 8.5) of the saturated CO_2 seawater at the bottom of the mesocosm bags to reduce the initial pH values by -0.2 and -0.3 for the ERCP 6.0 and ERCP 8.5 scenarios, respectively. During the rest of the experiment, the pH was influenced by the planktonic communities through photosynthesis and respiration, and by the atmospheric pCO_2 (see above). The experiment was conducted over 26 days.

Physical-chemical conditions in the mesocosm bags

Temperature, pH, light irradiance and salinity were measured every day at 9:00 (Supplementary Figure 3.1). Light intensity was measured just below the water surface with a Li-cor Li-250 Light meter (Bad Homburg, Germany). Temperature measurements were done directly inside the mesocosm bags using a Testo 110 – temperature meter (Lenzkirch, Germany). Total alkalinity (TA) samples were taken by plunging, filling, and closing an air-tighten 100 mL transparent glass bottle inside the mesocosm to avoid air bubbles. The samples were stored at 4°C before being analysed within 36 hours through linear Gran-titration (Dickson, 1981) using a TitroLine alpha plus (Schott, Mainz, Germany). Samples for dissolved inorganic nutrients and TA were taken at an interval of 1-3 days depending on the phytoplankton bloom development.

For further analyses, water was collected from each mesocosm bag with clean plastic beakers and brought to the lab for processing also at an interval of 1-3 days. The first parameter measured was pH using a WTW pH 330i equipped with a SenTix 81 pH electrode (Letchworth, England). Salinity was measured with a WTW CellOx 325 (probe Oxi 197-S, Letchworth, England). Dissolved inorganic nutrients samples were collected with a sterile plastic syringe and filtered through a 0.45 µm PTFE filter (Minisart, Sartorius, Goettingen, Germany) fitted to the syringe. For this step, the first 2 mL of the sample were used to rinse the filter and directly discarded. Samples for DIN and DIP were stored at -20°C, and the samples for DSi were stored at 4°C, until photometric analyses (Grasshoff et al. 1999) (Supplementary Figure 3.2a-c). Results of TA, pH, temperature, salinity, atmospheric pressure, DIP and DSi were computed to determine the carbonate system (Supplementary Table 3.1) using the CO2Sys Excel Macro (Pierrot et al., 2006) with a set of constants defined by Dickson and Millero (1987).

To quantify dissolved organic carbon (DOC), 20 mL of seawater were collected from the mesocosms with a sterile plastic syringe and filtered through a 0.45 µm PTFE filter. The first 2 mL of the sample was used to rinse the filter and were discarded. The samples were collected in technical duplicates and stored in HCl washed and precombusted glass vials. Samples were acidified with HCl and kept at -20°C until analysis. Dissolved organic carbon was determined by high temperature catalytic oxidation and subsequent nondispersive infrared spectroscopy and chemiluminescence detection, automatically conducted in a TOC-$L_{CPH/CPN}$ analyzer (Shimadzu, Kyoto, Japan). Results of DOC are displayed in the Supplementary Figure 3.2d.

Planktonic community

To determine phyto- and microzooplankton species composition and biomass, 100 mL of mesocosm seawater were sampled at an interval of 1-3 days and stored in amber glass bottles and immediately fixed with Lugol's iodine solution (2% final concentration). Phyto- and microzooplankton were identified using an inverted microscope Olympus IX51 following the method described in Utermöhl (1958). Planktonic organisms were identified to species level, or pooled into size-shape dependent groups when species identification was not possible.

Mesozooplankton was sampled on the days 4, 11, 20 and 26 of the experiment by sieving at least 5 L of seawater from the mesocosm through a 200 µm nylon mesh. The organisms caught on the mesh were flushed back into a 50 mL transparent Kautex container with sterile filtered seawater (0.2 µm), and immediately fixed with formaldehyde. The mesozooplankton community composition was determined by counting the whole sample, or three subsamples when splitting was necessary with a Folsom splitter (McEwen et al., 1954; Sell and Evans, 1982). The counting took place using a Bogorov chamber under stereomicroscope (Leica M205), and taxonomic identification was conducted as described in Boersma et al. (2015). Samples for bacterioplankton quantification were taken by sieving 5 mL of seawater through a 20 µm nylon mesh, and were fixed with glutaraldehyde (0.1% final concentration) and frozen at -80°C until analysis. The samples were thawed in a water bath (20°C) and stained with SYBR Green (Invitrogen) following the method described by Marie et al. (2005). Bacteria cells were enumerated by flow cytometry (BD AccuriTM C6 Plus, BD Biosciences) using a flow rate of 12 µL min^{-1} for 1-2 minutes and diluted in sterile filtered seawater (0.2 µm) when bacterial cell number was higher than 400 events s^{-1}. As SYBR Green stains DNA without distinguishing taxonomical groups, our results of bacterioplankton include any organisms within the range of picoplankton cell size (~0.2 – 2 µm), potentially also including picocyanobacteria. Biovolume of phytoplankton and microzooplankton was calculated from the measurement of cell dimensions using geometric formulae according to Hillebrand et al. (1999). Cell volume was converted into carbon following the equations of Menden-Deuer and Lessard (2000) for diatoms (pg C $cell^{-1}$ = 0.288 x $V^{0.811}$), dinoflagellates (pg C $cell^{-1}$ = 0.760 x $V^{0.819}$) and other protist plankton with the exception of ciliates (pg C $cell^{-1}$ = 0.216 x $V^{0.939}$), where V is the cell volume in μm^3. Ciliate carbon content was calculated as 0.19 pg C μm^{-3} according to Putt and Stoecker (1989). Bacteria cell counts were converted into carbon using the 20 fg C $cell^{-1}$ factor defined by Lee and Fuhrman (1987).

Elemental composition (CNP) of seston was determined by filtering 200 mL of seawater through precombusted GF/F filters. The filters were dried in a drying oven at 60°C until analysis. Carbon and nitrogen content were measured with a Vario Micro Cube elemental analyser (Elementar, Hanau, Germany). Phosphorus content was quantified as orthophosphate after oxidation by molybdate-antimony (Grasshoff et al. 1999). In the following, we characterized the planktonic community using functional groups: Phytoplankton, Bacterioplankton, Microzooplankton, and Mesozooplankton. The phytoplankton group included diatoms, phytoflagellates, and autotrophic dinoflagellates, according to the descriptions of trophic mode for each species (summarized by Kraberg et al. 2010). The microzooplankton group comprised heterotrophic and mixotrophic dinoflagellates and ciliates. Mesozooplankton species were all heterotrophic organisms larger than 200 µm.

Statistical analyses

Statistical analyses were performed using R 3.4.3 software (R Core Team, 2022). For all analyses, the threshold of significance was set at 0.05. Effect of the ERCP scenario on seston elemental stoichiometry and biomass of phytoplankton, microzooplankton, bacterioplankton as well as mesozooplankton biomass was assessed by linear mixed-effects models (LMM), applying day of the experiment as random effect. Posteriorly, Post-hoc test (Tukey test) was used to determine differences across scenarios. Data was log-transformed when normality and homoscedasticity of residuals was not met. Effects of the ERCP scenarios on the phyto- and microzooplankton species composition and affinity of species to the scenarios were analysed through the Principal Response Curve (PRC) using the 'vegan' R package. This test shows the degree of difference over time of the community composition in the ERCP scenarios in comparison to the Ambient condition, which is set as a control (effect '0'). Species weights are analysed as means of their regression coefficient against the control. When the curve of difference of the ERCP scenario has a positive slope, positive values for species weights represent affinity of this species to the scenario, whereas negative values would represent negative effect of the scenario on such species and *vice versa*.

3.4. Results

Seston stoichiometry

Seston C:N (molar) was constant around 8 during the first week of the experiment, and it increased from day 9 on to reach circa 15 from day 15 until the end of the experiment. Seston C:N was not statistically different across scenarios (LMM, $F_{149,8}$ 2.114, $p > 0.05$, Figure 3.1a). Seston C:P started at 227.4 in all scenarios and increased after day 9 to day 11. Throughout the experiment, seston C:P was lower in the Ambient than in both ERCP scenarios (LMM, $F_{149,8}$ 39.111, $p < 0.05$, Figure 3.1b). Seston N:P was 26.9 on day 1, but over the entire experiment, it was significantly lower in the Ambient than in the other two scenarios (LMM, $F_{149,8}$ 26.694, $p < 0.05$, Figure 3.1c).

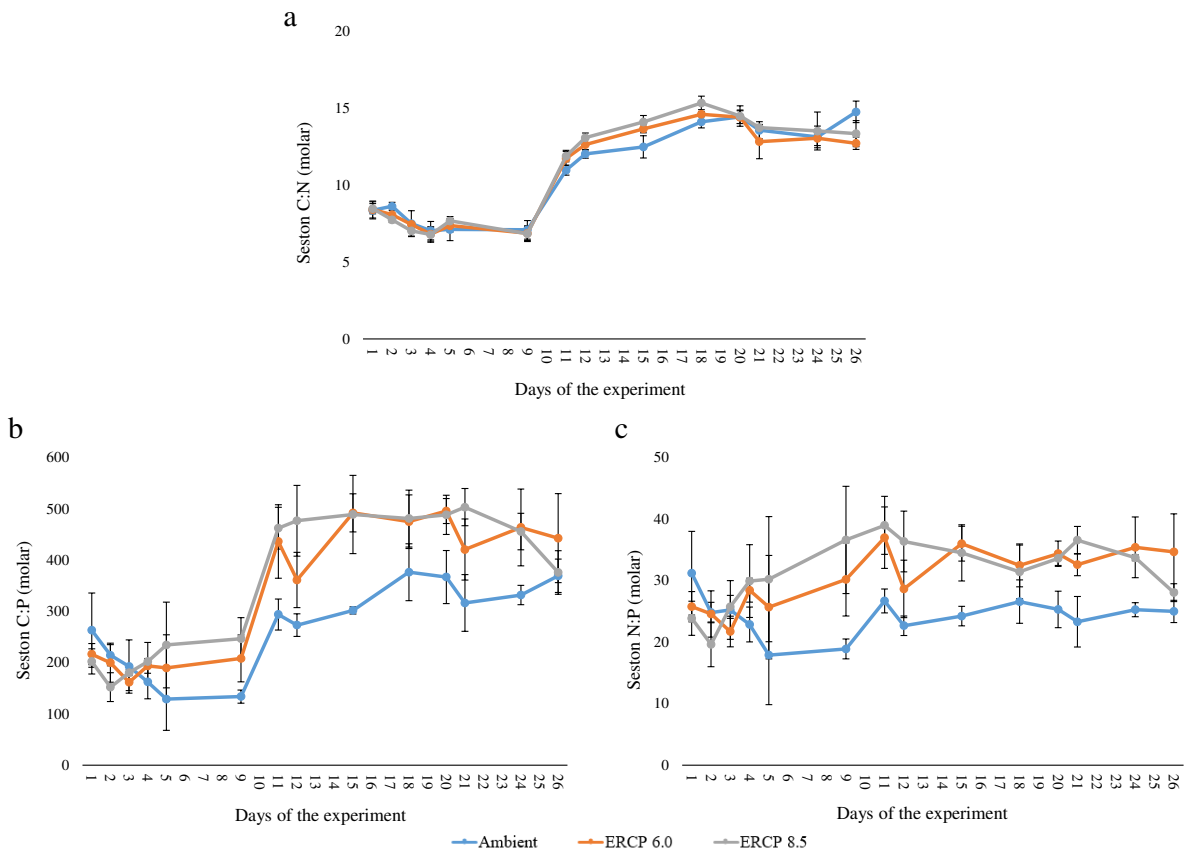

Figure 3.1: Seston elemental stoichiometry. (a) Seston Carbon:Nitrogen ratio. (b) Seston Carbon:Phosphorus ratio. (c) Seston Nitrogen:Phosphorus ratio. X-axis represents the days of the experiment, different colours represent the Ambient treatment and Extended Representative Concentration Pathway (ERCP) scenarios (blue = Ambient, orange = ERCP 6.0, grey = ERCP 8.5). Data as mean ± standard deviation

Phytoplankton

Across all scenarios, phytoplankton biomass exponentially increased from 329.3 µg C L^{-1} on day 1 to 2604.2 µg C L^{-1} (±659.5 SD) on day 11, when it started to decrease. At the end of the experiment (day 26) phytoplankton biomass was 890.5 µg C L^{-1}. No statistically significant difference in phytoplankton biomass was found across scenarios (LMM, $F_{95,9}$ 1.432, $p > 0.05$, Figure 3.2a). During the whole experiment, the phytoplankton community was dominated by diatoms, which made up approximately 80% of all phytoplankton biomass (Figure 3.2b-d). The most abundant taxa were *Thalassiosira sp*. and *Odontella sp*. As phytoplankton biomass started to decline after day 11, the proportion of phytoflagellates (< 20 µm) increased, which made up more than 20% of the phytoplankton biomass from day 20 onwards. The phytoplankton community was similar across all scenarios, and we did not observe any effect of the experimental treatments of the relative abundance of different species/groups of phytoplankton (Figure 3.2b-d and Supplementary Figure 3.3).

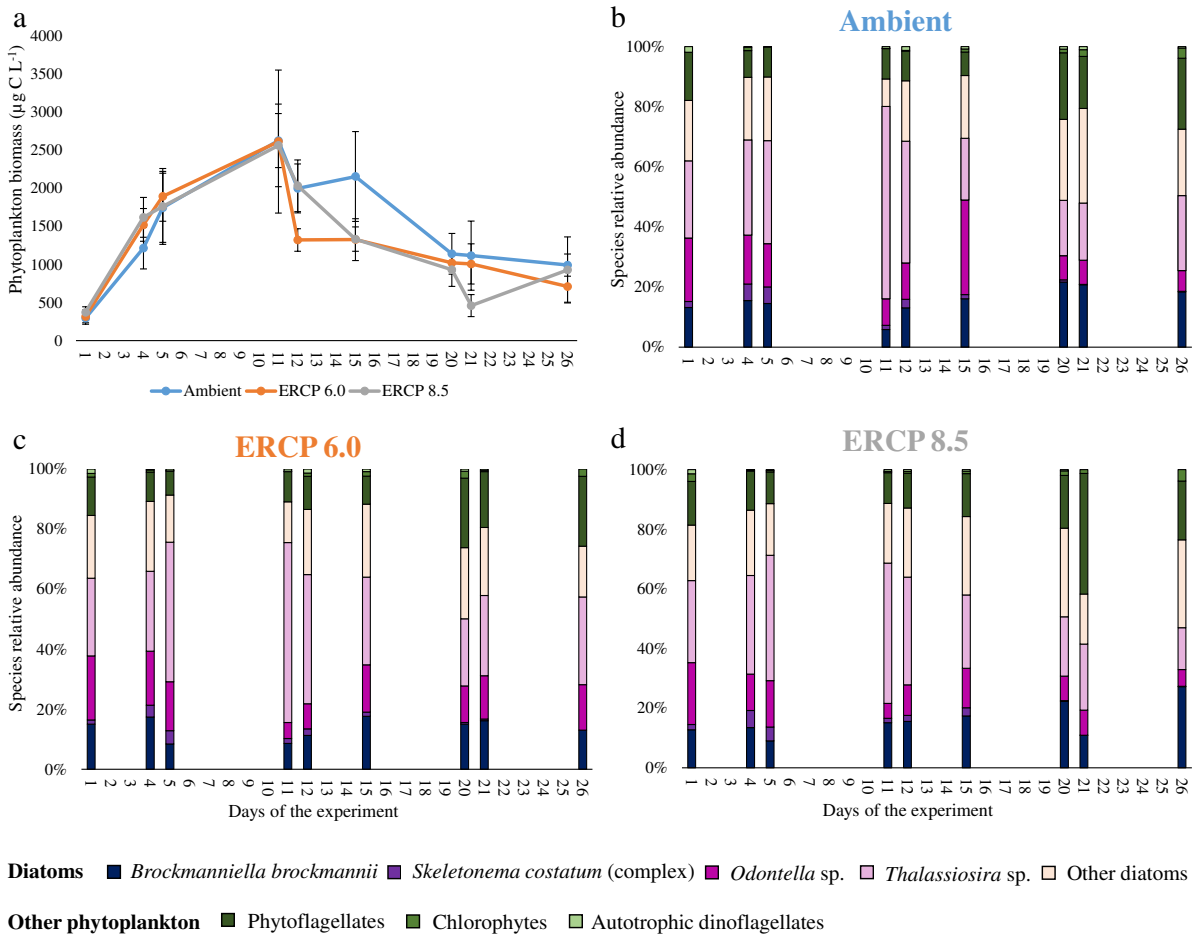

Figure 3.2: Phytoplankton community biomass and composition. (a) Phytoplankton biomass. (b,c,d) Relative abundances of different taxa of the phytoplankton communities under the different scenarios. X-axes represent the days of the experiment, different colours represent the Ambient treatment and Extended Representative

Concentration Pathway (ERCP) scenarios (blue = Ambient, orange = ERCP 6.0, grey = ERCP 8.5). Data as mean ± standard deviation.

Bacterioplankton

Bacterioplankton biomass was low at the beginning of the experiment in all scenarios (43.5 µg C L^{-1}), and steeply increased on two occasions, from day 7 to day 9, and from day 15 to day 18. After this second bloom, bacterioplankton biomass decreased to reach lower levels on day 21 (489.9 µg C L^{-1}) and stabilized until the end of the experiment. Despite the fluctuations seen in bacterioplankton biomass, it was not affected by the ERCP scenarios (LMM, $F_{156,9}$ 0.501, $p > 0.05$, Figure 3.3).

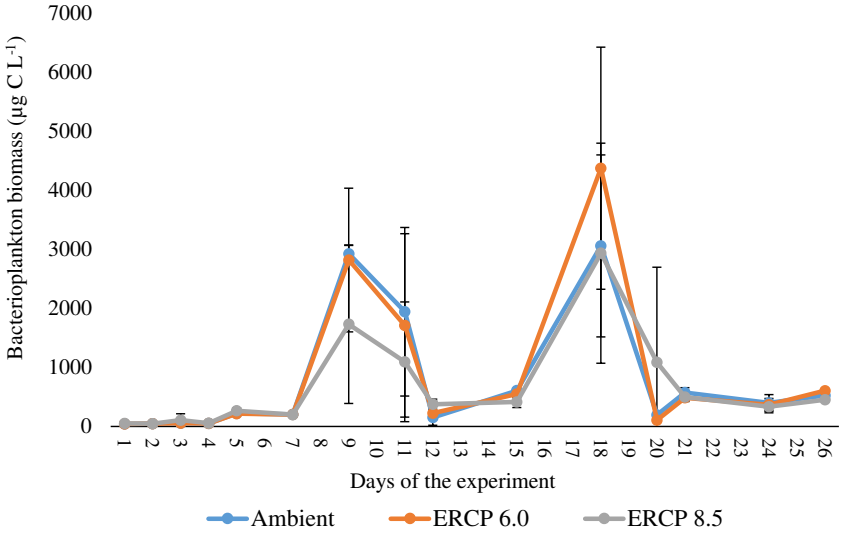

Figure 3.3: Bacterioplankton community biomass. X-axis represents the days of the experiment, different colours represent the Ambient treatment and Extended Representative Concentration Pathway (ERCP) scenarios (blue = Ambient, orange = ERCP 6.0, grey = ERCP 8.5). Data as mean ± standard deviation.

Microzooplankton

Overall, microzooplankton biomass continuously increased from the beginning to the end of the experiment in all treatments. Over the whole experiment, there was no significant effect of the ERCP scenarios on microzooplankton biomass (LMM, $F_{95,9}$ 0.257, $p > 0.05$, Figure 3.4a). The microzooplankton community was composed mostly of ciliates on day 1, but the relative proportion of ciliates gradually decreased, and the microzooplankton community was dominated by dinoflagellates from day 11 on (Figure 3.4b-d). The dominant dinoflagellate taxon was Gymnodiniales, about 60% of all microzooplankton on the last day of the experiment,

but biomass of this taxon was not statistically different across scenarios (LMM, $F_{95,9}$ 0.257, $p > 0.05$). The genera *Strobilidium* sp. and *Strombidium* sp. were the most abundant ciliates throughout the experiment.

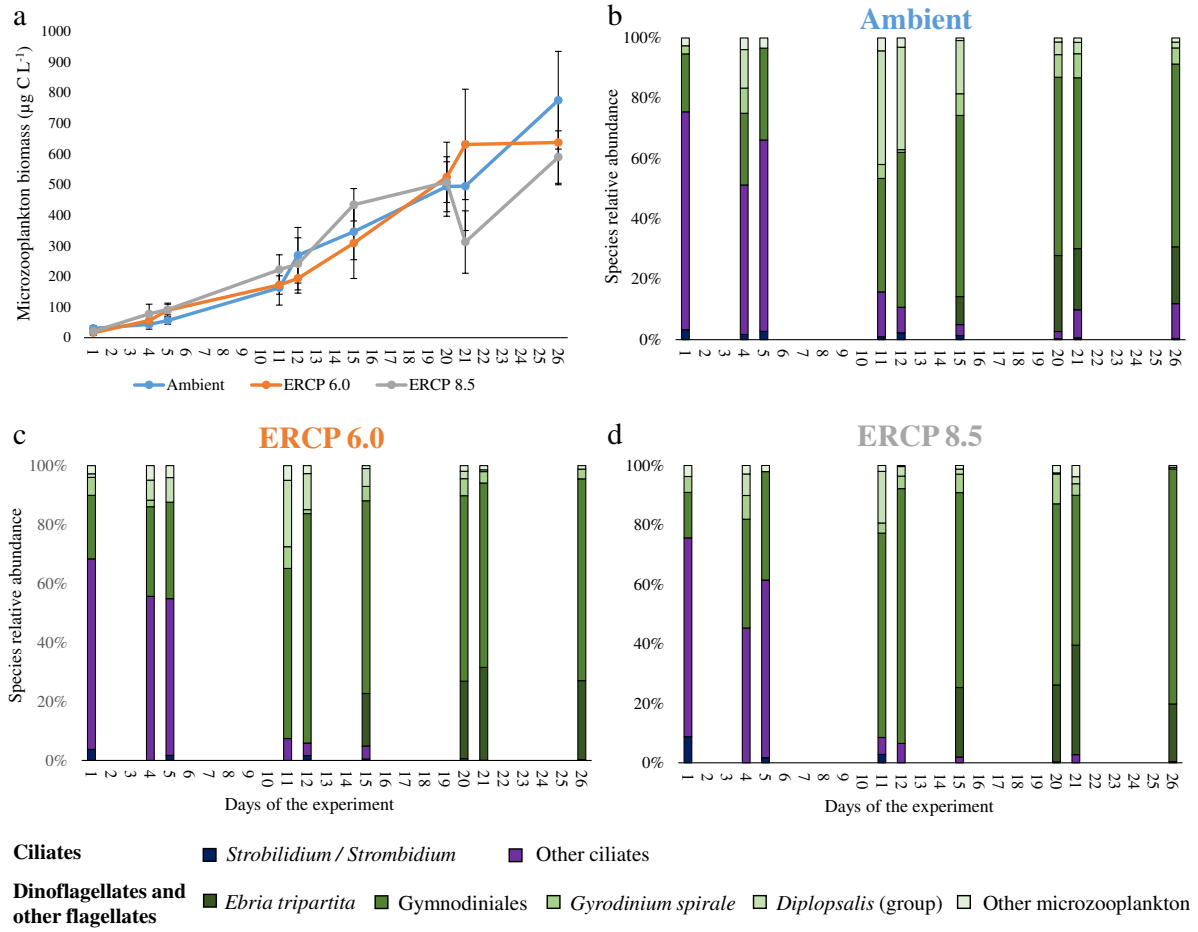

Figure 3.4: Microzooplankton community biomass and composition. (a) Microzooplankton biomass. (b,c,d) Relative abundances of different taxa of the microzooplankton communities under the different scenarios. X-axes represent the days of the experiment, different colours represent the Ambient treatment and Extended Representative Concentration Pathway (ERCP) scenarios (blue = Ambient, orange = ERCP 6.0, grey = ERCP 8.5). Data as mean ± standard deviation.

Mesozooplankton

In all scenarios, mesozooplankton abundance increased from day 4 to day 20, (Figure 3.5a). Mesozooplankton abundance was significantly higher in the ERCP 8.5 than in the Ambient (LMM, $F_{41,9}$ 5.994, $p < 0.05$), while the ERCP 6.0 scenario was not statistically different from the Ambient nor from the ERCP 8.5 scenarios. Throughout the experiment, the mesozooplankton community was dominated by copepods in all scenarios, mostly *Acartia* sp. and *Temora longicornis*. Overall, copepods were more abundant in the ERCP 8.5 (LMM, $F_{41,9}$ 7.691, $p < 0.05$, Figure 3.5b-d) than in the Ambient scenario. Similarly, copepod abundances in the ERCP 6.0 scenario were not statistically different from those in the Ambient and ERCP

8.5 scenarios (PostHoc, Tukey test, on LMM, $p > 0.05$). No other mesozooplankton group was affected by the ERCP scenarios (LMM, $p > 0.05$).

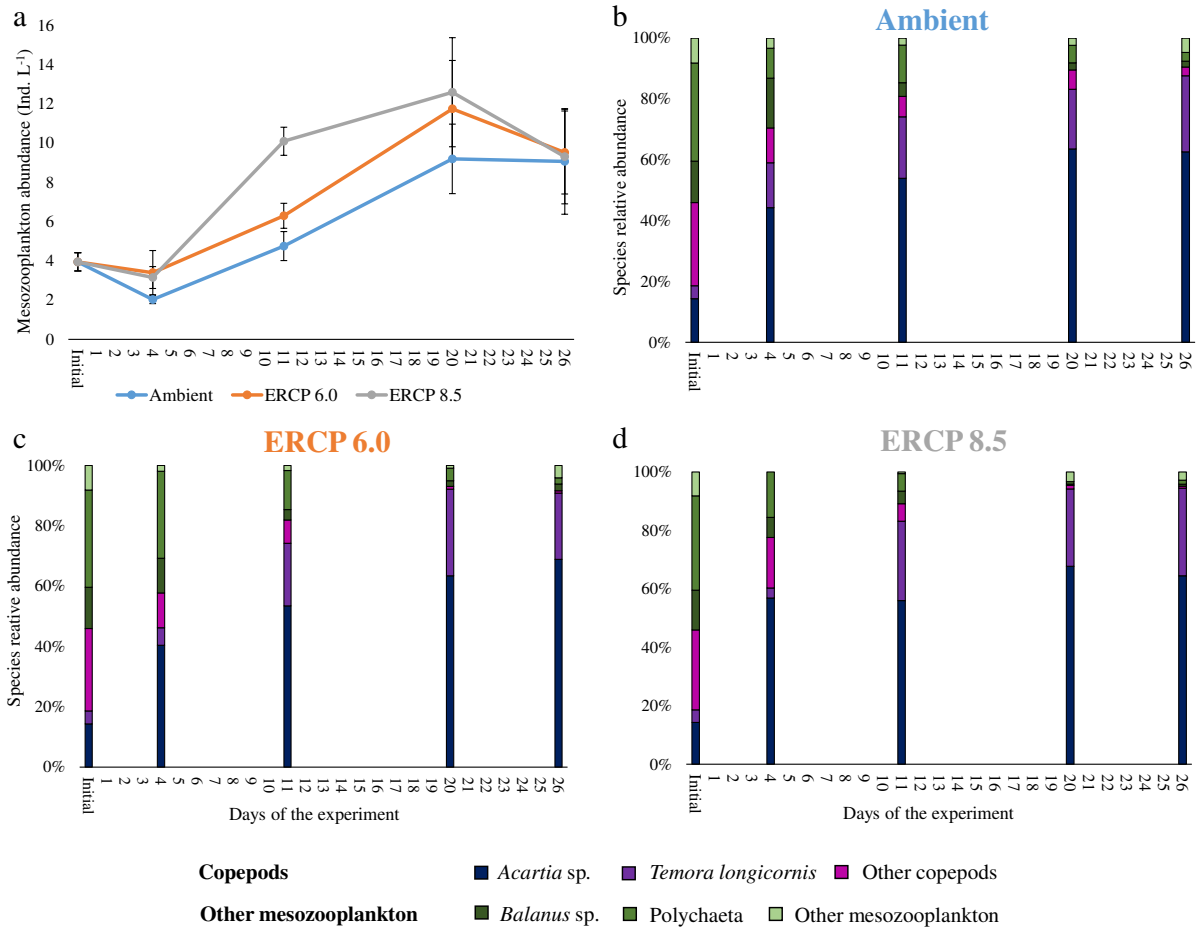

Figure 3.5: Mesozooplankton abundance and community composition. (a) Mesozooplankton abundance. (b,c,d) Relative abundances of different taxa of the mesozooplankton communities under the different scenarios. X-axes represent the days of the experiment, different colours represent the Ambient treatment and Extended Representative Concentration Pathway (ERCP) scenarios (blue = Ambient, orange = ERCP 6.0, grey = ERCP 8.5). Data as mean ± standard.

3.5. Discussion

Overall, our experiment indicates a remarkable stability of planktonic food web communities to global change during the spring bloom. We did not observe any significant influence of global change scenarios on the biomass and community composition of microzooplankton and phytoplankton. Only the abundance of mesozooplankton increased in the ERCP 8.5 scenario in comparison to the Ambient scenario.

Phytoplankton biomass increased rapidly at the beginning of the experiment, and, despite similar biomasses in all scenarios, nutrient depletion was more rapid under the ERCP scenarios in which dissolved silica was exhausted earlier than in the Ambient scenario. Higher temperature and pCO_2 likely enhance the nutrient uptake capacity of phytoplankton, as these drivers facilitate C acquisition and other metabolic processes related to nutrient uptake (van de Waal and Litchman, 2020). This may explain the difference seen here in the rate of dissolved inorganic nutrient decrease, indicating that phytoplankton demand for nutrients is likely to shift in the future, with supplies of silica and phosphorus becoming more critical for spring bloom dynamics. The faster nutrient depletion could also indicate higher phytoplankton production during the bloom. For instance, Feng et al. (2009) and Feng et al. (2021) found evidences of higher phytoplankton productivity during a spring bloom under warming and higher pCO_2 at the absence of large grazers. While higher phytoplankton production might have occurred in our experiment under the future scenarios, we did not observe any difference in phytoplankton biomass between scenarios. Since copepods were more abundant in the ERCP 8.5 scenario, they may have exerted a stronger top-down pressure over phytoplankton and prevented any visible increase in their biomass. The lower availability of phosphorus in the ERCP scenarios may not have been a large limitation for phytoplankton growth as silica was depleted before phosphate, suggesting that the phytoplankton bloom was limited by the availability of silica rather than phosphorus. Nevertheless, seston C:P and N:P stoichiometry rapidly increased at the end of the phytoplankton bloom in the ERCP scenarios, which is likely related to the lower availability of dissolved inorganic phosphorus in the future scenarios. The absence of stoichiometric homeostasis in autotrophs comes from the fact that these organisms obtain energy (sunlight) and nutrients from different, uncoupled, sources within their environment. When nutrient availability or light conditions change, acquisition and storage create the potential for large variations in the C:N:P ratios of autotrophs, which can be defined as conformers (Meunier et al., 2014). This potential shift in phytoplankton stoichiometric quality in the ERCP scenarios could explain the higher seston C:P and N:P ratios in the ERCP 6.0 and 8.5 scenarios compared to the aAmbient scenario. Van de Waal et al. (2010) predicted an increase in phytoplankton C-to-nutrient ratio, and especially in C:P, in response to climate change, which has been observed in other studies (Verschoor et al., 2013; Velthuis et al., 2022). This increase is expected due to the higher availability of DIC in the ocean, which can benefit photosynthesis, and due to lower availabilities of other dissolved inorganic phosphorus (Grizzetti et al., 2012). It has also been proposed that warming may favour protein synthesis,

which is temperature-dependent, and facilitate a decrease in P-rich ribosome intracellular concentration, thereby increasing the cellular C:P ratios (Toseland et al., 2013).

Phytoplankton exudate organic carbon when experiencing nutrient limitation in order to balance their stoichiometry, as carbon keeps being fixed through photosynthesis but other dissolved inorganic nutrients are no longer available (Thornton, 2014; Livanou et al., 2019). This may have occurred in all scenarios around day 7 to 10, when phytoplankton biomass reached its peak and dissolved nutrient were depleted, while DOC and seston C-to-nutrient ratio increased. Bacterioplankton dynamics appeared to be related to the availability of DOC, its biomass increased together with DOC concentrations. Indeed, dissolved organic carbon is the main sources of carbon for pelagic bacteria (Kieber et al., 1989), and is exuded by phytoplankton, especially when dissolved nutrients become depleted after a bloom (Jiao et al., 2010). A second bacterioplankton bloom took place between days 15 and 20, probably because decaying phytoplankton biomass led to an increase in DOC availability.

Microzooplankton biomass increased constantly from the beginning to the end of the experiment. While ciliates were more abundant at the onset of the experiment, dinoflagellates became dominant after phytoplankton biomass reached its maximum. The dominance of dinoflagellates within microzooplankton after a diatom bloom has been described before (Zhao et al., 2020; Song et al., 2021), and may result from a combination of bottom-up processes (availability of suitable prey) and top-down processes since copepods have been reported to preferentially consume ciliates over dinoflagellates (Stoecker and Sanders, 1985; Vincent and Hartmann, 2001). Microzooplankton are also sensitive to food quality (Meunier et al., 2012), and the shift in seston stoichiometry after day 10, may represent a challenge for the small grazers nutrition. Indeed, whereas seston C:P ratio was elevated after day 10, microzooplankton have high phosphorus requirements and preferentially consume prey with low C:P ratios (Meunier et al., 2012; Meunier et al., 2018). The continued microzooplankton growth suggests that microzooplankton efficiently coped with low resource quality. Several mechanisms, including selective and compensatory feeding, have been identified (Meunier et al., 2012), and microzooplankton may have matched their nutritional demands by increasing their consumption of P-rich bacterioplankton (Faithfull and Goetze, 2019). Nonetheless, the biomass of these compartments within the planktonic food web did not vary across the different scenarios, indicating that future environmental conditions may not lead to notable structural changes during a phytoplankton spring bloom event.

Copepods dominated the mesozooplankton and their abundance was positively influenced by the ERCP 8.5 scenario, but the different scenarios did not influence their species composition. Our results are supported by another mesocosm experiment showing that temperature increase can have positive effects on copepods development and reproduction rates (Sommer et al., 2007). In general, warming is expected to increase physiological processes rates in copepods, leading to increasing demand for energy and potentially higher grazing pressure (Isla et al., 2008), suggesting higher top-down control on phytoplankton. Hence, as previously discussed, we expect the higher abundance of copepods in the ERCP 8.5 scenarios to be responsible for a higher grazing pressure masking the positive effect of the environmental conditions under this scenario on phytoplankton biomass. Copepods have specific nutritional demands, and there is evidence of reduced development in copepods under phosphorus limitation (Klein Breteler et al., 2005; Meunier et al., 2016), indicating that even in the ERCP 8.5 scenario copepods were not P-limited. As for microzooplankton, copepods can select their prey to optimize the intake of needed nutrients (Meunier et al., 2015), and copepods can discard excessive carbon when consuming high C:P prey through increased cellular respiration and excretion (Schoo et al., 2013). Furthermore, Laspoumaderes et al. (2022) found a strong correlation between temperature and nutrient demand in ectotherms, and suggested that higher C:P food quality is beneficial for copepod development under warming. Therefore, the lower C:P and N:P ratio may not represent lower food quality, but in fact may match the physiological requirements of copepods under the ERCP 8.5 scenario.

Here, we applied an integrated multiple driver approach in a mesocosm experiment, to identify the effect of different global change scenarios on natural coastal plankton communities. This study suggests that marine planktonic communities may be little affected by global change during spring blooms in temperate systems. However, higher mesozooplankton abundances in the ERCP 8.5 scenario may increase the top-down control on phytoplankton in temperate coastal ecosystems during spring bloom events. Additionally, altered seston stoichiometry due to the lower availability of phosphorus, may shift trophic interactions. Yet, no significant effects of the ERCP scenarios were observed on the microbial loop and the plankton community composition.

3.6. Acknowledgements

We thank the colleagues from Alfred-Wegener-Institut for the technical and scientific support during the experiment, especially Julia Haafke, Petra Kadel, Silvia Peters, Andreas Kornmann, Inga Kirstein, Johannes Rick, Ragnhild Asmus and Harald Asmus. We thank Nelly Tremblay, Johanna Berlinghof and Jil Sonka for their support during the experiment. Sincere thanks to the colleagues who supported us in analysing some of the samples, including Ursula Ecker (mesozooplankton), Tatyana Romanova (dissolved inorganic nutrients) and Bernhard Fuchs (bacterioplankton). We thank Herwig Stibor, Helmut Hillebrand, and Ulf Riebesell for providing their expert opinion on the experimental design. We thank Herwig Stibor and Maria Stockenreiter for providing the LDPE bags in which the experiment was conducted. Special thanks to Bernhard Fuchs and Jan Brüwer for reviewing and commenting on the manuscript.

3.7. Supplementary Material

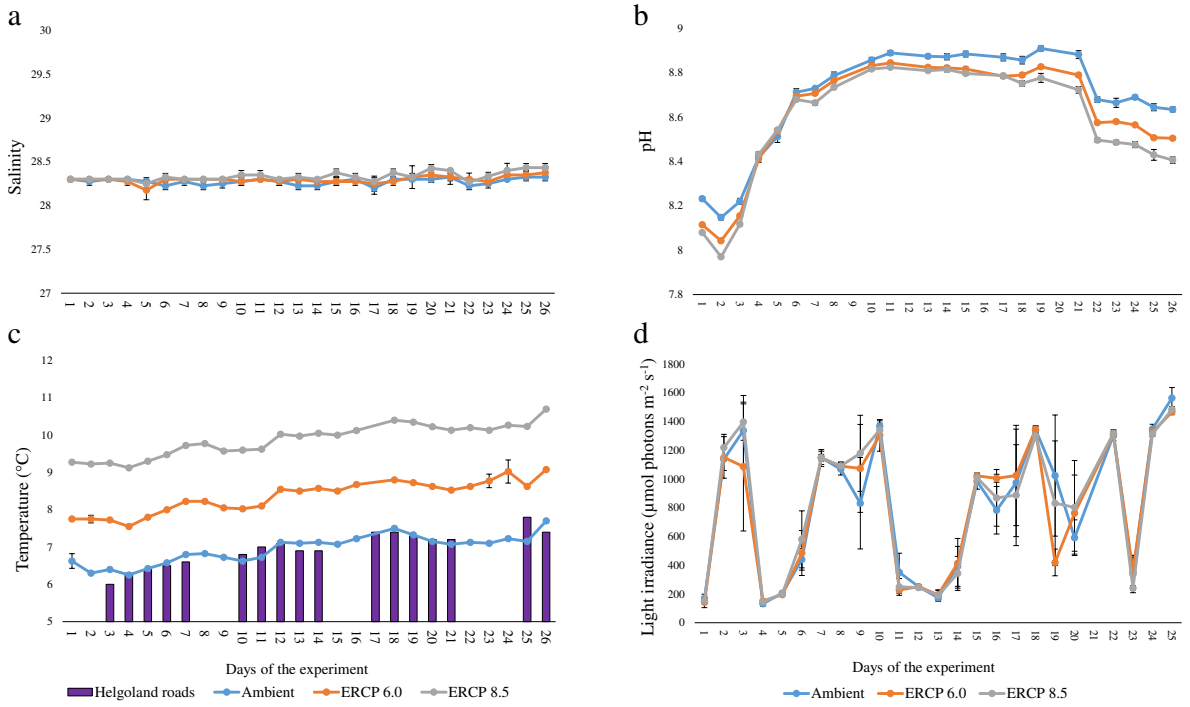

Supplementary Figure 3.1: Environmental conditions in the mesocosms during the experiment. (a) Salinity. (b) pH. (c) Temperature. (d) Light irradiance. Purple bars represent surface seawater temperature at Helgoland Roads; x-axis represents the days of the experiment, different colours represent the Ambient treatment and Extended Representative Concentration Pathway (ERCP) scenarios (blue = Ambient, orange = ERCP 6.0, grey = ERCP 8.5). Data as mean ± standard deviation.

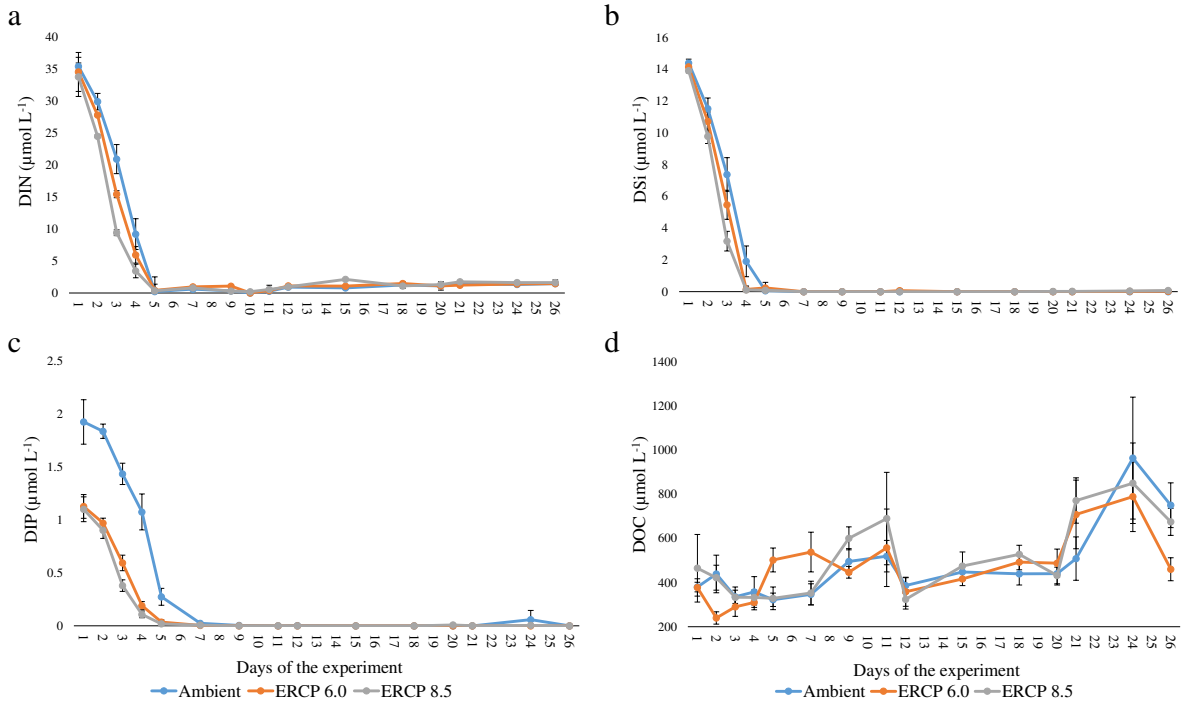

Supplementary Figure 3.2: Dissolved nutrient concentrations in the mesocosms during the experiment. (a) Dissolved inorganic nitrogen (DIN) = NO_x + NH_4^+. (b) Dissolved silicate (DSi) = SiO_3^-. (c) Dissolved inorganic phosphorus (DIP) = PO_4^{3-}. (d) Dissolved organic carbon (DOC); x-axis represents the days of the experiment, different colours represent the Ambient treatment and Extended Representative Concentration Pathway (ERCP) scenarios (blue = Ambient, orange = ERCP 6.0, grey = ERCP 8.5). Data as mean ± standard deviation.

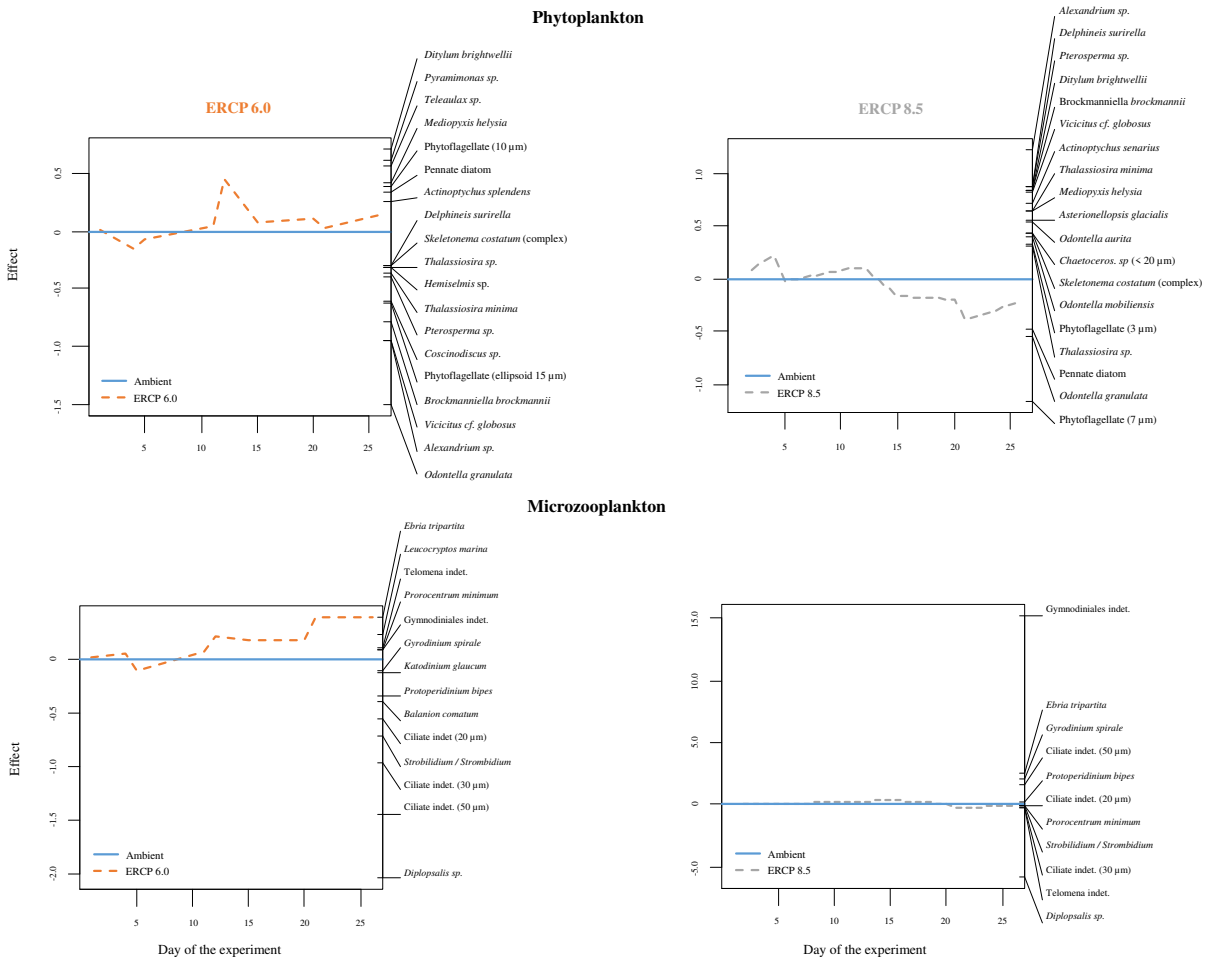

Supplementary Figure 3.3: Principal Response Curve of the plankton community. Graphic representation of the phytoplankton (top) and microzooplankton (bottom) community response over time in the extended Representative Concentration Pathway (ERCP) scenarios 6.0 and 8.5 in comparison to the Ambient treatment. For clarity, only the most affected taxa are displayed on the diagram.

Supplementary Table 3.1: Seawater carbonate chemistry. Seawater carbonate chemistry across scenarios during the experiment. Total alkalinity (TA), dissolved inorganic carbon (DIC), partial pressure of CO_2 (pCO_2), Bicarbonate (HCO_3^-), Carbonate (CO_3^{2-}) and Carbon dioxide (CO_2) were calculated based on pH and total alkalinity (TA) using CO2Sys (Pierrot et al., 2006). Data as mean ± standard deviation.

Day	Scenario	TA (µmol KgSW^{-1})	DIC (µmol KgSW^{-1})	pCO_2 (µatm)	HCO_3^- (µmol KgSW^{-1})	CO_3^{2-} (µmol KgSW^{-1})	CO_2 (µmol KgSW^{-1})	$\Omega_{calcite}$
1	Ambient	2260.3 (±10.3)	2103.3 (±15.3)	334.1 (±16.5)	1967.7 (±17.9)	118.6 (±4.0)	17.0 (±0.8)	2.92 (±0.10)
	ERCP 6.0	2262.7 (±3.8)	2143.5 (±6.1)	456.2 (±13.1)	2024.1 (±7.3)	96.9 (±2.3)	22.4 (±0.7)	2.39 (±0.05)
	ERCP 8.5	2259.7 (±7.6)	2145.4 (±7.4)	504.1 (±1.7)	2027.3 (±7.0)	94.6 (±0.3)	23.5 (±0.09)	2.33 (±0.01)
2	Ambient	2196.3 (±88.4)	2074.4 (±80.2)	402.3 (±17.5)	1957.6 (±73.4)	96.0 (±7.8)	20.7 (±0.9)	2.37 (±0.19)
	ERCP 6.0	2224.2 (±26.1)	2130.2 (±22.1)	538.4 (±11.9)	2021.9 (±19.7)	81.9 (±2.9)	26.4 (±0.5)	2.02 (±0.07)
	ERCP 8.5	2224.1 (±13.5)	2146.4 (±13.1)	653.8 (±11.5)	2042.0 (±12.5)	73.9 (±1.3)	30.5 (±0.5)	1.82 (±0.03)
3	Ambient	2250.5 (±14.1)	2100.4 (±12.7)	343.5 (±23.6)	1968.4 (±14.8)	114.4 (±6.6)	17.6 (±1.2)	2.82 (±0.16)
	ERCP 6.0	2259.2 (±21.6)	2126.8 (±25.8)	411.7 (±21.7)	2001.6 (±27.2)	105.0 (±3.3)	20.2 (±1.1)	2.59 (±0.08)
	ERCP 8.5	2260.3 (±8.8)	2133.9 (±8.5)	458.7 (±16.5)	2010.3 (±9.2)	102.3 (±3.3)	21.4 (±0.8)	2.52 (±0.08)
4	Ambient	2257.3 (±17.8)	2022.1 (±11.8)	203.4 (±24.2)	1842.3 (±24.3)	169.3 (±16.1)	10.5 (±1.3)	4.17 (±0.40)
	ERCP 6.0	2215.0 (±54.9)	1978.9 (±62.9)	204.7 (±20.1)	1799.2 (±66.1)	169.7 (±6.5)	10.1 (±1.0)	4.18 (±0.16)
	ERCP 8.5	2262.9 (±19.8)	2001.6 (±9.9)	199.1 (±10.5)	1803.5 (±8.5)	188.8 (±9.1)	9.3 (±0.5)	4.65 (±0.22)
5	Ambient	2276.4 (±28.4)	1992.0 (±54.0)	160.0 (±25.6)	1780.4 (±69.5)	203.4 (±17.1)	8.2 (±1.3)	5.01 (±0.42)
	ERCP 6.0	2275.7 (±13.8)	1966.8 (±19.7)	148.5 (±11.1)	1738.6 (±27.1)	220.9 (±10.1)	7.3 (±0.5)	5.44 (±0.25)
	ERCP 8.5	2272.5 (±33.4)	1948.4 (±30.7)	146.6 (±4.4)	1709.8 (±28.2)	231.8 (±4.6)	6.8 (±0.2)	5.72 (±0.46)
7	Ambient	2160.7 (±97.4)	1757.0 (±77.7)	79.5 (±2.4)	1472.0 (±60.1)	280.9 (±18.3)	4.0 (±0.12)	6.92 (±0.45)
	ERCP 6.0	2161.3 (±96.6)	1758.2 (±76.2)	85.3 (±4.0)	1472.8 (±58.9)	281.3 (±20.1)	4.1 (±0.2)	6.94 (±0.49)
	ERCP 8.5	2141.0 (±86.6)	1753.4 (±67.3)	96.2 (±4.6)	1478.7 (±51.6)	270.3 (±18.6)	4.4 (±0.2)	6.67 (±0.47)

Day	Scenario	TA (µmol KgSW^{-1})	DIC (µmol KgSW^{-1})	pCO_2 (µatm)	HCO_3^- (µmol KgSW^{-1})	CO_3^{2-} (µmol KgSW^{-1})	CO_2 (µmol KgSW^{-1})	$\Omega_{calcite}$
9	Ambient	2279.3 (±12.4)	1918.5 (±8.9)	110.2 (±4.7)	1656.8 (±13.0)	256.1 (±8.0)	5.6 (±0.2)	6.31 (±0.20)
	ERCP 6.0	2257.2 (±9.1)	1915.9 (±9.4)	125.6 (±3.1)	1667.5 (±10.7)	242.4 (±3.5)	6.1 (±0.1)	5.98 (±0.08)
	ERCP 8.5	2263.1 (±23.6)	1919.6 (±17.9)	133.9 (±3.4)	1668.6 (±14.7)	244.8 (±6.5)	6.2 (±0.2)	6.04 (±0.16)
11	Ambient	2332.9 (±86.8)	1791.2 (±57.0)	52.4 (±1.9)	1402.4 (±32.6)	386.1 (±26.5)	2.6 (±0.1)	9.51 (±0.65)
	ERCP 6.0	2323.3 (±77.8)	1801.7 (±63.0)	60.1 (±2.3)	1426.9 (±49.2)	371.8 (±15.3)	2.9 (±0.1)	9.17 (±0.38)
	ERCP 8.5	2338.3 (±94.8)	1811.7 (±71.1)	64.3 (±1.3)	1431.9 (±49.5)	376.8 (±21.9)	2.9 (±0.1)	9.29 (±0.54)
12	Ambient	2250.7 (±14.5)	1764.5 (±17.5)	61.6 (±3.5)	1418.8 (±23.7)	342.6 (±9.4)	3.1 (±0.2)	8.44 (±0.23)
	ERCP 6.0	2272.8 (±19.4)	1798.1 (±19.1)	70.9 (±1.6)	1458.4 (±18.1)	336.3 (±2.1)	3.4 (±0.1)	8.29 (±0.05)
	ERCP 8.5	2258.2 (±11.6)	1798.3 (±13.9)	79.8 (±4.4)	1468.8 (±21.1)	325.9 (±9.8)	3.6 (±0.2)	8.04 (±0.24)
15	Ambient	2251.3 (±15.1)	1724.1 (±11.1)	51.4 (±4.0)	1349.9 (±25.1)	371.6 (±16.0)	2.6 (±0.2)	9.2 (±0.40)
	ERCP 6.0	2250.4 (±8.8)	1756.6 (±13.8)	63.4 (±3.6)	1404.9 (±21.9)	348.6 (±9.7)	3.0 (±0.2)	8.59 (±0.24)
	ERCP 8.5	2237.8 (±26.5)	1744.5 (±35.5)	67.1 (±53.8)	1393.1 (±40.3)	348.2 (±5.4)	3.04 (±0.2)	8.59 (±0.13)
18	Ambient	2227.0 (±48.1)	1727.0 (±63.9)	57.6 (±7.2)	1372.9 (±72.1)	351.3 (±8.6)	2.8 (±0.4)	8.66 (±0.21)
	ERCP 6.0	2243.7 (±19.9)	1767.3 (±12.3)	68.9 (±3.7)	1427.7 (±16.1)	336.3 (±11.6)	3.3 (±0.2)	8.29 (±0.29)
	ERCP 8.5	2239 (±17.4)	1773.4 (±28.4)	77.4 (±6.3)	1440.5 (±37.5)	329.5 (±10.8)	3.5 (±0.3)	8.13 (±0.27)
20	Ambient	2209.5 (±108.9)	1771.3 (±101.6)	72.9 (±7.0)	1460.6 (±91.7)	307.0 (±11.8)	3.6 (±0.4)	7.57 (±0.29)
	ERCP 6.0	2233.7 (±74.4)	1841.6 (±68.1)	99.1 (±7.4)	1560.1 (±62.1)	330.1 (±13.4)	3.2 (±0.1)	8.14 (±0.33)
	ERCP 8.5	2227.6 (±84.8)	1864.3 (±87.3)	121.4 (±12.8)	1601.5 (±85.7)	257.4 (±6.8)	5.5 (±0.6)	6.35 (±0.17)
21	Ambient	2190.8 (±52.0)	1675.7 (±32.9)	50.4 (±5.2)	1313.2 (±34.6)	359.9 (±25.5)	2.5 (±0.3)	8.87 (±0.63)
	ERCP 6.0	2217.9 (±31.8)	1748.4 (±18.2)	68.1 (±3.2)	1415.1 (±14.1)	330.1 (±13.4)	3.2 (±0.1)	8.12 (±0.33)
	ERCP 8.5	2212.9 (±49.8)	1807.6 (±51.1)	102.7 (±32.7)	1516.8 (±86.9)	286.2 (±46.7)	4.6 (±1.5)	7.06 (±1.15)

Day	Scenario	TA (µmol KgSW^{-1})	DIC (µmol KgSW^{-1})	pCO_2 (µatm)	HCO_3^- (µmol KgSW^{-1})	CO_3^{2-} (µmol KgSW^{-1})	CO_2 (µmol KgSW^{-1})	$\Omega_{calcite}$
24	Ambient	2277.4 (±70.9)	1880.2 (±63.1)	95.1 (±6.3)	1593.9 (±56.7)	281.5 (±13.1)	4.7 (±0.3)	6.94 (±0.32)
	ERCP 6.0	2260.5 (±87.5)	1926.9 (±81.8)	136.6 (±7.1)	1682.8 (±174.5)	237.7 (±7.12)	6.4 (±0.36)	5.86 (±0.17)
	ERCP 8.5	2367.3 (±66.4)	2063.6 (±54.8)	185.3 (±10.8)	1833.7 (±46.8)	221.5 (±13.9)	8.3 (±0.5)	5.47 (±0.34)
26	Ambient	2193.9 (±51.8)	1837.2 (±52.9)	107.8 (±8.7)	1581.6 (±53.3)	250.4 (±53.3)	5.3 (±0.4)	6.17 (±0.23)
	ERCP 6.0	2212.7 (±19.3)	1917.7 (±11.6)	158.6 (±5.6)	1700.4 (±8.6)	209.8 (±7.1)	7.4 (±0.2)	5.18 (±0.17)
	ERCP 8.5	2210.4 (±32.4)	1955.1 (±30.7)	210.4 (±14.1)	1761.9 (±31.4)	183.9 (±9.2)	9.3 (±0.62)	4.54 (±0.23)

Chapter 4

An integrated multiple driver mesocosm experiment reveals the effect of global change on planktonic food web structure

Hugo Duarte Moreno[1], Martin Köring[1], Julien Di Pane[1], Nelly Tremblay[1], Karen H. Wiltshire[1,2], Maarten Boersma[1,3], Cédric L. Meunier[1]

[1]Alfred-Wegener-Institut, Helmholtz-Zentrum für Polar- und Meeresforschung, Biologische Anstalt Helgoland, Germany

[2]Alfred-Wegener-Institut, Helmholtz-Zentrum für Polar- und Meeresforschung, Wattenmeerstation, List auf Sylt, Germany

[3]University of Bremen, FB 2, Bremen, Germany

Published in *Communications Biology* 5(1), 1-9.

4.1. Abstract

Global change puts coastal marine systems under pressure, affecting community structure and functioning. Here, we conducted a mesocosm experiment with an integrated multiple driver design to assess the impact of future global change scenarios on plankton, a key component of marine food webs. The experimental treatments were based on the RCP 6.0 and 8.5 scenarios developed by the IPCC, which were Extended (ERCP) to integrate the future predicted changing nutrient inputs into coastal waters. We show that simultaneous influence of warming, acidification, and increased N:P ratios alter plankton dynamics, favours smaller phytoplankton species, benefits microzooplankton, and impairs mesozooplankton. We observed that future environmental conditions may lead to the rise of *Emiliania huxleyi* and demise of *Noctiluca scintillans,* key species for coastal planktonic food webs. In this study, we identified a tipping point between ERCP 6.0 and ERCP 8.5 scenarios, beyond which alterations of food web structure and dynamics are substantial.

4.2. Introduction

Human activities and associated increasing greenhouse gas emissions have caused simultaneous changes in a range of marine abiotic parameters. The Intergovernmental Panel on Climate Change (IPCC) established different scenarios projecting that, depending on humanity's effort to reduce greenhouse gas emissions, by 2100, temperature may increase by 1 to 6 °C and pH may decrease by 0.1 to 0.4 units in the ocean's upper layers (IPCC, 2014). In addition, urban, agricultural, and industrial development will continue to alter biogeochemical cycles through nutrient runoffs, increasing phosphorus limitations in European coastal marine systems (Grizzetti et al., 2012). Consequently, marine organisms are currently, and will continue to be, exposed to the simultaneous effects of multiple anthropogenic drivers. The pressure exerted by these changes on coastal marine systems threatens biological community structure and food web functioning (Hoegh-Guldberg and Bruno, 2010; Duarte, 2014). Planktonic organisms are particularly sensitive to ecosystem change, and, given their central role in marine food webs, these organisms are of vital importance for ecosystem health (Richardson and Schoeman, 2004). Despite the urgent need to understand and predict how global change will influence planktonic food webs, there is still a striking paucity of information on the integrated impact of multiple drivers, especially in a community context. The few studies addressing the combined effects on plankton communities showed, for example, negative effects on copepod abundance, as well as shifts in phytoplankton organismal size (Rose et al., 2009; Sommer et al., 2015; Garzke et al., 2016; Horn et al., 2020).

Among the different methods that can be employed to address community responses to multiple global change drivers experimentally and mechanically, mesocosm approaches provide the highest level of ecological relevance while still being conducive to experimental manipulations (Boyd et al., 2018). By incorporating natural assemblages and by addressing mechanistic relationships across trophic levels that take place in complex natural systems, mesocosms go beyond small, tightly controlled experiments which suffer from limited realism (Stewart et al., 2013). The main limitation of the mesocosm approach is the difficulty of replication, due to the high costs of acquiring and maintaining such systems (Boyd et al., 2018). For this reason, full-factorial mesocosm experiments are scarce. Although understanding the individual effect of global change drivers, such as temperature, pH, or dissolved nutrient concentrations, on the functioning of planktonic communities can inform specific mitigation strategies, it is important to consider that these drivers are simultaneously changing in natural environments. Hence, we applied an integrated multiple driver design to assess the potential

impact of global change on natural coastal plankton communities. We tested the influence of two future scenarios against current environmental conditions in triplicates: the Ambient condition (Ambient temperature and pH) and the Representative Concentration Pathway 6.0 (RCP 6.0, +1.5°C, -0.2 pH) and RCP 8.5 (+3.0°C, -0.3 pH), proposed by the IPCC for 2100 (IPCC, 2014). Additionally, as nutrient inputs are also predicted to change towards considerably higher nitrogen to phosphorus ratios (N:P) in coastal seas, especially those in Europe (Grizzetti et al., 2012), we extended the RCP scenarios (ERCP) to simulate changing nutrient regimes, with a N:P ratio (molar) of 16 (Redfield ratio) for the Ambient scenario and 25 for both future scenarios (ERCP 6.0 and 8.5). It is currently of utmost importance to make accurate and reliable predictions of the fate of planktonic communities in future conditions. Although our experimental design does not enable to draw conclusions about individual drivers effect, we believe that our work provides a more realistic assessment of these drivers' impact than an experiment addressing drivers singly would.

The mesocosm experiment was conducted over three weeks in late-summer (August-September) 2018. Seawater containing a natural plankton community was collected from the coastal North Sea. At the onset of the experiment, CO_2 saturated seawater was added to the ERCP scenario mesocosms to adjust pCO_2 and pH levels for each scenario. To create a realistic environment, we also manipulated the atmospheric pCO_2 in the enclosed mesocosm tanks throughout the experiment. Seawater temperature was adjusted daily according to the current North Sea temperature measured at the Helgoland Roads for the Ambient, and 1.5°C and 3.0°C warmer for the ERCP 6.0 and ERCP 8.5 scenarios, respectively. Dissolved nutrient concentrations were determined at the onset of the experiment and adjusted to reach the desired N:P ratios. Samples were taken in an interval of 1-3 days depending on the phytoplankton bloom development, and community composition, except for the large mesozooplankton, was monitored throughout the experiment period. Across scenarios, no significant difference was found in biomass of phytoplankton, microzooplankton and bacterioplankton on the first day of the experiment (Kruskal-Wallis test, $df = 2$, $p > 0.05$). The effects of the ERCP scenarios on plankton community biomass were statistically assessed through the Likelihood ratio test (LRT), and Principal Response Curve (PRC) analysis was applied to identify the influence of the ERCP scenarios on community composition.

4.3. Materials and Methods

Experimental design

With an integrated multiple driver approach, we tested the influence of two global change scenarios on the structure and dynamics of plankton food webs based on predictions by the Intergovernmental Panel on Climate Change for the end of the 21st century (IPCC, 2014)[1]. Temperature and pCO_2 levels were chosen to represent (1) Ambient conditions, (2) a moderate global change scenario based on RCP 6.0 (+1.5°C and -0.2 pH), and (3) a more severe global change scenario based on RCP 8.5 (+3°C and -0.3 pH). As nutrient inputs are also predicted to change towards considerably higher nitrogen to phosphorus ratio (N:P) in coastal European seas (Grizzetti et al., 2012), we extended the RCP scenarios (ERCP) to include the predicted changing nutrient regime, with the Ambient and the ERCP scenarios having an N:P ratio (molar) of 16 (Redfield ratio), and 25, respectively, at the onset of the experiment.

Mesocosm system

The experiment was conducted in the mesocosm facility located at the Alfred-Wegener-Institut, Helmholtz-Zentrum für Polar- und Meeresforschung (AWI) Wadden Sea Station on the Island of Sylt (Pansch et al., 2016). The outdoor facility consists of 12 double-hulled, insulated, cylindrical tanks, made of UV stabilised high-density polyethylene (HDPE; Spranger Kunststoffe, Plauen, Germany). Each tank has a height of 85 cm, an inner diameter of 170 cm, and a net volume of 1800 L. To avoid introduction of unwanted material, each mesocosm tank is covered with a translucent lid made of HDPE, which allows penetration of 90% of the photosynthetically active radiation. An adjustable flow-through system from the AWI Wadden Sea Station constantly supplies the tanks with fresh, unfiltered seawater. The temperature is regulated every 30 minutes by a Labview-based computer software (4H-Jena engineering, Jena, Germany), which periodically receives temperature data from Hydrolab DS5X Probes (OTT Messtechnik GmbH, Kempten, Germany) and controls external cooling units (Titan 2000 or Titan 4000 Aqua Medic, Bissendorf, Germany) and heaters (Titanium heater 500 W, Aqua Medic, Bissendorf, Germany).

We installed 450 L low-density polyethylene (LDPE) bags in each mesocosm tank (Supplementary Figure 4.1). The LDPE was chosen as material for the bags as it should not represent a risk for planktonic organisms either, since it also is used in food industry for packaging. The LDPE bags were filled with seawater collected from the open North Sea with natural plankton communities (see details about filling procedures below). The bags were fixed

in the centre of the tanks. By regulating the temperature and aerating the surrounding flow-through water as described above, we indirectly regulated temperature and pCO_2 in the LDPE bags. We replicated each treatment four times, for a total of 12 mesocosms. Due to damage to the bags and potential contamination of the plankton communities by the surrounding water, we excluded one replicate from each treatment, leaving triplicates for each of the three treatments. Despite the low number of replicates, the consistent response across scenarios and strong statistical results still reinforce the reliability of our results. The temperature in the Ambient conditions mesocosms was adjusted daily to the seawater temperature measured at the Helgoland Roads station (54°11.3'N, 7°54.0'E) and was increased by 1.5 and 3.0°C for the ERCP 6.0 and ERCP 8.5 scenarios, respectively. We mounted small mortar mixer engines (TC-MX 1400-2 E, Einhell Germany AG, Landau/Isar, Germany) on top of each mesocosm tank, which were connected to a custom-made HDPE propeller (AWI, Helgoland, Germany). To avoid sedimentation of the planktonic organisms and mimic the relatively well mixed water column condition found in the southern part of the North Sea (van Leeuwen et al., 2015), the submerged propellers gently homogenised the water column of the LDPE bags at 50 rpm in a 1-minute-mixing/30-minutes-pause interval. To reach the desired pCO_2 in the different ERCP scenarios, streaming pipes aerated each tank with the desired gas mixture in the water outside the LDPE bags (Supplementary Figure 4.1). The aeration outside the mesocosm bag was intended to prevent damage to fragile planktonic organisms that are sensitive to bubbling. The Ambient conditions mesocosms were bubbled with pressured air, ERCP 6.0 scenario with 800 µatm pCO_2 and the ERCP 8.5 with 1000 µatm pCO_2, which were determined by a central CO_2-mixing facility (GMZ 750, HTK, Hamburg, Germany). The mesocosm cover trapped the pCO_2-controlled atmosphere above the mesocosm water column, hence realistically mimicking future environmental conditions.

Seawater collection and filling of the mesocosm bags

On the 14th of August 2018, we collected water from the open North Sea 45 km west of the island of Sylt (55°01'20.0"N 7°38'41.0"E), during a cruise with the AWI research vessel Uthörn. During the water collection and filling procedure of the mesocosm bags, we did not use any pumps, but transferred seawater via gravity flow to prevent any damage to fragile organisms within the planktonic community. To sample seawater onboard, we submerged a 500 L tub attached to a crane to fill it with seawater from the upper 5 meters sea surface. The tub was subsequently lifted up to let the water flow through a hose connected to the tub into 1000 L polyethylene Intermediate Bulk Containers (IBC, AUER Packaging GmbH, Amerang,

Germany). We attached a 1000 µm mesh to the end of the hose, to exclude larger organisms, such as jellyfish and fish larvae. This procedure prevented any disproportionally large impact which larger consumers can have on the rest of the plankton community in a 450L enclosed water volume. Furthermore, this approach enabled us to focus on bottom-up processes since there was no top-down control on mesozooplankton. The procedure was repeated until eight IBC tanks were filled (8000 L), which took about three hours.

Before filling the mesocosm bags, we first gently homogenised the water in the IBC tanks. Then, we attached a four-way-distributor to one IBC tank, and the tank was lifted by a wheel-loader to allow gravity flow of the seawater into the mesocosm bags. At the end of each connected hose, a flowmeter measured the exact volume of water which was released into each mesocosm bag. We filled 80 L of seawater simultaneously to four bags, and then filled the next quadruplet of mesocosms. This enabled an equal distribution of the water contained in each IBC tank among the twelve mesocosms. This procedure was repeated until all mesocosm bags were filled with 450 L of North Sea water. This procedure enabled us to successfully tackle a major challenge when conducting mesocosm experiments, the difficulty of achieving homogenous replicates at the onset of the experiment (Boyd et al., 2018). Across scenarios, no significant difference was found in biomass of phytoplankton, microzooplankton and bacterioplankton on the first day of the experiment (Kruskal-Wallis test, $df = 2$, $p > 0.05$). Once the filling procedure was completed, we directly measured the dissolved N and P concentrations in each mesocosm bag according to the method described in Grasshoff et al. (1999), and subsequently adjusted the dissolved N:P ratios to 16 (Ambient conditions) and 25 (ERCP scenarios). We added DIN to reach 5 µmol L^{-1} in all scenarios, DIP to reach 0.31 µmol L^{-1} in the Ambient scenario and 0.2 µmol DIP L^{-1} in the ERCP 6.0 and 8.5 scenarios. These values correspond to mean values for that period of the year according to data from the Helgoland roads time series. At the onset of the experiment, we bubbled a small volume of seawater with pure CO_2, which lowered its pH to 4.8 at saturation. Using a 50 mL plastic syringe connected to a 1 m hose, we injected 400 mL (ERCP 6.0) and 760 mL (ERCP 8.5) of the saturated CO_2 seawater at the bottom of the mesocosm bags to reduce the initial pH values by -0.2 and -0.3 for the ERCP 6.0 and ERCP 8.5 scenarios, respectively. During the rest of the experiment, the pH was influenced by the planktonic communities through photosynthesis and respiration, and by the atmospheric pCO_2 (see above).

Physical-chemical conditions in the mesocosm bags

Temperature, pH, light irradiance and salinity were measured every day at 9:00 (Supplementary Figure 4.2). Light intensity was measured just below the water surface with a Li-cor Li-250 Light meter (Bad Homburg, Germany). Temperature measurements were done directly inside the mesocosm bags using a Testo 110 – temperature meter (Lenzkirch, Germany). Total alkalinity (TA) samples were taken by plunging, filling, and closing an air-tighten 100 mL transparent glass bottle inside the mesocosm to avoid air bubbles. The samples were stored at 4°C before being analysed within 36 hours through linear Gran-titration (Dickson, 1981) using a TitroLine alpha plus (Schott, Mainz, Germany). Samples for dissolved inorganic nutrients and TA were taken at an interval of 1-3 days depending on the phytoplankton bloom development.

For further analyses, water was collected from each mesocosm bag with clean plastic beakers and brought to the lab for processing. The first parameter measured was pH using a WTW pH 330i equipped with a SenTix 81 pH electrode (Letchworth, England). Salinity was measured with a WTW CellOx 325 (probe Oxi 197-S, Letchworth, England). Dissolved inorganic nutrients samples were collected with a sterile plastic syringe and filtered through a 0.45 µm PTFE filter (Minisart, Sartorius, Goettingen, Germany) fitted to the syringe. For this step, the first 2 mL of the sample were used to rinse the filter and directly discarded. Samples for dissolved inorganic nitrogen (DIN) and phosphorus (DIP) were stored at -20°C, and the samples for dissolved silica (DSi) were stored at 4°C, until photometric analyses (Grasshoff et al. 1999) (Supplementary Figure 4.3). Results of TA, pH, temperature, salinity, atmospheric pressure, DIP and DSi were computed to determine the carbonate system using the CO2Sys Excel Macro (Pierrot et al., 2006) with a set of constants defined by Dickson and Millero (1987) (Supplementary Table 4.1). Although pCO_2 in the mesocosms were below levels projected by the RCP scenarios during the experiment, CO_2 concentrations were always different across scenarios within the expected gradient (Supplementary Figure 4.2b and Supplementary Table 4.1), where Ambient is lower than ERCP 6.0 that is lower than ERCP 8.5. It is extreme complex to keep pCO_2 constant in mesocosm experiments, even with an appropriate CO_2 atmosphere, and especially throughout a phytoplankton bloom event that is able to change dissolved CO_2 even in the open sea (Arrigo et al., 1999). Therefore, our approach yields the most realistic of CO_2 time courses in a future ocean. The remaining of the water was used for analyses of the planktonic community.

Planktonic community

To determine plankton species composition and biomass, 100 mL of mesocosm seawater were stored in amber glass bottles and immediately fixed with neutral Lugol's iodine solution (1% final concentration) to preserve calcifying phytoplankton. Another 250 mL were fixed with acid Lugol's iodine solution (2% final concentration) to preserve other phytoplankton and microzooplankton species. Phytoplankton were identified using an inverted microscope Zeiss Anxiovert 135 (Jena, Germany) and microzooplankton using a Zeiss Axio Observer 7 A1 (New York, USA) following the method described in Utermöhl (1958). Due to the high biomass of the mesozooplankton *Noctiluca scintillans* during the experiment, this species was quantified and identified by the Utermöhl method as well, using chamber volumes ranging between 50 and 100 mL. Planktonic organisms were identified to species level, or pooled into size-shape dependent groups when species identification was not possible. Scanning electron microscopy (Philips XL30 SEM, Massachusetts, USA) was applied to identify coccolithophore species by the morphology of the coccoliths. For this procedure, prior to microscopy, 5 mL of the neutral lugol fixed sample were filtered through a 0.2 µm pore size polycarbonate membrane filter (Merck Millipore, Burlington, USA), dried in a drying oven at 40°C for 12 hours, placed on a metal stub using an adherent carbon disc with increased conductivity, and then sputter coated with a 10 nm gold layer.

Mesozooplankton, with the exception of *Noctiluca scintillans*, was sampled with a plankton net (200 µm) *in situ* (Initial) when seawater was collected, and on the day 15 of the experiment by sieving 5 L of seawater from the mesocosm through a 200 µm nylon mesh. The organisms caught on the mesh were flushed back into a 50 mL transparent Kautex container with sterile filtered seawater (0.2 µm), and immediately fixed with formaldehyde. The mesozooplankton community composition was determined by counting the whole sample or three subsamples when splitting was necessary with a Folsom splitter (McEwen et al., 1954; Sell and Evans, 1982). The counting took place using a Bogorov chamber under stereomicroscope (Leica M205), and taxonomic identification was conducted as in Boersma et al. (2015). Samples for bacterioplankton biomass were taken as 5 mL of seawater, sieved through 20 µm nylon mesh, fixed with glutaraldehyde (0.1% final concentration) and frozen at -80°C until analysis. The samples were thawed in a water bath (20°C) and stained with SYBR Green (Invitrogen) following the method described by Marie et al. (2005). Bacteria cells were enumerated by flow cytometry (BD AccuriTM C6 Plus, BD Biosciences) with a flow rate of 12 µL min^{-1} for 1-2 minutes and diluted in sterile filtered seawater (0.2 µm) when bacterial cell

number was higher than 400 events s^{-1}. As SYBR Green stains DNA molecules without distinguishing taxonomical groups, our results of bacterioplankton include any organisms within the range of picoplankton cell size (~0.2 – 2 µm), including picocyanobacteria.

Biovolume of each phytoplankton and microzooplankton species was calculated from the measurement of cell dimensions using geometric formulae according to Hillebrand et al. (1999). Cell volume was converted into carbon following the equations of Menden-Deuer and Lessard (2000) for diatoms (pg C $cell^{-1}$ = 0.288 x $V^{0.811}$), dinoflagellates (pg C $cell^{-1}$ = 0.760 x $V^{0.819}$) and other protist plankton with the exception of ciliates (pg C $cell^{-1}$ = 0.216 x $V^{0.939}$), where V is the cell volume in μm^3. Ciliate carbon content was calculated as 0.19 pg C μm^{-3} according to Putt and Stoecker (1989). *Noctiluca scintillans* C content was determined as 0.138 µg C $cell^{-1}$ (Beran et al., 2003). Bacteria cell counts were converted into carbon using the 20 fg C $cell^{-1}$ factor defined by Lee and Fuhrman (1987). The box size on the infographic of biomass (Figure 4.1) was determined by the integral area under the curve of the plankton biomass over time (Figures 4.2a, 4.3a, 4.4a and Supplementary Figure 4.4) and dominant taxa followed the values of the relative abundance of the most abundant taxa (Figures 4.2b-d, 4.3a-c and 4.4b-d). Elemental composition (CNP) of seston was determined by filtering 200 mL of seawater through precombusted GF/F filters. Carbon and nitrogen content were measured with a Vario Micro Cube elemental analyser (Elementar, Hanau, Germany). Phosphorus content was quantified as orthophosphate after oxidation by molybdate-antimony (Grasshoff et al. 1999). Functional groups were determined as Phytoplankton, Bacterioplankton, Microzooplankton and Mesozooplankton. The phytoplankton group included diatoms, phytoflagellates and autotrophic dinoflagellates, according to the descriptions of trophic mode for each species (summarized by Kraberg et al. 2010). The microzooplankton group comprised heterotrophic and mixotrophic dinoflagellates and ciliates, including nanociliates (< 20 µm). Mesozooplankton species were all the heterotrophic organisms larger than 200 µm.

Statistics and Reproducibility

Statistical analyses were performed using R 3.4.3 software (R Core Team, 2021). For all analyses, the threshold of significance was set at 0.05. All statistical analyses were applied considering the 3 individual replicates per scenario. Each replicate was determined as one tank of the mesocosm system. Effect of the ERCP scenario on planktonic biomass was assessed by the generalized linear model (GLM). We first fitted a model of total biomass (either phytoplankton or zooplankton) depending on treatments. It allowed us to check for general treatment effect on planktonic biomass. Then, we created a second model including treatment

and time. By comparing the constrained model (time and scenario) against the unconstrained one (only scenario) by Likelihood ratio test (LRT), we could test whether timing in planktonic biomasses were similar among treatments. Effects of the ERCP scenarios on the phyto- and microzooplankton species composition and affinity of species to the scenarios were analysed through the Principal Response Curve (PRC) using the 'vegan' R package. This test shows the degree of difference over time of the community composition in the ERCP scenarios in comparison to the Ambient condition, which is set as a control (effect '0'). Species weights are analysed as means of their regression coefficient against the control. When the curve of difference of the ERCP scenario has a positive slope, positive values for species weights represent affinity of this species to the scenario, whereas negative values would represent a negative effect of the scenario on such species and *vice versa*. Differences of mesozooplankton abundance were analysed through Analysis of Variance (ANOVA) followed by a PostHoc test (Tukey test). Data was log-transformed when normality and homoscedasticity of residuals was not met for ANOVA and LRT.

4.4. Results and Discussion

Overall: In all treatments, we observed a first phytoplankton bloom, which lasted roughly 10 days, followed by a second bloom of different magnitude and composition between the treatments. We observed that, throughout the experiment, the planktonic food web was relatively similar in the Ambient treatment and in the ERCP 6.0 scenario, whereas the ERCP 8.5 scenario substantially altered the biomass, structure, and dynamics of multiple trophic levels (Figure 4.1). The ERCP 8.5 scenario benefited the emergence of nanophytoplankton, specifically coccolithophores, at the expense of larger diatoms, especially in the second bloom. This has implications for the marine carbon pump due to the calcification capacity of coccolithophores (Rost and Riebesell, 2004). Mesozooplankton biomass was largely reduced in the ERCP 8.5 scenario, whilst the biomass of microzooplankton was higher in this treatment than in the other two. The increase of micrograzers and lower mesozooplankton biomass are indicative of a microbial loop dominance in this future scenario, and of a potential diminution of energy transfer to higher trophic levels. We wish to note that, due to the relatively short duration of the experiment, this study does not consider the potential adaptation of planktonic communities that may take place over longer periods of time.

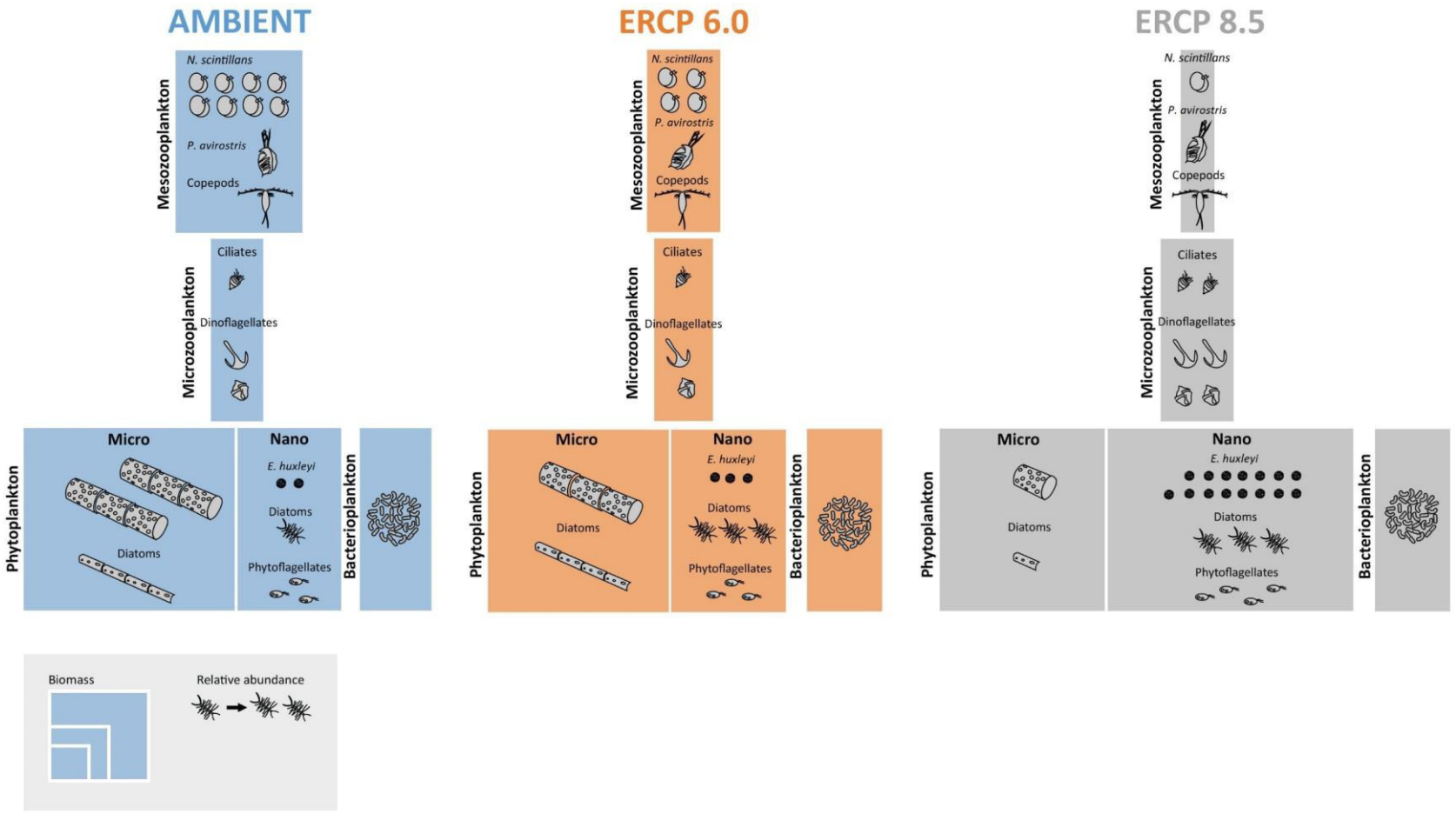

Figure 4.1: Infographic of biomass and dominant taxa for different food web compartments under the Ambient treatment and the ERCP scenarios. Colours represent the Ambient treatment and Extended Representative Concentration Pathway (ERCP) scenarios (blue = Ambient, orange = ERCP 6.0, grey = ERCP 8.5), box size represents the total biomass of each compartment, and the number of individuals represents the relative abundance of taxonomic groups within a scenario. Phytoplankton biomass is divided between microphytoplankton (> 20 µm) and nanophytoplankton (< 20 µm). Plankton biomass and relative abundance are displayed to scale.

The rise of nanophytoplankton: Total cumulative phytoplankton biomass was not affected by the experimental treatment (GLM, df 86, ERCP 6.0 $p = 0.90$, ERCP 8.5 $p = 0.17$, $n = 3$, Figure 4.2a). It appeared that the timing in phytoplankton biomass was also not statistically different among treatment (LRT; df 86, $p = 0.46$). Phytoplankton biomass increased exponentially from the beginning of the experiment in all treatments to reach a stationary phase on day 4. During this first phytoplankton bloom, we observed a gradient in the relative abundance of the large diatom *Guinardia flaccida* (GLM, df 86, ERCP 6.0 $p = 0.01$, ERCP 8.5 $p < 0.0001$, $n = 3$) from high in Ambient, to lower in ERCP 6.0 and ERCP 8.5, and the opposite in the contribution of nanophytoplankton (< 20 µm) to the total phytoplankton biomass (GLM, df 86, ERCP 6.0 $p = 0.88$, ERCP 8.5 $p = 0.04$, $n = 3$, Figure 4.1 and Figure 4.2b-d). During this first bloom, both ERCP scenarios yielded lower phytoplankton biomass and were largely favourable towards nanophytoplankton at the expense of larger microalgal species (Supplementary Figure 4.5). This result is similar to previous studies showing a negative effect of warming and acidification on the mean cell size of phytoplankton communities (Peter and Sommer, 2012; Bermúdez et. al, 2016), which can be exacerbated when nutrient availability is low (Peter and Sommer, 2015; Alvarez-Fernandez et al., 2018). For instance, Peter and Sommer (2015) used a semi-continuous microcosm approach to disentangle the direct temperature-mediated effects from indirect nutrient-limitation effects on phytoplankton size, and identified that nutrient effects largely dominate over direct temperature effects. While nutrient limitation has been associated with a reduction in light absorption leading to a reduction in cell size (Stramski et al., 2002), small cells have low surface:volume ratios, which facilitates nutrient uptake efficiency and is therefore an advantageous feature in low nutrient waters (Marañón, 2015). In contrast to the two future scenarios, DIN was depleted before DIP in the Ambient scenario (Supplementary Figure 4.3). These results are associated with our manipulation of N:P ratios, which are expected to increase in coastal seas (Grizzeti et al., 2012), and support predictions that human-induced nitrogen enrichment is altering the balance with P (Peñuelas et al., 2011). Since the phytoplankton bloom rapidly depleted DIP in the ERCP 6.0 and 8.5 scenarios (Supplementary Figure 4.3), we pose that the above-described phytoplankton biomass responses were mostly driven by DIP availability. The ERCP scenarios-induced smaller phytoplankton cell sizes are favourable for microzooplankton and as a consequence direct the flow of energy to the microbial food web, rather than efficiently fuelling higher trophic levels (Azam et al., 1983; Legendre and Le Fèvre, 1995).

Following the bloom decay phase, abundances of the small coccolithophore *Emiliania huxleyi* increased in all treatments, but *E. huxleyi* only remained dominant in the ERCP 8.5

scenario until the end of the experiment, forming, together with the diatom *Leptocylindrus danicus*, a second phytoplankton bloom (Figure 4.2a-d). The coccolithophore *E. huxleyi* has been the "canary" for ocean acidification research for a long time, as lower pH -values are predicted to be detrimental to calcification processes present in this species (Beaufort et al., 2011). Recent studies, however, challenge this view, showing strain-specific response of this species to higher pCO_2 (Langer et al., 2016). In fact, it has been suggested that this phytoplankton species may become more competitive at higher CO_2 concentrations due to increased carbon fixing enzymatic activity (Winter et al., 2014). Coccolithophore blooms, which are common during summer or early fall in temperate regions (Hopkins et al., 2015; León et al., 2018), have increased in intensity over the past decades in the North Atlantic (Rivero-Calle et al., 2015). Furthermore, *E. huxleyi* has been reported to outcompete diatom blooms when nutrients, such as silica and phosphorus, become depleted (Purdie and Finch, 1994; Nejstgaard et al., 1997; Leblanc et al., 2009). While calcification process in *E. huxleyi* under high pCO_2 is modulated by temperature (Sett et al., 2014), positive effects of warming coupled with high pCO_2 on calcification of this coccolithophore have been reported (Benner et al., 2013). This fact along with lower P availability may have created favourable growth conditions in the ERCP 8.5 scenario. Hence, we suggest that simultaneous pCO_2 and temperature increases, and lower dissolved nutrient concentrations, may promote intense *E. huxleyi* blooms in the future, which would significantly influence the role of this calcifying species in the marine carbon pump (Rost and Riebesell, 2004; Borchard et al., 2011).

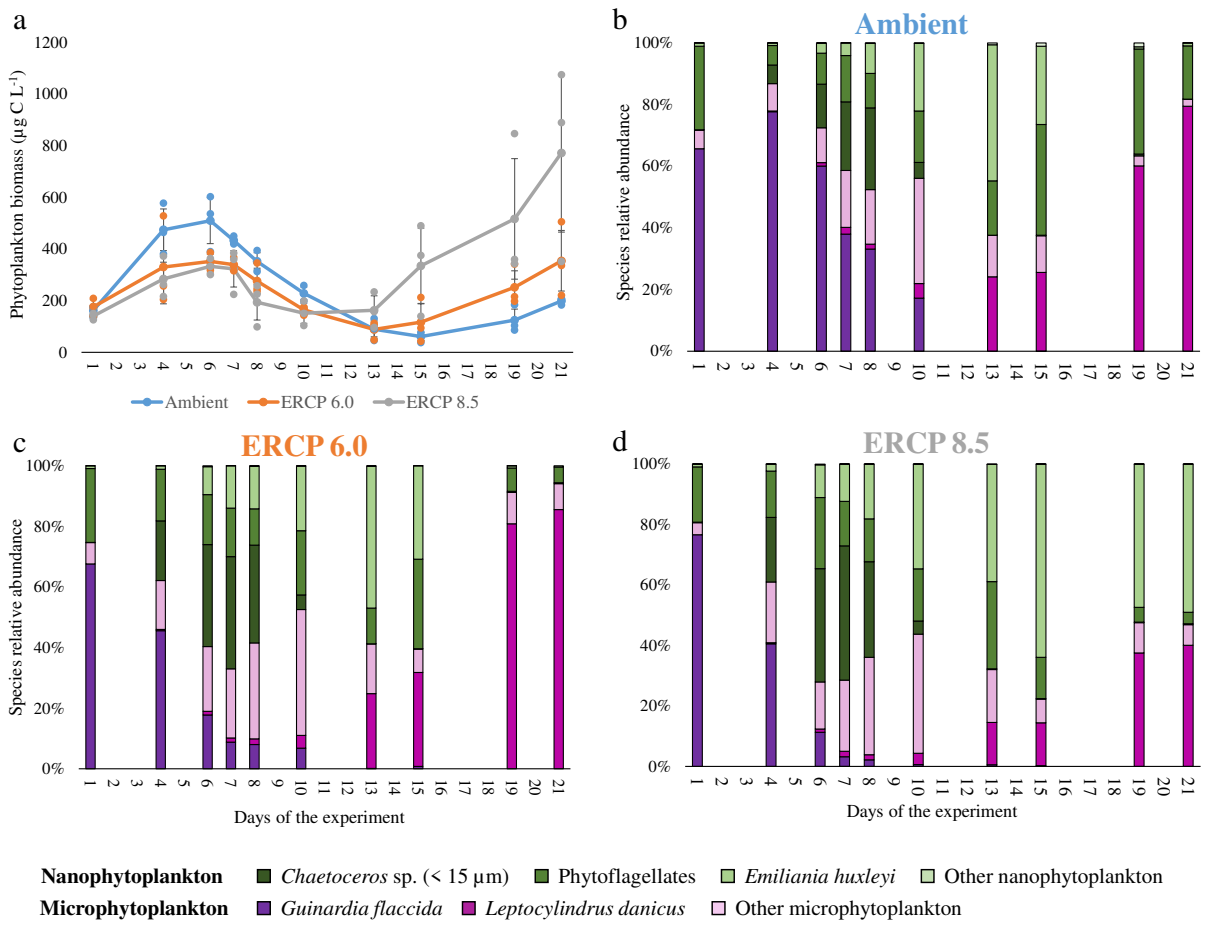

Figure 4.2: Phytoplankton biomass and community composition. (a) Phytoplankton biomass. (b,c,d) Relative abundances of different taxa of the phytoplankton communities under the different scenarios. x-axis represents the days of the experiment, different colours represent the Ambient treatment and Extended Representative Concentration Pathway (ERCP) scenarios (blue = Ambient, orange = ERCP 6.0, grey = ERCP 8.5), mean ± standard deviation. Cumulative phytoplankton biomass was not affected by the scenarios (LRT, df 86, p = 0.46, n = 3).

The fate of larger grazers: We observed a significant difference in the abundance of large grazers, from high in Ambient, to lower in ERCP 6.0, and even lower in ERCP 8.5 (Figure 4.1 and 4.3a, GLM, df 86, ERCP 6.0 p = 0.36, ERCP 8.5 p = 0.0003 and LRT, df 86, p < 0.0001, n = 3). The mesozooplankton community was largely dominated by the sea sparkle *Noctiluca scintillans*. Its abundance continuously increased from the beginning to the end of the experiment in the Ambient treatment (Figure 4.3a), whereas this species died out on days 13 and 21 in the ERCP 8.5 and ERCP 6.0 scenarios, respectively (Figure 4.3a). The abundance of copepods decreased during the experiment and was lower in both ERCP scenarios compared to the Ambient treatment (ANOVA, $F_{3,9}$ 276.1, p < 0.0001, n = 3, Figure 4.3b). The second most numerous mesozooplankton species, the cladoceran *Penilia avirostris*, was more numerous on day 15 compared to initial values and was present in higher abundances in the ERCP 6.0

scenario and in lower abundances in the ERCP 8.5 scenario and Ambient treatment (ANOVA, $F_{3,9}$ 26.62, p = 0.0003, n = 3 Figure 4.3c). This difference might result from an interaction between food availability, and nutritional requirements at elevated temperature and pCO_2. While temperatures during our experiment were well within the tolerance range of *N. scintillans* (Harrison et al., 2011 and references therein) and *P. avirostris* (Johns et al., 2005), this driver generally increases metabolic processes and energetic demands (O'Connor et al., 2009), and may intensify the sensitivity of consumers to low food availability. The scarcity of prey in the ERCP 8.5 might also have been the reason for the hump-shaped response of *P. avirostris* to both ERCP scenarios, as this species is not expected to be negatively affected by the temperature ranges used in our experiment. Given the correlation between temperature and metabolic rates, global warming could modify the metabolic demands of consumers, which, together with resource quality shifts, creates the potential for nutritional mismatches (Cross et al., 2015). Recent work shows that the nutritional requirements of zooplankton, and the resource quality which maximises the growth of these ectotherms, is not constant but rather varies with temperature (Boersma et al., 2016; Anderson et al., 2017). However, as seston C:N:P stoichiometry did not vary across treatments (Supplementary Figure 4.6), bottom-up effects were likely driven by resource availability rather than by elemental stoichiometric quality. *Noctiluca scintillans* and *Penilia avirostris* can feed on a broad range of prey sizes (Kirchner et al., 1996; Elbrächter and Qi, 1998; Atienza et al., 2006), and may have been little affected by the shift in size from micro- to nanophytoplankton. Rather, we suggest that the lower phytoplankton biomass, and hence food availability, in the ERCP 6.0 and 8.5 scenarios, during the first bloom and its decay phase, were responsible for the differences observed. However, as there was no top-down control on mesozooplankton during the experiment, it is important to note that the effects seen here could differ from communities in which their predators are present. In functional and numerical response experiments in which different phytoplankton taxa were fed to *N. scintillans*, Zhang et al. (2015) identified, in addition to the importance of nutrient availability that this large heterotrophic dinoflagellate grew fast when fed with diatoms. Hence, the collapse of *N. scintillans* may been driven by a marginally non-significant increase from Ambient, to ERCP 6.0, to ERCP 8.5, in the proportion of diatoms within the phytoplankton community (LRT, df 86, p = 0.05, n = 3). Altogether, we suggest that multiple global change stressors may act synergistically and reduce the abundance of mesozooplankton in the future via altered food availability and demand, with potential consequences for higher trophic levels (Reid et al., 2001; Beaugrand et al., 2003; Payne et al. 2009; Perälä et al., 2020). In parallel to bottom-up effects and to a lesser extent, we expect that the lower grazing pressure

from meszooplankton might also have contributed to the increase of *Emiliania huxleyi* in the ERCP 8.5 scenario (Behrenfeld et al., 2021).

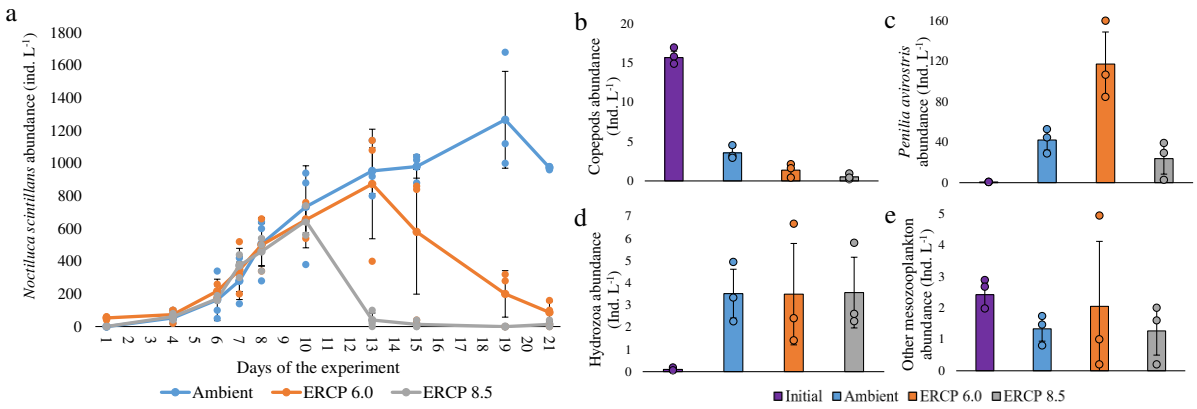

Figure 4.3: Mesozooplankton abundance and community composition. (a) Abundance of the dominant mesozooplankton species, *Noctiluca scintillans*, throughout the experiment period; x-axis represents the days of the experiment, different colours represent the Ambient treatment and Extended Representative Concentration Pathway (ERCP) scenarios (blue = Ambient, orange = ERCP 6.0, grey = ERCP 8.5), mean ± standard deviation. *Noctiluca scintillans* abundance was significantly different across scenarios (LRT, df 86, $p < 0.0001$, n = 3). (b) Abundance and composition of copepods. Copepods abundance is lower in all scenarios compared to Initial, but it is significantly higher in the Ambient compared to the ERCP scenarios (ANOVA, $F_{3,9}$ 276.1, $p < 0.0001$, n = 3). (c) Abundance and composition of *Penilia avirostris*. Abundance of the cladoceran *Penilia avirostris* is higher in all scenarios compared to Initial (ANOVA, $F_{3,9}$ 26.62, p = 0.0003, n = 3). (d) Abundance and composition of Hydrozoa. (e) Abundance and composition of other mesozooplankton. Initial corresponds to values *in situ* when seawater for the experiment was collected. Ambient treatment and ERCP scenarios represent samples from day 15. Data is displayed as mean ± standard deviation.

***Microzooplankton and the microbial loop**:* The scenarios we tested had the opposite effect on microzooplankton than on mesozooplankton. We observed a gradual increase in the biomass of microzooplankton from Ambient, to ERCP 6.0, to ERCP 8.5 scenarios (Figure 4.1). Although we found no significant difference across scenarios in microzooplankton community composition, their biomass increased along the first phytoplankton bloom and decreased after the phytoplankton bloom had decayed (Figure 4.4a-d). Whereas the microzooplankton biomass was not statistically different and continuously decreased until the end of the experiment in the Ambient and ERCP 6.0 treatments (GLM, df 86, p = 0.16, n = 3), the bloom of small coccolithophores in the ERCP 8.5 scenario coincided with an increase in microzooplankton biomass towards the end of the experiment (GLM, df 86, p = 0.0004, n = 3). Interestingly, coccoliths have been suggested as an effective defence mechanism against grazing from zooplankton (Monteiro et al., 2016), but a recent meta-analysis of data collected during mesocosm studies demonstrated that calcification of *E. huxleyi*, fails to deter microzooplankton grazing, thereby indicating that the possession of calcium carbonate scales does not provide *E. huxleyi* with effective protection from microzooplankton grazing (Mayers et al., 2020).

Moreover, bacterial biomass fluctuated during the experiment, it was higher at the end than at the beginning of the experiment in all treatments, and it reached higher levels in the ERCP 8.5 scenario than in the other two treatments during the decay phase of the first bloom (LRT, df 86, p = 0.02, n = 3, Supplementary Figure 4.4). The increase in microzooplankton biomass at the end of the experiment might also be related to the increasing bacterioplankton biomass during this time, as picoplankton also provides an important source of food for these small grazers (Zhao et al., 2020). Together with the collapse of mesozooplankton in the ERCP 8.5 scenario, these results indicate that marine coastal planktonic food webs may shift from being mesozooplankton-dominated towards a dominant role of the microbial loop in response to global change in (Figure 4.1). In support of this hypothesis, previous studies indicated that microzooplankton communities are rather unaffected by high pCO_2 (Aberle et al., 2013; Horn et al., 2016), and that the combination of warming and ocean acidification may in fact increase the interaction strength between microzooplankton and their phytoplanktonic as well as bacterial prey (Chen et al., 2012; Vázquez-Domínguez et al., 2012; Lara et al., 2013; Olson et al., 2018). Such shifts in bottom-up and top-down processes are not ecologically insignificant (Sherr and Sherr, 1994; Brander and Kiørboe, 2020). While microzooplankton are a natural trophic link between phytoplankton and bacteria, on the one hand, and mesozooplankton on the other hand (Irigoien et al., 1998), intensified trophic pathways through microzooplankton may diminish energy transfer efficiency to higher trophic levels. Strengthened energy flow through an additional trophic level leads to additional loss of organic carbon and, therefore, less efficient energy transfer to larger grazers (Fenchel, 2008; Aberle et al., 2015). The gain in prominence of microzooplankton over mesozooplankton we report here is supported by Berglund et al. (2007) and Aberle et al. (2015) who predicted lower energy transfer to higher trophic levels when the direct link from phytoplankton to mesozooplankton is shunted through an intermediary trophic level comprised of microzooplankton. Indeed, microzooplankton can directly compete with mesozooplankton for phytoplankton prey (Sherr and Sherr, 2007), and the addition of a trophic step between phytoplankton and mesozooplankton could reduce food web trophic efficiency, thereby creating a 'trophic sink' for production in the food web (Gifford, 1991; Rollwagen-Bollens et al., 2011; Anjusha et al., 2013).

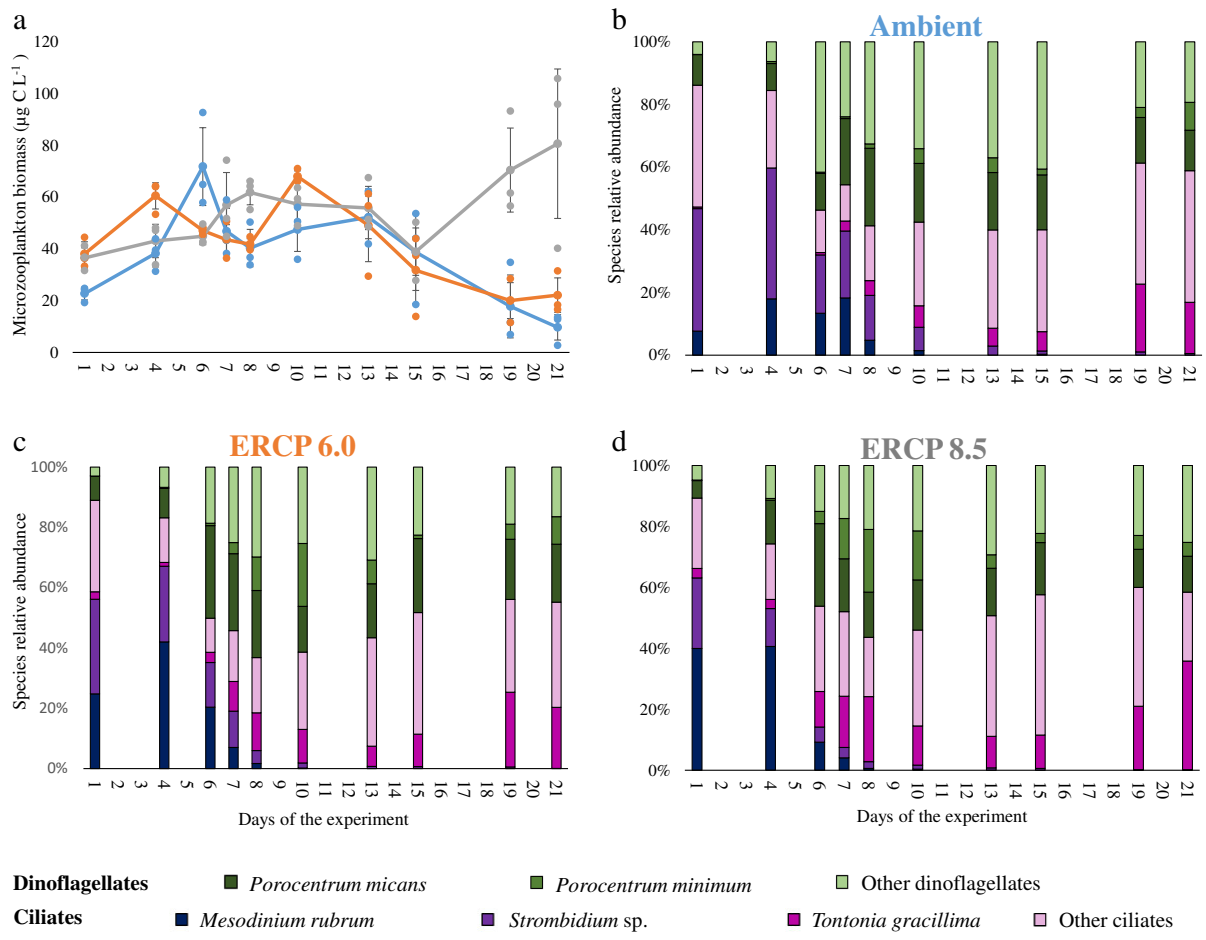

Figure 4.4: Microzooplankton biomass and community composition. (a) Microzooplankton biomass. (b,c,d) Relative abundances of different taxa of the microzooplankton communities under the different scenarios. X-axis represents the days of the experiment, different colours represent the Ambient treatment and Extended Representative Concentration Pathway (ERCP) scenarios (blue = Ambient, orange = ERCP 6.0, grey = ERCP 8.5), mean ± standard deviation. Microzooplankton biomass was significantly higher in the ERCP 8.5 (LRT, df 86, $p < 0.0001$, n = 3), compared to Ambient and ERCP scenarios.

Conclusions

Here, we applied an integrated multiple driver design in a mesocosm experiment, to test the short-term effect of different global change scenarios on natural coastal plankton communities. This study identifies a potential ecological tipping point between the ERCP 6.0 and the ERCP 8.5 scenarios (Figure 4.1). By promoting the growth of microzooplankton and nanophytoplankton, and by negatively impacting mesozooplankton, environmental conditions in the ERCP 8.5 scenario have the potential to considerably alter the structure and functioning of planktonic food webs in temperate coastal systems. In addition to these large structural shifts, we also observed that global change scenarios can cause the rise and demise of key species, such as *Emiliania huxleyi* and *Noctiluca scintillans*. The fact that planktonic food webs were relatively similar under Ambient and ERCP 6.0 conditions reinforces the goals of the "Special

Report on the impacts of global warming of 1.5°C above pre-industrial levels" (IPCC, 2018) to substantially reduce environmental risks and impacts of climate change.

4.5. Acknowledgements

We thank the colleagues from Alfred-Wegener-Institut for the technical and scientific support during the experiment, especially Julia Haafke, Petra Kadel, Silvia Peters, Andreas Kornmann, Inga Kirstein, Johannes Rick, Ragnhild Asmus and Harald Asmus. Sincere thanks to the colleagues who supported us in analysing some of the samples, including Ursula Ecker (mesozooplankton), Tatyana Romanova (dissolved inorganic nutrients), Bernhard Fuchs (bacterioplankton), Sebastian Rokitta and Gernot Nehrke (scanning electron microscopy). We thank Herwig Stibor, Helmut Hillebrand, and Ulf Riebesell for providing their expert opinion on the experimental design. We thank Herwig Stibor and Maria Stockenreiter for providing the LDPE bags in which the experiment was conducted.

4.6. Supplementary Material

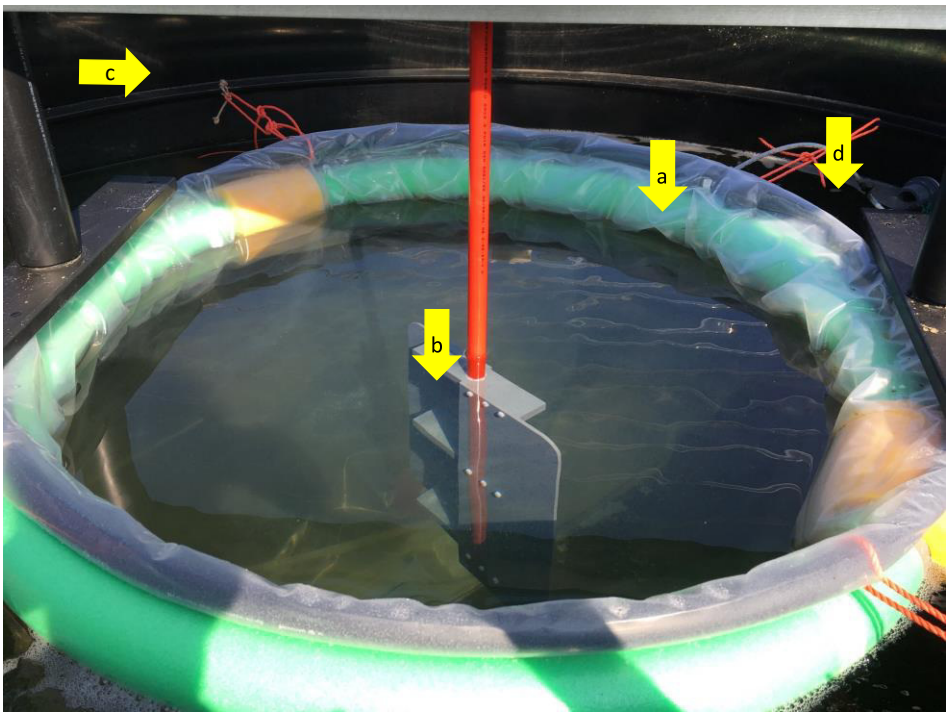

Supplementary Figure 4.1: Photo of the experimental setup. (a) The low-density polyethylene bag filled with seawater containing natural planktonic community, (b) The high-density polyethylene paddle for stirring, (c) the mesocosm tank and (d) surrounding temperature-controlled water bubbled with pCO_2-controlled air.

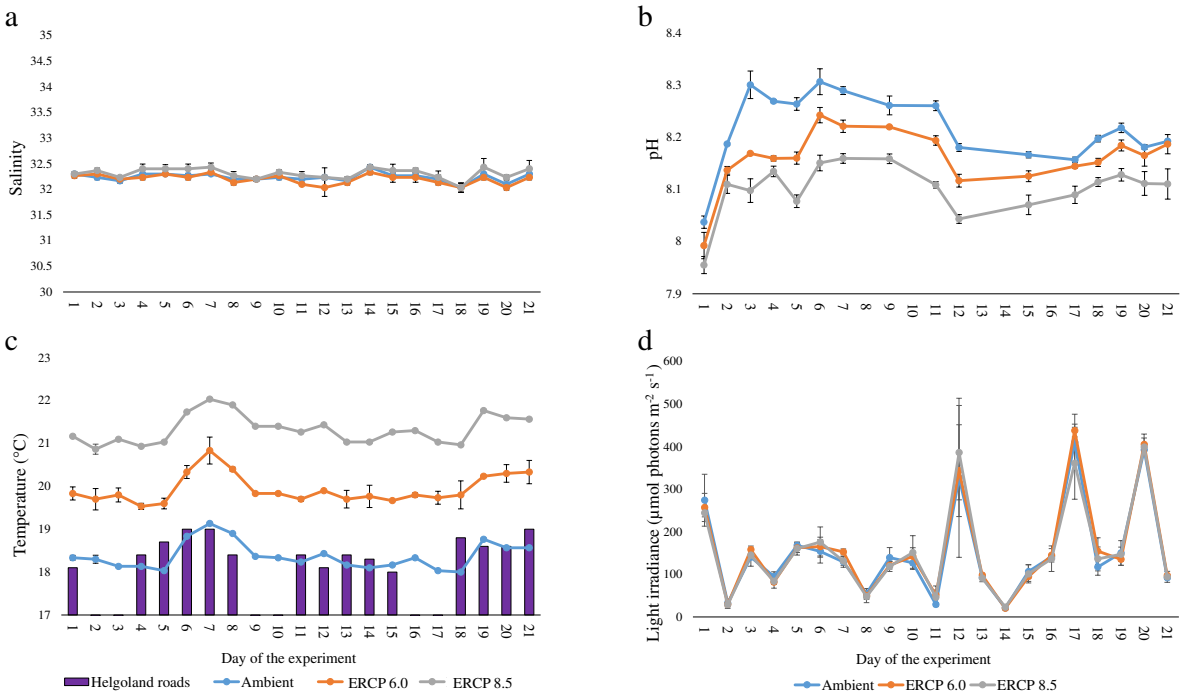

Supplementary Figure 4.2: Environmental conditions in the mesocosms during the experiment. (a) Salinity. (b) pH. (c) Temperature. (d) Light irradiance. Purple bars represent surface seawater temperature at Helgoland Roads; x-axis represents the days of the experiment, different colours represent the Ambient treatment and Extended Representative Concentration Pathway (ERCP) scenarios (blue = Ambient, orange = ERCP 6.0, grey = ERCP 8.5), mean ± standard deviation.

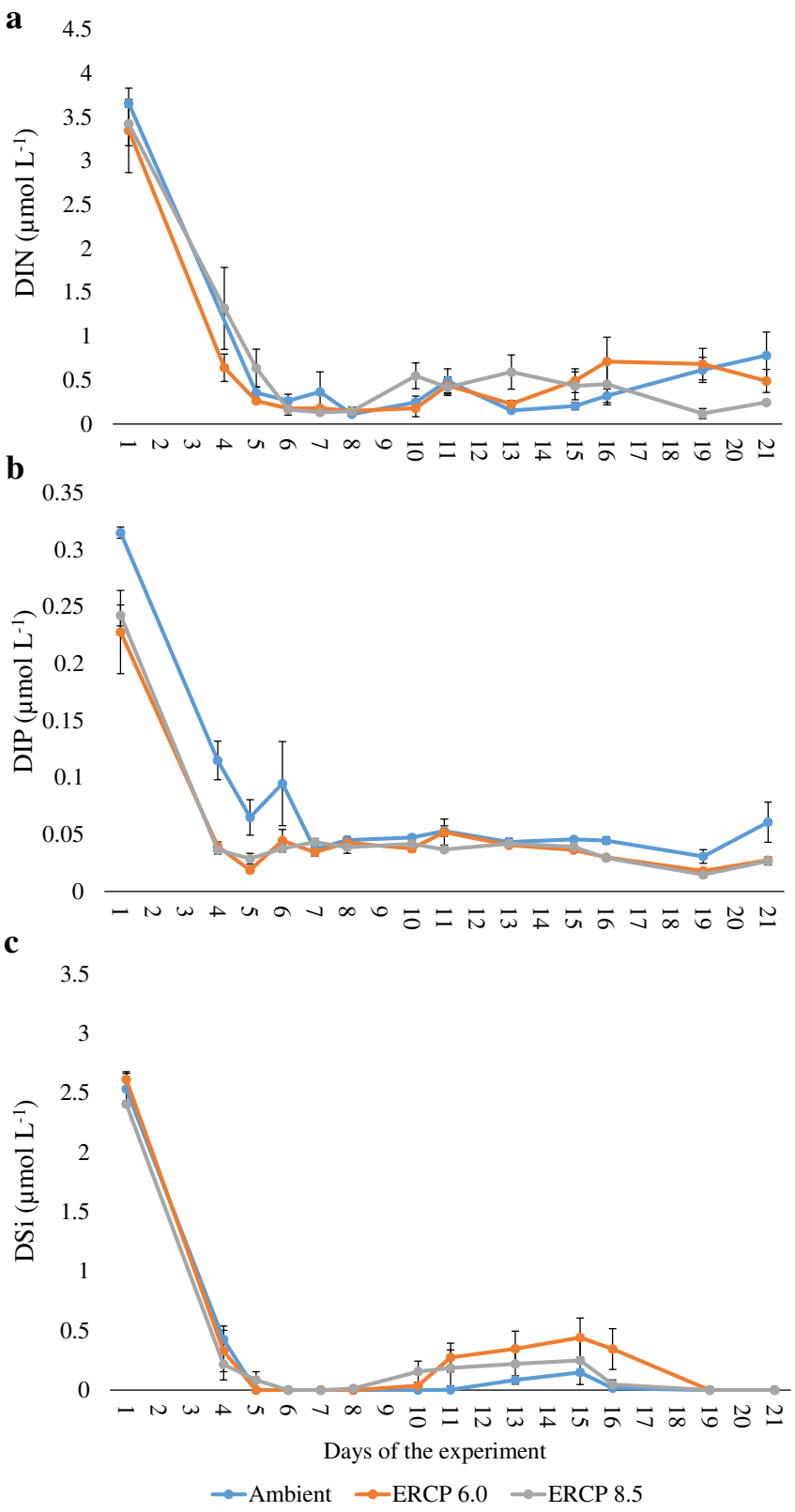

Supplementary Figure 4.3: Dissolved inorganic nutrient concentrations in the mesocosms during the experiment. (a) Dissolved inorganic nitrogen (DIN) = NO_x + NH_4^+. (b) Dissolved inorganic phosphorus (DIP) = PO_4^{3-}. (c) Dissolved inorganic silicate (DSi) = SiO_3^-; x-axis represents the days of the experiment, different colours represent the Ambient treatment and Extended Representative Concentration Pathway (ERCP) scenarios (blue = Ambient, orange = ERCP 6.0, grey = ERCP 8.5), mean ± standard deviation.

Supplementary Table 4.1: Carbonate chemistry in the mesocosms during the experiment. Dissolved inorganic carbon (DIC), partial pressure of CO_2 (pCO_2), Bicarbonate (HCO_3^-), Carbonate (CO_3^{2-}), Carbon dioxide (CO_2) and calcite saturation state ($\Omega_{calcite}$) were calculated based on pH and total alkalinity (TA) using CO2Sys (Pierrot et al., 2006); mean ± standard deviation.

Day	Scenario	TA (µmol KgSW^{-1})	DIC (µmol KgSW^{-1})	pCO_2 (µatm)	HCO_3^- (µmol KgSW^{-1})	CO_3^{2-} (µmol KgSW^{-1})	CO_2 (µmol KgSW^{-1})	$\Omega_{calcite}$
1	Ambient	2308.1 (±55.1)	2141.1 (±45.1)	586.7 (±20.6)	1991.4 (±38.3)	129.5 (±8.3)	20.1 (±0.7)	3.14 (±0.20)
	ERCP 6.0	2315.3 (±15.8)	2218.7 (±39.3)	658.5 (±57.6)	1974.8 (±27.4)	122.2 (±13.9)	21.7 (±1.9)	2.98 (±0.34)
	ERCP 8.5	2345.6 (±46.4)	2162.5 (±61.9)	744.1 (±58.1)	2019.9 (±59.4)	119.1 (±7.5)	23.6 (±1.8)	2.90 (±0.18)
4	Ambient	2341.9 (±20.8)	2061.1 (±19.4)	318.4 (±5.8)	1846.9 (±18.1)	203.1 (±2.7)	10.9 (±0.2)	4.90 (±0.06)
	ERCP 6.0	2332.1 (±32.4)	2079.5 (±42.7)	427.6 (±17.8)	1895.8 (±41.6)	169.5 (±0.9)	14.2 (±0.6)	4.12 (±0.02)
	ERCP 8.5	2335.1 (±6.8)	2100.4 (±19.1)	465.4 (±24.5)	1916.2 (±23.1)	169.3 (±4.8)	14.9 (±0.8)	4.13 (±0.12)
5	Ambient	2301.3 (±28.5)	2027.6 (±35.9)	317.8 (±21.2)	1819.6 (±39.8)	196.9 (±6.1)	11.0 (±0.7)	4.78 (±0.15)
	ERCP 6.0	2233.9 (±55.1)	2033.9 (±64.9)	418.5 (±32.6)	1853.7 (±65.9)	166.3 (±3.8)	13.9 (±1.2)	4.04 (±0.09)
	ERCP 8.5	2300.7 (±21.0)	2089.4 (±21.8)	533.1 (±28.6)	1922.8 (±21.2)	149.6 (±6.9)	16.9 (±0.9)	3.65 (±0.17)
6	Ambient	2227.9 (±82.1)	1929.9 (±55.3)	273.6 (±24.5)	1709.8 (±39.3)	210.8 (±23.6)	9.3 (±0.8)	5.12 (±0.57)
	ERCP 6.0	2269.6 (±42.7)	1973.8 (±53.7)	333.2 (±30.7)	1766.7 (±56.1)	196.2 (±4.6)	10.8 (±0.9)	4.78 (±0.11)
	ERCP 8.5	2321.8 (±45.2)	2095.7 (±39.9)	449.3 (±31.8)	1902.6 (±38.7)	179.1 (±10.1)	14.0 (±1.0)	4.37 (±0.25)
7	Ambient	2221.9 (±56.1)	1932.7 (±44.7)	285.8 (±5.9)	1718.4 (±35.6)	204.8 (±9.8)	9.6 (±0.2)	4.98 (±0.24)
	ERCP 6.0	2184.1 (±10.4)	1937.7 (±26.1)	345.6 (±18.6)	1739.4 (±30.3)	187.2 (±9.8)	11.1 (±0.7)	4.56 (±0.24)
	ERCP 8.5	2248.4 (±48.8)	2008.6 (±33.9)	421.8 (±16.7)	1819.2 (±29.8)	176.3 (±7.4)	13.1 (±0.5)	4.31 (±0.18)
8	Ambient	2232.8 (±18.1)	1852.8 (±12.4)	186.3 (±17.9)	1581.6 (±26.8)	264.9 (±17.2)	6.3 (±0.6)	6.44 (±0.42)
	ERCP 6.0	2237.9 (±15.2)	1862.5 (±35.2)	221.2 (±15.0)	1609.5 (±36.7)	245.8 (±10.4)	7.2 (±0.5)	5.99 (±0.25)
	ERCP 8.5	2254.1 (±40.3)	1922.4 (±28.4)	266.1 (±3.3)	1677.5 (±23.9)	236.6 (±4.4)	8.3 (±0.1)	5.78 (±0.11)

Day	Scenario	TA (µmol KgSW^{-1})	DIC (µmol KgSW^{-1})	pCO_2 (µatm)	HCO_3^- (µmol KgSW^{-1})	CO_3^{2-} (µmol KgSW^{-1})	CO_2 (µmol KgSW^{-1})	$\Omega_{calcite}$
10	Ambient	2262.6 (±47.4)	1865.6 (±31.0)	174.1 (±18.8)	1582.3 (±34.5)	277.3 (±23.1)	5.9 (±0.6)	6.74 (±0.56)
	ERCP 6.0	2233.8 (±13.9)	1867.2 (±8.7)	205.9 (±1.8)	1604.9 (±6.6)	255.5 (±2.6)	6.8 (±0.1)	6.22 (±0.06)
	ERCP 8.5	2249.9 (±33.0)	1969.8 (±76.2)	266.7 (±10.6)	1719.0 (±64.5)	242.4 (±13.1)	8.4 (±0.3)	5.92 (±0.32)
11	Ambient	2195.6 (±32.0)	1931.1 (±29.9)	305.4 (±14.3)	1733.1 (±28.7)	187.5 (±6.4)	10.5 (±0.5)	4.55 (±0.15)
	ERCP 6.0	2298.5 (±5.4)	1995.1 (±74.5)	377.1 (±16.4)	1806.6 (±65.3)	175.9 (±10.6)	12.5 (±0.5)	4.28 (±0.26)
	ERCP 8.5	2226.8 (±52.4)	2052.3 (±67.8)	485.6 (±26.2)	1878.9 (±64.3)	157.9 (±3.7)	15.4 (±0.8)	3.85 (±0.09)
13	Ambient	2289.7 (±52.0)	1972.0 (±51.6)	254.3 (±13.6)	1737.7 (±49.3)	225.5 (±4.6)	8.8 (±0.5)	5.48 (±0.11)
	ERCP 6.0	2249.3 (±35.8)	1979.8 (±64.6)	299.4 (±38.3)	1758.6 (±73.6)	211.3 (±11.5)	9.9 (±1.3)	5.14 (±0.28)
	ERCP 8.5	2292.0 (±49.5)	2034.0 (±36.2)	374.8 (±24.7)	1829.3 (±34.1)	192.8 (±10.7)	11.9 (±0.8)	4.70 (±0.26)
15	Ambient	2307.6 (±57.7)	2083.1 (±48.6)	415.6 (±1.9)	1903.2 (±41.1)	165.5 (±7.6)	14.3 (±0.1)	4.02 (±0.18)
	ERCP 6.0	2452.9 (±3.8)	2152.6 (±100.9)	481.2 (±12.6)	1972.5 (±87.8)	164.2 (±13.5)	15.9 (±0.4)	3.99 (±0.33)
	ERCP 8.5	2253.7 (±79.2)	2073.9 (±68.6)	540.9 (±53.8)	1909.5 (±66.9)	147.35 (±9.8)	17.1 (±1.7)	3.59 (±0.24)
16	Ambient	2287.3 (±67.6)	2008.9 (±51.9)	309.9 (±5.9)	1798.4 (±39.6)	199.8 (±12.5)	10.6 (±0.2)	4.86 (±0.30)
	ERCP 6.0	2326.5 (±6.1)	2056.3 (±7.1)	357.4 (±18.5)	1849.1 (±14.3)	195.5 (±8.1)	11.8 (±0.6)	4.76 (±0.19)
	ERCP 8.5	2310.9 (±35.6)	2059.2 (±30.4)	394.5 (±18.9)	1856.3 (±29.6)	190.4 (±6.5)	12.5 (±0.6)	4.64 (±0.16)
19	Ambient	2282.0 (±59.8)	2029.2 (±58.0)	358.5 (±20.4)	1833.9 (±54.9)	183.1 (±6.4)	12.2 (±0.71)	4.45 (±0.15)
	ERCP 6.0	2326.5 (±6.1)	2052.1 (±45.9)	399.3 (±23.5)	1858.8 (±45.2)	180.2 (±5.8)	13.0 (±0.76)	4.38 (±0.14)
	ERCP 8.5	2310.7 (±35.6)	2068.3 (±33.5)	468.8 (±24.2)	1884.9 (±29.6)	168.7 (±8.5)	14.6 (±0.75)	4.12 (±0.21)
21	Ambient	2297.5 (±28.9)	2058.1 (±27.3)	386.5 (±5.6)	1870.2 (±25.2)	174.8 (±1.9)	13.2 (±0.2)	4.25 (±0.05)
	ERCP 6.0	2283.7 (±16.1)	2024.1 (±7.7)	392.4 (±29.3)	1831.8 (±16.4)	179.6 (±14.9)	12.7 (±1.1)	4.38 (±0.37)
	ERCP 8.5	2204.0 (±99.1)	2014.7 (±77.6)	478 (±59.7)	1841.6 (±72.2)	158.1 (±18.9)	15.0 (±1.9)	3.86 (±0.46)

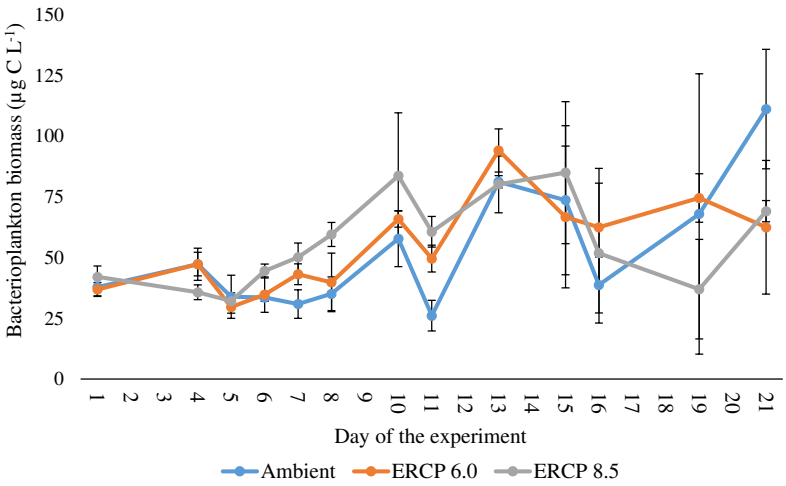

Supplementary Figure 4.4: Bacterioplankton biomass. X-axis represents the days of the experiment, different colours represent the Ambient treatment and Extended Representative Concentration Pathway (ERCP) scenarios (blue = Ambient, orange = ERCP 6.0, grey = ERCP 8.5), mean ± standard deviation.

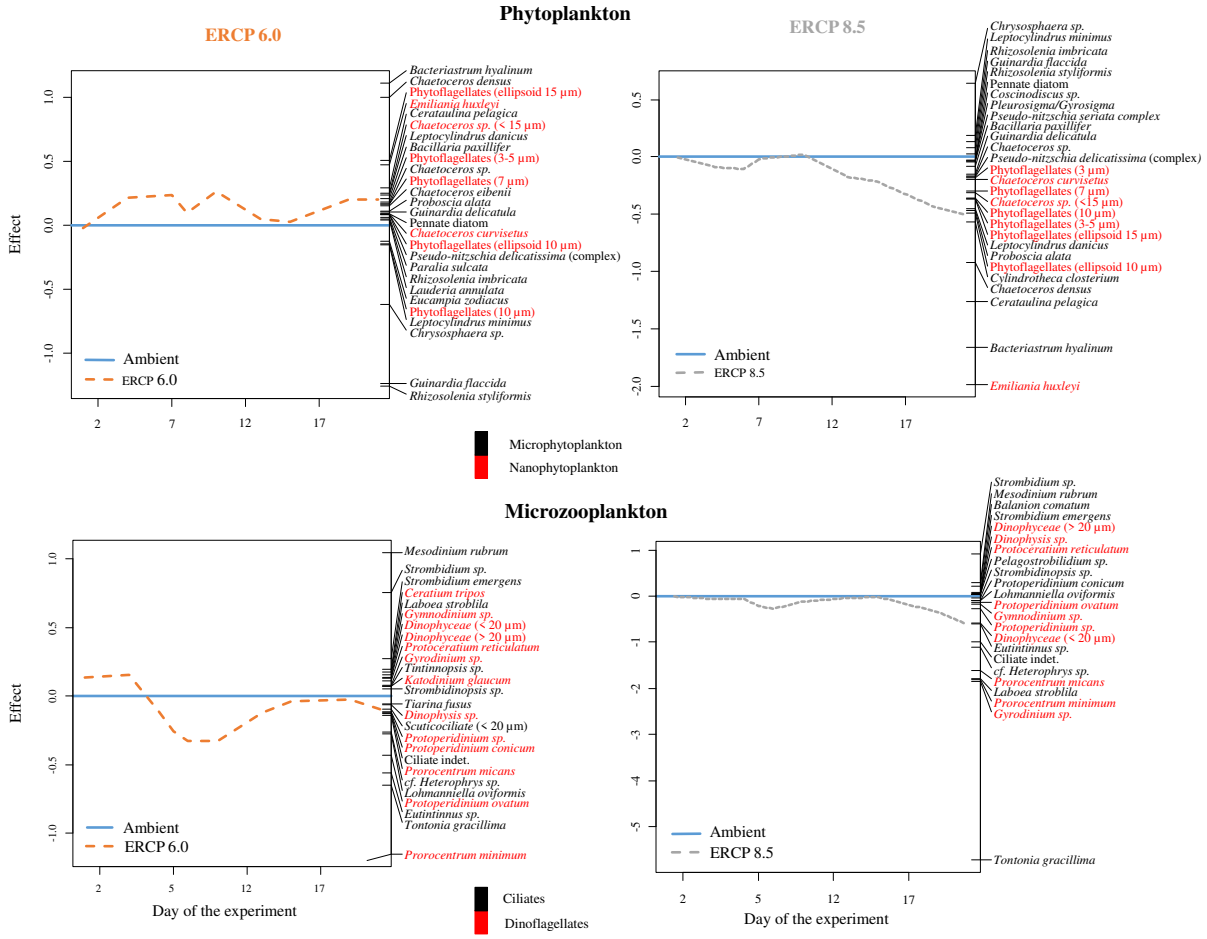

Supplementary Figure 4.5: Principal Response Curve of the plankton community. Graphic representation of the phytoplankton (top) and microzooplankton (bottom) community response over time in the extended Representative Concentration Pathway (ERCP) scenarios 6.0 and 8.5 in comparison to the Ambient treatment. Time and scenario explained 85% and 79% of the variation in phytoplankton community composition in the scenario ERCP 6.0 and ERCP 8.5, respectively. For microzooplankton community composition, it was 74% and 56%. For clarity, only the most affected taxa are displayed on the diagram.

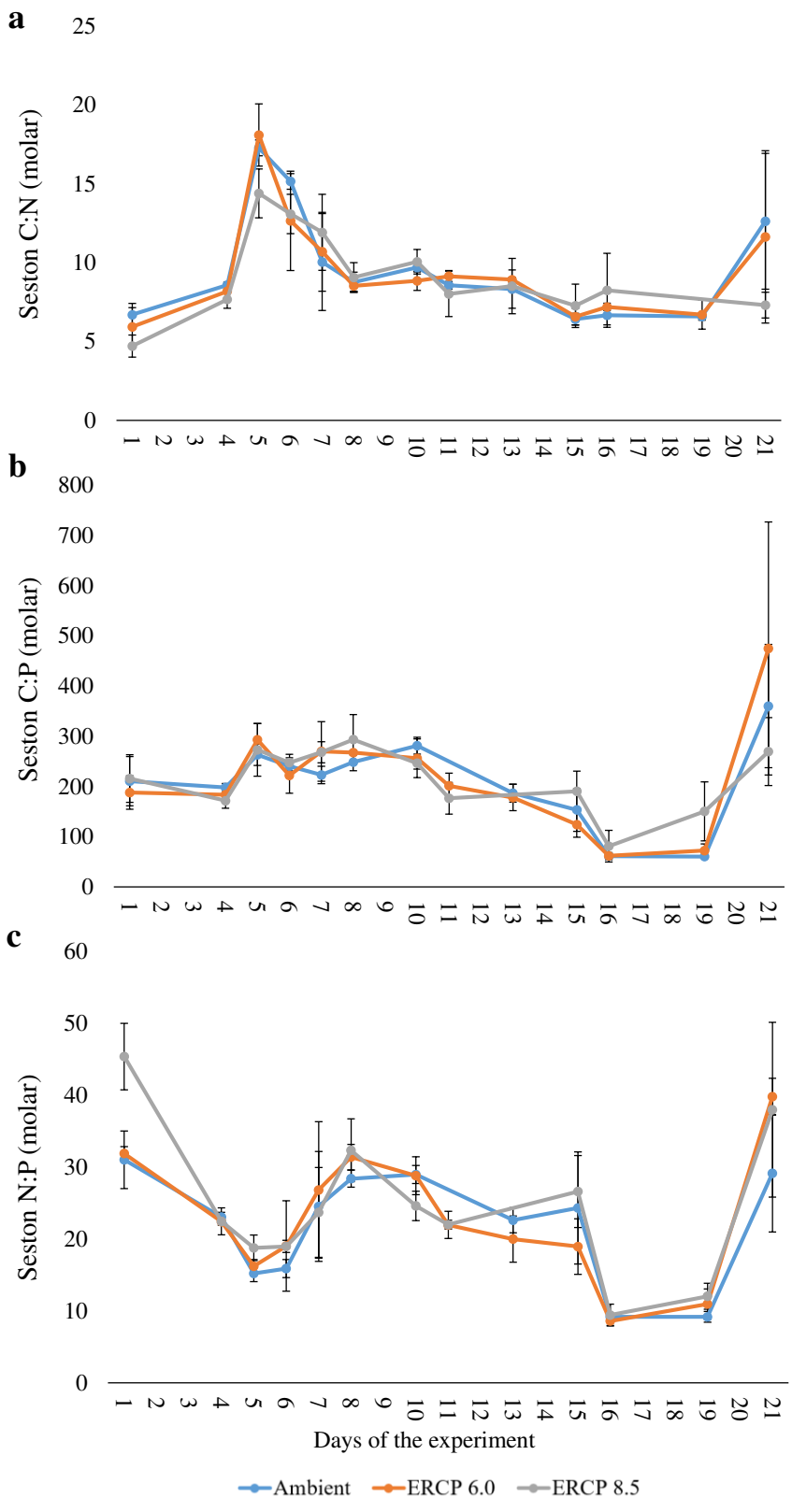

Supplementary Figure 4.6: Seston elemental stoichiometry. (a) Seston C:N stoichiometry (Carbon:Nitrogen). (b) Seston C:P stoichiometrym (Carbon:Phosphorus). (c) Seston N:P stoichiometry (Nitrogen:Phosphorus), x-axis represents the day of the experiment, different colours represent the Ambient and extended Representative Concentration Pathway (ERCP) scenarios (blue = Ambient, orange = ERCP 6.0, grey =ERCP 8.5), mean ± standard deviation.

Chapter 5

Global change alters plankton food webs by promoting the microbial loop: An inverse modelling and network analysis approach on a mesocosm experiment

Julien Di Pane[1,4], Pierre Bourdaud[2], Sabine Horn[3], Hugo Duarte Moreno[1], Cédric Léo Meunier[1]

[1]Alfred-Wegener-Institut, Helmholtz-Zentrum für Polar- und Meeresforschung, Biologische Anstalt Helgoland, Germany

[2]Research Unit EMH, IFREMER, Nantes, France

[3]Alfred-Wegener-Institut Helmholtz-Zentrum für Polar- und Meeresforschung, Wattenmeerstation, List auf Sylt, Germany

[4]Aix Marseille Univ, Université de Toulon, CNRS, IRD, MIO, Marseille, France

Under review in Oceanography and Limnology

5.1. Abstract

Marine organisms are exposed to the simultaneous effects of multiple environmental changes. Plankton forms the base of pelagic marine food webs and are particularly sensitive to ecosystem changes. Warming, acidification, and changes in dissolved nutrient concentrations may alter these assemblages, with consequences for the entire ecosystem. Global change may also cause less obvious alterations to the networks of interactions among species. Using inverse analyses applied to data collected during a mesocosm experiment, we aimed to compare the ecological functioning of plankton assemblages and the interactions within the plankton food web under different global change scenarios. The experimental treatments were based on the RCP 6.0 and 8.5 scenarios developed by the IPCC, which were extended (ERCP) to integrate the future predicted changes in coastal water nutrient concentrations. We identified that the functioning of the plankton food web was rather similar in the Ambient and ERCP 6.0 scenarios, but substantially altered in the ERCP 8.5 scenario. Global change strengthens the microbial loop, with a decrease of energy transfer to higher trophic levels. Microzooplankton responded by an increased degree of herbivory in their diet. We also observed that the organisation of the food web and its capacity to recycle carbon was higher under the ERCP 8.5 scenario, but flow diversity was significantly reduced, illustrating an increased food web stability at the expense of diversity. Here, we provide evidence that if global change goes beyond the ERCP 6.0 scenario, pelagic ecosystem functioning will be subjected to dramatic changes.

5.2. Introduction

Human activities and associated increasing greenhouse gas emissions cause simultaneous changes in a range of ocean abiotic parameters. The Intergovernmental Panel on Climate Change (IPCC) has computed different scenarios projecting that, by 2100, ocean's temperature may increase by 1 to 6 °C and pH may decrease by 0.1 to 0.4 (IPCC, 2022). In addition, urban, agricultural, and industrial development alter biogeochemical cycles through nutrient runoffs leading to a general increase of dissolved nitrogen:phosphorus (N:P) ratios in European coastal systems (Grizzetti et al., 2012). Consequently, marine organisms are currently, and will continue to be, exposed to the simultaneous effects of multiple anthropogenic-induced environmental changes (Hoegh-Guldberg and Bruno, 2010; Duarte, 2014). Such changes in environmental conditions can trigger cascading effects on species assemblages, on interactions between organisms, and therefore on overall ecosystem functioning. Despite the large body of research demonstrating effects of global change on population dynamics and community composition, the challenges associated with quantifying interactions between organisms have led to a paucity of information on the influence of global change on plankton food web functioning.

Plankton organisms form the base of pelagic marine food webs, and are particularly sensitive to ecosystem changes. For instance, warming and changes in dissolved nutrient concentrations in coastal seas observed over the past decades have altered phytoplankton and zooplankton assemblages, with consequences for the entire ecosystem such as nutrient turnover and fish recruitment (Alvarez-Fernandez et al., 2012; Capuzzo et al., 2018; Di Pane et al., 2022). However, less is known on how environmental changes could further impact plankton communities, and especially on the combined impact of multiple drivers (Sommer et al., 2015; Garzke et al., 2016; Horn et al., 2020). Moreno et al. (2022) addressed this topic in a mesocosm experiment, and showed that simultaneous warming, acidification, and increased dissolved N:P ratio altered plankton assemblages by favouring smaller phytoplankton and microzooplankton species, and by impairing mesozooplankton abundances. Previous studies also showed a deleterious combined effect of warming and acidification (Peter and Sommer, 2012; Bermúdez et al., 2016), which is further intensified when nutrient availability is low (Peter and Sommer, 2015). These studies provide essential information on the extent to which plankton communities may be restructured as a result of global change, but do not quantify how interactions between organisms may be altered, an information necessary to predict future energy transfer efficiency and food web connectance.

Despite the growing number of studies addressing the potential influence of multiple drivers on plankton organisms (Sala et al., 2000), global change may also cause less obvious alterations to the networks of interactions among species (Tylianakis et al., 2007). Yet, complex biotic interaction networks play an important role in determining the resilience and resistance of ecosystems (Ives and Carpenter, 2007), in maintaining biodiversity (Bascompte et al., 2006), and in mediating ecosystem responses to global change (Suttle et al., 2007). The lack of research on how multiple global change drivers can affect biotic interactions probably stems from difficulties in quantifying changes in interactions compared to changes in biodiversity (McCann, 2007). Nevertheless, interactions may be particularly susceptible to environmental changes, as they are sensitive to the phenology, behaviour, physiology, and relative abundances of multiple species (Tylianakis et al., 2007). In order to tackle this shortcoming, food web modelling represents a useful tool allowing to estimate energy fluxes between biotic compartments to obtain a representation of the ecosystem functioning from field or experimental studies.

Food web models have been widely used over the past years, aiming to reconstruct a network of components of an ecosystem (i.e. species, taxa or functional units) connected by trophic links (Coll and Libralato, 2012), and to estimate energy transfer and interaction strength between food web components. Despite the importance of energy transfer efficiency within the plankton food web for higher trophic levels, studies on food web processes often display a poor plankton resolution due to the lack of data on energy fluxes at lower trophic levels components (Richardson et al., 2006; Grami et al., 2008). Inverse analyses represent a useful tool to estimate unknown fluxes, which have been used to infer the properties of a system when insufficient data are available (Richardson et al., 2004). Although spatial and temporal variations are neglected in this approach, inverse analyses favour biological complexity of the food web and allow considering a high diversity of components (Tortajada et al., 2012). Since the seminal study of Vezina and Platt (1988) in which inverse analyses were used to provide a complete description of the plankton food web at steady state, many studies successfully used a similar approach to examine plankton food web dynamics (e.g. Hlaili et al., 2014; Meddeb et al., 2019; Tortajada et al., 2012). However, to the best of our knowledge, no study has attended yet to model the potential future functioning of plankton food web under simultaneous changes of multiple global change drivers.

Using inverse analyses applied to data collected during a mesocosm experiment (Moreno et al., 2022), we aimed to compare the ecological functioning of plankton assemblages and the

interactions within the plankton food web under different global change scenarios. Our objectives were to 1) estimate and compare carbon fluxes across compartments, 2) predict ecological properties of the plankton food web, and 3) evaluate how the plankton food web could be impacted in the future by global change. Therefore, this study provides unique insights into the extent and direction of changes in plankton trophic systems in response to global change.

5.3. Materials and Methods

Experiment and data acquisition

The data used in the study were obtained during a mesocosm experiment conducted over three weeks in the mesocosm facilities at the Wadden Sea station of the Alfred Wegener Institute Helmholtz Centre for Polar and Marine Research on the island of Sylt, Germany, in late summer (August-September) 2018 (Meunier et al., 2022; Moreno et al., 2022). Using a multiple driver approach, Moreno et al. (2022) tested the influence of two global change scenarios, based on predictions by the Intergovernmental Panel on Climate Change for the end of the 21st century (IPCC, 2014), on the structure and dynamics of plankton assemblages. Temperature and pCO_2 levels were chosen to represent (1) Ambient conditions (i.e. condition observed in the field in real time; T: 18.4 ± 0.3°C; pH: 8.3 ± 0.1), (2) a moderate global change scenario based on RCP 6.0 (+1.5°C and -0.2 pH), and (3) a more severe global change scenario based on RCP 8.5 (+3°C and -0.3 pH). Additionally, dissolved inorganic nutrient concentrations were also manipulated to simulate the predicted increase in N:P ratios in coastal European seas (Grizzetti et al., 2012), with the Ambient and the Extended RCP scenarios (ERCP) having an N:P ratio (molar) of 16 (Redfield ratio), and 25, respectively, at the onset of the experiment. More detailed information about the experimental design can be found in Moreno et al. (2022).

During the three weeks of the experiment, plankton (i.e. bacterioplankton, phytoplankton, micro- and mesozooplankton) was sampled ten times (~ every two days) in order to determine carbon biomass ($\mu gC.ind^{-1}$) and species composition. For the three scenarios, we grouped all plankton organisms reported in Moreno et al. (2022) into 10 compartments (Table 5.1) according to their morphotype, feeding behaviour, and size class (Tortajada et al., 2012). Pelagic bacteria (bac) represented the lowest non-autotroph trophic level. Phytoplankton was composed of four compartments, namely nano-diatoms (ndi), coccolithophores (coc), phytoflagellates (phf) and micro-phytoplankton (mph). Microzooplankton was composed of two groups, heterotrophic dinoflagellates (din) and ciliates (cil). Mesozooplankton was

composed of three compartments, copepods (cop), cladocerans (cla) and the species *Noctiluca scintillans* (Nsc).

Table 5.1: Overview of the main taxa representing each compartment used in the model. These groups were created regarding their differences in trophic level, size class and feeding strategies.

Group	Code	Compartment	Dominant taxa	Number of taxa
Bacteria	bac	Pelagic bacteria	-	1
Nano-phytoplankton [2-20µm]	coc	Coccolithophores	*Emiliania huxleyi*	1
	ndi	Nano diatoms	*Chaetoceros* sp. |10 µm x10 µm | (68%), *Chaetoceros* sp. |15 µm x10 µm | (28%)	9
	phf	Phytoflagellates	Flagellate (ellipsoid) indet. |8 µm x15 µm | (22%), Flagellate (ellipsoid) indet. |5 µm x10 µm | (18%), Flagellate (sphere) indet. |3 µm-5 µm | (16%), *Phaeocystis* sp. (13%)	10
Micro phytoplankton >20µm	mph	Micro phytoplankton	*Guinardia flaccida* (43%), *Leptocylindrus danicus* (27%), *Cylindrotheca closterium* (6%)	37
Microzooplankton <200µm	din	Heterotrophic dinoflagellates	*Prorocentrum micans* (30%), *Gyrodinium* sp. (18%), *Prorocentrum minimum* (12%)	20
	cil	Ciliates	*Mesodinium rubrum* (22%), *Strombidium* sp. (11%), *Heterophrys* sp. (8%)	22
Mesozooplankton >200µm	cla	Cladocera	*Penilia avirostris*	1
	cop	Copepods	*Oithona* sp. (32%), *Temora longicornis* (22%), *Tisbe* sp. (16%)	8
	Nsc	*Noctiluca scintillans*	-	1

Since plankton organisms are highly cyclic, and in order to obtain one value of biomass per compartment for each scenario, we calculated the median carbon biomass by compartment for each scenario (Supplementary Figure 5.1). This approach is preferable when the data display some extreme low and high values (typical for blooming organisms) in their distribution as it provides a good measure of central tendency.

Inverse analysis

The main objective of this study was to reconstruct the food web structure of plankton assemblages from controlled environment experiments, to quantify interactions and fluxes within the food web, and to assess how those may be influenced by global change. Food webs are represented by energy fluxes between organisms, which are often difficult to quantify, but can be mathematically estimated (van Oevelen et al., 2010). Here, we used inverse Monte Carlo modelling coupled with Markov chains to determine daily carbon flows in the three scenarios at equilibrium ($mgC.m^{-3}.d^{-1}$) using the *LimSolve* package (Meersche et al., 2009) of the R software (R core Team, 2022). Inverse modelling (LIM; Meersche et al., 2009; Van Oevelen et al., 2010) allows to model a food web from *in situ* or mesocosm measurements and equations, estimating the possible values of the unknown fluxes in the food web at equilibrium. LIM is well suited to describe the eco-physiological processes of plankton food web that are often neglected in other types of models (Niquil et al., 2012). In addition, the Monte Carlo Markov chain approach allows the variability built into the model to be considered via minimum and maximum values assigned to each flow. After compartment creation, the LIM approach follows four main steps, starting by (1) constructing an *a priori* model considering the topology of the food web; i.e. all possible flows between compartments as well as all different import and export flows, (2) setting mass balance equations between flows as equalities, (3) setting inequalities, from either *in situ* measurements or from literature, consisting in a number of biological constraints to reduce the range of possible values for each flow, and (4) calculating a large sample of possible solutions for unknown flows (Meddeb et al., 2019).

Food web topology

Since the experiment was performed in a closed environment (mesocosm bags), gross primary production (GPP) of the four phytoplankton compartments was the only source of carbon import within the biological system. Carbon exports, or losses were driven by respiration of all living compartments. Losses by sinking were not considered since the experimental set up simulated a well-mixed water column by constant stirring. Bacterial and phytoplankton exudation, as well as zooplankton excretion contributed to the dissolved organic carbon (doc) pool, while natural mortality (senescence) contributed to the detrital pool (det). Doc was only consumed by bacteria, while det was used by bacteria, ciliates, dinoflagellates, copepods and *N. scintillans*. The dissolution of det into doc was also considered. The microzooplankton compartment (dinoflagellates and ciliates) grazed on phytoplankton (ndi, phf, coc, mph) and bacteria (bac). In the mesozooplankton compartment, copepods were predating on

microzooplankton (din and cil) and grazing on micro-phytoplankton and det (Nakamura and Turner, 1997; Suzuki et al., 1999; Castellani et al., 2005). *Noctiluca scintillans (Nsc)* and

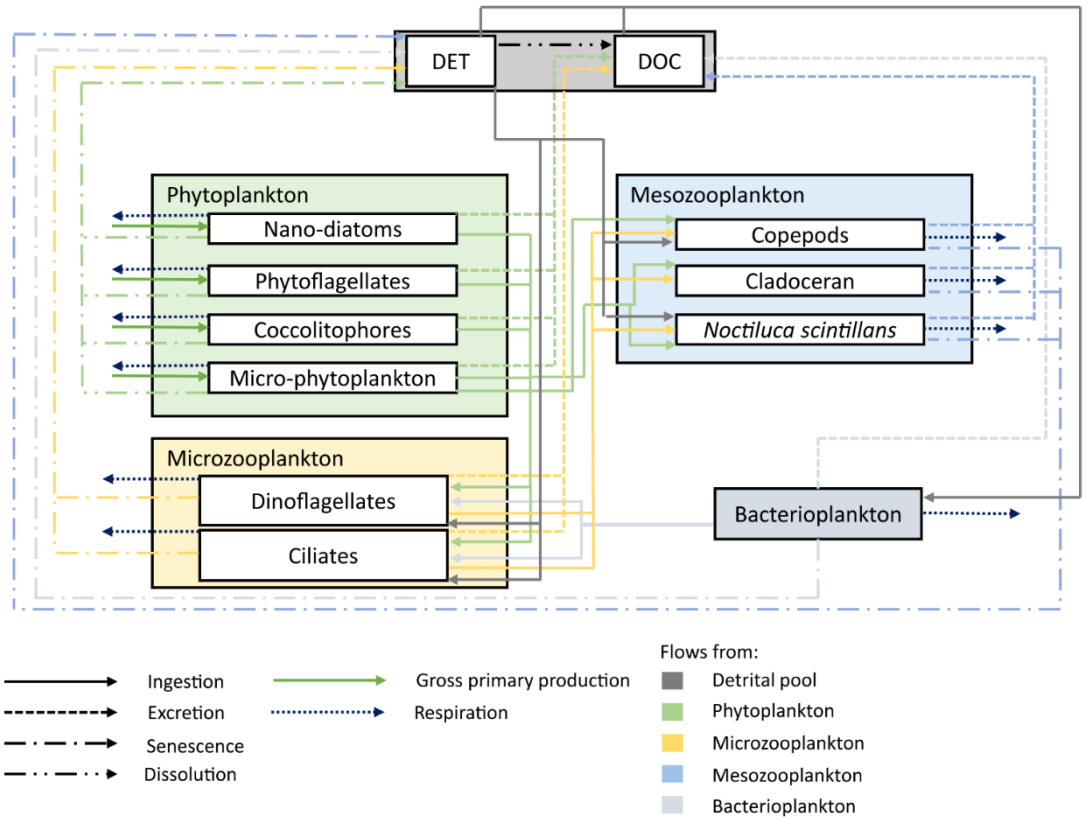

Figure 5.1: A priori model structure summarising all compartments and possible flows considered in the food web model.

cladocerans (cla) can consume a wide variety of prey and have a relatively limited ability to actively select food due to their feeding mode (Turner et al., 1988; Kirchner et al., 1996; Zhang et al., 2016). Both Nsc and cla were feeding on all phytoplankton and microzooplankton compartments, but only Nsc on det (Atienza et al., 2006; Zhang et al., 2015). A total of 66 flows were considered in the *a priori* model of each scenario (Figure 5.1).

Model constraints

The system was considered stable and at equilibrium. In other words, the sum of the inflows was equal to the sum of the outflows. The mass balance equations are given in Table 5.2.

Table 5.2: Mass equilibrium and equations used for the LIM. Flow names were composed of the three letters code of the origin compartment followed by the one of the receiving compartments (see Table 5.1 for code names correspondence), separated by "TO". R = respiration, P = production, B = biomass, GPP = gross primary production.

Compartments	Mass balanced equation
bac	(docTObac + detTObac) – (R-bac + bacTOdoc + bacTOdet + bacTOdin + bacTOcil) = 0
ndi	GPPndi – (R-ndi + ndiTOdet + ndiTOdoc + ndiTOdin + ndiTOcil + ndiTOcla + ndiTONsc) = 0
coc	GPPcoc – (R-coc + cocTOdet + cocTOdoc + cocTOdin + cocTOcil + cocTOcla + cocTONsc) = 0
phf	GPPphf – (R-phf + phfTOdet + phfTOdoc + phfTOdin + phfTOcil + phfTOcla + phfTONsc) = 0
mph	GPPmph – (R-mph + mphTOdet + mphTOdoc + mphTOdin + mphTOcil + mphTOcla + mphTONsc + mphTOcop) = 0
din	(bacTOdin + ndiTOdin + mphTOdin + phfTOdin + bacTOdin + detTOdin) – (din-R + dinTOdet + dinTOdoc+ dinTOcla + dinTOcop + dinTONsc) = 0
cil	(bacTOcil + ndiTOcil + mphTOcil + phfTOcil + bacTOcil + detTOcil) – (cil-R + cilTOdet + cilTOdoc + cilTOcla + cilTOcop + cilTONsc) = 0
cop	(dinTOcop + cilTOcop + mphTOcop + detTOcop) – (cop-R + copTOdet + copTOdoc) = 0
cla	(dinTOcla + cilTOcla + mphTOcla + cocTOcla + ndiTOcla + phfTOcla) – (cla-R + claTOdet + claTOdoc) = 0
Nsc	(dinTONsc + cilTONsc + mphTONsc + cocTONsc + ndiTONsc + phfTONsc + detTONsc) – (R-Nsc + NscTOdet + NscTOdoc) = 0
doc	(claTOdoc + copTOdoc + NscTOdoc + cilTOdoc + dinTOdoc + ndiTOdoc + pfhTOdoc + mphTOdoc + cocTOdoc + bacTOdoc + detTOdoc) – docTObac = 0
det	(claTOdet + copTOdet + NscTOdet + cilTOdet + dinTOdet + ndiTOdet + pfhTOdet + mphTOdet + cocTOdet + bacTOdet) – (detTObac + detTOdoc + detTOcil + detTOdin + detTOcop + detTONsc) = 0

Compartments	Description	Equation	Reference
cop, cla, Nsc	Mesozooplankton production is equal to about 15% of their biomass	P = B * 0.153424	Sautour and Castel (1998)
bac	Bacterial production is equal to 31% of their ingestion	P = C * 0.31	Newell and Linley (1984)
detTOdoc	2% of det is dissolved into doc	detTOdoc = det * 0.02	Moloney and Field (1991); Moloney et al. (1991)

In order to make the model consistent with the biological reality of the system, the solutions of the flows estimated by the model were constrained by equations and inequations taken from the literature which have been used in numerous studies (Table 5.3). These inequalities represented the threshold constraining the values of biological processes (e.g.

ingestion rate) within realistic limits. In order to be as accurate as possible, and where the literature allowed it, predation and grazing rates on specific prey compartments were also used as upper limits.

The maximum specific respiration rate (MSR, Moloney and Field, 1991) represented the maximum respiration boundary for all compartments and was calculated as function of community weighted mean (CommWM) body mass of the compartment, temperature, and biomass (Richardson et al., 2004; Marquis et al., 2007; Grami et al., 2008). Calculating CommWM body mass for each mesocosm and each sampling day permitted to account for variation in relative abundances of taxa within compartments composed by more than one taxon. To do so, the CommWM body mass, i.e. the mean body mass of a compartment at each sampling day was calculated as follow:

$$CommWMmc = \sum_{i=1}^{n} pi * Bi$$

With *CommWMmc* being the community weighted mean body mass (pgC.ind^{-1}) of the compartment *c* within the mesocosm (experimental unit + day) *m, n* the number of taxa composing the compartment *C*, *pi* the proportion of the taxon *i*, and *Bi* the biomass of the taxon *i* (pgC.ind^{-1}). Following that, the MSR at 20°C was calculated for each compartment within each plot:

$$MSRmc^{@20°C} = a * CommWMmc^{-0.25}$$

With $MSRmc^{@20°C}$ being the maximum specific respiration rate (d^{-1}) of the compartment *c* within the mesocosm *m* at 20°C, and *a* (pgC$^{0.25}$ d^{-1}) the allometric argument either equal to 1.7 for phytoplankton and bacteria, or to 14 for heterotrophs (Moloney and Field, 1991). On the same basis, maximum specific uptake (MSU) and its relative maximum specific senescence (MSS) were calculated for phytoplankton and bacterial compartments respectively. The same formula was applied but the allometric argument (*a*) was equal to 3.6 (Moloney and Field, 1991). As these values were calculated for a temperature of 20°C, a Q10 correction, i.e. the factor by which rate changes due to 10 °C increase in temperature, of 2 was applied, as suggested by Moloney and Field (1991). The rates were therefore corrected according to the measured daily temperature of each experimental unit.

Table 5.3: List of constraints used in the linear inverse modelling. GPP = Gross primary production, NPP = net primary production, B = biomass, R = respiration, C = consumption, S = senescence, E = Excretion, MSR = maximum specific respiration rate, MSU = maximum specific uptake rate, MSS = maximum specific senescence.

Process	Concerned compartment	Bound	Description	Inequation	Reference
GPP	coc, ndi, mph, phf	Both	Gross primary production of phytoplankton ranges between 3.3 and 20 times of their respiration	$R * 3.3 \leq GPP \leq R * 20$	Vézina and Piatt (1988)
Respiration	bac, cla, cop, Nsc, din, cil	Lower	At least 20% of total ingestion	$R \geq C * 0.2$	Vézina and Savenkoff (1999)
	cla, cop, Nsc, din, cil	Upper	Does not exceed MSR (d^{-1}) as function of biomass ($mgC.m^{-3}$)	$R \leq MSR * B$	Moloney et al. (1989, 1991)
	bac	Upper	Does not exceed MSR (d^{-1}) as function of biomass ($mgC.m^{-3}$)	$R \leq MSR * B$	Moloney et al. (1989, 1991); Vézina and Savenkoff (1999)
	coc, ndi, mph, phf,	Both	Autotroph respiration ranges between 50% and 100% of MSR (d^{-1}) as function of biomass ($mgC.m^{-3}$)	$(MSR * B) *0.5 \leq R \leq MSR * B$	Moloney et al. (1989, 1991)
Consumption	bac	Upper	Does not exceed MSU (d^{-1}) as function of biomass ($mgC.m^{-3}$)	$C \leq MSU * B$	Moloney et al. (1989, 1991) ; Vézina et al. (2000)
	doc → bac	Upper	Bacteria total uptake of doc does not exceed 5 times their total respiration	doc → bac ≤ R * 5	Vézina and Savenkoff (1999)
	din → cop	Upper	Cop feeding on din do not exceed 27% of cop biomass	$din \rightarrow cop \leq B_{cop} * 0.27$	Nakamura and Turner (1997)
	mph→ cop	Upper	Cop feeding on din do not exceed 17% of cop biomass	$mph \rightarrow cop \leq B_{cop} * 0.27$	Castellani et al. (2005)
	cil →cop	Upper	Cop feeding on din does not exceed the maximum feeding rate multiplicated by cop biomass	$cil \rightarrow cop \leq B_{cop} * ((-1.12*3.64*B_{cil})/340)$	Nakamura and Turner (1997)
	coc, ndi, phf, mph, din, cil → cla	Upper	Cla feeding on preys do not exceed the maximum feeding rate multiplicated by cla biomass	$Prey_i \rightarrow cla \leq B_{cla}*(0.25+0.012* B_i)$	Vézina and Savenkoff (1999)
	coc, ndi, phf, mph → Nsc	Upper	Nsc feeding on phytoplankton preys do not exceed the maximum feeding rate multiplicated by Nsc biomass	$Preyi \rightarrow Nsc \leq B_{Nsc} * (((2.93_{10^{-4}} * B_i) / (3.58_{10^{-3}} + B_i)) / 1.02_{10^{-3}})$	Zhang et al. (2015)

	din, cil → Nsc	Upper	Nsc feeding on microzooplankton preys does not exceed the maximum feeding rate multiplicated by Nsc biomass	$Prey_i \rightarrow Nsc \leq B_{Nsc} * (((3.31_{10}^{-4} * B_i) / (5.38_{10}^{-3} + B_i)) / 1.02_{10}^{-3})$	
Senescence	bac → det	Both	Viral lysis of bacteria ranges between 10% and 40% of their production rate	$P_{bac} * 0.10 \leq S \leq P_{bac} * 0.40$	Fuhrman (2000)
	coc, ndi, phf, mph → det	Upper	Does not exceed MSS (d^{-1}) as function of biomass ($mgC.m^{-3}$)	$S \leq MSS * B$	Moloney et al. (1991); Moloney and Field (1991)
		Lower	Natural mortality is at least 1 % of biomass	$S \geq B * 0.01$	Arnous et al. (2010)
	din, cil, cla, cop, Nsc	Upper	Not more than respiration	$S \leq R$	Vézina and Pace (1994)
		Lower	At least 10% of total ingestion	$S \geq C * 0.1$	
Excretion	bac→ doc	Upper	Lower than respiration	$E < R$	
	coc, ndi, phf, mph → doc	Both	Ranges between 10 and 55% of NPP	$NPP * 0.10 \leq E \leq NPP * 0.55$	Baines and Pace (1991)
	cla, cop, Nsc, din, cil → doc	Upper	No more than their respiration	$E \leq R$	Vézina and Piatt (1988); Vézina and Pace (1994)
		Lower	At least 10 % of their total ingestion	$E \geq C * 0.1$	
Assimilation	din, cil, cla, cop, Nsc	Both	Zooplankton assimilation efficiency ranges between 50 and 90% of their consumption	$C * 0.5 \leq$ assimilation $\leq C * 0.9$	Vézina et al. (2000); van Oevelen et al. (2006)

Calculation of LIM solutions

The different equations and constraints were integrated into the LIM-MCMC to calculate the unknown carbon flows between compartments. The vectors of unknown flows were thus sampled through a solutions space of 500,000 iterations with a jump size of 0.5. Model simulations were realised via the *LimSolve* package (Meersche et al., 2009). Visual observations were realised to ensure that the distribution of possible values follows a Gaussian distribution, meaning a good sampling (van Oevelen et al., 2010).

Indices, trophic pathways and ecological network analysis

The range of values obtained for each flux from the LIM were used to calculate indices allowing to extract ecological tendencies for each global change scenario. These indices were ratios of fluxes and ecological network analysis.

Ecological network analysis

Ecological network analysis (ENA) allows to summarise information hidden from the different flows of carbon extracted from the model by providing a set of global system indices representing an overview of food web functioning and efficiency (Ulanowicz, 2004; Fath et al., 2019). Following literature (Fath et al., 2019; van der Heijden et al., 2020) and ecological issues specific to this study, we selected six ENA indices in order to compare the organisation and functioning of the plankton food web between the different scenarios.

Total system throughput (TSTp) is the sum all flows in the system and is considered as proxy of the total power generated by the system. Average path length (APL) is defined as the sum of all the flows between the compartments and the inputs or the outputs (called total system throughflow or TSTf) divided by the total boundary input into the system (Finn, 1976). This index represents the average number of compartments a unit of energy passes from its entry to the system until it leaves (Finn, 1976). Thus, a higher APL indicates a longer pathway length in the system. The Finn Cycling Index (FCI) calculates the fraction of the TSTf that is cycled in the network, traducing how much of the flow would revisit the same compartment multiple times before exiting the system (Fath et al., 2019). A high FCI is then highlighting a high recycling capacity of the system. The flow diversity is calculated by applying Shannon's diversity index to the flow structure, the higher the value, the more diverse and even are the food web flows. The last index calculated was the relative internal Ascendency (rASCi) which represents the efficiency and definitiveness by which the carbon is transferred internally. The higher the rASCi value, the greater the internal organisation of the food web (Heymans et al., 2014). These indices were calculated from the 500,000 iterations via the *enaR* package (Borrett and Lau, 2014).

A Lindeman spine was created for each scenario using the function *enaTroAgg* (package *enaR*, Borrett and Lau, 2014) which uses the mean of each carbon flow obtained from the 500,000 iterations. This linear chain represents a food web where each compartment is allocated to a discrete trophic level (Fath et al., 2019). In this representation, autotrophs belong to the trophic group I and represent the discrete level where the energy is entering the food web. The following trophic levels represent the integer trophic levels of the consumers. The losses due to respiration, trophic efficiencies, and output as detritus are also detailed. Ultimately, this enables to extract ecological properties such as the relation between detritivory and herbivory (D:H ratio), the degree of omnivory (Omnivory index), the ratio between autotrophic production and respiration, as well as compartment-specific trophic levels.

Proportion of different food sources in zooplankton diet

In addition to ENA, we calculated a series of ecological trophic pathway ratios following (Legendre and Rassoulzadegan, 1995). These ratios of carbon flows are useful tools to summarize and compare processes such as grazing or detritivory between ecological systems, and allow the identification of the trophic pathway that dominates a given plankton assemblage (Hlaili et al., 2014). Concretely, they permitted to see whether the proportion of the different food sources changed between global change scenarios. All ratios were ranged from 0 to 1. We used the flow values obtained from the LIM to compute six ratios (Table 5.4) for each scenario before comparing them (see paragraph Statistical analyses for the method used). The ratio 1 to 3 allow the calculation of the feeding proportion of microzooplankton on its different food source (i.e. phytoplankton, bacteria, detritus), while ratio 4 and 5 refer to the proportion of herbivory and carnivory in mesozooplankton diet, respectively. Finally, ratio 6 illustrate the grazing pressure of microzooplankton versus mesozooplankton, a value of 1 defining a grazing pressure exclusively exerted by microzooplankton.

Table 5.4: Ratios of carbon fluxes used in the study, adapted from Hlaili et al. (2014) and Legendre and Rassoulzadegan (1995). det = detrital organic carbon, bac = bacteria, pht = phytoplankton, mic = microzooplankton, mes = mesozooplankton. foodTOmic = phtTOmic + bacTOmic + detTOmic. foodTOmes = phtTOmes + micTOmes + detTOmes.

Ratio	Formula	Description	Ecological meaning
Ratio 1	: / foodTOmic	Consumption rate of total phytoplankton by microzooplankton divided by total consumption rate by microzooplankton	Proportion of pht in mic diet
Ratio 2	bacTOmic / foodTOmic	Consumption rate of bacteria by microzooplankton divided by total consumption rate by microzooplankton	Proportion of bac in mic diet
Ratio 3	detTOmic / foodTOmic	Consumption rate of detritus by microzooplankton divided by total consumption rate by microzooplankton	Proportion of det in mic diet
Ratio 4	phtTOmes / foodTOmes	Consumption rate of total phytoplankton by mesozooplankton divided by total consumption rate by mesozooplankton	Proportion of pht in mes diet
Ratio 5	micTOmes / foodTOmes	Consumption rate of mic by mesozooplankton divided by total consumption rate by mesozooplankton	Proportion of mic in mes diet
Ratio 6	phtTOmic / (phtTOmic + phtTOmes)	Consumption rate of total phytoplankton by microzooplankton divided by the consumption rate of total phytoplankton by micro- and mesozooplankton	Grazing pressure exerted by mic versus mes

Statistical analyses

ENA indices and carbon flow ratios were compared pairwise between scenarios using the Cliff's delta statistic (*effsize* package; Torchiano et al., 2020). This non-parametric effect size statistic quantifies the amount of differences between groups of observations beyond p-values

interpretation (Macbeth et al., 2011). In other words, it estimates the probability that a randomly selected value in one group is higher than a randomly selected value from another group, minus reverse probability. Threshold values are then used to determine significance or magnitude. Low threshold values, < 0.15 considered as negligible and < 0.33 as small, mean no statistical difference. Delta values ranged between 0.33 and 0.47 are considered medium and equal or superior than 0.47, means large difference, both highlighting a statistically difference between groups.

5.4. Results

Ecological network indices

The food web structure and functioning, summarised by ENA indices, shows differences between the scenarios (Figure 5.2, Supplementary Figure 5.1). Overall, the structure and functioning of the plankton food web were rather similar in the Ambient and ERCP 6.0 scenarios, whereas the ERCP 8.5 scenario substantially altered ENA indices. The sum of energy flows (i.e TSTp) was significantly different among all scenarios. The lowest TSTp was observed in the Ambient scenario (1603 $mgC.m^{-3}.d^{-1}$), and the highest in the ERCP 6.0 (1986 $mgC.m^{-3}.d^{-1}$). Relative internal ascendancy (rASCi) did not significantly differ between the Ambient (31.8%) and ERCP 6.0 (31.5%) scenarios, but was statistically higher in the ERCP 8.5 (34%) compared to the other two scenarios. Flow diversity was higher in the Ambient and ERCP 6.0 scenarios (3.20 and 3.24, respectively) than in the ERCP 8.5 scenario (3.02). Finn cycling index showed the opposite pattern, with the highest value in the ERCP 8.5 scenario (14.2%), and lower ones in the Ambient (12.7%) and ERCP 6.0 (12%) scenarios. Despite relatively similar APL values in the three scenarios, we observed statistically significant differences between the Ambient and ERCP 8.5 scenarios, with the lowest APL values in the ERCP 8.5 scenario (3.33).

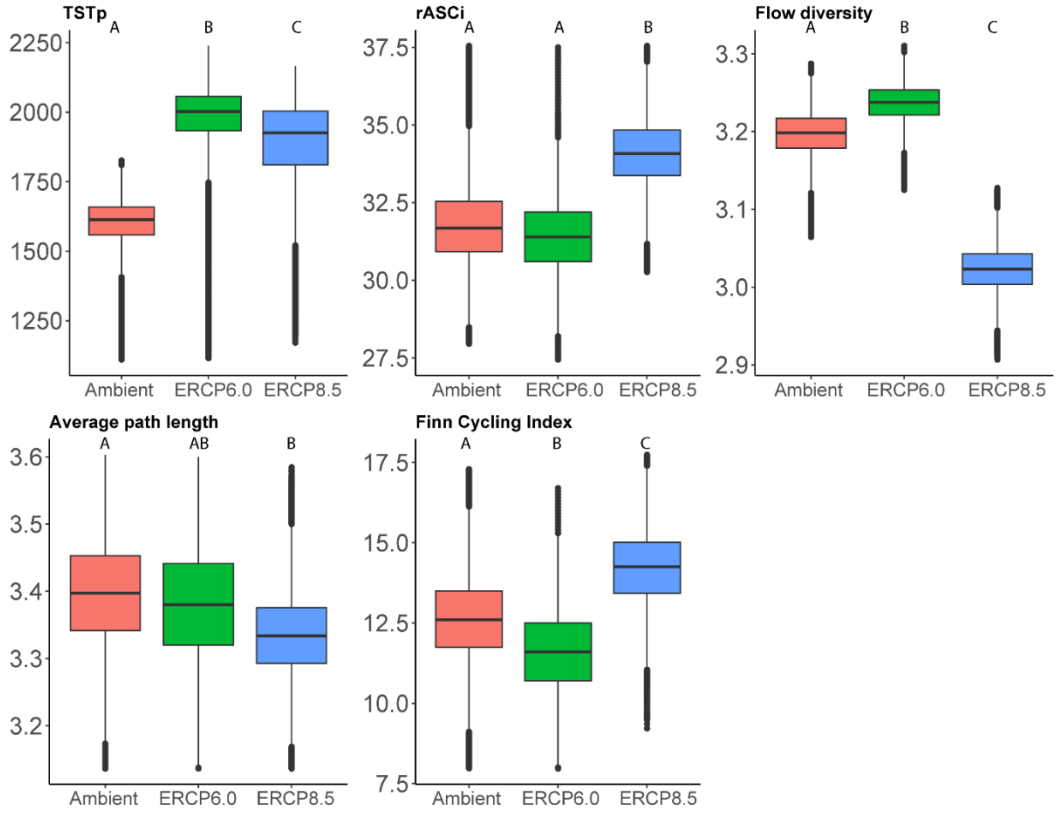

Figure 5.2: ENA indices calculated for each scenario. TSTp unit is in $mgC.m^{-3}.d^{-1}$. Flow diversity and Average path length are unitless values. Finn Cycling Index and rASCi are percentage values. Letters highlight significant differences resulting from a Cliff's delta superior than 0.33. Two boxplots with a common letter illustrate no statistical difference at this threshold. Cliff's delta values for each pair of comparison are given in Supplementary Table 5.1.

Structural network calculations were performed based on the interaction of the living and non-living compartments in order to determine the mean trophic structure in each scenario (Table 5.5 and Figure 5.3).

Table 5.5: Food wed indices referring to the mean trophic level (MTL), detritivory to herbivory (D:H) ratio, and gross primary production (GPP) to autotroph respiration (RI) for each scenario. The trophic level specific to each consumer was also added.

Scenario	MTL	D:H	GPP:RI		Trophic level
Ambient	2.25	1.88	5.21	din	2.12
				cil	2.15
				cop	2.42
				Nsc	2.41
				cla	2.40
ERCP 6.0	2.25	1.63	5.20	din	2.16
				cil	2.15
				cop	2.41
				Nsc	2.36
				cla	2.42
ERCP 8.5	2.09	2.22	5.08	din	2.08
				cil	2.13
				cop	2.36
				Nsc	2.33
				cla	2.39

The highest degree of herbivory (i.e., from trophic level I to II) was observed in the ERCP 6.0 scenario (234 mgC.m-^{3}.d^{-1}), while the highest detritivory level (i.e., from D to II) was in the ERCP 8.5 scenario (405 mgC.m-^{3}.d^{-1}). The Detritivory:Herbivory ratio was similar in the Ambient and ERCP 6.0 scenarios (1.88 and 1.63, respectively), and was higher in the in ERCP 8.5 scenario (2.22). While the mean trophic level did not change between the Ambient and ERCP 6.0 scenarios, it dropped to 2.09 in the ERCP 8.5 scenario, showing a general decrease in trophic level performed by all compartments, especially dinoflagellates and copepods (Table 5.5). Efficiency of energy transfer to the trophic level III (i.e., predation on trophic level II) was more than twice lower in the ERCP 8.5 compared to the two other scenarios.

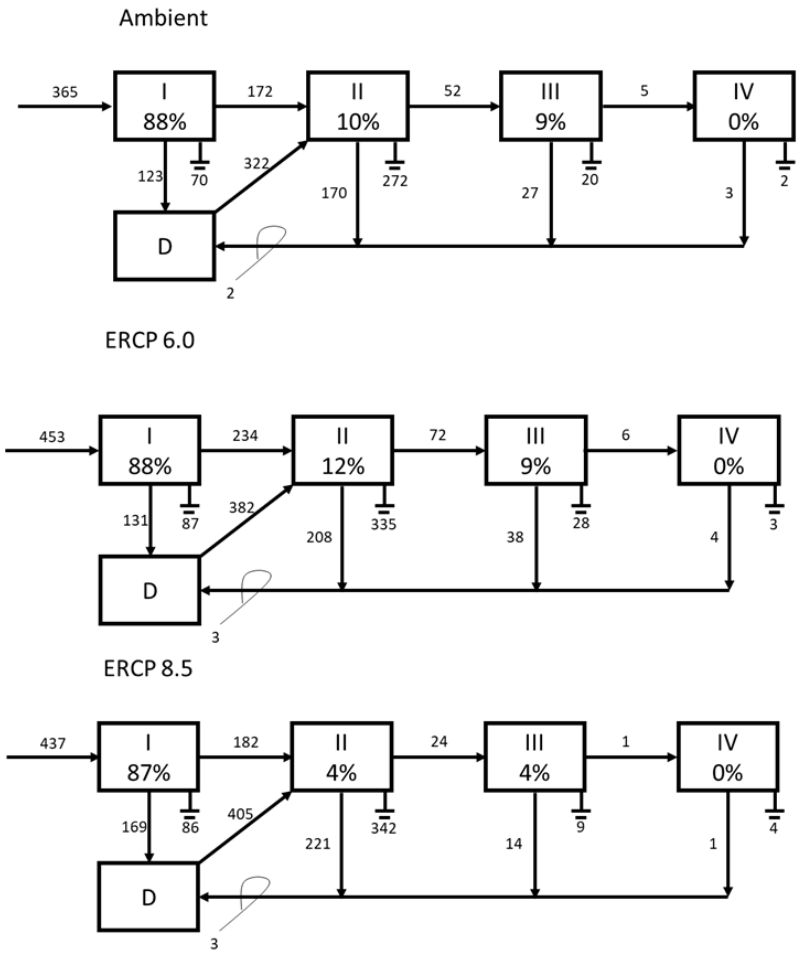

Figure 5.3: Lindeman spine of the three scenarios. Flows are in mgC.m^{-3}.d^{-1}. Boxes refer to the integer or discrete trophic levels (I, II, III and IV) and detrital pool (D). Percent values refer to the efficiency of energy transfer between the integer trophic levels, i.e. the ratio of input to a trophic level to the amount of flow that is passed on the next level from it. Dashed arrows represent the vector of canonical respirations. Black arrows refer to the vector of the input flow to a trophic level from the preceding trophic level, i.e. the Grazing Chain for the network, and the vector of the returns to detrital pool from each trophic level. The loop refers to the detrital circle, i.e. the flow circulation within the detrital pool.

Zooplankton diet and grazing pressure

Using the previously calculated carbon fluxes, we computed trophic pathways to determine the proportion of each food source in the diet of microzooplankton and mesozooplankton. We identified that microzooplankton trophic pathways were overall similar in the Ambient and ERCP 6.0 scenarios, but significantly changed in the ERCP 8.5 scenario (Figure 5.4 and Supplementary Figure 5.1). For instance, the proportion of phytoplankton (i.e. ratio 1), bacteria (i.e. ratio 2), and detritus (i.e. ratio 3) in microzooplankton diet, were not statistically different between the Ambient and ERCP 6.0 scenarios. In contrast, the proportion of phytoplankton in microzooplankton diet was significantly higher, and the proportion of bacteria and detritus in microzooplankton diet were significantly lower in the ERCP 8.5 scenario than in the other two scenarios. Similarly, the proportion of phytoplankton in the diet of mesozooplankton (i.e. ratio 4) was significantly higher in the ERCP 8.5 than in the Ambient scenario. Interestingly, we did not see significant change in the proportion of microzooplankton in mesozooplankton diet (i.e. ratio 5) between the different scenarios, the proportion of carnivory in mesozooplankton diet being around 35% in all scenarios. The grazing pressure exerted by mesozooplankton on phytoplankton compared to that exerted by microzooplankton (i.e. ratio 6) was significantly lower in the ERCP 8.5 than in the two others scenarios.

5.5. Discussion

Overall, we identified that the functioning of the plankton food web was rather similar in the Ambient and ERCP 6.0 scenarios, but substantially altered in the ERCP 8.5 scenario, highlighting a tipping point between the ERCP 6.0 and 8.5 beyond which considerable changes occur. Using food web modelling and ecological network analysis, we identified that simultaneous warming, acidification, and increased dissolved N:P ratio favoured the microbial oop, and decreased energy transfer to higher trophic levels. At the organismal level, autotrophs displayed a lower metabolic balance while omnivorous organisms increased the degree of herbivory in their diet. Regarding functioning, we also observed that the organisation of the food web and its capacity to recycle carbon were higher under the ERCP 8.5 scenario, but flow diversity and carbon path length were significantly reduced. We provide evidence that if global

change goes beyond the ERCP 6.0 scenario, dramatic changes in pelagic ecosystem functioning may occur.

Impacts of multiple drivers on size structure through changes in metabolic balance

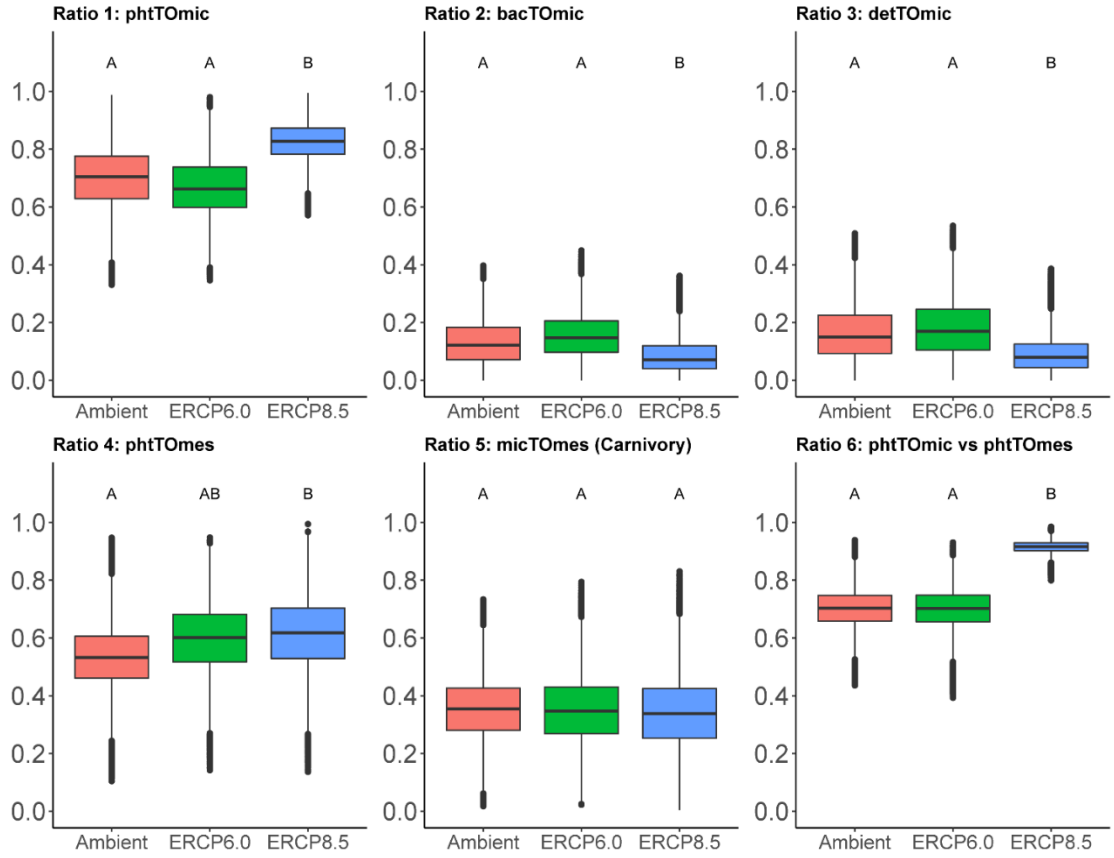

Figure 5.4: Distribution of carbon flow ratios for each scenario. Ratios from 1 to 3 refer to realised proportion of phytoplankton, bacteria and detritus in microzooplankton diet. Ratio 4 refers to herbivory proportion in mesozooplankton diet and ratio 5 to its proportion of carnivory. The ratio 6 refers to the grazing pressure exerted by microzooplankton over mesozooplankton. See Table 5.4 for more descriptions. Letters highlight significant differences resulting from a Cliff's delta superior than 0.33. Cliff's delta values for each pair of comparison are given in Supplementary Table 5.1. det = detrital organic carbon, bac = bacteria, pht = phytoplankton, mic = microzooplankton, mes = mesozooplankton.

We observed that in the ERCP 8.5 scenario, the simultaneous influence of warming, acidification and increased N:P ratio lowered the metabolic balance (GPP versus respiration) for autotrophs, showing a relatively higher respiration rate per unit of primary production. As summarized by the Metabolic Theory of Ecology (Brown et al., 2004), both phytoplankton respiration and photosynthetic rates should increase with increasing temperature (Gillooly et al., 2001). Energetic costs associated with increased metabolism favour smaller organisms as stated by the temperature size rule, which mentions that warming negatively impacts body/cell size due to the increasing metabolism and energy costs (Atkinson, 1995; Angilletta et al., 2004). Regarding acidification, most observations report little or no negative effects on phytoplankton

(Maugendre et al., 2017) and microbes (Joint et al., 2011), but could benefit some microorganisms, especially under low nutrient availability (Sala et al., 2016). When nutrient availability is low, the temperature-size-rule can also be reinforced for phytoplankton (Peter and Sommer, 2015). Small cells have a low surface-to-volume ratio, improving nutrient uptake efficiency and making them more competitive under lower nutrient availability (Marañón, 2015). Hence, the lower metabolic balance we observed in response to global change may explain the positive selection for smaller plankton organisms reported by Moreno et al., (2022), as well as other studies (Moore and Folt, 1993; Daufresne et al., 2009; Sheridan and Bickford, 2011; Peter and Sommer, 2012; Bermúdez et al., 2016). This positive selection could be due to the additive or synergistic effect of warming, acidification and increased N:P ratios, with a tipping point between the ERCP 6.0 and 8.5 scenarios. A shift in plankton size structure through metabolic balance has the potential to dramatically impact plankton assemblages and therefore food web functioning. Microzooplankton is particularly well suited to consume small phytoplankton cells, and a reduction in phytoplankton size may redirect energy flows to the microbial food web, instead of efficiently fuelling higher trophic levels (Azam et al., 1983; Legendre and Le Fèvre, 1995).

Global change strengthens the microbial loop

Microzooplankton play a key role in plankton food web by consuming a substantial part of primary and bacterial production (Fenchel, 2008), and transferring energy to higher trophic levels, thereby substantially impacting the carbon cycling (López-Abbate, 2021). For instance, microzooplankton grazers can have a higher effect than copepods in structuring and controlling phytoplankton spring blooms (Löder et al., 2011). Microzooplankton and their food sources (i.e., detritus, bacteria, phytoplankton), represent together the “microbial food web” (Azam et al., 1983). Bigger plankton organisms, such as mesozooplankton, link this microbial food web to upper trophic levels via predation (Tortajada et al., 2012), representing an essential top-down regulator of microzooplankton (Löder et al., 2011). Moreover, omnivorous mesozooplankton do also feed directly on phytoplankton, representing the “herbivorous food web” (Pomeroy, 1974). The dominance of one food web over another has been shown to be largely influenced by the size structure of primary producers (Azam et al., 1983; Thingstad and Rassoulzadegan, 1999). Legendre and Rassoulzadegan (1995) showed that phytoplankton blooms of large species lead to a dominance of the herbivorous over the microbial food web. In contrast, microzooplankton primarily consume smaller phytoplankton species, and blooms of nanophytoplankton (Burkill et al., 1987) , or reductions in phytoplankton size structure, as we

reported here, may benefit the microbial food web because small phytoplankton are less edible for mesozooplankton, and do not support the herbivorous food web efficiently.

The strength of carbon flows in the microbial food web appeared to be highly influenced by the different scenarios (Figure 5.5). We identified a tipping point between ERCP 6.0 and 8.5, with significantly more carbon going to microzooplankton and bacteria, and much less carbon going to the mesozooplankton compartment. Thus, simultaneously increasing temperature, acidification, and N:P ratios in the ERCP 8.5 scenario, shifted the food web structure to a more pronounced flux of carbon through the microbial loop, while Ambient and ERCP 6.0 scenarios were displaying a more balanced multivorous food web (association between microbial and herbivorous food webs; Tortajada et al., 2012).

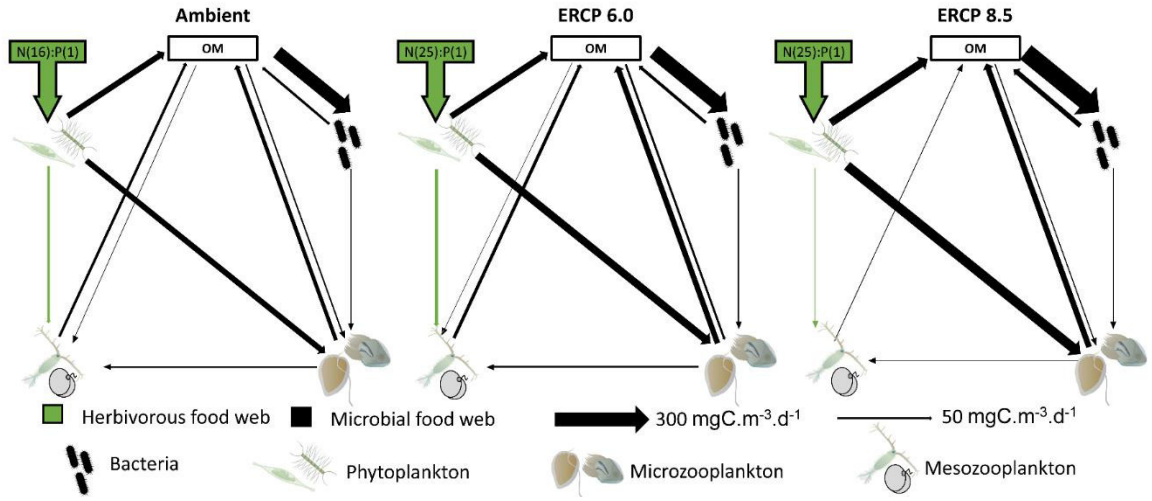

Figure 5.5*:* Simplified food web diagram of carbon flows for each scenario. The height of the arrows is scaled (except for nutrients) according to the amount of carbon (See Supplementary Table 5.2 for values). The herbivorous and microbial food webs are differentiated by colour code. Under global change scenario, the herbivorous food web is weakening due to small cell size phytoplankton selection. In addition to increased grazing availability for microzooplankton, a substantial part of primary producers, being not consumed, goes to the detrital pool, fuelling the microbial food web. OM = Dissolved and particulate organic matter.

In addition to increased carbon flows through microzooplankton, we also observed a higher detrital (both particulate and dissolved organic matter) and bacterial production in the ERCP 8.5 scenario. Due to the gap left by mesozooplankton, large phytoplankton cells were not consumed, which led to higher amount of organic matter going from phytoplankton to the detrital pool (Figure 5.5). Moreover, senescence is not the only source of organic matter since phytoplankton exude a significant proportion of dissolved carbon (Fogg, 1983), and exudation has been shown to increase under higher pCO_2 and temperature conditions (Thornton, 2014). Higher metabolism under warming also leads to a higher excretion rate for secondary producers (Vézina and Pace, 1994). The combination of unconsumed phytoplankton and increased

excretion/exudation rates likely strengthened detrital production, which in turn enhanced bacterial activity (Arístegui et al., 2014), and fuelled the microbial food web (Ory et al., 2010).

Global change enhances the degree of herbivory in zooplankton diet

The enhanced bacterial production in the ERCP 8.5 led to an overall higher detritivory at the entire food web level. Our study also shows that the proportion of phytoplankton in the diet of microzooplankton and mesozooplankton was the highest in the ERCP 8.5 scenario. Conversely, the proportion of bacteria and detritus in microzooplankton diet was the lowest in this scenario. Two of the ways through which trophic interactions can be affected by higher temperatures are either by an increase in food intake, as metabolic rates and energetic demands increase with temperature, but also by a qualitative change in diet composition (Zhang et al., 2020). For instance, an increased level of herbivory in response to warming has been observed for many omnivorous taxa (Zhang et al., 2020), including zooplankton. This has been linked to the need for ectotherms to consume food with a higher carbon:nutrient ratio at higher temperatures (Croll and Watts, 2004; Laspoumaderes et al., 2022; Malzahn et al., 2016) to fulfil increased carbon metabolic demands in response to warming (Karl and Fischer, 2008; Forster et al., 2011). As primary producers have higher relative carbon content compared to consumers (Sterner and Elser, 2002), omnivores may increase the degree of herbivory in their diet in order to sustain their increased metabolic demands for carbon. However, there is still no clear consensus, as warming has also been shown to drive a decrease or a non-linear cubic thermal response of consumers nutrient requirements (Ruiz et al., 2020; Laspoumaderes et al., 2022). Additionally, increased feeding rate under warmer conditions may offset higher metabolic demand, resulting in an unchanged carbon demand relative to nutrients (Anderson et al., 2017). While the specific physiological processes remain to be clarified, our study indicates that global change is likely to alter plankton food web by increasing the top–down control of omnivores on primary producers.

In brief, our results are showing a higher bacterial and detrital production in addition to an increased top down pressure of microzooplankton on primary producers, altogether reinforcing the carbon flows through the microbial loop. This is in line with previous studies stating that, despite a low effect of acidification on microzooplankton (Aberle et al., 2013; Horn et al., 2016), the combination of warming and elevated pCO_2 could enhance the interaction strength between the microbial loop's compartments (Chen et al., 2012; Lara et al., 2013; Olson et al., 2018). Such changes on diet preference and food web structure can alter ecosystem processes, by impacting both carbon cycling and upper trophic levels.

Implications for ecosystem functioning

ENA indices have been defined and used in order to quantify key properties of food web functioning and stability (Fath et al., 2019). Indices related to cycling, resilience, and organisation such as FCI or rASCi inform on stability properties of the food web (Finn, 1976; Tortajada et al., 2012), and we identified that stability was highest in the ERCP 8.5 scenario. Increased carbon flows through the microbial food web are likely responsible for this, since lower energy transfer to higher trophic levels reduces overall food chain lengths which is known to increase food web stability (McCann, 2011; Dettner et al., 2012). This is supported by flow diversity which was the lowest in the ERCP 8.5 scenario, indicating that the energy flows between different compartments were concentrated on few pathways, leading consequently to the lowest amount of system activity generated by each compartment (APL), and lowest system complexity. In addition, the ERCP 8.5 scenario was characterized by a particularly high TSTp and a low trophic efficiency. Similar results were found in a simulation with increased temperature (Baird et al., 2019), which resulted in an increased detrital production and consumption, a substantial increase in TSTp, and a decline of the herbivorous food web, overall illustrating a shift towards detritus-based food web under warming conditions. In our study, the simultaneous effects of warming, acidification, and elevated N:P ratios produced a more stable and less diverse food web, characterised by few dominant and specialized pathways (low flow diversity and high rASCi) and by low transfer efficiency to higher trophic levels (low trophic efficiency, low APL, high FCI).

The direction of the diversity-stability relationship in food webs has been the topic of numerous debates among ecologists (Rooney and McCann, 2012). Historically, poorly diverse systems have been considered as less stable than richer ones, with a higher diversity of links positively correlated with an increased stability (MacArthur, 1955). However, laboratory experiments on food web structure have shown the stabilizing properties of poor interaction diversity (Rip et al., 2010), and that the relationship diversity-stability can be altered depending on predation pressure in the system; i.e. negative without predators and positive with predators (Jiang et al., 2009). Following this hypothesis, the sharp decrease in predation pressure experienced by the microbial loop in the ERCP 8.5 scenario could have increased stability over diversity. Although our experimental design, limited to plankton, limits our ability to extend our findings to higher trophic levels, we can reasonably expect bottom-up cascading effects on upper planktivorous trophic levels.

Within marine food web, the response of plankton to climate change is crucial for fish. Shifts in plankton assemblages have already shown major effects on fish recruitment over the past decades (Beaugrand et al., 2003; van Deurs et al., 2009; Reid et al., 2016). An increasing dominance of the microbial food web, to the detriment of a more multivorous food web, as reported here, could impact the upper trophic levels. Indeed, the reduction of food web trophic efficiency may create a 'trophic sink' for many planktivorous species which will cascade to higher trophic levels.

Furthermore, an enhanced microbial food web can also have major effects on carbon cycling. Although it has long been debated whether the microbial food web leads to losses of fixed carbon to the system or whether it primarily channels fixed carbon to higher levels, it is now generally accepted that the microbial food web is a carbon sink (Fenchel, 2008). In addition, the microbial food web plays an important role in the mineralisation of nutrients. Hence, the result presented here of an enhanced microbial food web under future environmental conditions suggests that both carbon losses from the pelagic system, as well as nutrient cycling rates in the water column, are likely to increase.

Conclusion

We explored the impact that multiple global change drivers may have simultaneously on the plankton food web. We identified a tipping point between the ERCP 6.0 and 8.5 scenarios, beyond which plankton food web structure and functioning are substantially altered. In particular, we identified that the microbial food web gained in prominence, which impaired upper trophic levels, and ultimately the carbon flow diversity. These results, and the shift towards smaller plankton organisms, may be attributed to direct influences of warming, elevated pCO_2 and N:P ratio on metabolism as well as to their indirect effects on prey availability. Moreover, we identified shifts in interaction strengths, with, for instance, higher degrees of herbivory in the diet of microzooplankton and mesozooplankton. These changes are not anodyne, and may have important consequences for ecosystem services, such as nutrient biomineralization, carbon cycling, and fish recruitment.

5.7. Supplementary Material

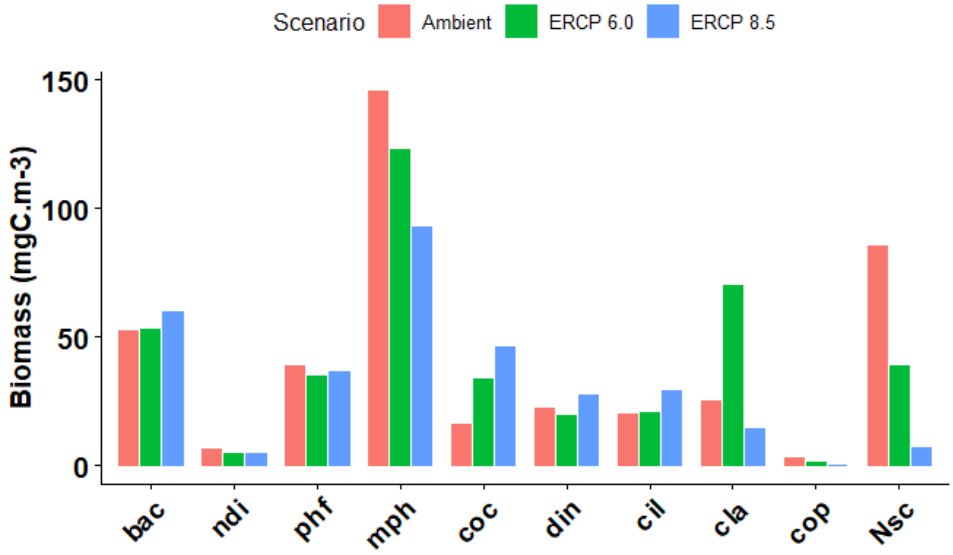

Supplementary Figure 5.1: Median values of biomass for each compartment within each scenario. Abbreviation of compartments are given in Table 5.1.

Supplementary Table 5.1: Detailed Cliff's delta statistic results obtained from the comparison between the scenarios for flow ratios and ENA indices.

Food web structural index	Index	Comparison	Cliff's delta statistic	Magnitude	Significant
Ratio	Ratio 1	Ambient- ERCP6.0	0.19	Small	No
		Ambient- ERCP8.5	0.67	Large	Yes
		ERCP6.0- ERCP8.5	0.79	Large	Yes
	Ratio 2	Ambient- ERCP6.0	0.17	Small	No
		Ambient- ERCP8.5	0.38	Medium	Yes
		ERCP6.0- ERCP8.5	0.54	Large	Yes
	Ratio 3	Ambient- ERCP6.0	0.09	Negligible	No
		Ambient- ERCP8.5	0.5	Large	Yes
		ERCP6.0- ERCP8.5	0.57	Large	Yes
	Ratio 4	Ambient- ERCP6.0	0.32	Small	No
		Ambient- ERCP8.5	0.38	Medium	Yes
		ERCP6.0- ERCP8.5	0.08	Negligible	No
	Ratio 5	Ambient- ERCP6.0	0.02	Negligible	No
		Ambient- ERCP8.5	0.07	Negligible	No
		ERCP6.0- ERCP8.5	0.05	Negligible	No
	Ratio 6	Ambient- ERCP6.0	0.01	Negligible	No
		Ambient- ERCP8.5	0.98	Large	Yes
		ERCP6.0- ERCP8.5	0.98	Large	Yes
ENA	APL	Ambient- ERCP6.0	0.11	Negligible	No
		Ambient- ERCP8.5	0.47	Large	Yes
		ERCP6.0- ERCP8.5	0.32	Small	No
	FCI	Ambient- ERCP6.0	0.41	Medium	Yes
		Ambient- ERCP8.5	0.61	Large	Yes
		ERCP6.0- ERCP8.5	0.85	Large	Yes

TSTp	Ambient- ERCP6.0	0.99	Large	Yes
	Ambient- ERCP8.5	0.9	Large	Yes
	ERCP6.0- ERCP8.5	0.4	Medium	Yes
TSTf	Ambient- ERCP6.0	0.98	Large	Yes
	Ambient- ERCP8.5	0.88	Large	Yes
	ERCP6.0- ERCP8.5	0.41	Medium	Yes
Flow diversity	Ambient- ERCP6.0	0.71	Large	Yes
	Ambient- ERCP8.5	0.99	Large	Yes
	ERCP6.0- ERCP8.5	0.99	Large	Yes
rASCi	Ambient- ERCP6.0	0.14	Negligible	Yes
	Ambient- ERCP8.5	0.85	Large	Yes
	ERCP6.0- ERCP8.5	0.89	Large	Yes

Supplementary Table 5.2: Mean and standard deviation of each flow estimated from the 500,000 iterations.

Flow	Ambient		ERCP 6.0		ERCP 8.5	
	Mean	SD	Mean	SD	Mean	SD
FIX->coc	58.76521	13.63366	112.2043	19.11991	147.9326	24.82522
FIX->phf	97.18078	15.6948	111.5535	20.8388	109.4597	19.36419
FIX->mph	172.2672	14.50669	195.3043	18.568	150.8185	18.76925
FIX->ndi	36.34407	11.15726	34.10608	9.649031	29.11457	10.67524
bac->CO2	195.0049	13.68802	228.9109	15.9015	266.0768	25.87393
ndi->CO2	2.833041	0.51622	2.236847	0.370686	2.419414	0.445367
phf->CO2	19.71346	3.135743	21.60428	3.924771	21.78405	3.619856
mph->CO2	37.6059	2.69267	42.26777	3.642434	31.64147	3.928407
coc->CO2	9.681267	1.899179	21.37497	3.929204	29.93251	5.006558
din->CO2	41.997	3.923066	38.24455	4.148164	63.70604	3.551093
cil->CO2	15.69255	1.715271	49.92671	4.908389	11.54831	1.181535
cla->CO2	10.53699	0.580103	32.71445	1.617102	7.36869	0.399416
cop->CO2	0.877651	0.196665	0.351973	0.083779	0.076469	0.020922
Nsc->CO2	30.61448	3.144077	15.53582	2.134558	2.771673	0.400865
bac->din	14.29923	11.65734	17.73286	14.73341	12.95708	11.81129
bac->cil	8.545379	7.05753	20.32325	15.10564	4.348668	4.053672
bac->POC	20.97116	7.661939	25.89304	9.087691	29.50664	10.43051
bac->DOC	43.79511	16.5334	38.89487	19.23173	72.72936	20.88438
coc->din	12.60619	9.13036	17.1817	12.70702	50.0095	14.76947
coc->cil	8.167756	6.627703	25.18855	16.45404	6.24566	5.284632
coc->Nsc	7.790103	5.863632	4.239232	2.998645	0.763809	0.536731
coc->cla	3.818061	2.883644	15.28761	11.04259	3.501796	2.653268
coc->POC	1.502194	0.777268	3.542649	1.826531	5.747678	2.764291
coc->DOC	15.19963	9.009116	25.38963	15.0959	51.73168	17.4317
ndi->din	8.743271	7.12499	7.097881	6.013976	10.45911	7.121597
ndi->cil	5.940046	4.868284	7.43316	6.018856	4.495945	3.783146
ndi->Nsc	5.996065	5.055805	3.529794	2.755676	0.749475	0.532466
ndi->cla	2.954982	2.188282	5.622785	4.651522	1.769724	1.199936
ndi->POC	0.41773	0.205304	0.312638	0.155678	0.355852	0.178847
ndi->DOC	9.458935	6.763957	7.872973	5.75078	8.865051	6.0104

phf->din	19.42893	12.04798	15.32933	12.45119	35.50757	12.85671
phf->cil	10.57624	8.194305	26.83706	17.29095	6.402065	5.494413
phf->Nsc	9.343421	6.4308	4.306751	3.024345	0.766153	0.536788
phf->cla	5.171061	3.948732	11.98573	9.002033	3.32046	2.460015
phf->POC	3.654948	1.835556	3.711834	1.935084	4.104061	1.994253
phf->DOC	29.29272	12.46178	27.77853	14.85056	37.5753	13.24745
mph->din	41.01604	16.67155	29.98565	19.81237	47.29245	13.07961
mph->cil	14.41352	10.22048	35.70665	20.18905	6.664168	5.5849
mph->Nsc	9.861394	6.542529	4.504077	3.097306	0.768028	0.53784
mph->cla	5.592998	4.367656	19.99899	14.06263	3.609452	2.796908
mph->cop	0.242282	0.140905	0.089911	0.052394	0.014147	0.008241
mph->POC	8.467909	3.804796	9.031249	4.320298	6.765567	2.97097
mph->DOC	55.0671	16.95945	53.72001	24.59955	54.06326	13.9989
din->cla	4.52777	3.338137	15.8796	9.343431	2.996357	2.135966
din->cop	0.382562	0.222549	0.141884	0.082785	0.022322	0.013063
din->Nsc	10.33675	7.340955	5.01064	3.399825	0.83273	0.595275
din->POC	28.444	9.333637	25.5013	8.662125	51.18164	10.26595
din->DOC	30.46451	8.77287	26.46103	8.747606	51.48848	10.79681
cil->cla	4.814689	3.274108	14.62522	9.619319	3.703341	2.301306
cil->cop	0.299015	0.173868	0.115834	0.067618	0.025656	0.014981
cil->Nsc	13.35549	7.572056	4.928014	3.407533	0.873616	0.604801
cil->POC	11.112	3.262619	32.8263	11.12818	8.309119	2.513794
cil->DOC	11.25106	3.266783	33.5231	10.8645	8.329081	2.524327
cop->DOC	0.515421	0.240638	0.206045	0.098458	0.044095	0.022595
cop->POC	0.441905	0	0.16403	0	0.025794	0
Nsc->DOC	22.75827	6.52577	10.66243	3.701859	1.93578	0.662528
Nsc->POC	13.12701	0	5.963616	0	1.05863	0
cla->DOC	7.325068	2.297686	22.71409	7.122472	5.172825	1.587806
cla->POC	9.017507	1.440243	27.97139	4.225258	6.359614	0.985881
POC->bac	55.54479	20.23962	81.83382	25.5932	91.41533	18.73948
POC->DOC	1.943127	0.254174	2.698361	0.351956	2.268292	0.299987
DOC->bac	227.0709	28.04444	249.9211	32.13079	294.2032	41.23564
POC->cil	8.88185	7.411058	20.45651	16.6893	4.632616	4.173198
POC->cop	0.911118	0.462512	0.37442	0.187471	0.084233	0.041896
POC->Nsc	9.816547	8.151762	5.643365	4.426963	1.012271	0.830579
POC->din	20.05893	16.09345	23.91158	18.9319	14.00185	12.41748

Chapter 6

General Discussion

6.1. General response of plankton food webs to the ERCP scenarios

The overall goal of this thesis was to identify the effect of multiple global change drivers on phytoplankton carbon metabolism and antioxidant capacity as key aspects also influencing seasonal bloom dynamics, biomass, community composition and interactions within the planktonic food web. The first research question was regarding the effect of the global change drivers of the ERCP 8.5 scenario on the carbon metabolism and antioxidant capacity of the diatom *Phaeodactylum tricornutum* in a full-factorial approach. The hypothesis that the multiple global change drivers will lead to increase of primary production, respiration and DOC exudation rate, resulting in cells with lower POC can be partially accepted. Cells had in fact lower POC, although no increase in respiration rate was found. However, the second hypothesis that cells would invest more energy in antioxidant capacity under the future ERCP 8.5 scenario, can be rejected. Results reported in the Chapter II reveal that under the conditions of the ERCP 8.5 scenarios had lower antioxidant capacity and higher oxidative damage, indicating an even worse response to global change drivers than expected. In particular, I observed that temperature is the major abiotic driver inducing shifts in carbon fluxes within the cells of the diatom *Phaeodactylum tricornutum*. Temperature positively affected its growth rate, DOC exudation and primary production, and negatively affected dark respiration and antioxidant capacity, whilst the additional effect of higher pCO_2 and N:P ratio further stimulated primary production and DOC exudation. Consequently, phytoplankton cells had lower C content under the ERCP 8.5 scenario and higher oxidative damage. These results suggest that more carbon may flow into the microbial loop via DOC exudation, and that less energy may be available to higher trophic levels. The consequences of the findings from Chapter II for the planktonic food web as a whole, was further investigated in Chapters III, IV and V. Chapters III and IV answered the questions regarding the impact of global change drivers on biomass and community composition of planktonic food webs during the phytoplankton seasonal blooms, spring and fall, respectively. Chapter V provided answers regarding the effect of global change

drivers on interactions and carbon fluxes between compartments of the plankton community during the fall bloom. The hypothesis that under the conditions of future scenarios plankton communities will be dominated by smaller species, including an enhancement of the microbial loop, as well as diminished populations of mezoooplankton can be accepted for the fall season (Chapter IV and V), but has to be rejected for the spring season (Chapter III). By applying a multiple-driver approach and testing two ERCP scenarios, 6.0 and 8.5, I was able to demonstrate a gradient effect of the changing abiotic conditions on the plankton community biomass, food web structure, and carbon fluxes. Planktonic food webs under the ERCP 6.0 scenario remained relatively similar to current conditions, whereas environmental circumstances under the ERCP 8.5 scenario led to significant changes in the structure of different compartments of the food web. In spring, the communities in the ERCP 8.5 scenario had a larger abundance of mesozooplankton, while the opposite occurred in fall, when mesozooplankton abundance was largely diminished. At the same time, growth of nanophytoplankton, including the coccolithophore *Emiliania huxleyi*, was stimulated in fall. The contrasting effects found in fall and spring show that the interactive impact of global change drivers depend on seasonal environmental conditions. Therefore, the main hypothesis that future scenarios will lead to alterations in phytoplankton carbon metabolism and food web structure channelling a higher amount of primary production into the microbial loop can be accepted only for the fall season and rejected for the spring season. Overall, this thesis shows the importance of more realistic approaches to assess the effect of global change on planktonic food webs. The results reinforce the goals of the 'Special Report on the impacts of global warming of 1.5 °C above pre-industrial levels' to substantially reduce environmental risks and impacts of climate change.

6.2. Diatom carbon metabolism and antioxidant capacity under global change drivers and its implications for the planktonic food web

The specific processes underlying the negative effect of the ERCP scenarios on carbon metabolism and antioxidant capacity of a diatom were assessed in Chapter II. The full-factorial approach of this experiment allowed the identification of major changes in carbon metabolism and antioxidant capacity in the diatom *Phaeodactylum tricornutum* exposed to environmental conditions of the ERCP 8.5 scenario. The results showing that warming induced mitochondria malfunction, higher AOX activity, lower antioxidant enzymes and accumulation of MDA in the diatom cells demonstrate the metabolic stress suffered by a phytoplankton due to global

change. The inability of phytoplankton to cope with reactive oxygen species can be crucial for its survival, as ROS can cause oxidative damage to different cellular apparatus, such as lipids, proteins, and nucleic acid (Halliwell, 1987). Oxidative stress can lead to lower photosynthetic rate due to membrane lipid peroxidation (Rajagopal et al., 2000; Juan et al., 2004; Carrara, et al., 2021), lower growth rates as well as chlorophyll *a* content (Mallick et al., 2002) and, therefore loss of metabolic fitness and, ultimately, cell death (Bidle, 2016). Warming and ocean acidification have been found to induce oxidative damage in different phytoplankton groups (Lesser, 1997; Yakovleva et al., 2009; Brutemark et al., 2015; Kvernvik et al., 2020). Additionally, lipid peroxidation caused by ROS can lead to changes in the fatty acid profile in microalgae, which can, in turn, influence the development of grazers that rely on the quality of essential fatty acids in their prey (Hessen et al., 1997). Oxidative stress in phytoplankton is specially problematic for grazers because lipid peroxidation preferentially oxidizes polyunsaturated fatty acids (Gaschler and Stockwell, 2017), which play an important role in the somatic growth of zooplankton, such as copepods (Rossoll et al., 2012). These results illustrate how phytoplankton adapted to the North Sea environmental conditions can face physiological stress and challenges to maintain a health metabolism under future conditions. Phytoplankton species under stress due to abiotic conditions can be outcompeted by other species better adapted, leading to changes in food web interactions and functioning (Litchman et al., 2012).

The results presented in Chapter II are supported by findings from Chapter IV and V that indicated an increasing flow of energy into the microbial loop. An important change caused by the environmental conditions under the ERCP 8.5 scenario was the increase of DOC exudation by the phytoplankton in fall. The tested global change drivers, higher pCO_2, temperature, and N:P ratio, are known to induce DOC exudation by phytoplankton (Zlotnik and Dubinsky, 1989; Baines and Pace, 1991; Riebesell et al., 2007; Wetz and Wheeler, 2007; Engel et al., 2011; Thornton, 2014; Torstensson et al., 2015; Li and Sun, 2016), while bacterioplankton rely on DOC as a major energy source (Azam et al., 1983, Kieber et al., 1989; Mühlenbruch et al., 2018). These experiments show that the abiotic conditions under the ERCP 8.5 scenario can diminish important carbon fluxes derived from phytoplankton to higher trophic levels, where instead of being transferred up to higher trophic levels, primary production is exported to the microbial loop. Despite the fact that photosynthetic rate was enhanced by temperature and pCO_2, phytoplankton cells presented lower carbon content caused by the higher growth rate and DOC exudation. Processes leading to phytoplankton cell division are known to be positively affected by temperature (Zhao et al., 2022), while primary production is expected to be stimulated by higher pCO_2 and temperature as long as phytoplankton are not

light- or nutrient-limited (Tilzer et al., 1986; Riebesell, 2004; Winder and Sommer, 2012). However, even the increased primary production rate was not able to compensate the higher growth rate under warmer conditions and *P. tricornutum* cells had lower carbon content. A reduction in cellular C content represents lower availability of energy for higher trophic levels, especially under warmer conditions, when heterotrophic ectotherms have a higher demand for carbon, due to the increase of metabolic rates at higher temperature (Boersma et al., 2016). Hence, the environmental conditions under the ERCP 8.5 scenarios have detrimental effects to phytoplankton antioxidant capacity, generating cellular oxidative stress, as well as leads to changes in metabolism that would instead of channel carbon to higher trophic levels, exports carbon into the microbial loop.

6.3. Global change scenarios effects on the phytoplankton bloom biomass and community composition – differences between spring and fall

The contrasting effects of ERCP scenarios on the planktonic food web during the two seasonal blooms, such as mesozooplankton abundance and phytoplankton community composition, are not unexpected as the North Sea naturally presents different environmental conditions and plankton community between the end of summer and beginning of spring (Bresnan et al., 2009). The temperature was about 12°C higher at the beginning of fall compared to the beginning of spring during the mesocom experiments, while dissolved inorganic nutrients were almost 8 times higher in spring than in fall. Typical summer/fall stratificantion is not expected in the southern North Sea, as it is a relatively well mixed system throughout the year (van Leeuwen et al., 2015). Thus, stratification effect was not considered for the experiments, and the mesocosms were constantly mixed. The species dominating the blooms in spring were common species for the region and for the season: *Odontella* sp., *Skeletonema costatum*, *Thalassiosira* sp. and other diatoms. In fall, the community in the Ambient scenario were also common taxa found during this time of the year: *Guinardia flaccida*, *Leptocylindrus danicus*, *Noctiluca scintillans* and *Prorocentrum* sp. Additionally, the spring blooms start when the zooplankton biomass is low, whereas the phytoplankton bloom in fall starts already under higher top-down control, with a stablished zooplankton community. Therefore, differences in the plankton biomass, community composition and their response to changes in environmental drivers are to be expected between the two seasons. However, the baseline sea surface temperature for the experiments measured at the Helgoland roads was ~1.5°C higher than the mean temperature found in the previous decades during spring and fall mesocosm experiments

(Wiltshire et al., 2015), indicating that the years when the experiment were conducted were relatively warmer than usual, but following the warming trend seen in the region (Di Pane, et al., 2022).

It has been observed before by Wiltshire et al. (2008) that the spring diatom bloom in the North Sea has been resilient to environmental changes over the last decades, an indicative that, so far, increases in temperature, pCO_2 and N:P ratio were not intensive enough to disrupt spring bloom dynamics. However, future increases in temperature and pCO_2 are expected to stimulate primary production, metabolic rates, and growth of phytoplankton. Hare et al. (2007) and Feng et al. (2009) incubated natural phytoplankton communities and exposed them to higher temperature and pCO_2, which resulted in higher phytoplankton productivity, as well as shifts in species composition. Nonetheless, higher phytoplankton productivity was not seen in the spring mesocosm experiment, potentially because of a higher copepod grazing pressure. Although copepod grazing rate was not measured, the higher abundance of copepods in the ERCP 8.5 scenario may have increased the grazing pressure on phytoplankton and consumed the additional primary production in this scenario. In addition, warming can increase grazing rates to fulfil elevated energy demands in zooplankton (Heine et al., 2019; López-Abbate, 2021), which may have prevented me from observing any change in phytoplankton biomass. The lower availability of phosphorus also proved not to be an obstacle for phytoplankton growth in spring as dissolved silica was depleted before phosphorus even in the ERCP scenarios. However, lower P contributed to a higher N:P and C:P ratio of seston. The N:P ratio of phytoplankton is expected to be increased further by warming, as less ribosomes, and therefore phosphorus, are necessary to synthesize protein (Toseland et al., 2013). Warming and elevated pCO_2 is also expected to further increase C:P ratios, since more carbon can be fixed under higher temperature and pCO_2 (Hare et al., 2007; Feng et al., 2009). The phenology of phytoplankton spring bloom has also been a point of debate, as shifts in the time of the bloom peak due to changing environmental conditions can lead to mismatch with the phenology of zooplankton (Edwards and Richardson, 2004). Despite predictions of shifts in phytoplankton bloom phenology related to climate change (Lewandowska and Sommer, 2010; Asch et al., 2019), this was not evidenced in any of the two season, neither in fall nor in spring. Nevertheless, phytoplankton biomass is not the only aspect influencing food web structure, community composition also plays an important role in this matter.

The phytoplankton species composition remained similar across scenarios in spring, reinforcing the resilience of the spring bloom to global change. In fall, however, the community

was largely altered under the ERCP 8.5 scenario, where the coccolithophore *Emiliania huxleyi* and other nanophytoplankton dominated over diatoms. In support of this result, Scharfe and Wiltshire (2019) already found effects of climate change on the phytoplankton community in the North Sea over the last decades, showing that response of phytoplankton to changing environmental conditions are species-specific, with losers and winners. *Emiliania huxleyi* can largely benefit from future environmental conditions as the photosynthetic carbon fixation of this species is below saturation under current pCO_2, which contrasts with diatoms which are close to or at CO_2-saturation at present day (Burkhardt et al., 1999; Riebesell et al., 2000; Burkhardt et al., 2001; Rost et al., 2003). Warming and higher N:P can also be beneficial to *E. huxleyi* competitiveness, since this species is known for being very effective in P acquisition (Xu et al., 2006; Xu et al., 2010), as well as for presenting high growth rate at temperatures around 20°C (Rosas-navarro et al., 2016). The calcification capacity of *E. huxleyi* is responsible for the precipitating of $CaCO_3$, which removes dissolved carbonate from the water column, the major component of the oceanic alkalinity pool. Therefore, *Emilania huxleyi* is a major player in the oceanic carbon cycle as more intense and more frequent blooms of this species in the future can reduce local total alkalinity levels, which diminishes the ocean capacity to absorb CO_2 from the atmosphere or could even lead to CO_2 release from the seawater (Rost and Riebesell, 2004). These changes in the phytoplankton community composition are, however, not isolated and can have cascading effects to higher trophic levels.

The positive effect of warming on metabolic processes is known to increase energy demand in ectotherms, such as copepods and microzooplankton (Heine et al., 2019; López-Abbate, 2021). Indeed, Boersma et al. (2016) and Malzahn et al. (2016) found mesozooplankton preferring phytoplankton prey over microzooplankton under warming, probably due to the high carbon content of microalgae that better support their energetic demand in such conditions. Therefore, higher grazing pressure on phytoplankton is expected under global conditions. While zooplankton metabolic demands can change, simultaneous alteration of food quality induced by global change drivers may prevent zooplankton from obtaining resources matching their nutritional demands (Meunier et al., 2016; Mathews et al., 2018; McLaskey et al., 2019). At the same time, no direct effect of realistic expected ocean acidification has been seen on zooplankton (Aberle et al., 2013; McConville et al., 2013; Horn et al., 2016; Bailey et al., 2017). Chapters III and IV show that environmental conditions under the ERCP 8.5 scenario had significant impacts on the zooplankton community in both seasons, spring and fall, yet, with contrasting effects. In spring, the copepods *Acartia* sp. and *Temora longicornis* dominated in all scenarios, but in the ERCP 8.5 scenario they were more abundant, indicating that conditions

under this scenario were beneficial for copepod development, and more carbon fixed by phytoplankton was transferred to higher trophic levels compared to the ERCP 6.0 scenario and Ambient. Different from other temperate regions where copepod production is highly correlated to phytoplankton blooms (Kiøboe and Nielsen, 1994), Halsband and Hirche (2001) found that the copepods production was uncoupled from the spring phytoplankton bloom in the North Sea. This desynchronized behaviour is probably due to the colder temperatures seen at the beginning of spring in the North Sea, when the phytoplankton bloom occurs, which limit egg production and hatching. As result, a large fraction of the primary production from the bloom is not transferred to higher trophic levels under Ambient conditions. In turn, environmental conditions of the ERCP 8.5 scenario during the phytoplankton bloom allow higher copepod abundance, creating a better match between primary production and mesozooplankton in spring. In fall, the effect was the opposite, with mesozooplankton being negatively impacted and microzooplankton dominating as grazers. Since elemental stoichiometry of seston in fall was not different across scenarios, there is no indication that C:N:P ratio of prey had a negative impact on mesozooplankton abundance. The most numerous species of large grazers in fall, *Noctiluca scintillans* and *Penilia avirostris*, which are able to feed on a broad range of prey sizes (Kirchner et al., 1996; Atienza et al., 2006). Temperature was also well within the tolerance of these species (Johns et al., 2005; Harrison et al., 2011). Thus, the shift from large diatoms to nanophytoplankton in the ERCP 8.5 scenario and warmer conditions likely had little effect on these species, rather, I suggest that food availability was a limiting factor for the development of mesozooplankton. Since under warmer conditions energy demand in ectotherms is expected to be higher (Heine et al., 2019; López-Abbate, 2021), as well as higher preference for phytoplankton in their diet (Boersma et al., 2016; Malzahn et al., 2016). On the other hand, there was no difference in phytoplankton biomass in the ERCP 8.5 compared to other scenarios. These results indicate that the conditions in the ERCP 8.5 reached a threshold for the mesozooplankton community in the context of the fall in the North Sea and the fluxes of energy through the microbial loop became more significant. Therefore, the environmental conditions under the ERCP 8.5 scenario led to a higher mesozooplankton productivity during the spring bloom, while presented lower mesozooplankton productivity during the fall bloom coupled with increase of microzooplankton biomass.

Key components of the microbial loop, bacterioplankton and microzooplankton, were not significantly affected by the ERCP scenarios in the spring bloom. In fall, bacterioplankton reached higher biomass in the ERCP 8.5 scenario during the phytoplankton bloom decay phase than in the other scenarios. Pelagic bacteria production is known to increase after phytoplankton

blooms, due to the higher availability of DOC that is mostly released by dead phytoplankton cells or exuded from living cells (Ducklow et al., 1993; Thornton, 2014). This fuels bacterioplankton production that rely on DOC as energy source (Kieber et al., 1989). Thus, the increase of bacterioplankton in the ERCP 8.5 scenario in fall shows that more energy was channelized from phytoplankton to the microbial loop. At the same time, microzooplankton community in the ERCP 8.5 scenario in fall was dominated by ciliates, which benefited on the larger availability of their prey, bacterioplankton and nanophytoplankton (Azam et al., 1983; Legendre and Le Fèvre, 1995). Therefore, due to the reduction of mesozooplankton under the ERCP 8.5 scenario, the microzooplankton became the dominant grazer in the planktonic food web. This indicates that not only more energy was redirected to the microbial loop, but also less energy went up to higher trophic levels, demonstrating changes in nutrient fluxes and interactions within the food web.

6.4. Global change scenarios effects on planktonic food web structure and interactions during the fall bloom

The changes in plankton biomass and community under the ERCP scenarios in fall were further assessed in Chapter V. By applying an inverse network analysis to create a food web model based on the data collected from the fall mesocosm experiment, Chapter V quantifies carbon fluxes between compartments of the food web and reveals alterations in the ecosystem functioning in the ERCP 8.5 scenario. Food webs under the Ambient and ERCP 6.0 conditions showed similar carbon fluxes and functioning. On the other hand, results of the model showed the increased carbon flow from primary producers to the microbial loop in the ERCP 8.5 scenario, either via grazing from microzooplankton or from POC and DOC. The gap left in the food web by the reduced abundances of mesozooplankton, allowed higher amounts of senescent phytoplankton cells to end up in the detrital pool, which together with DOC, fuelled bacterioplankton production. The enhancement of the microbial loop in the ERCP 8.5 scenario also led to increasing degree of detritivory, as well as higher capacity to recycle carbon. In the ERCP 8.5 scenario, omnivorous zooplankton also showed a higher degree of herbivory, agreeing with the expectations of Boersma et al. (2016) and Malzahn et al. (2016) that copepods prefer carbon-rich prey under warmer conditions. Results of the inverse network analysis are also aligned with assumptions of Laws et al. (2000) that imply that smaller cell size phytoplankton contribute more to the dissolved organic carbon pool than larger cells. Hilligsøe et al. (2011) also predicted lower mesozooplankton abundance in food webs dominated by

smaller cell phytoplankton. Moreover, the changes in carbon fluxes induced by global change drivers in the planktonic food web are also a reflection of changed carbon fluxes and metabolic stress within phytoplankton cells.

6.5. What does an enhanced microbial loop mean?

The importance of the microbial loop for the biogeochemical cycle of carbon and other elements has long been recognized (Pomeroy, 1974). The microbial loop itself is an intricate network of interactions between its components (Azam et al., 1983). While bacterioplankton exploit DOC (Kieber et al., 1989), microzooplankton, and even smaller zooplankton, can also graze on bacteria and other smaller nano- or picophytoplankton (Wright and Coffin, 1984). Sloppy feeding by zooplankton, viral lysis, excretion and particulate organic material also provide substrate for heterotrophic bacteria growth. However, dissolved organic carbon exuded by phytoplankton is accounted as the major organic carbon source for pelagic bacteria (Fuhrman and Azam, 1982; Peterson, 1984) and is influenced by environmental conditions (Thornton, 2014; Torstensson et al., 2015). Chapter II indicates an increased in DOC exudation by phytoplankton under the ERCP 8.5 scenario, suggesting that future environmental conditions will lead to a higher flow of organic carbon from phytoplankton to the microbial loop. On the one hand, dissolved photosynthates supply organic carbon to bacteria and microzooplankton, on the other hand, mineralization of organic nutrients, such as nitrogen and phosphorus, is carried out by heterotrophic bacteria, making these elements again available for primary producers (Legendre and Rassoulzadegan, 1995). Interestingly, the phytoplankton community under the ERCP 8.5 scenario in the fall was also composed mostly by smaller species in comparison to the ERCP 6.0 and Ambient. Since microzooplankton prefer smaller phytoplankton prey (Bernard and Rassoulzadegan, 1990; Calbet et al., 2007), a potential shrinking in phytoplankton size may further fuel carbon into the microbial via grazing as well.

Mesozooplankton are also able to feed on microzooplankton and, to some extent, on bacteria (Stoecker and Sanders, 1985; Kirchner et al., 1996; Vincent and Hartmann, 2001) thus, transferring some of the carbon from the microbial loop to higher trophic levels. Nevertheless, additional carbon transfer through the microbial loop to large grazers, instead of direct trophic link to primary producers, leads to further loss of organic carbon and lower trophic efficiency (Fenchel, 2008; Aberle et al., 2015). Therefore, the strengthened fluxes of carbon through the microbial loop may lower the productivity of mesozooplankton and constrain energy fluxes

within lower trophic levels in the pelagic food web. This was evidenced in chapters IV and V, where the microbial loop and microzooplankton dominated over mesozooplankton, as well as the lower mean trophic level and higher detritivory degree in the ERCP 8.5 scenario, while the ERCP 6.0 scenario still presented similar food web structure in this matter compared to the Ambient. These findings are also in line with results from models of Taucher and Oschlies (2011) that proposed an enhanced microbial loop activity due to warming. Pomeroy and Deibel (1986) and Kirchman et al. (2009) also predicted a decrease of energy transfer from primary producers to higher trophic levels due to the strengthening of the microbial loop fuelled by organic carbon derived from phytoplankton primary production. Nonetheless, the changes caused by the abiotic factors in the ERCP scenarios were less critical for the microbial loop in spring, indicating that the threshold for a restructuring of the microbial loop was not reached in the spring bloom.

6.6. Limitations

The main limitation of experiments evaluating the effect of global change drivers on plankton physiology and ecology is time. In natural systems plankton species and communities will experience environmental changes gradually under longer periods of time than in the experimental setups. The results of Chapter II were obtained from a period after acclimation of the diatom *P. tricornutum* to the future scenarios (over 20 generations). While this excludes results showing stress response the environmental conditions, 20 generations is still much less time than almost 80 years that this species will have in the sea to reach the conditions predicted in the tested scenario. On the other hand, the plankton communities in the mesocosm experiments had even less time to get accustomed to the ERCP scenarios conditions, only one day. A longer period of acclimatization would yield even less representative results, as the species and interactions among them gradually shift away from natural conditions, due to the artificial setup in the mesocosm tanks.

The use of a single species to assess the effect of global change drivers on carbon metabolism and antioxidant response of a phytoplankton proved to be adequate. Yet, it is important to note that each species presents different environmental thresholds and the overall effect of the changes in phytoplankton cell physiology for the plankton community will largely depend on the assemblages of phytoplankton in such communities. Another limitation present in the experiment using *P. tricornutum* is the importance of this species for the regional

community. Despite the global distribution of this diatom, it is generally not a dominant or bloom-forming species in the North Sea, which limits the extrapolation of the results obtained from this species to other phytoplankton. Nevertheless, this species was still chosen for the experiment as it is as representative of the Bacillariophyceae group, which is a dominant group for the global phytoplankton primary production, including the North Sea, and because there is a paucity of scientific literature on diatoms ecophysiology. Additionally, the fact that the strain used for the single species experiment was isolated in 1910 is also a point to be considered. Because the strain has been living in lab and not under natural conditions over the last century, the extrapolation of the results are limited to some extent.

The mesocosm experiments also have limitations considering the structure of the food web, since trophic levels higher than mesozooplankton were excluded from the experiment. The inclusion of larger animals would have had a large and disproportional impact on the top-down control mechanisms within the small and limited mesocosm space, therefore higher trophic levels were sieved out from the communities. However, I have to consider that the effect of the tested scenarios could have yielded different results if larger organisms were present, preying on mesozooplankton. Another limitation for the experiments was the timing. Baselines for the experiment derived from environmental conditions and natural plankton assemblages found in those particular years (2018 and 2019), which were relatively warmer years compared to previous ones. Although expected due to climate change, it is unclear, if the temperature baseline applied in the experiment will become common for the southern North Sea or if it was merely an unsual warm year. Yet, this feature has to be considered as temperature is also a major driver in environmental selection of species present when the seawater for the mesocosm experiments was sampled.

6.7. Conclusions

The multiple-driver approach is a useful tool to identify shifts in plankton biomass, community composition and carbon fluxes between compartments of the planktonic food web, as well as phytoplankton carbon metabolism and antioxidant capacity at species level. The use of the Representative Concentration Pathway scenarios developed by the Intergovernmental Panel on Climate Change also proved to be valuable for a more realistic approach to assess global change impact on natural plankton communities and on single species. This approach also showed that the combination of relatively small changes in environmental conditions, such

as only +3°C, can have significant impacts on ecophysiological dynamics of planktonic organisms. The response of the diatom *Phaeodactylum tricornutum* to warming, pCO_2 and elevated N:P ratio of dissolved inorganic nutrients revealed the high interactivity of these drivers, which together synergistically affect carbon fluxes and antioxidant capacity within the phytoplankton cell. These changes translate to higher growth rate and primary production, lower respiration rate and increased DOC exudation, leading to lower carbon content cells under the ERCP 8.5 scenario. Such changes imply higher energetic input into the microbial loop as well as lower carbon availability to higher trophic via grazing. In addition, cells faced higher oxidative stress due to warming, which can make this diatom less competitive at higher temperatures. Hence, when extrapolated to other diatoms from temperate coastal areas, the effect of the environmental conditions under the ERCP 8.5 scenario could lead to a decrease in populations of diatoms species in those areas, opening space for species, such as *E. huxleyi*, better suited to future conditions to thrive and restructure the planktonic food web.

This thesis also identified the gradient effect of the ERCP 6.0 and 8.5 scenario compared to Ambient conditions, indicating again the interactivity of global change drivers in the context of natural plankton community. Results showed the resilience of the phytoplankton spring bloom to alterations due to global change drivers, where plankton species assemblages remained similar across scenarios. Nonetheless, I cannot exclude phytoplankton productivity may increase in spring under the ERCP 8.5 scenario conditions, since copepod abundance was also enhanced, indicating a higher energy transfer from primary producers to higher trophic levels in this scenario. Despite the lower dissolved inorganic phosphorus availability, phytoplankton biomass was not hindered, instead, stoichiometric quality of seston showed a higher N:P and C:P ratios, agreeing with current available literature that expect lower demand of P by ectotherms at warmer temperature. The fall phytoplankton bloom was more sensitive to global change drivers, where the abiotic conditions of the ERCP 8.5 scenario favoured the coccolithophore *Emiliania huxleyi* and other nanophytoplankton at the expense of larger diatoms, as well as decrease of mesozooplankton, which were partially replaced by microzooplankton. Further assessment via food web reverse modelling also revealed lower mean trophic level, higher degree of detritivory and changes in carbon fluxes within the plankton community caused by abiotic conditions of the ERCP 8.5 scenario. Thus, the fall phytoplankton bloom under the ERCP 8.5 scenario presented a community composition restructuring and significant higher dominance of the microbial loop coupled with lower energy transfer to higher trophic levels.

Overall, this thesis shows the importance of realistic approaches to assess the effect of global change on planktonic food webs. The results presented here indicate that plankton spring bloom productivity in temperate regions are likely to increase towards higher trophic levels, such as copepods, and species composition are expected to remain similar. The low temperature at the beginning of spring might be responsible to buffer additional stress caused by changing environmental conditions, here warming, ocean acidification and higher N:P ratio. On the other hand, plankton communities in late summer and beginning of fall will likely be more affected by global change drivers, including the rise and demise of key species, such as *Emiliania huxleyi* and *Noctiluca scintillans*. Due to the fact that plankton communities and ecosystem fluxes remained relatively similar between the ERCP 6.0 and Ambient conditions, compared to the ERCP 8.5, this thesis also reinforces the goals of the 'Special Report on the impacts of global warming of 1.5 °C above pre-industrial levels' to substantially reduce changes in ecosystem structure and functioning.

6.8. Outlook

The long-term effect of global change scenarios on the complete annual cycle of phytoplankton throughout the seasons still remains poorly understood. Although the effect of the global change scenarios on the phytoplankton blooms were analysed in this thesis, an experiment showing how a post-bloom plankton community will develop and affect the next bloom is an interesting proposal. Sommer and Lewandowska (2011) tested, for instance, the effect of overwintering zooplankton on the spring phytoplankton bloom triggering, as warmer winters may stimulate zooplankton grazing rate, which showed to have a negative effect on phytoplankton biomass at the beginning of spring. Specific grazing experiment would also help to elucidate the impact of the ERCP scenarios on zooplankton grazing rate and selectivity and how it can shape the phytoplankton community. Indeed, some experiments have shown that temperature has an impact on grazing rate and selectivity (Garrido et al., 2013; Boersma et al., 2016; Malzahn et al., 2016), but evidences of this grazing patterns on the phytoplankton community under multiple-drivers effect remain scarce. At the same time, bottom-up effects can also be further investigated, for instance, if the ERCP scenarios also affect phytoplankton demand for dissolved inorganic nutrients. This is seen in the spring mesocosm experiment, where silica is depleted in the ERCP scenarios before the Ambient. This could be better analysed through bioassays under the different ERCP scenarios conditions, where carbon,

nitrogen, phosphorus and silica can be assessed separately. Such experiment would elucidate if phytoplankton growth under global change conditions can become more or less limited by these nutrients in the future.

Shifts in distribution of marine organisms due to climate change have been found (Brierley and Kingsford, 2009; Poloczanska et al., 2013) as well as impact of invasive species on local food webs (Keller et al., 2011). Hence, such species are likely to play a role in competing with local species under a changing abiotic conditions. During the fall mesocosm experiment, the presence of the cladoceran *Penilia avirostris* was found, an invasive species in the North Sea that thrived in the ERCP 6.0 scenarios but was less abundant in the ERCP 8.5, suggesting that this mesozooplankton also reached a tipping point in between this two future scenarios. Interactions between local species can also be modified due to global change drivers. Therefore, local species that once were under optimal conditions can become competitive, as it was the case with the *Emiliania huxleyi* during the fall mesocosm experiment. Thus, it is important to further investigate species competition under global change within an ecosystem including local and invasive species to better understand food web restructuring under such conditions.

Environmental conditions, such as temperature, also influence bacterioplankton species compositions (Rajeev et al., 2021). Therefore, an experiment able to realistic assess species compositions would elucidate more about the effects of global change on bacterioplankton and their function in the ecosystem, given the high importance of prokaryotes for the nutrient fluxes as well. Additionally, the enhancement of the microbial loop under warmer conditions seen here also raises questions about structural and functional changes taking place in this compartment of the planktonic food web. The increase of DOC exudation showed by the diatom *P. tricornutum* in the ERCP 8.5 scenario illustrates an increase of energy input into the microbial loop, but does not reveal much about the quality of such exudates. The quality of dissolved organic matter is an important factor for bacterioplankton growth and community composition, as different components support different groups and species of prokaryotes and, thus, may influence the species selection (Sapp et al., 2007; Pete et al., 2010). Hence, further investigation of phytoplankton-bacterioplankton interactions via DOC quality and exudation rate can also assist the understanding of indirect effects of global change on the microbial loop through phytoplankton. This can be done, for instance, by growing phytoplankton isolated species or natural communities in microcosms under the ERCP conditions, quantifying DOC production and determining its qualities, such as the composition of polysaccharides and

monosaccharides. Additionally, samples for bacterioplankton quantification and sequencing can be taken to determine prokaryote community composition and their function.

Processes governing the fall of the *Noctiluca sinctillans* should also be investigated, as this is an important mesozooplankton species able to compete with copepods. Grazing experiments with *N. scintillans* and phytoplankton species grown under ERCP scenarios can include different groups, such as diatoms, flagellates, dinoflagellates and coccolithophores, as well as size classes, nano-, pico- or microphytoplankton, in different quantities. Such trials would provide answers on how global change affect *N. scintillans* grazing rate, prey preference, growth rate and survival. Grazing experiments combined with different C:N:P ratio of prey can provide additional knowledge on the nutritional demand of *N. scintillans* under the ERCP scenarios conditions as well. It is known, for instance, that this species grows faster when fed with diatoms, rather than dinaflagellates or green algae under current conditions (Zhang et al., 2015). Furthermore, bacterioplankton and microzooplankton could also be added to grazing experiments in order to determine if heterotrophic organisms are also a good nutritional option for this mesozooplankton. This would also reveal more about what was the real cause of the diminishment of this species when facing the ERCP scenarios conditions.

Multiple-driver experiment on natural communities including higher trophic levels other than mesozooplankton, such as fish larvae, would also draw a larger picture of global change impact on marine food webs. For instance, temperature influences survival rate of fish larvae (Yin and Blaxter, 1987), which can, in turn, affect top-down control mechanisms on plankton and the fluxes of nutrients through these food web compartments. Nutrient flows are indeed a great concern regarding global change. As seen in this thesis, increase in mesozooplankton abundance in spring coupled with higher C:P and N:P ratios are indicative of changes in ecological stoichiometry and nutrient fluxes throughout trophic levels. On top, the rise of coccolithophores in a warmer season can additionally impact the biological carbon pump. The shift from large diatom to nanophytoplankton can further impact the biological carbon pump, due to the reduced sinking rate of smaller cells (Feng et al., 2021), which decreases the carbon export to the deeper layers of the sea. Therefore, further investigation on how nutrients fluxes in plankton food webs can be impacted by global change drivers would be of use to better predict future shifts in nutrient cycling at large scale.

Bibliography

Aberle, N., Lengfellner, K. & Sommer, U. (2007). Spring bloom succession, grazing impact and herbivore selectivity of ciliate communities in response to winter warming. Oecologia, 150, 668-681. doi:10.1007/s00442-006-0540-y

Aberle, N., Malzahn, A. M., Lewandowska, A. M. & Sommer, U. (2015). Some like it hot: the protozooplankton − copepod link in a warming ocean. Marine Ecology Progress Series, 519, 103–113. doi:10.3354/meps11081

Aberle, N., Schulz, K. G., Stuhr, A., Malzahn, A. M., Ludwig, A. & Riebesell, U. (2013). High tolerance of microzooplankton to ocean acidification in an Artic coastal plankton community. Biogeosciences, 10, 1471-1481. doi:10.5194/bg-10-1471-2013

Aebi, H. (1984). Catalase in vitro. In: Packer L, eds. Methods in Enzymology Vol. 105: Oxygen Radicals in Biological Systems. New York, USA: Academic Press/Elsevier, 121–126. doi:10.1016/S0076-6879(84)05016-3

Agawin, N. S. R., Duarte, C. M. & Agustí, S. (2000). Nutrient and temperature control of the contribution of picoplankton to phytoplankton biomass and production. Limnology and Oceanography, 45 (3), 591-600. doi:10.4319/lo.2000.45.3.0591

Ahmad, S. & Pardini, R. S. (1988). Evidence for the presence of glutathione peroxidase activity towards an organic hydroperoxide in larvae of the cabbage looper moth, *Trichoplusia ni*. Insect Biochemistry, 18, 861–866. doi:10.1016/0020-1790(88)90111-4

Alipanah, L., Rohloff, J., Winge, P., Bones, A. M. & Brembu, T. (2015). Whole-cell response to nitrogen deprivation in the diatom *Phaeodactylum tricornutum*. Journal of Experimental Botany, 66 (20), 6281-6296. doi:10.1093/jxb/erv340

Allen, A. E., Laroche, J., Maheswari, U., Lommer, M., Schauer, N., Lopez, P. J., Finazzie, G., Fernie, A. R. & Bowler, C. (2008). Whole-cell response of the pennate diatom *Phaeodactylum tricornutum* to iron starvation. Proceedings of the National Academy of Sciences, 105 (30), 10438-10443. doi:10.1073/pnas.0711370105

Allesson, L., Ström, L. & Berggren, M. (2016). Impact of photochemical processing of DOC on the bacterioplankton respiratory quotient in aquatic ecosystems. Geophysical Research Letters, 43 (14), 7538-7545. doi:10.1002/2016GL069621

Alvarez-Fernandez, S., Bach, L. T., Taucher, J., Riebesell, U., Sommer, U., Aberle, N., Brussaard, C. P. D. & Boersma, M. (2018). Plankton responses to ocean acidification. The role of nutrient limitation. Progress in Oceanography, 165, 11-18. doi:10.1016/j.pocean.2018.04.006

Alvarez-Fernandez, S., Lindeboom, H. & Meesters, E. (2012). Temporal changes in plankton of the North Sea: community shifts and environmental drivers. Marine Ecology Progress Series, 462, 21–38. doi:10.3354/meps09817

Andersen, C. B. (2002). Understanding carbonate equilibria by measuring alkalinity in experimental and natural systems. Journal of Geoscience Education, 50(4), 389-403. doi:10.5408/1089-9995-50.4.389

Anderson, T. R., Hawkins, E. & Jones, P. D. (2016). CO_2, the greenhouse effect and global warming: from the pioneering work of Arrhenius and Callendar to today's Earth System Models. Endeavour, 40 (3), 178-187. doi:10.1016/j.endeavour.2016.07.002

Anderson, T. R., Hessen, D. O., Boersma, M., Urabe, J., & Mayor, D. J. (2017). Will invertebrates require increasingly carbon-rich food in a warming world? The American Naturalist, 190 (6), 725-742. doi:10.1086/694122

Angilletta, M. J., Steury, Jr., T. D. & Sears, M. W. (2004). Temperature, growth rate, and body size in ectotherms: fitting pieces of a life-history puzzle. Integrative and Comparative Biology, 44, 498–509. doi:10.1093/icb/44.6.498

Anjusha, A., Jyothibabu, R., Jagadeesan, L., Mohan, A. P., Sudheesh, K., Krishna, K., Ullas,

N. & Deepak, M. P. (2013). Trophic efficiency of plankton food webs: Observations from the Gulf of Mannar and the Palk Bay, Southeast Coast of India. Journal of Marine Systems, 115, 40-61. doi:10.1016/j.jmarsys.2013.02.003

Arbones, B., Figueiras, F. G. & Varela, R. (2000). Action spectrum and maximum quantum yield of carbon fixation in natural phytoplankton populations : implications for primary production estimates in the ocean. Journal of Marine Systems, 26 (1), 97-114. doi:10.1016/S0924-7963(00)00042-7

Arístegui, J., Duarte, C. M., Reche, I. & Gómez-Pinchetti, J. L. (2014). Krill excretion boosts microbial activity in the Southern Ocean. PLoS ONE, 9, e89391. doi:10.1371/journal.pone.0089391

Arnous, M.-B., Courcol, N. & Carrias, J.-F. (2010). The significance of transparent exopolymeric particles in the vertical distribution of bacteria and heterotrophic nanoflagellates in Lake Pavin. Aquatic Sciences, 72, 245–253. doi:10.1007/s00027-010-0127-x

Arrigo, K. R., Robinson, D. H., Worthen, D. L., Dunbar, R. B., DiTullio, G. R., Vanwoert, M. & Lizotte, M. P. (1999). Phytoplankton community structure and the drawdown of nutrients and CO_2 in the Southern Ocean. Science, 283, 365–368. doi:10.1126/science.283.5400.365

Asch, R. G., Stock, C. A. & Sarmiento, J. L. (2019). Climate change impacts on mismatches between phytoplankton blooms and fish spawning phenology. Global Change Biology, 8, 2544-2559. doi:10.1111/gcb.14650

Atienza, D., Saiz, E. & Calbet, A. (2006). Feeding ecology of the marine cladoceran *Penilia avirostris*: natural diet, prey selectivity and daily ration. Marine Ecology Progress Series, 315, 211-220. doi:10.3354/meps315211

Atkinson, D. (1995). Effects of temperature on the size of aquatic ectotherms: Exceptions to the general rule. Journal of Thermal Biology, 20, 61–74. doi:10.1016/0306-4565(94)00028-H

Azam, F., Fenchel, T., Field, J. G., Gray, J. S., Meyer-Reil, L. A. & Thingstad, F. (1983). The ecological role of water-column microbes in the sea. Marine Ecology Progress Series, 10, 257-263.

Bach, L. T., Hernández-Hernández, N., Taucher, J., Spisla, C., Sforna, C., Riebesell, U. & Arístegui, J. (2019). Effects of elevated CO_2 on a natural diatom community in the subtropical NE Atlantic. Frontiers in Marine Science, 6, 75. doi:10.3389/fmars.2019.00075

Bailey, A., Thor, P., Browman, H. I., Fields, D. M., Runge, J., Vermont, A., Bjelland, R., Thompson, C., Shema, S., Durif, C. M. F. & Hop, H. (2017). Early life stages of the Artic copepod Calanus glacialis are unaffected by increased seawater pCO_2. ICES Journal of Marine Science, 74 (4), 996-1004. doi:10.1093/icesjms/fsw066

Bailleul, B., Berne, N., Murik, O., Petroutsos, D., Prihoda, J., Tanaka, A., Villanova, V., Bligny, R., Flori, S., Falconet, D., Krieger-Liszkay, A., Santabarbara, S., Rappaport, F., Joliot, P., Tirichine, L., Falkowski, P. G., Cardol, P., Bowler, C. & Finazzi, G. (2015). Energetic coupling between plastids and mitochondria drives CO_2 assimilation in diatoms. Nature, 524, 366-369. doi:10.1038/nature14599

Baines, S. B. & Pace, M. L. (1991). The production of dissolved organic matter by phytoplankton and its importance to bacteria : Patterns across marine and freshwater systems. Limnology and Oceanography, 36, 1078–1090. doi:10.4319/lo.1991.36.6.1078

Baird, D., Asmus, H., Asmus, R., Horn, S. & de la Vega, C. (2019). Ecosystem response to increasing Ambient water temperatures due to climate warming in the Sylt- Rømø Bight, northern Wadden Sea, Germany. Estuarine, Coastal and Shelf Science, 228, 106322. doi:10.1016/j.ecss.2019.106322

Barros, M. P., Pedersén, M., Colepicolo, P. & Snoeijs, P. (2003). Self-shading protects

phytoplankton communities against H_2O_2-induced oxidative damage. Aquatic Microbial Ecology, 30 (3), 275–282. doi:10.3354/ame030275

Bascompte, J., Jordano, P. & Olesen, J. M. (2006). Asymmetric coevolutionary networks facilitate biodiversity maintenance. Science, 312, 431–433. doi:10.1126/science.1123412

Beardall, J. & Raven, J. A. (2004). The potential effects of global climate change on microalgal photosynthesis, growth and ecology. Phycologia, 43 (1), 26-40. doi:10.2216/i0031-8884-43-1-26.1

Beaufort, L., Probert, I., de Gabriel-Thoron, T., Bendif, E. M., Ruiz-Pino, D., Metzl, N., Goyet, C., Buchet, N., Coupel, P., Grelaud, M., Rost, B., Rickaby, R. E. M. & de Chagas, C. (2011). Sensitivity of coccolithophores to carbonate chemistry and ocean acidification. Nature, 476, 80-83. doi:10.1038/nature10295

Beaugrand, G., Brander, K. M., Lindley, J. A., Souissi, S., & Reid, P. C. (2003). Plankton effect on cod recruitment in the North Sea. Nature, 426 (6967), 661-664. doi:10.1038/nature02164

Behrenfeld, M. J., Boss, E. S. & Halsey, K. H. (2021). Phytoplankton community structuring and succession in a competition-neutral resource landscape. ISME Communications, 1 (12). doi:10.1038/s43705-021-00011-5

Behrenfeld, M. J., Randerson, J. T., McClain, C. R., Feldman, G. C., Los, S. O., Tucker, C. J., Falkowski, P. G., Field, C. B., Frouin, R. & Esaias, W. E. (2001). Biospheric primary production during an ENSO transition. Science, 291, 2594–2597. doi:10.1126/science.1055071

Beliaeff, B. & Burgeot, T. (2002). Integrated Biomarker Response: a useful tool ecological risk. Environmental Toxicology and Chemistry, 21 (6), 1316-1322. doi:10.1002/etc.5620210629

Beman, J. M., Arrigo, K. R. & Matson, P. A. (2005). Agricultural runoff fuels large phytoplankton blooms in vulnerable areas of the ocean. Nature, 434, 211-214. doi:10.1038/nature03370

Benner, I., Diner, R. E., Lefebvre, S. C., Li, D., Komada, T., Carpenter, E. J. & Stillman, J. H. (2013). *Emiliania huxleyi* increases calcification but not expression of calcification-related genes in long-term exposure to elevated temperature and pCO_2. Philosophical Transactions of the Royal Society B, 368, 20130049. doi:10.1098/rstb.2013.0049

Beran, A., Guardiani, B., Tamberlich, F., Kamburska, L. & Fonda Umani, S. (2003). Carbon content and biovolume of the heterotrophic dinoflagellate *Noctiluca scintillans* from the Northern Adriatic Sea. Proceedings of the CESUM-BS 2003, Varna. Book of Abstracts, UNESCO, Paris, 28.

Berdalet, E., Latasa, M., Estrada, M., Ciencies, I. De, Borbo, P. J. De, & Barcelona, C. De. (1994). Effects of nitrogen and phosphorus starvation on nucleic acid and protein content of *Heterocapsa* sp. Journal of Plankton Research, 16(4), 303–316. doi:10.1093/plankt/16.4.303

Berge, T., Daugbjerg, N., Andersen, B. B. & Hansen, P. J. (2010). Effect of lowered pH on marine phytoplankton growth rates. Marine Ecology Progress Series, 416, 79-91. doi:10.3354/meps08780

Berges, J. A., Franklin, D. J. & Harrison, P. J. (2001). Evolution of an artificial seawater medium: improvements in enriched seawater, artificial water over the last two decades. Journal of Phycology, 37, 1138-1145. doi:10.1046/j.1529-8817.2001.01052.x

Berglund, J., Müren, U., Båmstedt, U. & Andersson, A. (2007). Efficiency of a phytoplankton-based and a bacteria-based food web in a pelagic marine system. Limnology and Oceanography, 52 (1), 121–131. doi:10.4319/lo.2007.52.1.0121

Bermúdez, J. R., Riebesell, U., Larsen, A. & Winder, M. (2016). Ocean acidification reduces transfer of essential biomolecules in a natural plankton community. Scientific Reports, 6, 1–8. doi:10.1038/srep27749

Bernard, C. & Rassoulzadegan, F. (1990). Bacteria or microflagellates as a major food source for marine ciliates: possible implications for the microzooplankton. Marine Ecology Progress Series, 64 (1-2), 147-155.

Bi, R. & Sommer, U. (2020). Food quantity and quality interactions at phytoplankton-zooplankton interface: chemical and reproductive responses in calanoid copepod. Frontiers in Marine Science, 7, 274. doi:10.3389/fmars.2020.00274

Bidle, K. D. (2016). Programmed cell death in unicellular phytoplankton. Current Biology, 26, R594-R607. doi:10.1016/j.cub.2016.05.056

Bitaubé Pérez, E., Pina, I. C. & Pérez Rodríguez, L. (2008). Kinetic model of growth of *Phaeodactylum tricornutum* in intensive culture photobioreactor. Biochemical Engineering Journal, 40, 520-525. doi:10.1016/j.bej.2008.02.007

Boersma, M., Mathew, K. A., Niehoff, B., Schoo, K. L., Franco-Santos, R. M. & Meunier, C. L. (2016). Temperature driven changes in the diet preference of omnivorous copepods: no more meat when it's hot? Ecology Letters, 19 (1), 45-53. doi:10.1111/ele.12541

Boersma, M., Wiltshire, K. H., Kong, S. M., Greve, W. & Renz, J. (2015). Long-term change in the copepod community in the southern German Bight. Journal of Sea Research, 101, 41–50. doi:10.1016/j.seares.2014.12.004

Bopp, L., Aumont, O., Cadule, P., Alvain, S. & Gehlen, M. (2005). Response of diatoms distribution to global warming and potential implications: A global model study. Geophysical Research Letters, 32, L19606. doi:10.1029/2005GL023653

Borchard, C., Borges, A. V., Händel, N. & Engel, A. (2011). Biogeochemical response of *Emiliania huxleyi* (PML B92/11) to elevated CO_2 and temperature under phosphorous limitation : A chemostat study. Journal of Experimental Marine Biology and Ecology, 410, 61–71. doi:10.1016/j.jembe.2011.10.004

Borrett, S. R. & Lau, M- K. (2014). enaR: An r package for Ecosystem Network Analysis. Methods in Ecology and Evolution, 5, 1206–1213. doi:10.1111/2041-210X.12282

Bowler, C. et al. (2008). The *Phaeodactylum* genome reveals the evolutionary history of diatom genomes. Nature, 456 (7219), 239–244. doi:10.1038/nature07410

Bowler, C., Vardi, A. & Allen, A. E. (2010). Oceanographic and biogeochemical insights from diatom genomes. Annual Review of Marine Science, 2, 333-365. doi:10.1146/annurev-marine-120308-081051

Boyce, D. G., Lewis, M. R. & Worm, B. (2010). Global phytoplankton decline over the past century. Nature, 466, 591-596. doi:10.1038/nature09268

Boyd, P. W., Collins, S., Dupont, S., Fabricius, K., Gattuso, J. P., Havenhand, J., Hutchins, D. A., Riebesell, U., Sintoul, M. S., Vichi, M., Biswas, H., Ciotti, A., Gao, K., Gehlen, M., Hurd, C. L., Kurihara, H., McGraw, C. M., Navarro, J. M., Nilsson, G. E., Passow, U. & Pörtner, H. O. (2018). Experimental strategies to assess the biological ramifications of multiple drivers of global ocean change - A review. Global Change Biology. 24, 2239–2261. doi:10.1111/gcb.14102

Bradford, M. M. (1976). A rapid and sensitive method for the quantitation of microgram quantities of protein utilizing the principle of protein-dye binding. Analytical Biochemistry, 72, 248–254. doi:10.1016/0003-2697(76)90527-3

Brander, K. & Kiørboe, T. (2020). Decreasing phytoplankton size adversely affects ocean food chains. Global Change Biology, 26, 5356-5357. doi:10.1111/gcb.15216

Bresnan, E., Hay, S., Hughes, S. L., Fraser, S., Rasmussen, J., Webster, L., Slesser, G., Dunn, J. & Heath, M. R. (2009). Seasonal and interannual variation in the phytoplankton community in the north east of Scotland. Journal of Sea Research, 61, 17–25. doi:10.1016/j.seares.2008.05.007

Brierley, A. S. & Kingsford, M. J. (2009). Impacts of climate change on marine organisms and ecosystems. Current Biology, 19 (14), R602-R614. doi:10.1016/j.cub.2009.05.046

Brown, J. H., Gillooly, J. F, Allen, A. P., Savage, V. M. & West, G. B. (2004). Toward a

metabolic theory of ecology. Ecology, 85, 1771–1789. doi:10.1890/03-9000
Brutemark, A., Engström-Öst, J., Vehmaa, A. & Gorokhova, E. (2015). Growth, toxicity and oxidative stress of a cultured cyanobacterium (*Dolichospermum* sp.) under different CO_2 / pH and temperature conditions. Phycological Research, 63 (1), 56–63. doi:10.1111/pre.12075
Buesseler, K. O. (1998). The decoupling of production and particulate export in the surface. Global Biogeochemical cycles, 12 (2), 297–310. doi:10.1029/97GB03366
Burkhardt, S., Amoroso, G., Riebesell, U. & Sültemeyer, D. (2001). CO_2 and HCO_3^- uptake in marine diatoms acclimated to different CO_2 concentrations. Limnology and Oceanography, 46 (6), 1378-1391. doi:10.4319/lo.2001.46.6.1378
Burkhardt, S., Zondervan, I. & Riebesell, U. (1999). Effect of CO_2 concentration on C:N:P ratio in marine phytoplankton: a species comparison. Limnology and Oceanography, 44 (3), 683-690. doi:10.4319/lo.1999.44.3.0683
Burkill, P. H., Mantoura, R. F. C., Llewellyn, C. A. & Owens, N. J. P. (1987). Microzooplankton grazing and selectivity of phytoplankton in coastal waters. Marine Biology, 93, 581–590. doi:10.1007/BF00392796
Burson, A., Stomp, M., Akil, L., Brussaard, C. P. D. & Huisman, J. (2016). Unbalanced reduction of nutrient loads has created an offshore gradient from phosphorus to nitrogen limitation in the North Sea. Limnology and Oceanography, 61, 869-888. doi: 10.1002/lno.10257
Calbet, A., Carlotti, F. & Gaudy, R. (2007). The feeding ecology of the copepod C*entropages typicus* (Kröyer). Progress in Oceanography, 72 (2-3), 137-150. doi:10.1016/j.pocean.2007.01.003
Capuzzo, E., Lynam, C. P., Barry, J., Stephens, D., Forster, R. M., Greenwood, N., McQuatters-gollop, A., Silva, T., van Leeuwen, S. M. & Engelhard, G. H. (2018). A decline in primary production in the North Sea over 25 years, associated with reductions in zooplankton abundance and fish stock recruitment. Global Change Biology, 24, e352–e364. doi:10.1111/gcb.13916
Carrara, F., Sengupta, A., Behrendt, L., Vardi, A. & Stocker, R. (2021). Bistability in oxidative stress response determines the migration behavior of phytoplankton in turbulence. Proceedings of the National Academy of Sciences, 118 (5), e2005944118. doi:10.1073/pnas.2005944118
Castellani, C., Irigoien, X., Harris, R. & Lampitt, R. S. (2005). Feeding and egg production of *Oithona similis* in the North Atlantic. Marine Ecology Progress Series, 288, 173–182. doi:10.3354/meps288173
Castellani, C., Robinson, C., Smith, T. & Lampitt, R. S. (2005). Temperature affects respiration rate of *Oithona similis*. Marine Ecology Progress Series, 285, 129-135. doi:10.3354/meps285129
Chen, B., Landry, M. R., Huang, B. & Liu, H. (2012). Does warming enhance the effect of microzooplankton grazing on marine phytoplankton in the ocean? Limnology and Oceanography, 57 (2), 519–526. doi:10.4319/lo.2012.57.2.0519
Choo, K., Snoeijs, P. & Pederse, M. (2004). Oxidative stress tolerance in the filamentous green algae *Cladophora glomerata* and *Enteromorpha ahlneriana*. Journal of Experimental Marine Biology and Ecology, 298 (1), 111–123. doi:10.1016/j.jembe.2003.08.007
Coll, M. & Libralato, S. (2012). Contributions of food web modelling to the ecosystem approach to marine resource management in the Mediterranean Sea. Fish and Fisheries, 13, 60–88. doi:10.1111/j.1467-2979.2011.00420.x
Croll, S. L. & Watts, S. A. (2004). The effect of temperature on feed consumption and nutrient absorption in *Procambarus clarkii* and *Procambarus zonangulus*. Journal of the World Aquaculture Society, 35, 478–488. doi:10.1111/j.1749-7345.2004.tb00113.x
Cross, W. F., Hood, J. M., Benstead, J. P., Huryn, A. D. & Nelson, D. (2015). Interactions

between temperature and nutrients across levels of ecological organization. Global Change Biology, 21 (3), 1025-1040. doi:10.1111/gcb.12809
Cullen, J. J., Franks, P. J., Karl, D. M., & Longhurst, A. L. A. N. (2002). Physical influences on marine ecosystem dynamics. In The Sea (eds. Robinson, A. R., McCarthy, J. J. & Rothschild, B. J.) pp. 297-336. New York, The USA: John Wiley & Sons, Inc.
Cushing, D. H. (1990). Plankton production and year-class strength in fish populations: an update of the match/mismatch hypothesis. Advances in Marine Biology, 26, 249-293. doi:10.1016/S0065-2881(08)60202-3
Daufresne, M., Lengfellner, K. & Sommer, U. (2009). Global warming benefits the small in aquatic ecosystems. Proceedings of the National Academy of Sciences, 106, 12788–12793. doi:10.1073/pnas.0902080106
Day, D. A. & Wiskich, J. T. (1995). Regulation of alternative oxidase activity in higher plants. Journal of Bioenergetics and Biomembranes, 27 (4), 379-385. doi:10.1007/BF02110000
De Senerpont Domis, L. N., Van de Waal, D. B., Helmsing, N. R., Van Donk, E. & Mooij, W. M. (2014). Community stoichiometry in a changing world: combined effects of warming and eutrophication on phytoplankton dynamics. Ecology, 95 (6), 1485-1495. doi:10.1890/13-1251.1
Del Giorgio, P. A. & Duarte, C. M. (2002). Respiration in the open ocean. Nature, 420, 379-384. doi:10.1038/nature01165
Dettner, K., Bauer, G. & Völkl, W. (2012). Vertical food web interactions: evolutionary patterns and driving forces. Springer Science & Business Media. doi:10.1007/978-3-642-60725-7_19
Di Pane, J., Wiltshire, K. H., McLean, M., Boersma, M. & Meunier, C. L. (2022). Environmentally induced functional shifts in phytoplankton and their potential consequences for ecosystem functioning. Global Change Biology, 28, 2804–2819. doi:10.1111/gcb.16098
Dickson, A. G. (1981). An exact definition of total alkalinity and a procedure for the estimation of alkalinity and total inorganic carbon from titration data. Deep-Sea Research. 28, 609–623. doi:10.1016/0198-0149(81)90121-7
Dickson A. G. & Millero, F. J. (1987). A comparison of the equilibrium constants for the dissociation of carbonic acid in seawater media. Deep-Sea Research, 34, 1733–1743. doi:10.1016/0198-0149(87)90021-5
Di Pane, J., Wiltshire, K. H., McLean, M., Boersma, M. & Meunier, C. L. (2022). Environmentally induced functional shifts in phytoplankton and their potential consequences for ecosystem functioning. Global Change Biology, 28, 2804-2819. doi: 10.1111/gcb.16098
Doney, S. C., Fabry, V. J., Feely, R. A. & Kleypas, K. A. (2009). Ocean acidification: the other CO_2 problem. Annual Review of Marine Science, 1, 169-192. doi:10.1146/annurev.marine.010908.163834
Duarte, C. M. (2014). Global change and the future ocean : a grand challenge for marine sciences. Frontiers in Marine Science, 1, 1–16. doi:10.3389/fmars.2014.00063
Duarte, C. M. & Cebrián, J. (1996). The fate of marine autotrophic production. Limnology and Oceanography, 41 (8), 1758-1766. doi:10.4319/lo.1996.41.8.1758
Dubinsky, Z. & Stambler, N. (2009). Photoacclimation processes in phytoplankton : mechanisms, consequences and applications. Aquatic Microbial Ecology, 56 (2-3), 163-176. doi:10.3354/ame01345
Ducklow, H. W., Kirchman, D. L., Quinby, H. L., Carlson, C. A. & Dam, H. G. (1993). Stocks and dynamics of bacterioplankton carbon during the spring bloom in the eastern North Atlantic Ocean. Deep-Sea Research II, 40 (1-2), 245-263. doi:10.1016/0967-0645(93)90016-G
Dyhrman, S. T., Jenkins, B. D., Rynearson, T. A., Saito, M. A., Mercier, M. L., Alexander, H.,

Whitney, L. P., Drzewianowski, A., Bulygin, V. V., Bertrand, E. M, Wu, Z., Benitez-Nelson, C & Heithoff, A. (2012). The transcriptome and proteome of the diatom *Thalassiosira pseudonana* reveal a diverse phosphorus stress response. PLoS ONE, 7(3), e33768. doi:10.1371/journal.pone.0033768

Easterbrook, D. J. (2016). Greenhouse gases. In Evidence-Based Climate Science, pp. 163-173, Amsterdam, The Netherlands: Elsevier. doi:10.1016/B978-0-12-804588-6.00009-4

Edwards, K. F., Thomas, M. K., Klausmeier, C. A. & Litchman, E. (2016). Phytoplankton growth and the interaction of light and temperature: A synthesis at the species and community level. Limnology and Oceanography, 61, 1232-1244. doi:10.1002/lno.10282

Edwards, M. & Richardson, A. J. (2004). Impact of climate change on marine pelagic phenology and trophic mismatch. Nature, 430, 881-884. doi:10.1038/nature02808

Elbrächter, M. & Qi, Y. (1998). Aspects of *Noctiluca* (Dinophyceae) population dynamics. In: Anderson, M. D. (ed) Physiological Ecology of harmful algal blooms. Springer-Verlag, Berlin, 315−335.

Engel, A., Händel, N., Wohlers, J., Lunau, M., Grossart, H. P., Sommer, U. & Riebesell, U. (2010). Effects of sea surface warming on the production and composition of dissolved organic matter during phytoplankton blooms: results from a mesocosm study. Journal of Plankton Research, 33 (3), 357-372. doi:10.1093/plankt/fbq122

Engel, A., Piontek, J., Grossart, H., Riebesell, U., Schulz, K. G. & Sperling, M. (2014). Impact of CO_2 enrichment on organic matter dynamics during nutrient induced coastal phytoplankton blooms. Journal of Plankton Research, 36 (3), 641-657. doi:10.1093/plankt/fbt125

EPA (2020). Sea Surface Temperature (Technical Documentation). United States Environmental Protection Agency. https://www.epa.gov/sites/default/files/2021-04/documents/sea-surface-temp_td.pdf

Faithfull, C. & Goetze, E. (2019). Copepod nauplii use phosphorus from bacteria, creating a short circuit in the microbial loop. Ecology Letters, 22, 1462-1471. doi:10.1111/ele.13332

Falkowski, P. G. (1994). The role of phytoplankton photosynthesis in global biogeochemical cycles. Photosynthesis Research, 39, 235-258. doi:10.1007/BF00014586

Falkowski, P. G., Barber, R. T. & Smetacek, V. (1998). Biogeochemical controls and feedbacks on ocean primary production. Science, 281, 200-206. doi:10.1126/science.281.5374.200

Fath, B. D., Asmus, H., Asmus, R., Baird, D., Borrett, S. R., de Jonge, V. N., Ludovisi, A., Niquil, N., Scharler, U. M., Schückel, U. & Wolff, M. (2019). Ecological network analysis metrics: The need for an entire ecosystem approach in management and policy. Ocean & Coastal Management, 174, 1–14. doi:10.1016/j.ocecoaman.2019.03.007

Fenchel, T. (2008). The microbial loop – 25 years later. Journal of Experimental Marine Biology and Ecology, 366, 99-103. doi:10.1016/j.jembe.2008.07.013

Feng, Y., Chai, F., Wells, M. L., Liao, Y., Li, P., Cai, T., Zhao, T., Fu, F. & Hutchins, D. A. (2021). The combined effects of increased pCO_2 and warming on a coastal phytoplankton assemblage: from species composition to sinking rate. Frontiers in Marine Science, 8, 622319. doi:10.3389/fmars.2021.622319

Feng, Y., Hare, C. E., Leblanc, K., Rose, J., Zhang, Y., DiTullio, G. R., Lee, P. A., Wilhelm, S. W., Rowe, J. M., Sun, J., Nemcek, N., Gueguen, C., Passow, U., Benner, I., Brown, C. & Hutchins, D. A. (2009). Effects of increased pCO_2 and temperature on the North Atlantic spring bloom. I. The phytoplankton community and biogeochemical response. Marine Ecology Progress Series, 388, 13-25. doi:10.3354/meps08133

Field, C. B., Behrenfeld, M. J., Randerson, J. T. & Falkowski, P. (1998). Primary production of the biosphere: integrating terrestrial and oceanic components. Science, 281, 237-240.

Finn, J. T. (1976). Measures of ecosystem structure and function derived from analysis of flows. Journal of Theoretical Biology, 56, 363–380. doi:10.1016/S0022-5193(76)80080-X

Fogg, G. E. (1983). The ecological significance of extracellular products of phytoplankton

photosynthesis. Botanica Marina, 26, 3–14. doi:10.1515/botm.1983.26.1.3
Fogg, G. E. (2001). Algal adaptation to stress - some general remarks. In Algal adaptation to environmental stresses: physiological, biochemical and molecular mechanisms (eds. L. C. Rai & J. P. Gaur), pp. 1-20. Berlin, Germany: Springer. doi:10.1007/978-3-642-59491-5_1
Forster, J., Hirst, A. G. & Woodward, G. (2011). Growth and development rates have different thermal responses. The Aerican. Naturalist, 178, 668–678. doi:10.1086/662174
Friedlingstein, P. et al. (2022). Global Carbon Budget 2021. Earth System Science Data, 14, 1917-2005. doi:10.5194/essd-14-1917-2022
Fuhrman, J. (2000). Impact of viruses on bacterial processes. Kirchman, D, Ed. Microbial Ecology of the Oceans. Wiley-Liss. 327–350.
Fuhrman, J. A. & Azam, F. (1982). Thymidine incorporation as a measure of heterotrophic bacterioplankton production in marine surface waters: evaluation and field results. Marine Biology, 66 (2), 109-120. doi:10.1007/BF00397184
Gaedke, U., Ruhenstroth-Bauer, M., Wiegand, I., Tirok, K., Aberle, N., Breithaupt, P., Lengfellner, K., Wohlers, J. & Sommer, U. (2010). Biotic interactions may overrule direct climate effects on spring phytoplankton dynamics. Global Change Biology, 16, 1122-1136. doi:10.1111/j.1365-2486.2009.02009.x
Gao, K. & Campbell, D. A. (2014). Photophysiological responses of marine diatoms to elevated CO_2 and decreased pH: a review. Functional Plant Biology, 41, 449-459. doi:10.1071/FP13247
Gao, K., Helbling, E. W., Häder, D. P. & Hutchins, D. A. (2012). Responses of marine primary producers to interactions between ocean acidification, solar radiation, and warming. Marine Ecology Progress Series, 470, 167-189. doi:10.3354/meps10043
Gao, G., Jin, P., Liu, N., Li, F., Tong, S., Hutchins, D. A. & Gao, K. (2017). The acclimation process of phytoplankton biomass, carbon fixation and respiration to the combined effects of elevated temperature and pCO_2 in the northern South China Sea. Marine Pollution Bulletin, 118, 213-220. doi:10.1016/j.marpolbul.2017.02.063
Garrido, S., Cruz, J., Santos, A. M. P., Ré, P. & Saiz; E. (2013). Effects of temperature, food type and food concentration on the grazing of the calanoid copepod *Centropages chierchiae*. Journal of Plankton Research, 35 (4), 843-854. doi:10.1093/plankt/fbt037
Garzke, J., Hansen, T., Ismar, S. M. H. & Sommer, U. (2016). Combined effects of ocean warming and acidification on copepod abundance, body size and fatty acid content. PLoS ONE, 11 (5), 1–22. doi:10.1371/journal.pone.0155952
Gaschler, M. M. & Stockwell, B. R. (2017). Lipid peroxidation in cell death. Biochemical and Biophysical Research Communications, 482 (3), 419-425. doi:10.1016/j.bbrc.2016.10.086
Gechev, T. S., Van Breusegem, F., Stone, J. M., Denev, I. & Laloi, C. (2006). Reactive oxygen species as signals that modulate plant stress responses and programmed cell death. BioEssays, 28, 1091–1101. doi:10.1002/bies.20493
Geider, R. J., La Roche, J., Greene, R. M. & Olaizola, M. (1993). Response of the photosynthetic apparatus of *Phaeodactylum tricornutum* (Bacillariophyceae) to nitrate, phosphate, or iron starvation. Journal of Phycology, 29 (6), 755-766. doi:10.1111/j.0022-3646.1993.00755.x
Gifford, D. J. (1991). The Protozoan-Metazoan trophic link in pelagic ecosystems. The Journal of Protozoology, 38 (1), 81–86. doi:10.1111/j.1550-7408.1991.tb04806.x
Gillespie, K. M., Rogers, A. & Ainsworth, E. A. (2011). Growth at elevated ozone or elevated carbon dioxide concentration alters antioxidant capacity and response to acute oxidative stress in soybean (*Glycine max*). Journal of Experimental Botany, 62 (8), 2667-2678. doi:10.1093/jxb/erq435
Gillooly, J. F., Brown, J. H., West, G. B., Savage, V. M. & Charnov, E. L. (2001). Effects of size and temperature on metabolic rate. Science, 293, 2248–2251.

doi:10.1126/science.1061967
Giordano, M., Beardall, J. & Raven, J. A. (2005). CO_2 concentrating mechanisms in algae: mechanisms, environmental modulation, and evolution. Annual Review of Plant Biology, 56, 99-131. doi: 10.1146/annurev.arplant.56.032604.144052
Goldman, J. A. L., Bender, M. L. & Morel, F. M. M. (2017). The effects of pH and pCO_2 on photosynthesis and respiration in the diatom *Thalassiosira weissflogii*. Photosynthesis Research, 132 (1), 83–93. doi:10.1007/s11120-016-0330-2
Grami, B., Niquil, N., Sakka Hlaili, A., Gosselin, M., Hamel, D. & Mabrouk, H. H. (2008). The plankton food web of the Bizerte Lagoon (South-western Mediterranean): II. Carbon steady-state modelling using inverse analysis. Estuarine, Coastal and Shelf Science, 79, 101–113. doi:10.1016/j.ecss.2008.03.009
Grasshoff K., Kremling, K. & Ehrhardt, M. (1999). Methods of seawater analysis, 3rd edn. Wiley-VCH Verlag, Weinheim.
Grizzetti, B., Bouraoui, F. & Aloe, A. (2012). Changes of nitrogen and phosphorus loads to European seas. Global Change Biology, 18, 769-782. doi:10.1111/j.1365-2486.2011.02576.x
Guillard, R. R. L. (1975). Culture of phytoplankton for feeding marine invertebrate. In: Smith WL, Chanley MH, eds, Culture of Marine Invertebrates Animals. New York, USA: Plenum, 296 – 360. doi:10.1007/978-1-4615-8714-9_3
Guo, K., Chen, J., Yuan, J., Wang, X., Xu, S., Hou, S. & Wang, Y. (2022). Effects of temperature on transparent exopolymer particle production and organic carbon allocation of four marine phytoplankton species. Biology, 11, 1056. doi:10.3390/biology11071056
Habig, W. H. & Jakoby, W. B. (1981). Glutathione S-transferases (rat and human). In: Jakoby WB, eds, Methods in Enzymology: Detoxication and Drug Metabolism: Conjugation and Related Systems 77. New York, USA: Academic Press/Elsevier, 218–235. doi:10.1016/S0076-6879(81)77029-0
Häder, D. P. & Gao, K. (2015). Interactions of anthropogenic stress factors on marine phytoplankton. Frontiers in Environmental Science, 3, 1-14. doi:10.3389/fenvs.2015.00014
Halliwell, B. (1987). Oxidative damage, lipid peroxidation and antioxidant protection in chloroplasts. Chemistry and Physics of Lipids, 44 (2-4), 327-340. doi:10.1016/0009-3084(87)90056-9
Halsband, C. & Hirche, H. J. (2001). Reproductive cycles of dominant calanoid copepods in the North Sea. Marine Ecology Progress Series, 209, 219-229. doi:10.3354/meps209219
Hancke, K., Hancke, T. B., Olsen, L. M. & Johnsen, G. (2008). Temperature effects on microalgal photosynthesis-light responses measured by O_2 production, pulse-amplitude-modulated fluorescence, and ^{14}C assimilation. Journal of Phycology, 44, 501-514. doi:10.1111/j.1529-8817.2008.00487.x
Hare, C. E., Leblanc, K., DiTullio, G. R., Kudela, R. M., Zhang, Y., Lee, P. A., Riseman, S. & Hutchins, D. A. (2007). Consequences of increased temperature and CO_2 for phytoplankton community structure in the Bering Sea. Marine Ecology Progress Series, 352 (9), 9-16. doi:10.3354/meps07182
Harrison, P. J., Furuya, K., Gilbert, P. M., Xu, J., Liu, H. B., Yin, K., Lee, J. H. W., Anderson, D. M., Gowen, R., Al-Azri, A. R. & Ho, A. Y. T. (2011). Geographical distribution of red and green *Noctiluca scintillans*. Chinese Journal of Oceanology and Limnology, 29 (4), 807–831. doi:10.1007/s00343-011-0510-z
Harrison, P. J., Waters, R. E. & Taylor, F. J. R. (1980). A broad spectrum artificial seawater medium for coastal and open ocean phytoplankton. Journal of Phycololgy, 16, 28–35. doi:10.1111/j.0022-3646.1980.00028.x
He, L., Han, X. & Yu, Z. (2014). A rare *Phaeodactylum tricornutum* cruciform morphotype: culture conditions, transformation and unique fatty acid characteristics. PLoS ONE, 9 (4),

e93922. doi:10.1371/journal.pone.0093922
Heil, C. A., Revilla, M, Glibert, P. M. & Murasko, S. (2007). Nutrient quality drives differential phytoplankton community composition on the southwest Florida shelf. Limnology and Oceanography, 52(3), 1067-1078. doi:10.4319/lo.2007.52.3.1067
Hein, M. & Sand-Jensen, K. (1997). CO_2 increases oceanic primary production. Nature, 388 (6642), 526-527. doi:10.1038/41457
Heine, K. B., Abebe, A., Wilson, A. E. & Hood, W. R. (2019). Copepod respiration increases by 7% per °C increase in temperature: A meta-analysis. Limnology and Oceanography Letters, 4, 53-61. doi:10.1002/lol2.10106
Hendey, N. I. (1954). Note on the Plymouth *Nitzschia* culture. Journal of the Marine Biological Association of the United Kingdom, 33 (2), 335-339. doi:10.1017/S0025315400008377
Hendey, N. I. (1964). An introductory account of the smaller algae of British coastal waters. Fishery Investigations Series IV. Part V Bacillariophyceae (Diatoms). Her Majesty's Stationery Office, F. Midler and Sons (eds), London, pp. 317. doi:10.1017/S0025315400016660
Hessen, D. O., de Lange, H. J. & van Donk, E. (1997). UV-induced changes in phytoplankton cells and its effects on grazers. Freshwater Biology, 38, 513-524. doi:10.1046/j.1365-2427.1997.00223.x
Heymans, J. J., Coll, M., Libralato, S., Morissette, L. & Christensen, V. (2014). Global patterns in ecological indicators of marine food webs: A modelling approach. PLoS ONE, 9, e95845. doi:10.1371/journal.pone.0095845
Hillebrand, H., Acevedo-Trejos, E., Moorthi, S. D., Ryabov, A., Striebel, M., Thomas, P. K. & Schneider, M. (2021). Cell size as driver and sentinel of phytoplankton community structure and functioning. Functional Ecology, 36, 276-293. doi:10.1111/1365-2435.13986
Hillebrand, H., Dürselen, C. D., Kirschtel, D., Pollingher, U. & Zohary, T. (1999). Biovolume calculation for pelagic and benthic microalgae. Journal of Phycology. 35, 403–424. doi:10.1046/j.1529-8817.1999.3520403.x
Hilligsøe, K. M., Richardson, K., Bendtsen, J., Sørensen, L.-L., Nielsen, T. G., Lyngsgaard, M. M. (2011). Linking phytoplankton community size composition with temperature, plankton food web structure and sea-air CO_2 flux. Deep-Sea Research I, 58, 826-838. doi:10.1016/j.dsr.2011.06.004
Hjerne, O., Hadju, S., Larsson, U., Downing, A. S. & Winder, M. (2019). Climate driven changes in timing, composition and magnitude of the Baltic Sea phytoplankton spring bloom. Frontiers in Marine Science, 6:482. doi:10.3389/fmars.2019.00482
Hlaili, A. S., Niquil, N. & Legendre, L. (2014). Planktonic food webs revisited: Reanalysis of results from the linear inverse approach. Progress in Oceanography, 120, 216–229. doi:10.1016/j.pocean.2013.09.003
Hoegh-Guldberg, O. & Bruno, J. F. (2010). The Impact of Climate Change on the World's Marine Ecosystems. Science, 328, 1523-1528. doi:10.1126/science.1189930
Honjo, S. & Manganini, S. J. (1993). Annual biogenic particle fluxes to the interior of the North Atlantic Ocean; studied at 34°N 21°W and 48°N 21°W. Deep Sea Research Part II: Topical Studies in Oceanography, 40 (1-2), 587-607. doi:10.1016/0967-0645(93)90034-K
Hopkins, J., Henson, S. A., Painter, S. C., Tyrrell, T. & Poulton, A. J. (2015). Phenological characteristics of global coccolithophore blooms. Global Biogeochemical Cycles, 29, 239–253. doi:10.1002/2014GB004919
Horn, H. G., Boersma, M., Garzke, J., Sommer, U. & Aberle, N. (2020). High CO_2 and warming affect microzooplankton food web dynamics in a Baltic Sea summer plankton community. Marine Biology, 167 (5), 1-17. doi:10.1007/s00227-020-03683-0
Horn, H. G., Sander, N., Stuhr, A., Algueró-Muñiz, M., Bach, L. T., Löder, M. G. J., Boersma, M., Riebesell, U. & Aberle, N. (2016). Low CO_2 sensitivity of microzooplankton

communities in the Gullmar Fjord, Skagerrak: Evidence from a long-term mesocosm study. PLoS ONE, 11 (11), E0165800. doi:10.1371/journal.pone.0165800

Huertas, I. E., Rouco, M., López-Rodas, V. & Costas, E. (2011). Warming will affect phytoplankton differently: evidence through a mechanistic approach. Proceedings of the Royal Society B, 278, 3534-3543. doi:10.1098/rspb.2011.0160

Huppert, A., Blasius, B. & Stone, L. (2002). A model of phytoplankton blooms. The American Naturalist, 159 (2), 156-171. doi:10.1086/324789

Hyun, B., Kim, J., Jang, P., Jang, M., Choi, K., Lee, K., Yang, E. J., Noh, J. H. & Shin, K. (2020). The effects of ocean acidification and warming on growth of a natural community of coastal phytoplankton. Journal of Marine Science and Engineering, 8, 821. doi:10.3390/jmse8100821

IEA (2022). Global Energy Review: CO_2 Emissions in 2021. Global emissions rebound sharply to highest ever level. International Energy Agency. https://www.iea.org/reports/global-energy-review-co2-emissions-in-2021-2

IPCC (2018). Global Warming of 1.5°C. An IPCC Special Report on the impacts of global warming of 1.5°C above pre-industrial levels and related global greenhouse gas emission pathways, in the context of strengthening the global response to the threat of climate change, sustainable development, and efforts to eradicate poverty [Masson-Delmotte, V., P. Zhai, H.-O. Pörtner, D. Roberts, J. Skea, P.R. Shukla, A. Pirani, W. Moufouma-Okia, C. Péan, R. Pidcock, S. Connors, J.B.R. Matthews, Y. Chen, X. Zhou, M.I. Gomis, E. Lonnoy, T. Maycock, M. Tignor, and T. Waterfield (eds.)].

IPCC (2021): Summary for Policymakers. In: Climate Change 2021: The Physical Science Basis. Contribution of Working Group I to the Sixth Assessment Report of the Intergovernmental Panel on Climate Change [Masson-Delmotte, V., P. Zhai, A. Pirani, S. L. Connors, C. Péan, S. Berger, N. Caud, Y. Chen, L. Goldfarb, M. I. Gomis, M. Huang, K. Leitzell, E. Lonnoy, J.B.R. Matthews, T. K. Maycock, T. Waterfield, O. Yelekçi, R. Yu and B. Zhou (eds.)]. Cambridge University Press. doi:10.1017/9781009157896

IPCC (2022): Climate Change 2022: Impacts, Adaptation and Vulnerability. Contribution of Working Group II to the Sixth Assessment Report of the Intergovernmental Panel on Climate Change [H.-O. Pörtner, D.C. Roberts, M. Tignor, E.S. Poloczanska, K. Mintenbeck, A. Alegría, M. Craig, S. Langsdorf, S. Löschke, V. Möller, A. Okem, B. Rama (eds.)]. Cambridge University Press. Cambridge University Press, Cambridge, UK and New York, NY, USA, 3056 pp. doi:10.1017/9781009325844

IPCC Climate Change (2014): Synthesis Report. Contribution of Working Groups I, II and III to the Fifth Assessment Report of the Intergovernmental Panel on Climate Change [Core Writing Team, R.K. Pachauri and L.A. Meyer (eds.)]. IPCC, Geneva, Switzerland, 151 pp.

Irigoien, X., Head, R., Klenke, U., Meyer-Harms, B., Harbour, D., Niehoff, B., Hirche, H.-J. & Harris, R. (1998). A high frequency time series at weathership M, Norwegian Sea, during the 1997 spring bloom: feeding of adult female *Calanus finmarchicus*. Marine Ecology Progress Series, 172, 127-137. doi:10.3354/meps172127

Isla, J. A., Lengfellner, K. & Sommer, U. (2008). Physiological response of the copepod *Pseudocalanus* sp. in the Baltic Sea at different thermal scenarios. Global Change Biology, 14, 895-906. doi:10.1111/j.1365-2486.2008.01531.x

Ives, A. R. & Carpenter, S. R. (2007). Stability and diversity of ecosystems. Science, 317, 58–62. doi:10.1126/science.1133258

Janknegt, P.J., Van De Poll, W. H., Visser, R. J. W., Rijstenbil, J. W. & Buma, A. G. J. (2008). Oxidative stress response in the marine antartic diatom *Chaetoceros brevis* (Bacillariophyceae) during photoacclimation. Journal of Phycology, 44 (4), 957-966. doi:10.1111/j.1529-8817.2008.00553.x

Jiang, L., Joshi, H. & Patel, S. N. (2009). Predation alters relationships between biodiversity and temporal stability. The American Naturalist, 173, 389–399. doi:10.1086/596540

Jiao, N., Herndl, G. J., Hansell, D. A., Benner, R., Kattner, G., Wilhelm, S. W., Kirchman, D. L., Weinbauer, M. G., Luo, T., Chen, F. & Azam, F. (2010). Microbial production of recalcitrant dissolved organic matter: long-term carbon storage in the global ocean. Nature Reviews Microbiology, 8(8), 593–599. doi:10.1038/nrmicro2386

Johns, D. G., Edwards, M., Greve, W. & SJohn, A. W. G. (2005). Increasing prevelance of the marine cladoceran *Penilia avirostris* (Dana, 1852) in the North Sea. Helgoland Marine Research, 59, 215-218. doi:10.1007/s10152-005-0221-y

Joint, I., Doney, S. C. & Karl, D. M. (2011). Will ocean acidification affect marine microbes? The ISME Journal, 5, 1–7. doi:10.1038/ismej.2010.79

Jones, K., J. & Gowen, R. J. (1990). Influences of stratification and irradiance regime on summer phytoplankton composition in coastal and shelf seas of the British Isles. Estuarine, Coastal and Shelf Science, 30, 557-567. doi: 10.1016/0272-7714(90)90092-6

Juan, Y. U., Xue-xi, T., Pei-yu, Z., Ji-yuan, T. & Heng-jiang, C. A. I. (2004). Effects of CO_2 enrichment on photosynthesis, lipid peroxidation and activities of antioxidative enzymes of *Platymonas subcordiformis* subjected to UV-B radiation stress. Acta Botanica Sinica, 46 (6), 682-690.

Karl, I. & Fischer, K. (2008). Why get big in the cold? Towards a solution to a life-history puzzle. Oecologia, 155, 215–225. doi:10.1007/s00442-007-0902-0

Keller, R. P., Geist, J., Jeschke, J. M. & Kühn, I. (2011). Invasive species in Europe: ecology, status, and policy. Environmental Sciences Europe, 23 (1), 1-17. doi:10.1186/2190-4715-23-23

Kieber, D. J., McDaniel, J. & Mopper, K. (1989). Photochemical source of biological substrates in sea water: implications for carbon cycling. Nature, 341, 637-639. doi:10.1038/341637a0

Kiøboe, T. & Nielsen, T. G. (1994). Regulation of zooplankton biomass and production in a temperate, coastal ecosystem. 1. Copepods. Limnology and Oceanography, 39 (3), 493-507. doi:10.4319/lo.1994.39.3.0493

Kirchman, D. L., Morán, X. A. G. & Ducklow, H. (2009). Microbial growth in the polar oceans – role of temperature and potential impact of climate change. Nature Reviews Microbiology, 7, 451-459. doi:10.1038/nrmicro2115

Kirchner, M., Sahling, G., Uhlig, G, Gunkel, W. & Klings, K-W. (2015). Does the red tide-forming dinoflagellate *Noctiluca scintillans* feed on bacteria? Sarsia, 81, 45-55. doi:10.1080/00364827.1996.10413610

Klein Breteler, W. C. M., Schogt, N. & Rampen, S. (2005). Effect of diatom nutrient limitation on copepod development: role of essential lipids. Marine Ecology Progress Series, 291, 125-133. doi:10.3354/meps291125

Kraberg, A., Baumann, M. & Dürselen, C. D. (2010). Coastal phytoplankton: Photo Guide for Northern European Seas. (Publisher Dr. Friedrich Pfeil, München, 2010).

Kuczynska, P., Jemiola-Rzeminska, M. & Strzalka, K. (2015). Photosynthetic pigments in diatoms. Marine Drugs, 13, 5847–5881. doi:10.3390/md13095847

Kvernvik, A. C., Rokitta, S. D., Leu, E., Harms, L., Gabrielsen, T. M., Rost, B. & Hoppe, C. J. (2020). Higher sensitivity towards light stress and ocean acidification in an Arctic sea-ice-associated diatom compared to a pelagic diatom. New Phytologist, 226 (6), 1708-1724. doi:10.1111/nph.16501

Langer, G., Nehrke, G., Probert, I., Ly, J. & Ziveri, P. (2009). Strain-specific responses of *Emiliania huxleyi* to changing seawater carbonate chemistry. Biogeosciences, 6 (11), 2637-2646. doi:10.5194/bg-6-2637-2009

Lara, E., Arrieta. J. M., Garcia-Zaradona, I., Boras, J. A., Duarte, C. M., Agustí, S., Wassmann, P. F. & Vaqué, D. (2013). Experimental evaluation of the warming effect on viral, bacterial and protistan communities in two contrasting Arctic systems. Aquatic Microbial Ecology, 70, 17-32. doi:10.3354/ame01636

Larsson, U. & Hagström, A. (1979). Phytoplankton exudate release as an energy source for the

growth of pelagic bacteria. Marine Biology, 52, 199-206. doi:10.1007/BF00398133
Laspoumaderes, C., Meunier, C. L., Magnin, A., Berlinghof, J., Elser, J. J., Balseiro, E., Torres, G., Modenutti, B., Tremblay, N. & Boersma, M. (2022). A common temperature dependence of nutritional demands in ectotherms. Ecology Letters, 0 (1), 1-14. doi:10.1111/ele.14093
Launay, H., Huang, W., Maberly, S. C. & Gontero, B. (2020). Regulation of carbon metabolism by environmental conditions: a perspective from diatoms and other chromalveolates. Frontiers in Plant Science, 11, 1033. doi:10.3389/fpls.2020.01033
Laws, E. A., Falkowski, P. G., Smith Jr., W. O., Ducklow, H. & McCarthy, J. (2000). Temperature effects on export production in the open ocean. Global Biogeochemical Cycles, 14 (4), 1231-1246. doi:10.1029/1999GB001229
Leblanc, K., Hare, C. E., Feng, Y., Berg, G. M., DiTullio, G. R., Neeley, A., Benner, I., Sprengel, C., Beck, A., Sanudo-Wilhelmy, S. A., Passow, U., Klinck, K., Rowe, J. M., Wilhelm, S. W., Brown, C. W. & Hutchins, D. A. (2009). Distribution of calcifying and silicifying phytoplankton in relation to environmental and biogeochemical parameters during the late stages of the 2005 North East Atlantic Spring Bloom. Biogeosciences, 6, 2155–2179. doi:10.5194/bg-6-2155-2009
Lee, S. & Fuhrman, J. A. (1987). Relationships between biovolume and biomass of naturally derived marine bacterioplankton. Applied and Environmental Microbiology, 53 (6), 1298-1303. doi:10.1128/aem.53.6.1298-1303.1987
Legendre, L. & Le Fèvre, J. (1995). Microbial food webs and the export of biogenic carbon in oceans. Aquatic Microbial Ecology, 9, 69-77. doi:10.3354/ame009069
Legendre, L. & Rassoulzadegan, F. (1995). Plankton and nutrient dynamics in marine waters. Ophelia, 41 (1), 153-172. doi:10.1080/00785236.1995.10422042
León, P., Walsham, P., Bresnan, E., Hartman, S., Hughes, S., Mackenzie, K. & Webster, L. (2018). Seasonal variability of the carbonate system and coccolithophore *Emiliania huxleyi* at a Scottish Coastal Observatory monitoring site. Estuarine, Coastal and Shelf Science, 202, 302-314. doi:10.1016/j.ecss.2018.01.011
Le Quéré, C., Takahashi, T., Buitenhuis, E. T., Rödenbeck, C. & Sutherland, S. C. (2010). Impact of climate change and variability on the global oceanic sink of CO_2. Global Biogeochemical Cycles, 24, 1-10. doi:10.1029/2009GB003599
Lesser, M. P. (1997). Oxidative stress causes coral bleaching during exposure to elevated temperatures. Coral Reefs, 16 (3), 187–192. doi:10.1007/s003380050073
Lewandowska, A. & Sommer, U. (2010). Climate change and the spring bloom: a mesocosm study on the influence of light and temperature on phytoplankton and mesozooplankton. Marine Ecology Progress Series, 405, 101-111. doi:10.3354/meps08520
Li, J., & Sun, X. (2016). Effects of different phosphorus concentrations and N/P ratios on the growth and photosynthetic characteristics of *Skeletonema costatum* and *Prorocentrum donghaiense*. Chinese Journal of Oceanology and Limnology, 34 (6), 1158-1172. doi:10.1007/s00343-016-5169-z
Litchman, E., Edwards, K. F., Klausmeier, C. A. & Thomas, M. K. (2012). Phytoplankton niches, traits and eco-evolutionary responses to global environmental change. Marine Ecology Progress Series, 470, 235-248. doi: 0.3354/meps09912
Litchman, E., Klausmeier, C. A., Miller, J. R., Schofield, O. M. & Falkowski, P. G. (2006). Multi-nutrient, multi-group model of present and future oceanic phytoplankton communities. Biogeosciences, 3, 585-606. doi:10.5194/bg-3-585-2006
Livanou, E., Lagaria, A., Psarra, S. & Lika, K. (2018). A DEB-based approach of modelling dissolved organic matter release by phytoplankton. Journal of Sea Research, 143, 140-151. doi:10.1016/j.seares.2018.07.016
Löder, M G. J., Kraberg, A. C., Aberle, N., Peters, S. & Wilsthire, K. H. (2010). Dinoflagellates and ciliates at Helgoland Roads, North Sea. Helgoland Marine Research, 66, 11-23. doi:

10.1007/s10152-010-0242-z
Löder, M. G. J., Meunier, C., Wiltshire, K. H., Boersma, M. & Aberle, N. (2011). The role of ciliates, heterotrophic dinoflagellates and copepods in structuring spring plankton communities at Helgoland Roads, North Sea. Marine Biology, 158, 1551–1580. doi:10.1007/s00227-011-1670-2
Lòpez-Abbate, M. C. (2021). Microzooplankton communities in a changing ocean: a risk assessment. Diversity, 13, 82. doi:10.3390/d13020082
MacArthur, R. (1955). Fluctuations of animal populations and a measure of community stability. Ecology, 36, 533–536. doi:10.2307/1929601
Macbeth, G., Razumiejczyk, E. & Ledesma, R. D. (2011). Cliff's Delta Calculator: A non-parametric effect size program for two groups of observations. Universitas Psychologica, 10, 545–555.
Mallick, N., Mohn, F. H., Soeder, C. J. & Grobbelaar, J. U. (2002). Ameliorative role of nitric oxide on H_2O_2 toxicity to a chlorophycean alga *Scenedesmus obliquus*. The Journal of General and Applied Microbiology, 48 (1), 1-7.
Malzahn, A. M., Doerfler, D. & Boersma, M. (2016). Junk food gets healthier when it's warm. Limnology and Oceanography, 61, 1677-1685. doi:10.1002/lno.10330
Mantickci, M., Hansen, J. L. S. & Markager, S. (2017). Photosynthesis enhanced dark respiration in three marine phytoplankton species. Journal of Experimental Marine Biology and Ecology, 497, 188-196. doi:10.1016/j.jembe.2017.09.015
Marañón, E. (2015). Cell size as a key determinant of phytoplankton metabolism and community structure. Annual Review of Marine Science, 7, 241–264. doi:10.1146/annurev-marine-010814-015955
Margalef, R. (1978). Life-forms of phytoplankton as survival alternatives in an unstable environment. Oceanologica Acta, 1, 493-509.
Marie, D., Simon, N. & Vaulot, D. (2005). Phytoplankton cell counting by flow cytometry. Algal Culturing Techniques, 1, 253-267.
Marquis, E., Niquil, N., Delmas, D., Hartmann, H. J., Bonnet, D., Carlotti, F., Herbland, A., Labry, C., Sautour, B., Laborde, P., Vézina, A. & Dupuy, C. (2007). Inverse analysis of the planktonic food web dynamics related to phytoplankton bloom development on the continental shelf of the Bay of Biscay, French coast. Estuarine, Coastal and Shelf Science, 73, 223–235. doi:10.1016/j.ecss.2007.01.003
Marra, J. & Barber, R. T. (2004). Phytoplankton and heterotrophic respiration in the surface layer of the ocean. Geophysical Research Letters, 31 (9), 1–4. doi:10.1029/2004GL019664
Martin-Jézéquel, V. & Tesson, B. (2012). *Phaeodactylum tricornutum* polymorphism: an overview. Advances in Algal Cell Biology, 43-80. doi:10.1515/9783110229615.43
Mathews, L., Faithfull, C. L., Lenz, P. H. & Nelson, C. E. (2018). The effects of food stoichiometry and temperature on copepods are mediated by ontogeny. Physiological Ecology, 188, 75-84. doi:10.1007/s00442-018-4183-6
Maugendre, L., Gattuso, J.-P., Louis, J., de Kluijver, A., Marro, S., Soetaert, K. & Gazeau, F. (2015). Effect of ocean warming and acidification on a plankton community in the NW Mediterranean Sea. ICES Journal of Marine Science, 72 (6), 1744-1755. doi:10.1093/icesjms/fsu161
Maugendre, L., Gattuso, J.-P., Poulton, A. J., Dellisanti, W., Gaubert, M., Guieu, C. & Gazeau, F. (2017). No detectable effect of ocean acidification on plankton metabolism in the NW oligotrophic Mediterranean Sea: Results from two mesocosm studies. Estuarine, Coastal and Shelf Science, 186, 89–99. doi:10.1016/j.ecss.2015.03.009
Mayers, K. M. J., Poulton, A. J., Bidle, K., Thamatrakoln, K., Schieler, B., Giering, S. L. C., Wells, S. R., Tarran, G. A., Mayor, D., Johnson, M., Riebesell, U., Larsen, A., Vardi, A. & Harvey, E. L. (2020). The possession of coccoliths fails to deter microzooplankton grazers. Frontiers in Marine Science, 7, 976. doi:10.3389/fmars.2020.569896

McCann, K. (2007). Protecting biostructure. Nature, 446, 29–29. doi:10.1038/446029a
McCann, K. S. (2011). Food Webs (MPB-50), Princeton University Press.
McConville, K., Halsband, C., Fileman, E. S., Somerfield, P. J., Findlay, H. S. & Spicer, J. I. (2013). Effects of elevated CO_2 on the reproduction of two calanoid copepods. Marine Pollution Bulletin, 73, 428-434. doi:10.1016/j.marpolbul.2013.02.010
McEwen, G. F., Johnson, M. W. & Folsom, T. R. (1954). A statistical analysis of the performance of the Folsom plankton sample splitter, based upon test observations. Archiv für Meteorologie, Geophysik und Bioklimatologie, Serie A, 7 (1), 502-527. doi:10.1007/BF02277939
McLaskey, A. K., Keister, J. E., Schoo, K. L., Olson, M. B. & Love, B. A. (2019). Direct and indirect effects of elevated CO_2 are revealed through shifts in phytoplankton, copepod development, and fatty acid accumulation. PLoS ONE, 14 (3), e0213931. doi:10.1371/journal.pone.0213931
Meddeb, M., Niquil, N., Grami, B., Mejri, K., Haraldsson, M., Chaalali, A., Pringault, O. & Hlaili, A. S. (2019). A new type of plankton food web functioning in coastal waters revealed by coupling Monte Carlo Markov chain linear inverse method and ecological network analysis. Ecological Indicators, 104, 67–85. doi:10.1016/j.ecolind.2019.04.077
Meersche, K. V. den, Soetaert, K. & Oevelen, D. V. (2009). xsample() : An R Function for Sampling Linear Inverse Problems. Journal of Statistical Software, 30, 1-15. doi:10.18637/jss.v030.c01
Mehrbach, C., Culberson, C. H., Hawley, J. E. & Pytkowicx, R. M. (1973). Measurement of the apparent dissociation constants of carbonic acid in seawater at atmospheric pressure. Limnology and Oceanography, 18 (6), 897-907. doi:10.4319/lo.1973.18.6.0897
Menden-Deuer, S. & Lessard, E. J. (2000). Carbon to volume relationships for dinoflagellates, diatoms, and other protist plankton. Limnology and Oceanography, 45 (3), 569–579. doi:10.4319/lo.2000.45.3.0569
Meunier, C. L., Algueró-Muñiz, M., Horn, H. G., Lange, J. A. F. & Boersma, M. (2016). Direct and indirect effects of near-future pCO_2 levels on zooplankton dynamics. Marine and Freshwater Research, 68 (2), 373-380. doi:10.1071/MF15296
Meunier, C. L., Alvarez-Fernandez, S., Cunha-Dupont, A. Ö., Geisen, C., Malzahn, A. M., Boersma, M. & Wiltshire, K. H. (2018). The craving for phosphorus in heterotrophic dinoflagellates and its potential implications for biogeochemical cycles. Limmnology and Oceanography, 63, 1774-1784. doi:10.1002/lno.10807
Meunier, C. L., Boersma, M., Wiltshire, K. H. & Malzahn, A. M. (2015). Zooplankton eat what they need: copepod selective feeding and potential consequences for marine systems. Oikos, 125, 50-58. doi:10.1111/oik.02072
Meunier, C. L., Hantzche, F. M., Cunha-Dupont, A. Ö., Haafke, J., Oppermann, B., Malzahn, A. M. & Boersma, M. (2012). Intraspecific selectivity, compensatory feeding and flexible homeostasis in the phagotrophic flagellate *Oxyrrhis marina*: three ways to handle food quality fluctuations. Hydrobiologia, 680, 53-62. doi:10.1007/s10750-011-0900-4
Meunier, C. L., Malzahn, A. M. & Boersma, M. (2014). A new approach to homeostatic regulation: towards a unified view of physiological and ecological concepts. PLoS ONE, 9 (9), e107737. doi:10.1371/journal.pone.0107737
Meunier, C. L., Moreno, H. D., Köring, M., Di Pane, J., Tremblay, N., Wiltshire, K. H. & Boersma, M. (2022). An integrated multiple driver mesocosm experiment reveals the effect of global change on planktonic food web structure. doi:10.1594/PANGAEA.940529
Mittler, R., Vanderauwera, S., Gollery, M. & Van Breusegem, F. (2004). Reactive oxygen gene network of plants. Trends in Plant Science, 9 (10), 490-498. doi:10.1016/j.tplants.2004.08.009
Mohamed, Z. A. (2008). Polysaccharides as a protective response against microcystin-induced oxidative stress in *Chlorella vulgaris* and *Scenedesmus quadricauda* and their possible

significance in the aquatic ecosystem. Ecotoxicology, 17, 504–516. doi:10.1007/s10646-008-0204-2

Moloney, C. L. & Field, J. G. (1989). General allometric equations for rates of nutrient uptake, ingestion, and respiration in plankton organisms. Limnology and Oceanography, 34, 1290–1299. doi:10.4319/lo.1989.34.7.1290

Moloney, C. L. & Field, J. G. (1991). The size-based dynamics of plankton food webs. I. A simulation model of carbon and nitrogen flows. Journal of Plankton Research, 13, 1003–1038. doi:10.1093/plankt/13.5.1003

Moloney, C. L., Field, J. G. & Lucas, M. I. (1991). The size-based dynamics of plankton food webs. II. Simulations of three contrasting southern Benguela food webs. Journal of Plankton Research, 13, 1039–1092. doi:10.1093/plankt/13.5.1039

Monteiro, F. M., Bach, L. T., Brownlee, C., Bown, P., Rickaby, R. E. M., Poulton, A. J., Tyrrel, T., Beuafort, L., Dutkiewicz, S., Gibbs, S., Gutowska, M. G., Lee, R., Riebesell, U., Young, J. & Ridgwell, A. (2016). Why marine phytoplankton calcify. Science Advances, 2 (7), 1–14. doi:10.1126/sciadv.1501822

Moore, M. and Folt, C. (1993). Zooplankton body size and community structure: Effects of thermal and toxicant stress. Trends in Ecology and Evolution, 8, 178–83. doi:10.1016/0169-5347(93)90144-E

Morán, X. A. G., López-Urrutia, A., Calvo-Díaz, A. & Li, W. K. W. (2010). Increasing importance of small phytoplankton in a warmer ocean. Global Change Biology, 16, 1137-1144. doi:10.1111/j.1365-2486.2009.01960.x

Moreno, H. D., Köring, M., Di Pane, J., Tremblay, N., Wiltshire, K. H., Boersma, M. & Meunier, C. L. (2022). An integrated multiple driver mesocosm experiment reveals the effect of global change on planktonic food web structure. Communications Biology, 5 (1), 1-9. doi:10.1038/s42003-022-03105-5

Mühlenruch, M., Grossart, H.-P., Eigemann, F. & Voss, M. (2018). Mini-review: Phytoplankton-derived polysaccharides in the marine environment and their interactions with heterotrophic bacteria. Environmental Microbiology, 20 (8), 2671-2685. doi:10.1111/1462-2920.14302

Nakamura, Y. & Turner, J. T. (1997). Predation and respiration by the small cyclopoid copepod *Oithona similisr* : How important is feeding on ciliates and heterotrophic flagellates? Journal of Plankton Research, 19, 1275–1288. doi:10.1093/plankt/19.9.1275

Neori, A. & Holm-Hansen, O. (1982). Effect of temperature on rate of photosynthesis in Antarctic phytoplankton. Polar Biology, 1, 33-38. doi:10.1007/BF00568752

Nejstgaard, J. C., Gismervik, I. & Solberg, P. T. (1997). Feeding and reproduction by *Calanus finmarchicus*, and microzooplankton grazing during mesocosm blooms of diatoms and the coccolithophore *Emiliania huxleyi*. Marine Ecology Progress Series, 147, 197-217. doi:10.3354/meps147197

Newell, R. & Linley, E. (1984). Significance of microheterotrophs in the decomposition of phytoplankton: estimates of carbon and nitrogen flow based on the biomass of plankton communities. Marine Ecology Progress Series, 16, 105–119. doi:10.3354/meps016105

Niquil, N., Saint-Béat, B., Johnson, G. A., Soetaert, K., Oevelen, D., Bacher, C. & Vézina, A. F. (2012). Inverse Modeling in Modern Ecology and Application to Coastal Ecosystems, Elsevier Inc.

Obernosterer, I. & Herndl, G. J. (1995). Phytoplankton extracellular release and bacterial growth: dependence on the inorganic N:P ratio. Marine Ecology Progress Series, 116 (1), 247-257.

O'Connor, M. I. O., Piehler, M. F., Leech, D. M., Anton, A. & Bruno, J. F. (2009). Warming and resource availability shift food web structure and metabolism. PLoS Biology, 7 (8), 1–6. doi:10.1371/journal.pbio.1000178

Olson, M. B., Solem, K. & Love, B. (2018). Microzooplankton grazing responds to simulated

ocean acidification indirectly through changes in prey cellular characteristics. Marine Ecology Progress Series, 604, 83-97. doi:10.3354/meps12716

Ory, P., Hartmann, H. J., Jude, F., Dupuy, C., Del Amo, Y., Catala, P., Mornet, F., Huet, V., Jan, B., Vincent, D., Sautor, B. & Montanié, H. (2010). Pelagic food web patterns: do they modulate virus and nanoflagellate effects on picoplankton during the phytoplankton spring bloom? Environmental Microbiology, 12, 2755–2772. doi:10.1111/j.1462-2920.2010.02243.x

Oudot-Le Secq, M. P., Grimwood, J., Shapiro, H., Armbrust, E. V., Bowler, C. & Green, B. R. (2007). Chloroplast genomes of the diatoms *Phaeodactylum tricornutum* and *Thalassiosira pseudonana*: comparison with other plastid genomes of the red lineage. Molecular Genetics and Genomics, 277, 427–439. doi: 10.1007/s00438-006-0199-4.

Padfield, D., Yvon-Durocher, G., Buckling, A., Jennings, S. & Yvon-Durocher, G. (2016). Rapid evolution of metabolic traits explains thermal adaptation in phytoplankton. Ecology Letters, 19, 133-142. doi:10.1111/ele.12545

Pansch, A., Winde, V., Asmus, R. & Asmus, H. (2016). Tidal benthic mesocosms simulating future climate change scenarios in the field of marine ecology. Limnology and Oceanography: Methods, 14 (4), 257–267. doi:10.1002/lom3.10086

Payne, M. R., Hatfield, E. M. C., Dickey-Collas, M., Falkenhaug, T., Gallego, A., Gröger, J., Licandro, P., Llope, M., Munk, P., Röckmann, C., Schmidt, J. O. & Nash, R. D. M. (2009). Recruitment in a changing environment: the 2000s North Sea herring recruitment failure. ICES Journal of Marine Science, 66 (2), 272-277. doi:10.1093/icesjms/fsn211

Peñuelas, J., Poulter, B., Sardans, J., Ciais, P., van der Velde, M., Bopp, L., Boucher, O., Godderis, Y., Hinsinger, P., Llusia, J., Nardin, E., Vicca, S., Obersteiner, M. & Janssens, I. A. (2013). Human-induced nitrogen-phosphorus imbalances alter natural and managed ecosystems across the globe. Nature Communications, 4, 2934. doi:10.1038/ncomms3934

Peñuelas, J., Sardans, J., Rivas-Ubach, A., & Janssens, I. A. (2011). The human-induced imbalance between C, N and P in Earth's life system. Global Change Biology, 18, 3-6. doi:10.1038/ncomms3934

Perälä, T., Olsen, E. M. & Hutchings, J. A. (2020). Disentangling conditional effects of multiple regime shifts on Atlantic cod productivity. PLoS ONE, 15 (11), e0237414. doi:10.1371/journal.pone.0237414

Perelman, A., Dubinsky, Z. & Martínez, R. (2006). Temperature dependence of superoxide dismutase activity in plankton. Journal of Experimental Marine Biology and Ecology, 334 (2), 229-235. doi:10.1016/j.jembe.2006.02.009

Pete, R., Davidson, K., Hart, M. C., Gutierrez, T. & Miller, A. E. (2010). Diatom derived dissolved organic matter as a driver of bacterial productivity: the role of nutrient limitation. Journal of Experimental Marine Biology and Ecology, 391 (1-2), 20-26. doi:10.1016/j.jembe.2010.06.002

Peter, K. H. & Sommer, U. (2012). Phytoplankton cell size reduction in response to warming mediated by nutrient limitation. PLoS ONE, 8 (9), e71528. doi:10.1371/journal.pone.0049632

Peter, K. H. & Sommer, U. (2015). Interactive effect of warming, nitrogen and phosphorus limitation on phytoplankton cell size. Ecology and Evolution, 5 (5), 1011-1024. doi:10.1002/ece3.1241

Peterson, B. J. (1984). Synthesis of carbon stocks and flows in the open ocean mixed layer, p. 547-554. In J. E. Hobbie and P. J. LeB. Williams. doi:10.1007/978-1-4684-9010-7_24

Pierrot, D. E., Lewis, E. & Wallace, D. W. R. (2006). MS Excel program developed for CO2 system calculations. Carbon Dioxide Information Analysis Center, Oak Ridge National Laboratory, U.S. Department of Energy.

Poloczanska, E. S., Brown, C. J., Sydeman, W. J., Kiessling, W., Schoeman, D. S., Moore, P. J., Brander, K., Bruno, J. F., Buckley, L. B., Burrows, M. T., Duarte, C. M., Halpern, B.

S., Holding, J., Kappel, C. V., O'Connor, M. I., Pandofil, J. M., Parmesan, C., Schwing, F., Thompson, S. A. & Richardson, A. J. (2013). Global imprint of climate change on marine life. Nature Climate Change, 3 (10), 919-925. doi:10.1038/nclimate1958

Pomeroy, L. R. (1974). The ocean's food web, a changing paradigm. Bioscience, 24 (9), 499-504. doi:10.2307/1296885

Pomeroy, L R. & Deibel, D. (1986). Temperature regulation of bacterial activity during the spring bloom in Newfoundland Coastal Waters. Science, 233, 359-361. doi:10.1126/science.233.4761.359

Prihoda, J., Tanaka, A., de Paula, W. B., Allen, J., Tirichine, L. & Bowler, C. (2012). Chloroplast-mitochondria cross-talk in diatoms. Journal of Experimental Botany, 63 (4), 1543-1557. doi:10.1093/jxb/err441

Purdie, D. A. & Finch, M. S. (1994). Impact of a coccolithophorid bloom on dissolved carbon dioxide in sea water enclosures in a Norwegian fjord. Sarsia, 79 (4), 379-387. doi:10.1080/00364827.1994.10413569

Putt, M. & Stoecker, D. K. (1989). An experimentally determined carbon : volume ratio for marine "oligotrichous" ciliates from estuarine and coastal waters. Limnology and Oceanography. 34 (6), 1097-1103. doi:10.4319/lo.1989.34.6.1097

Rajagopal, S., Murthy, S. D. S. & Mohanty, P. (2000). Effect of ultraviolet-B radiation on intact cells of the cyanobacterium *Spirulina platensis*: characterization of the alterations in the thylakoid membranes. Journal of Photochemistry and Photobiology, 54, 61–66. doi:10.1016/S1011-1344(99)00156-6

Rajeev, M., Sushmitha, T. J., Aravindraja, C., Toleti, S. R. & Pandian, S. K. (2021). Thermal discharge-induced seawater warming alters richness, community composition and interactions of bacterioplankton assemblages in a coastal ecosystem. Scientific Reports, 11 (1), 1-13. doi:10.1038/s41598-021-96969-2

Ras, M., Steyer, J. & Bernard, O. (2013). Temperature effect on microalgae: a crucial factor for outdoor production. Reviews in Environmental Science and Bio/Technology, 12 (2), 153-164. doi:10.1007/s11157-013-9310-6

Rasdi, N. W. & Qin, J. G. (2014). Effect of N:P ratio on growth and chemical composition of *Nannochloropsis oculata* and *Tisochrysis lutea*. Journal of Applied Phycology, 27 (6), 2221-2230. doi:10.1007/s10811-014-0495-z

Raven, J. A. & Falkowski, P. G. (1999). Oceanic sinks for atmospheric CO_2. Plant, Cell and Environment, 22, 741-755. doi:10.1046/j.1365-3040.1999.00419.x

R Core Team. (2021). R: A language and environment for statistical computing. R Foundation for Statistical Computing, Vienna, Austria. URL https://www.R-project.org/.

R Core Team. (2022). R: A language and environment for statistical computing. R Foundation for Statistical Computing, Vienna, Austria. URL https://www.R-project.org/.

Reid, P. C., Borges, M. F. & Svendsen, E. (2001). A regime shift in the North Sea circa 1988 linked to changes in the North Sea horse mackerel fishery. Fisheries Research, 50 (1-2), 163-171. doi:10.1016/S0165-7836(00)00249-6

Reid, P. C., et al. (2016). Global impacts of the 1980s regime shift. Global Change Biology, 22, 682–703. doi:10.1111/gcb.13106

Richardson, A. J. & Schoeman, D. S. (2004). Climate impact on plankton ecosystems in the Northeast Atlantic. Science, 305, 1609–1612. doi:10.1126/science.1100958

Richardson, T. L., Jackson, G. A., Ducklow, H. W. & Roman, M. R. (2004). Carbon fluxes through food webs of the eastern equatorial Pacific: an inverse approach. Deep Sea Research Part I: Oceanographic Research Papers, 51, 1245–1274. doi:10.1016/j.dsr.2004.05.005

Richardson, T. L., Jackson, G. A., Ducklow, H. W. & Roman, M. R. (2006). Spatial and

seasonal patterns of carbon cycling through planktonic food webs of the Arabian Sea determined by inverse analysis. Deep Sea Research Part II: Topical Studies in Oceanography, 53, 555–575. doi:10.1016/j.dsr2.2006.01.015

Riebesell, U. (2004). Effects of CO_2 enrichment on marine phytoplankton. Journal of Oceanography, 60, 719-729. doi:10.1007/s10872-004-5764-z

Riebesell, U., Aberle-Malzah, N., Achterber, E. P., Alguéro-Muñiz, M., Alvarez-Fernandez, S., Arístegui, J., Bach, L. T., Boersma, M., Boxhammer, T., Guan, W., Haunost, M., Horn, H. G., Löscher, C. R., Ludwig, A., Spisla, C., Sswat, M., Stange, P. & Taucher, J. (2018). Toxic algal bloom induced by ocean acidification disrupts the pelagic food web. Nature Climate Change, 8, 1082-1086. doi:10.1038/s41558-018-0344-1

Riebesell, U., Schulz, K. G., Bellerby, R. G. J., Botros, M., Fritsche, P., Meyerhöfer, M., Neil, C., Nondal, G., Oschlies, A., Wohlers, J. & Zöllner, E. (2007). Enhanced biological carbon consumption in a high CO_2 ocean. Nature, 450 (7169), 545-548. doi:10.1038/nature06267

Riebesell, U., Zondervan, I., Rost, B., Tortell, P. D., Zeebe, R. E. & Morel, F. M. M. (2000). Reduced calcification of marine plankton in response to increased atmospheric CO_2. Nature, 407, 364-367. doi:10.1038/35030078

Rip, J. M. K., McCann, K. S., Lynn, D. H. & Fawcett, S. (2010). An experimental test of a fundamental food web motif. Proceedings of the Royal Society B Biological Sciences, 277, 1743–1749. doi:10.1098/rspb.2009.2191

Rivero-Calle, S., Gnanadesikan, A., Del Castillo, C. E., Balch, W. M. & Guikema, S. D. (2015). Multidecadal increase in North Atlantic coccolithophores and the potential role of rising CO_2. Science, 350 (6267), 1533–1537. doi:10.1126/science.aaa8026

Rokitta, S. D., John, U. & Rost, B. (2012). Ocean acidification affects redox-balance and ion-homeostasis in the life-cycle stages of *Emiliania huxleyi*. PLoS ONE, 12, e52212. doi:10.1371/journal.pone.0052212

Rokitta, S. D., Kranz, S. A. & Rost, B. (2022). Inorganic carbon acquisition by aquatic primary producers. In: Maberly SC, Gontero B, eds. Blue planet, red and green photosynthesis. London, UK: ISTE-Wiley, 81-114. doi:10.1002/9781119986782.ch4

Rokitta, S. D. & Rost, B. (2012). Effects of CO_2 and their modulation by light in the life-cycle stages of the coccolithophore *Emiliania huxleyi*. Limnology and Oceanography, 57 (2), 607-618. doi:10.4319/lo.2012.57.2.0607

Rokitta, S. D., von Dassow, P., Rost, B. & John, U. (2016). P- and N-depletion trigger similar cellular responses to promote senescence in eukaryotic phytoplankton. Frontiers in Marine Science, 3:109. doi:10.3389/fmars.2016.00109

Rollwagen-Bollens, G. & Gifford, S. (2011). The role of protistan microzooplankton in the upper San Francisco estuary planktonic food web: source or sink? Estuaries and Coasts, 34, 1026–1038. doi:10.1007/s12237-011-9374-x

Rooney, N. & McCann, K. S. (2012). Integrating food web diversity, structure and stability. Trends in Ecology and Evolution, 27, 40–46. doi:10.1016/j.tree.2011.09.001

Rosas-Navarro, A., Langer, G. & Ziveri, P. (2016). Temperature affects the morphology and calcification of *Emiliania huxleyi* strains. Biogeosciences, 13, 2913-2926. doi:10.5194/bg-13-2913-2016

Rose, J. M., Feng, Y., Gobler, C. J., Gutierrez, R., Hare, C. E., Leblanc, K. & Hutchins, D. A. (2009). Effects of increased pCO_2 and temperature on the North Atlantic spring bloom. II. Microzooplankton abundance and grazing. Marine Ecology Progress Series, 388, 27-40. doi:10.3354/meps08134

Rossoll, D., Bermúdez, R., Hauss, H., Schulz, K. G., Riebesell, U., Sommer, U. & Winder, M. (2012). Ocean acidification-induced food quality deterioration constrains trophic transfer. PLoS ONE, 7 (4), e34737. doi:10.1371/journal.pone.0034737

Rost, B. & Riebesell, U. (2004). Coccolithophores and the biological pump: responses to environmental changes, In: Coccolithophores: from molecular processes to global impact

/ Hans R. Thierstein; Jeremy R. Young (Eds.) Berlin [u.a.]: Springer, 99-125. doi:10.1007/978-3-662-06278-4_5

Rost, B., Riebesell, U. & Burkhardt, S. (2003). Carbon acquisition of bloom-forming marine phytoplankton. Limnology and Oceanography, 48 (1), 55-67. doi:10.4319/lo.2003.48.1.0055

Ruiz, T., Koussoroplis, A.-M., Danger, M., Aguer, J.-P., Morel-Desrosiers, N. & Bec, A. (2020). U-shaped response unifies views on temperature dependency of stoichiometric requirements. Ecology Letters, 23, 860–869. doi:10.1111/ele.13493

Sala, M. M. et al. (2016). Contrasting effects of ocean acidification on the microbial food web under different trophic conditions. ICES Journal of Marine Science, 73, 670–679. doi:10.1093/icesjms/fsv130

Sala, O. E., F. Stuart Chapin, III, Armesto, J. J., Berlow, E., Bloomfield, J., Dirzo, R., Huber-Sanwald, E., Huenneke, L. F., Jackson, R. B., Kinzig, A., Leemans, R., Lodge, D. M., Mooney, H. A., Oesterheld, M., Poff, N. L., Sykes, M. T., Walker, B. H., Walker, M., Wall, D. H. (2000). Global biodiversity scenarios for the year 2100. Science 287: 1770–1774. doi:10.1126/science.287.5459.1770

Sapp, M., Schwaderer, A. S., Wiltshire, K. H., Hoppe, H. G., Gerdts, G. & Wichels, A. (2007). Species-specific bacterial communities in the phycosphere of microalgae? Microbial Ecology, 53 (4), 683-699. doi:10.1007/s00248-006-9162-5

Sarker, S. (2018). What explains phytoplankton dynamics? An analysis of the Helgoland Roads Time Series data sets. Doctoral dissertation, Jacobs University Bremen.

Sautour, B. & Castel, J. (1998). Importance of microzooplanktonic crustaceans in the coastal food chain: Bay of Marennes-Oléron, France. Oceanologica Acta, 21, 105–112. doi:10.1016/S0399-1784(98)80054-6

Scharfe, M. & Wiltshire, K. H. (2019). Modeling of intra-annual abundance distributions: Constancy and variation in the phenology of marine phytoplankton species over five decades at Helgoland Roads (North Sea). Ecological Modelling, 404, 46-60. doi:10.1016/j.ecolmodel.2019.01.001

Schoo, K. L., Malzahn, A. M., Krause, E. & Boersma, M. (2013). Increased carbon dioxide availability alters phytoplankton stoichiometry and affects carbon cycling and growth of a marine planktonic herbivore. Marine Biology, 160, 2145-2155. doi:10.1007/s00227-012-2121-4

Sell, D. W., & Evans, M. S. (1982). A statistical analysis of subsampling and an evaluation of the Folsom plankton splitter. Hydrobiologia, 94, 223–230. doi:10.1007/BF00016403

Sett, S., Bach, L. T., Schulz, K. G., Koch-Klaven, S., Lebrato, M. & Riebesell, U. (2014). Temperature modulates coccolithophorid sensitivity of growth, photosynthesis and calcification to increasing seawater pCO_2. PLoS ONE, 9 (2), e88308. doi:10.1371/journal.pone.0088308

Sett, S., Schulz, K. G., Bach, L. T. & Riebesell, U. (2018). Shift towards larger diatoms in a natural phytoplankton assemblage under combined high-CO_2 and warming conditions. Journal of Plankton Research, 40 (4), 391-406. doi:10.1093/plankt/fby018

Sheridan, J. A. & Bickford, D. (2011). Shrinking body size as an ecological response to climate change. Nature Climate Change, 1, 401–406. doi:10.1038/nclimate1259

Sherr, E. B. & Sherr, B. F. (1994). Bacterivory and herbivory: key roles of phagotrophic protists in pelagic food webs. Microbial Ecology, 28, 223-235. doi:10.1007/BF00166812

Sherr, E. B., & Sherr, B. F. (2007). Heterotrophic dinoflagellates: a significant component of microzooplankton biomass and major grazers of diatoms in the sea. Marine Ecology Progress Series, 352, 187–197. doi:10.3354/meps07161

Shi, D., Hong, H., Su, X., Liao, L., Chang, S. & Lin, W. (2019). The physiological response of marine diatoms to ocean acidification: differential roles of seawater pCO_2 and pH. Journal of Phycology, 55, 521–533. doi:10.1111/jpy.12855

Siedlewicz, G., Żak, A., Sharma, L., Kosakowska, A. & Pazdro, K. (2020). Effects of oxytetracycline on growth and chlorophyll a fluorescence in green algae (*Chlorella vulgaris*), diatom (*Phaeodactylum tricornutum*) and cyanobacteria (*Microcystis aeruginosa* and *Nodularia spumigena*). Oceanologia, 62, 214-225. doi:10.1016/j.oceano.2019.12.002

Smayda, T. J. & Reynolds, C. S. (2001). Community assembly in marine phytoplankton: application of recent models to harmful dinoflagellates blooms. Journal of Plankton Research, 23 (5), 447-461. doi: 10.1093/plankt/23.5.447

Sommer, U., Aberle, N., Engel, A., Hansen, T., Lengfellner, K., Sandow, M., Wohlers, J., Zöllner, E. & Riebesell, U. (2007). An indoor mesocosm system to study the effect of climate change on the late winter and spring succession of Baltic Sea phyto- and zooplankton. Global Change and Conservation Ecology, 150, 655-667. doi:10.1007/s00442-006-0539-4

Sommer, U. & Lengfellner, K. (2008). Climate change and the timing, magnitude, and composition of the phytoplankton spring bloom. Global Change Biology, 14, 1199-1208. doi:10.1111/j.1365-2486.2008.01571.x

Sommer, U. & Lewandowska, A. (2011). Climate change and the phytoplankton spring bloom: warming and overwintering zooplankton have similar effects on phytoplankton. Global Change Biology, 17, 154-162. doi:10.1111/j.1365-2486.2010.02182.x

Sommer, U., Paul, C. & Moustaka-Gouni, M. (2015). Warming and ocean acidification effects on phytoplankton – from species shifts to size shifts within species in a mesocosm experiment. PLoS ONE, 10 (5), e0125239. doi:10.1371/journal.pone.0125239

Song, X., Li, Y., Xiang, C., Su, X., Xu, G., Tan, M., Huang, Y., Liu, J., Ma, Z., Huang, L. & Li, G. (2021). Nitrogen and phosphorus enrichments alter the dynamics of the plankton community in Daya Bay, northern South China Sea: results of mesocosm studies. Marine and Freshwater Research, 72, 1632-1642. doi:10.1071/MF21097

Sterner, R. W. & Elser, J. J. (2002). Ecological stoichiometry: the biology of elements from molecules to the biosphere. – Princeton Univ. Press. doi:10.1515/9781400885695

Stewart, R. I. A., Dossena, M., Bohan, D. A., Jeppesen, E., Kordas, R. L., Ledger, M. E., Meerhof, M., Moss, B., Mulder, C., Shurin, J. B., Suttle, B., Thompson, R., Trimmer, M. & Woodward, G. (2013). Mesocosm experiments as a tool for ecological climate-change Research. In Advances in ecological research / Guy Woodward; Eoin J. O'Gorman (Eds.). Amsterdam: Academic Press, 71-181. doi:10.1016/B978-0-12-417199-2.00002-1

Stock, W., Blommaert, L., De Troch, M., Mangelinckx, S., Willems, A., Vyverman, W. & Sabbe, K. (2019). Host specificity in diatom-bacteria interactions alleviates antagonistic effects. FEMS Microbiology Ecology, 95 (11), fiz171. doi:10.1093/femsec/fiz171

Stoecker, D. K. & Sanders, N. K. (1985). Differential grazing by *Acartia tonsa* on a dinoflagellate and a tintinnid. Journal of Plankton Research, 7 (1), 85-100. doi:10.1093/plankt/7.1.85

Stoll, M. H. C., Bakker, K., Nobbe, G. H., Haese, R. R. (2001). Continuous-Flow analysis of dissolved inorganic carbon content in seawater. Analytical Chemistry, 73, 4111-4116. doi:10.1021/ac010303r

Stramski, D., Sciandra, A. & Claustre, H. (2002). Effects of temperature, nitrogen, and light limitation on the optical properties of the marine diatom *Thalassiosira pseudonana*. Limnology and Oceanography. 47(2),392-403. doi:10.4319/lo.2002.47.2.0392

Strickland, J. D. H. & Parsons, T. R. (1972). Practical Handbook of Seawater Analysis. Fisheries Research Board of Canada. doi:10.25607/OBP-1791

Strom, S. L., Brainard, M. A., Holmes, J. L. & Olson, M. B. (2001). Phytoplankton blooms are strongly impacted by microzooplankton grazing in coastal North Pacific waters. Marine Biology, 138, 355-368. doi:10.1007/s002270000461

Sun, J., Feng, Y., Zhou, F., Song, S., Jiang, Y. & Ding, C. (2013). Top-down control of spring

surface phytoplankton blooms by microzooplankton in the Central Yellow Sea, China. Deep-Research II, 97, 51-60. doi:10.1016/j.dsr2.2013.05.005

Suttle, K. B., Thomsen, M. A. & Power, M. E. (2007). Species interactions reverse grassland responses to changing climate. Science, 315, 640–642. doi:10.1126/science.1136401

Suzuki, K. (2000). Measurement of Mn-SOD and Cu, Zn-SOD. In: Taniguchi N, Gutteridge J, eds. Experimental Protocols for Reactive Oxygen and Nitrogen Species. Oxford, UK: Oxford University Press: 91–95.

Suzuki, K., Nakamura, Y. & Hiromi, J. (1999). Feeding by the small calanoid copepod *Paracalanus* sp. on heterotrophic dinoflagellates and ciliates. Aquatic Microbial Ecology, 17, 99–103. doi:10.3354/ame017099

Taucher, J., Jones, J., James, A., Brzezinski, M. A., Carlson, C. A., Riebesell, U. & Passow, U. (2015). Combined effects of CO_2 and temperature on carbon uptake and partitioning by the marine diatoms *Thalassiosira weissflogii* and *Dactyliosolen fragilissimus*. Limnology and Oceanography, 60 (3), 901-919. doi:10.1002/lno.10063

Taucher, J. & Oschlies, A. (2011). Can we predict the direction of marine primary production change under global warming? Geophysical Research Letters, 38, L02603. doi:10.1029/2010GL045934

Thangaraj, S. & Sun, J. (2021). Transcriptomic reprogramming of the oceanic diatom *Skeletonema dohrnii* under warming ocean and acidification. Environmental Microbiology, 23 (2), 980-995. doi:10.1111/1462-2920.15248

Thingstad, T. F. & Rassoulzadegan, F. (1999). Conceptual models for the biogeochemical role of the photic zone microbial food web, with particular reference to the Mediterranean Sea. Progress in Oceanography, 44, 271–286. doi:10.1016/S0079-6611(99)00029-4

Thornton, D. C. O. (2014). Dissolved organic matter (DOM) release by phytoplankton in the contemporary and future ocean. European Journal of Phycology, 49 (1), 20-46. doi:10.1080/09670262.2013.875596

Tilzer, M. M., Elbrächter, M., Gieskes, W. W. & Beese, B. (1986). Light-temperature interactions in the control of photosynthesis in Antarctic phytoplankton. Polar Biology, 5, 105–111. doi:10.1007/BF00443382

Tinker, J. P. & Howes, E. L. (2020). The impacts of climate change on temperature (air and sea), relevant to the coastal and marine environment around the UK. MCCIP, Science Review, 2020, 1-30. doi: 10.14465/2020.arc01.tem

Tong, S., Xu, D., Wang, Y., Zhang, X., Li, Y., Wu, H. & Ye, N. (2021). Influence of ocean acidification on thermal reaction norms of carbon metabolism in the marine diatom *Phaeodactylum tricornutum*. Marine Environmental Research, 164, 105233.

Torchiano, M. (2020). effsize: Efficient Effect Size Computation. doi:10.5281/zenodo.1480624

Torstensson, A., Hedblom, M., Björk, M. M., Chierici, M. & Wulff, A. (2015). Long-term acclimation to elevated pCO_2 alters carbon metabolism and reduces growth in the Antarctic diatom *Nitzschia lecointei*. Proceedings of the Royal Society B: Biological Sciences, 282 (1815), 20151513. doi:10.1098/rspb.2015.1513

Tortajada, S., Niquil, N., Blanchet, H., Grami, B., Montanié, H., David, V., Glé, C., Saint-Béat, B., Johnson, G. A., Marquis, E., Del Amo, Y., Dubois, S., Vincent, D., Dupuy, C., Jude, F., Hartmann, H. J. & Sautour, B. (2012). Network analysis of the planktonic food web during the spring bloom in a semi enclosed lagoon (Arcachon, SW France). Acta Oecologica, 40, 40–50. doi:10.1016/j.actao.2012.02.002

Tortell, P. D., Payne, C., Gueguen, C., Strzepek, R. F., Boyd, P. W. & Rost, B. (2008). Inorganic carbon uptake by Southern Ocean phytoplankton. Limnology and Oceanography, 53 (4), 1266–1278. doi:10.4319/lo.2008.53.4.1266

Toseland, A., Daines, S. J., Clark, J. R., Kirkham, A., Strauss, J., Uhlig, C., Lenton, T. M., Valentin, K., Pearson, G. A., Moulton, V. & Mock, T. (2013). The impact of temperature on marine phytoplankton resource allocation and metabolism. Nature Climate Change, 3

(11), 979-984. doi:10.1038/nclimate1989
Townsend, D. W., Cammen, L. M., Holligan, P. M., Campbell, D. E. & Pettigrew, N. R. (1994). Causes and consequences of variability in the timing of spring phytoplankton blooms. Deep-Sea Research, 41 (5-6), 747-765. doi:10.1016/0967-0637(94)90075-2
Turner, J. T., Tester, P. A. & Ferguson, R. L. (1988). The marine cladoceran *Penilia avirostris* and the "microbial loop" of pelagic food webs. Limnology and Oceanography, 33, 245–255. doi:10.4319/lo.1988.33.2.0245
Tylianakis, J. M., Tscharntke, T. & Lewis, O. T. (2007). Habitat modification alters the structure of tropical host–parasitoid food webs. Nature, 445, 202–205. doi:10.1038/nature05429
Uchiyama, M. & Mihara, M. (1978). Determination of malondialdehyde precursor in tissues by thiobarbituric acid test. Analytical Biochemistry, 86, 271-278. doi:10.1016/0003-2697(78)90342-1
Ulanowicz, R. E. (2004). Quantitative methods for ecological network analysis. Computational Biology and Chemistry, 28, 321–339. doi:10.1016/j.compbiolchem.2004.09.001
Utermöhl, H. (1958). Zur Vervollkommnung der quantitativen Phytoplankton-Methodik. Internationale Vereinigung für Theoretische und Angewandte Limnologie: Mitteilungen, 9 (1), 1-38. doi:10.1080/05384680.1958.11904091
van de Waal, D. B. & Litchman, E. (2020). Multiple global change stressor effects on phytoplankton nutrient acquisition in a future ocean. Philosophical Transactions B, 375, 20190706. doi:10.1098/rstb.2019.0706
van de Waal, D. B., Verschoor, A. M., Verspagen, J. M. H., van Donk, E. & Huisman, J. (2010). Climate-driven changes in the ecological stoichiometry of aquatic ecosystems. Frontiers in Ecology and the Environment, 8 (3), 145-152. doi:10.1890/080178
van der Heijden, L. H., Niquil, N., Haraldsson, M., Asmus, R. M., Pacella, S. R., Graeve, M., Rzeznik-Orignac, J., Asmus, H., Saint-Béat, B. & Lebreton, B. (2020). Quantitative food web modeling unravels the importance of the microphytobenthos-meiofauna pathway for a high trophic transfer by meiofauna in soft-bottom intertidal food webs. Ecological Modelling, 430, 109129. doi:10.1016/j.ecolmodel.2020.109129
van Deurs, M., van Hal, R., Tomczak, M. T., Jónasdóttir, S. H. & Dolmer, P. (2009). Recruitment of lesser sandeel *Ammodytes marinus* in relation to density dependence and zooplankton composition. Marine Ecology Progress Series, 381, 249–258. doi:10.3354/meps07960
van Leeuwen, S., Tett, P., Mills, D. & van der Molen, J. (2015). Stratified and nonstratified areas in the North Sea: Long-term variability and biological and policy implications. Journal of Geophysical Research: Oceans, 120, 4670-4686. doi:10.1002/2014JC010485
van Mooy, B. A. S., Fredricks, H. F., Pedler, B. E., Dyhrman, S. T., Karl, D. M., Koblizek, M., Lomas, M . W., Mincer, T. J., Moore, L. R., Moutin, T., Rappé, M. S., & Webb, E. A. (2009). Phytoplankton in the ocean use non-phosphorus lipids in response to phosphorus scarcity. Nature Letters, 458, 69–72. doi:10.1038/nature07659
van Oevelen, D., Soetaert, K., Middelburg, J. J., Herman, P. M. J., Moodley, L., Hamels, I., Moens, T. & Heip, C. H. R. (2006). Carbon flows through a benthic food web: Integrating biomass, isotope and tracer data. Journal of Marine Research, 64, 453–482. doi:10.1357/002224006778189581
van Oevelen, D., van den Meersche, K., Meysman, F. J. R., Soetaert, K., Middelburg, J. J. & Vézina, A. F. (2010). Quantifying food web flows using linear inverse models. Ecosystems, 13, 32–45. doi:10.1007/s10021-009-9297-6
Vázquez-Domínguez, E., Vaqué, D. & Gasol, J. M. (2012). Temperature effects on the heterotrophic bacteria, heterotrophic nanoflagellates, and microbial top predators of the NW Mediterranean. Aquatic Microbial Ecology, 67, 107-121. doi:10.3354/ame01583
Vega-López, A., Ayala-López, G., Posadas-Espadas, B. P., Olivares-Rubio, H. F. & Dzul-

Caamal, R. (2013). Relations of oxidative stress in freshwater phytoplankton with heavy metals and polycyclic aromatic hydrocarbons. Comparative Biochemistry and Physiology Part A: Molecular & Integrative Physiology, 165 (4), 498-507. doi:10.1016/j.cbpa.2013.01.026

Velthuis, M., Keuskamp, J. A., Bakker, E. S., Boersma, M., Sommer, U., van Donk, E. & van de Waal, D. B. (2022). Differential effects of elevated pCO_2 and warming on marine phytoplankton stoichiometry. Limnology and Oceanography, 67, 598-607. doi:10.1002/lno.12020

Verschoor, A. M., van Dijk, M. A., Huisman, J. & van Donk, E. (2013). Elevated CO_2 concentrations affect the elemental stoichiometry and species composition of an experimental phytoplankton community. Freshwater Biology, 58, 597-611. doi:10.1111/j.1365-2427.2012.02833.x

Vézina, A. F. & Pace, M. L. (1994). An inverse model analysis of planktonic food webs in experimental lakes. Canadian Journal of Fisheries and Aquatic Science, 51, 2034–2044. doi:10.1139/f94-206

Vézina, A. F. & Platt, T. (1988). Food web dynamics in the ocean. I Best-estimates of flow networks using inverse methods. Marine Ecology Progress Series, 42, 269-287. doi:10.3354/meps042269

Vézina, A. F. & Savenkoff, C. (1999). Inverse modeling of carbon and nitrogen flows in the pelagic food web of the northeast subarctic Pacific. Deep Sea Research Part II: Topical Studies in Oceanography, 46, 2909–2939. doi:10.1016/S0967-0645(99)00088-0

Vézina, A. F., Savenkoff, C., Roy, S., Klein, B., Rivkin, R., Therriault, J.-C. & Legendre, L. (2000). Export of biogenic carbon and structure and dynamics of the pelagic food web in the Gulf of St. Lawrence Part 2. Inverse analysis. Deep Sea Research Part II: Topical Studies in Oceanography, 47, 609–635. doi:10.1016/S0967-0645(99)00120-4

Villanova, V., Fortunato, A. E., Singh, D., Dal Bo, D., Conte, M., Obata, T., Jouhet, J., Fernie, A. R., Marechal, E., Falciatore, A., Pagliardini, J., Le Monnier, A., Poolman, M., Curien, G., Petroutsos, D. & Finazzi, G. (2017). Investigating mixotrophic metabolism in the model diatom *Phaeodactylum tricornutum*. Philosophical Transactions Royal Society B, 372, 20160404. doi:10.1098/rstb.2016.0404

Vincent, D. & Hartmann, H. J. (2001). Contribution of ciliated microprotozoans and dinoflagellates to the diet of three copepod species in the Bay of Biscay. Hydrobiologia, 443, 193-204. doi:10.1023/A:1017502813154

Wagner, H., Jakob, T. & Wilhelm, C. (2006). Balancing the energy flow from captured light to biomass under fluctuating light conditions. New Phytologist, 169, 95-108. doi:10.1111/j.1469-8137.2005.01550.x

Wei, H., Sun, J., Moll, A. & Zhao, L. (2004). Phytoplankton dynamics in the Bohai Sea – observations and modelling. Journal of Marine Systems, 44, 233-251. doi:10.1016/j.jmarsys.2003.09.012

Wetz, M. S. & Wheeler, P. A. (2007). Release of dissolved organic matter by coastal diatoms. Limnology and Oceanography, 52 (2), 798–807. doi:10.4319/lo.2007.52.2.0798

Wiltshire, K. H., Boersma, M., Carstens, K., Kraberg, A. C., Peters, S. & Scharfe, M. (2015). Control of phytoplantkon in a shelf sea: Determination of the main drivers based on the Helgoland Roads Time Series. Journal of Sea Research, 105, 42-45. doi: 10.1016/j.seares.2015.06.022

Wiltshire, K. H., Boersma, M., Möller, A. & Buhtz, H. (2000). Extraction of pigments and fatty acids from the green alga *Scenedesmus obliquus* (Chlorophyceae). Aquatic Ecology, 34, 119–126. doi:10.1023/A:1009911418606

Wiltshire, K. H., Kraberg, A., Bartsch, I., Boersma, M., Franke, H., Freund, J., Gebühr, C., Gerdts, G., Stockmann, K. & Wichels, A. (2010). Helgoland Roads, North Sea : 45 Years of Change. Estuaries and Coasts, 33, 295–310. doi:10.1007/s12237-009-9228-y

Wiltshire, K. H., Malzahn, A. M., Wirtz, K., Greve, W., Janisch, S., Mangelsdorf, P., Manly, B. F. J. & Boersma, M. (2008). Resilience of North Sea phytoplankton spring bloom dynamics: An analysis of long-term data at Helgoland Roads. Limnology and Oceanography, 53 (4), 1294-1302. doi:10.4319/lo.2008.53.4.1294

Winder, M. & Sommer, U. (2012). Phytoplankton response to a changing climate. Hydrobiologia, 698(5), 5–16. doi:10.1007/s10750-012-1149-2

Winter, A., Henderiks, J., Beaufort, L., Rickaby, R. E. M. & Brown, C. W. (2014). Poleward expansion of the coccolithophore *Emiliania huxleyi*. Journal of Plankton Research, 36(2), 316-325. doi:10.1093/plankt/fbt110

Wolf, K. K. E., Romanelli, E., Rost, B., John, U., Collins, S., Weigand, H. & Hoppe, C. J. M. (2019). Company matters : The presence of other genotypes alters traits and intraspecific selection in an Arctic diatom under climate change. Global Change Biology, 25, 2869–2884. doi:10.1111/gcb.14675

Wright, R. T. & Coffin, R. B. (1984). Measuring microzooplankton grazing on planktonic marine bacteria by its impact on bacterial production. Microbial Ecology, 10 (2), 137-149. doi:10.1007/BF02011421

Wu, Y., Gao, K. & Riebesell, U. (2010). CO_2-induced seawater acidification affects physiological performance of the marine diatom *Phaeodactylum tricornutum*. Biogeosciences, 7, 2915-2923. doi:10.5194/bg-7-2915-2010

Xu, K., Gao, K., Villafañe, V. E. & Helbling, E. W. (2011). Photosynthetic responses of *Emiliania huxleyi* to UV radiation and elevated temperature: roles of calcified coccoliths. Biogeosciences, 8, 1441-1452. doi:10.5194/bg-8-1441-2011

Xu, Y., Boucher, J. M. & Morel, F. M. M. (2010). Expression and diversity of alkaline phosphatase EHAP1 in *Emiliania huxleyi* (Prymnesiophyceae). Journal of Phycology, 46, 85-92. doi:10.1111/j.1529-8817.2009.00788.x

Xu, Y., Wahlund, T. M., Feng, L., Shaked, Y. & Morel, F. M. M. (2006). A novel alkaline phosphatase in the coccolithophore *Emiliania huxleyi* (Prymensiophyceae) and its regulation by phosphorus. Journal of Phycology, 42, 835-844. doi:10.1111/j.1529-8817.2006.00243.x

Yakovleva, I. M., Baird, A. H., Yamamoto, H. H., Bhagooli, R., Nonaka, M. & Hidaka, M. (2009). Algal symbionts increase oxidative damage and death in coral larvae at high temperatures. Marine Ecology Progress Series, 378, 105-112. doi:10.3354/meps07857

Yamaguchi, H., Arisaka, H., Otsuka, N., & Tomaru, Y. (2014). Utilization of phosphate diesters by phosphodiesterase-producing marine diatoms. Journal of Plankton Research, 36 (1), 281–285. doi:10.1093/plankt/fbt091

Yin, M. C. & Blaxter, J. H. S. (1987). Temperature, salinity tolerance, and buoyancy during early development and starvation of Clyde and North Sea herring, cod, and flounder larvae. Journal of Experimental Marine Biology and Ecology, 107 (3), 279-290. doi:10.1016/0022-0981(87)90044-X

Yoshida, K., Terashima, I. & Noguchi, K. (2007). Up-Regulation of Mitochondrial Alternative Oxidase concomitant with chloroplast over-reduction by excess light. Plant Cell Physiology, 48 (4), 606–614. doi:10.1093/pcp/pcm033

Young, J. N., Kranz, S. A., Goldman, J. A. L., Tortell, P. D. & Morel, F. M. M. (2015). Antarctic phytoplankton down-regulate their carbon-concentrating mechanisms under high CO_2 with no change in growth rates. Marine Ecology Progress Series, 532, 13-28. doi:10.3354/meps11336

Zhang, P., van Leeuwen, C. H. A., Bogers, D., Poelman, M., Xu, J. & Bakker, E. S. (2020). Ectothermic omnivores increase herbivory in response to rising temperature. Oikos, 129, 1028–1039. doi:10.1111/oik.07082

Zhang, S., Liu, H., Chen, B. & Chih-Jung, W. (2015). Effects of diet nutritional quality on the growth and grazing of *Noctiluca scintillans*. Scientific Reports, 527 (73), 73-85.

doi:10.3354/meps11219
Zhang, S., Liu, H., Guo, C. & Harrison, P. (2016). Differential feeding and growth of *Noctiluca scintillans* on monospecific and mixed diets. Marine Ecology Progress Series, 549, 27–40. doi:10.3354/meps11702
Zhao, P. Z., Ouyang, L. L., Shen, A. L., & Wang, Y. L. (2022). The cell cycle of phytoplankton: A review. Journal of the World Aquaculture Society, 53 (4), 799-815. doi:10.1111/jwas.12916
Zhao, Y., Dong, Y., Li, H., Lin, S., Huang, L., Xiao, T., Gregori, G., Zhao, L. & Zang, W. (2020). Grazing by microzooplankton and copepods on the microbial food web in spring in the southern Yellow Sea, China. Marine Life Science & Technology, 2, 442-455. doi:10.1007/s42995-020-00047-x
Zlotnik, I. & Dubinsky, Z. (1989). The effect of light and temperature on DOC excretion by phytoplankton. Limnology and Oceanography, 34 (5), 831–839. doi:10.4319/lo.1989.34.5.0831

Universität Bremen

Versicherung an Eides Statt

Name, Vorname	
Matrikel-Nr.	
Straße	
Ort, PLZ	

Ich, _____ (Vorname, Name)

versichere an Eides Statt durch meine Unterschrift, dass ich die vorstehende Arbeit selbständig und ohne fremde Hilfe angefertigt und alle Stellen, die ich wörtlich dem Sinne nach aus Veröffentlichungen entnommen habe, als solche kenntlich gemacht habe, mich auch keiner anderen als der angegebenen Literatur oder sonstiger Hilfsmittel bedient habe.

Ich versichere an Eides Statt, dass ich die vorgenannten Angaben nach bestem Wissen und Gewissen gemacht habe und dass die Angaben der Wahrheit entsprechen und ich nichts verschwiegen habe.

Die Strafbarkeit einer falschen eidesstattlichen Versicherung ist mir bekannt, namentlich die Strafandrohung gemäß § 156 StGB bis zu drei Jahren Freiheitsstrafe oder Geldstrafe bei vorsätzlicher Begehung der Tat bzw. gemäß § 161 Abs. 1 StGB bis zu einem Jahr Freiheitsstrafe oder Geldstrafe bei fahrlässiger Begehung.

_____

Ort, Datum / Unterschrift